SEDIMENT TRANSPORT AND PROCESSES IN A HIGHLY REGULATED RIVER. THE LOWER EBRO, NE IBERIAN PENINSULA

TRANSPORT DE SEDIMENT I PROCESSOS ASSOCIATS EN UN RIU ALTAMENT REGULAT. EL TRAM BAIX DEL RIU EBRE, NE PENÍNSULA IBÈRICA

Tesi Doctoral

Memòria presentada per
DAMIÀ VERICAT
per optar al títol de Doctorat Europeu en Geografia

Departament de Medi Ambient i Ciències del Sòl
Universitat de Lleida

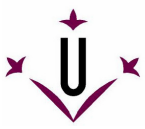

El Director de la Tesi:

Dr. Ramon J. Batalla
Departament de Medi Ambient
i Ciències del Sòl
Universitat de Lleida

El Co-Director de la Tesi:

Dr. Celso Garcia
Departament de Ciències de la
Terra
Universitat de les Illes Balears

Lleida, 9 de juny de 2005

Note

This file contains papers that have been revised and modified according to the comments made by the referees. Results of the work have not changed after the revisions, although some figures and tables have been redrawn. Papers C4P1 and C4P2 have been assembled into one prior submission to *Geomorphology*.

Als presents: els meus familiars i la Dolors, que han confiat amb la meva feina

Als absents: els meus avis i la Neus, que sempre romandran en el meu record

AGRAÏMENTS

Quan emprens l'aventura de fer el doctorat (o la tesi doctoral) no et pots arribar a imaginar el difícil que és escriure aquest apartat: els agraïments. Són moltes les persones que t'han ajudat a tirar endavant, i ara, com puc expressar-me?

En primer instant vull donar les gràcies a la persona què, sense la seva ajuda i suport, no s'hagués pogut realitzar aquesta tesi. Em refereixo a Ramon J. Batalla, el meu director de tesi. Han estat incomptables les hores que ha passat al meu darrera. Hi havia campanya de camp, no s'ho perdia; feina de laboratori acumulada, allà estava; errors en els càlculs, el perfecte corrector; ..., i com no, necessitava consells, l'ideal assessor. Ah! m'oblidava, articles per corregir o per fer, on estan i quins són?, envia'm l'arxiu original de les dades, de les figures, i del text, ja està sobre la pila - deia. Moltes gràcies Ramon, gràcies de tot cor!

Mallorca ..., quin paradís ..., les contrades on resideix Cels Garcia. Cels ha estat un excel·lent co-director. El seu suport i coneixements han estat claus per poder tirar endavant el treball, especialment pel que fa al disseny de les campanyes granulomètriques, sí, el que alguns anomenen *comptar pedretes*, i al posterior anàlisi i interpretació de les dades. Aquest treball conjunt ha fet possible escriure alguns dels articles fonamentals de la tesi que, sens dubte, contribuiran a difondre la recerca del tram baix del riu Ebre. Moltes gràcies Cels!

La persona que ha conviscut més i més hores amb mi durant la realització de la tesi ha estat l'Albert Rovira. Quin home!, l'Albert ha col·laborat amb el treball de camp i el de laboratori, i com no, ens ha farcit de grans idees. Moltes gràcies *piltra*! En relació directa amb l'Albert la vaig conèixer, gràcies Mariona per la teva ajuda! Gràcies nois per fer-me un forat al vostre *niu*!

Són diverses les institucions i empreses que han possibilitat la meva feina i a les quals ells vull agrair el suport i col·laboració: Ministerio de Educación Cultura y Deporte, ENDESA (gràcies a l'Antoni Palau), Confederació Hidrogràfica de l'Ebre (incloent-hi el SAIH), Ajuntament de Móra d'Ebre, Consell Comarcal de la Ribera d'Ebre, Policia Local de Móra d'Ebre, Mossos d'Esquadra, Servei Català del Trànsit, Guàrdia Civil (incloent-hi els submarinistes), i COPISA.

Durant la realització de campanyes de camp he rebut molts ajuts, tant en el mostreig de sediment des de dalt dels ponts amb aquells aparells tant estranys que algú ha arribat a pensar

que serveixen per pescar silurs, com en les reconstruccions de les seccions aigües avall de l'embassament de Flix, el que podríem anomenar com els *passeigs amb barca*. Tal i com es sol dir, 'la primera vegada mai s'oblida': el Joan, el Ramon, l'Albert i el Will, varen ser presents en la primera campanya de camp al tram baix del riu Ebre. Campanya d'aproximadament dues setmanes en la que es van garbellar i pesar 1,2 tones de graves, i mesurar 4.600 partícules. Quina gran ajuda!, quina calor!, ..., gràcies nois! També dono les gràcies a la resta d'*ajudants*: Joan Manuel, Laura, Benja, Dolors, M. Alba, Tània, Pere, Matt, Carles, Óscar, i Núria. De la mateixa manera, a totes aquelles persones que s'han esperat en el bell mig del trajecte Roquetes-Lleida a què agafés mostres de sediment en suspensió: gràcies Anna, Laia, Dolors, ... Vull donar les gràcies en particular a una persona que va restar perduda durant molt temps cercant el pont de Sástago degut a un error meu, gràcies al Carles Balasch!, gràcies per la teva cerca i pel teu gran interès en el meu treball durant el transcurs de la tesi. De la mateixa manera, la feina de camp no s'hauria pogut realitzar sense una bona logística. Donar les gràcies al *catering*, gràcies mama i papa!; agrair els esforços dels meus germans per solucionar tot tipus de problemes, gràcies germanets!; i també a l'empresa TMC per modificar aparells, fer puntades de soldadura aquí i allí ... Darrera del treball de camp sempre que ha fet falta he tingut un gran equip de transportistes: papa, Benjamín, i Toni, moltes gràcies! I com no, la gran infrastructura facilitada per emmagatzemar el material: els papes i padrins, el meu germà Narcis, la família Cuevas-Sànchez, l'Ajuntament de Móra d'Ebre, i el Ramon, han fet veure que tot el material que he deixat en els seus garatges, *muntanyes*, escales, ..., no molestava, moltes gràcies!, i perdoneu per les molèsties.

També vull donar les gràcies a tots els professors que van facilitar-me la realització d'estades de recerca: Peter Ergenzinger (Freie Uniersität Berlin, Alemanya), Alan Werritty (University of Dundee, Escòcia, UK), Helmut Habersack (Universität für Bodenkultur, Àustria), Cels Garcia (Universitat de les Illes Balears, Espanya), Michael Church i Marwan Hassan (University of British Columbia, Canadà). Són llocs en els que he deixat amics que sempre els tindré presents, gràcies nois! Són indrets on m'he atipat de dolços gràcies als subministraments a llarga distància de Maribel, Llorenç, Joan, Narcis, Toni, Montse i Ares. També agrair a les persones que m'han visitat i que m'han fet passar uns magnífics dies, gràcies Carme (la meva cosineta, per cert, gràcies pels incomptables *xats*), Salvador, Dolors, Albert, Ramon, Cels, Maria, i Eli.

No vull oblidar-me de la gent que m'ha envoltat en l'entorn de la Universitat de Lleida. Donar les gràcies a tot el Departament de Medi Ambient i Ciències del Sòl. Gràcies Joan Ignasi, Manel i Pedro per deixar-me ubicar la segona residència al Laboratori d'Agrometeorologia i Energia Solar durant el transcurs de la tesi. No vull oblidar-me de la gent que ha treballat i encara treballa en aquest laboratori: Elisenda, Cristina, Xavi, Dani, Jordi, Jérôme, Toni i Eva. De manera especial donar les gràcies a una *gran persona*: gràcies Eli! Crec que és millor utilitzar una de les teves frases: 'gràcies pel teu suport científic però, sobretot gràcies per la teva gran amistat'. No s'ha d'oblidar la secretària del departament, és impossible d'oblidar la Clara, gràcies per tot! per tota la paperassa, gestions, ... que t'he demanat i que tant amablement has realitzat.

Gràcies a tots els *traficants de papers*, els quals han estat clau per a la meva formació: Ramon, Cels, Carles, Albert, Xavier, i Joan.

Donar les gràcies a totes aquelles persones que han suggerit canvis o retocs en el primer esborrany de tesi: Maria Sala, Alan Werritty, Phil Owens, Des Walling, i Carles Balasch. De la mateixa manera, a tots aquells que han fet millorar la presentació d'aquesta: Pedro J. Pérez, Carles Balasch, Josep M. Villar, José A. Martínez, Rosa M. Poch, i Ildefons Pla. Finalment, agraeixo al conjunt de membres del tribunal l'interès mostrat per aquest treball i la seva col·laboració per a què hagi arribat al final.

No queda gaire bé però, quan us hi trobeu ho entendreu. Dono les gràcies a tots els que m'he pogut oblidar en aquest document sense ser-ho, en cap dels casos, per voluntat pròpia.

Per últim, donar les gràcies d'una manera especial als meus pares i a la Dolors Cuevas. Tot i que és difícil entendre que fa un fill tantes hores al mig del riu, davant de l'ordinador, i tant de temps a l'estranger, crec que ells ho han comprès: fer allò en el que creu i li agrada, gràcies pares! La Dolors és la persona que ha vetllat per a què no se m'esgotin les forces durant el transcurs de la tesi, la persona que m'ha ajudat en els moments difícils molt lluny de casa, la persona que ho ha donat tot per mi, la persona que sap tant de l'Ebre com jo degut als meus inacabables comentaris, la persona que mai oblidaré ..., la persona què degut al seu retorn des de Vancouver (Canadà) a Catalunya el 7 d'octubre de 2004 em va donar l'empenta per tirar endavant una dura i important estada a l'estranger. Gràcies amor meu!

INDEX

ANNEXES

Summary

The sediment transport and the associated fluvial processes have been analysed in the large impounded lower Ebro River during two representative hydrological years (2002-2004). Sediment transport, including both suspended and bedload, have been measured upstream and downstream the Mequinenza-Riba-roja-Flix reservoirs chain. Fluvial adjustments have been monitored downstream from the Flix Dam. Results indicate that the mean annual total load upstream from the dams is estimated at $1.64 \cdot 10^6$ tonnes, of which more than 99% is transported in suspension. The mean annual total load below the dams is estimated at $0.45 \cdot 10^6$ tonnes, of which 60% is transported in suspension and 40% as bedload. Reservoirs retain up to 95% of fine sediments transported by the river. Total load represents 3% of what was transported at the beginning of the 20th century in the absence of dams. Nowadays, sediment load downstream from the dams is almost all entrained from the riverbed, causing a mean riverbed incision of 30 mm per year. Sediment transport was particularly high during floods. Around 1,700,000 tonnes were transported upstream from the dams during the February and March 2003 floods (Q_{10} with a peak discharge of 2,600 m^3/s), with mean suspended sediment concentrations of 0.5 g/l and mean bedload rates of 100 g/ms. Bedload represented approximately 1.5% of the total load. In contrast, 175,000 tonnes were transported at the downstream monitoring section, with mean suspended sediment concentrations of 0.05 g/l and mean bedload rates of 150 g/ms, showing a high degree of temporal and spatial variability. Bedload represented approximately half of the total load. The grain-size distribution of the riverbed materials has shown to be strongly related to flow competence and sediment availability. On one side, high competent discharges during 2002-2003 were able to entrain most coarse surface material (i.e., armour layer), increasing the availability of sediment to be transported (subsurface material), causing remarkable incision. On the other, discharges during 2003-2004 were not competent to move coarse particles and a re-armouring process occurred. Both years, including five natural floods and two flushing flows, have shown a complete incision-armouring cycle. River-channel adjustments during the second half of the 20th century include the loss of active sedimentary areas, hence sediment availability, due to vegetation encroachment (i.e. riparian forest), and channel narrowing (20%), thus reducing the active section of the channel. The lack of sediment transport and the reduction of frequent floods below the dams control the medium and long-term changes observed in river's channel morphology.

Key words: sediment transport, river morphology, regulated river, grain-size distribution, Ebro River

Resum

Aquesta tesi estudia el transport de sediment i els processos fluvials associats al tram baix del riu Ebre al llarg de dos anys hidrològicament mitjans (2002-2004). El transport de sediment, que inclou tant la càrrega de fons com el sediment en suspensió, s'ha mesurat aigües amunt i avall del complex d'embassaments Mequinenza-Riba-roja-Flix. Els canvis morfològics i granulomètrics s'han analitzat aigües avall de la presa de Flix. La càrrega mitjana anual de sediment aigües amunt de les preses és de $1{,}64 \cdot 10^6$ tones, de les quals un 99% ho són en suspensió. El transport mig anual aigües avall dels embassaments és de $0{,}45 \cdot 10^6$ tones (60% en suspensió i 40% com a càrrega de fons). Els embassaments retenen al voltant del 95% de la càrrega transportada en suspensió. El transport mitjà anual aigües avall de la presa de Flix representa el 3% del que el riu transportava a l'inici del segle XX en absència d'embassaments. La major part del sediment que el riu transporta actualment prové, per tant, de la pròpia llera, fet que causa una incisió mitjana anual d'uns 30 mm. Una part molt important de la càrrega transportada anualment es produeix durant avingudes d'alta magnitud. Per exemple, el transport aigües amunt de les preses durant les crescudes de febrer i març de 2003 (Q_{10}, 2.600 m^3/s) va ser de 1.700.000 tones de sediment. La concentració mitjana de sediment en suspensió durant aquests episodis va ser de 0,5 g/l i la taxa mitjana de càrrega de fons de 100 g/ms. El sediment transportat com a càrrega de fons va representar un 1,5% del total del sediment transportat. Aigües avall de la presa de Flix el riu va transportar 175.000 tones de sediment durant les mateixes crescudes, la meitat com a càrrega de fons. La concentració mitjana de sediment en suspensió fou de 0,05 g/l i la taxa mitjana de càrrega de fons va ser de 150 g/ms. Ambdós modes de transport tenen una gran variabilitat temporal i espacial. La distribució granulomètrica del material del llit està directament controlada per la competència del flux i per la disponibilitat de sediment. Les crescudes d'alta magnitud de 2002-2003 van mobilitzar la cuirassa superficial, incrementant la disponibilitat de sediment (material subsuperficial) i causant una notable incisió de la llera. Contràriament, durant el 2003-2004 el cabal no fou suficientment competent per mobilitzar les fraccions més grolleres i, conseqüentment, el procés dominat fou el de re-acuirassament del llit del riu. Ambdós anys mostren un cicle complert de incisió-acuirassament. Els canvis en la morfologia fluvial aigües avall de la presa de Flix durant la segona meitat del segle XX mostren la pèrdua d'àrees sedimentàries actives (disponibilitat de sediment) degut a la colonització per la vegetació de ribera, i la disminució de l'amplada de la llera (20%), reduint, conseqüentment, la secció activa d'aquesta. La manca de sediment i la reducció de les crescudes controlen els canvis en la morfologia fluvial a mig i llarg termini.

Paraules clau: transport de sediment, morfologia fluvial, riu regulat, distribució granulomètrica, riu Ebre

Resumen

Esta tesis estudia el transporte de sedimento y los procesos fluviales asociados en el tramo bajo del río Ebro durante dos años hidrológicamente medios (2002-2004). El transporte de sedimento, que incluye tanto la carga de fondo como el sedimento en suspensión, se ha muestreado aguas arriba y abajo del complejo de embalses Mequinenza-Ribarroja-Flix. Los cambios morfológicos y granulométricos se han analizado aguas abajo de la presa de Flix. La carga media anual de sedimento aguas arriba de las presas es de $1{,}64 \cdot 10^6$ toneladas, de las cuales un 99% lo son en suspensión. El transporte medio anual aguas abajo de los embalses es de $0{,}45 \cdot 10^6$ toneladas (60% en suspensión y 40% como carga de fondo). Los embalses retienen alrededor del 95% de la carga en suspensión. El transporte medio anual aguas abajo de la presa de Flix representa el 3% de lo que el río transportaba al principio del siglo XX en ausencia d'embalses. La mayor parte del sedimento que el río transporta actualmente proviene, por lo tanto, del propio cauce, hecho que causa una incisión media anual de 30 mm. Una parte muy importante de la carga transportada anualmente lo es durante avenidas de alta magnitud. Por ejemplo, el transporte aguas arriba de las presas durante las crecidas de febrero y marzo de 2003 (Q_{10}, 2.600 m^3/s) fue de 1.700.000 toneladas de sedimento. La concentración media de sedimento en suspensión durante estos episodios fue de 0,5 g/l y la tasa media de carga de fondo de 100 g/ms. El sedimento transportado como carga de fondo representó un 1,5% del total del sedimento transportado. Aguas abajo de la presa de Flix el río transportó 175.000 toneladas de sedimento durante las mismas crecidas, la mitad como carga de fondo. La concentración media de sedimento en suspensión fue de 0,05 g/l y la tasa media de carga de fondo fue de 150 g/ms. Ambos modos de transporte tienen una gran variabilidad temporal y espacial. La distribución granulométrica del material del lecho está directamente controlada por la competencia del flujo y por la disponibilidad de sedimento. Las crecidas de alta magnitud de 2002-2003 movilizaron la coraza superficial, incrementando la disponibilidad de sedimento (material subsuperficial) y causando una notable incisión del cauce. Contrariamente, durante 2003-2004 el caudal no fue suficientemente competente para movilizar las fracciones más gruesas y, consecuentemente, el proceso dominante fue el de re-acorazamiento del lecho del río. Ambos años muestran un ciclo completo de incisión- acorazamiento. Los cambios en la morfología fluvial aguas abajo de la presa de Flix durante la segunda mitad del siglo XX muestran la pérdida de áreas sedimentarias activas (disponibilidad de sedimento) debido a la colonización por vegetación de ribera, y la disminución de la anchura del cauce (20%), reduciendo, como consecuencia, la sección activa. La falta de sedimento y la reducción de las crecidas controlan los cambios en la morfología fluvial a medio y largo plazo.

Palabras clave: transporte de sedimento, morfología fluvial, río regulado, distribución granulométrica, río Ebro

CHAPTER 1
INTRODUCTION

INDEX CHAPTER 1: INTRODUCTION

Figure captions (figures in the paper not included)

Figure 1.1. Classification of the effects on dammed rivers (after Petts, 1987)

Figure 1.2. The Ebro Basin in the Iberian Peninsula. Water divides, drainage network and main dams and cities are indicated

Figure 1.3. Distribution of the main lithologic units of the Ebro Depression

Figure 1.4. Irregular and turtuous meanders in the Ebro River near Escatrón. Flow direction is from left to right

Figure 1.5. Annual rainfall and runoff in the Ebro Basin during the 2002-2003 hydrological year

Figure 1.6. Annual rainfall and runoff in the Ebro Basin during the 2003-2004 hydrological year

Figure 1.7. Reservoir construction and capacity in the Ebro Basin during the twentieth century

Figure 1.8. Monthly flood frequency during pre and post-dams periods

Figure 1.9. (a) Mean monthly discharge in the Guadalope River (EA99) during pre (1973-1991) and post (1992-1995) dams periods. (b) Mean monthly discharge in the Ebro River (EA27) during pre (1913-1974) and post (1975-2002) dams periods

Figure 1.10. (**a**) The lower Ebro River: tributaries, dams and villages. Note than Sástago and Móra d'Ebre (underline villages) conform the study reach in this research. (**b**) Morphostructural units downstream Flix Dam. Note than Ribar-roja and Flix dams are plotted as a reference elements in the diagram.

Figure 1.11. Mean monthly discharges at Tortosa gauging station (n.27). Note than percentages on top of the bars represent the monthly percentage in the mean annual runoff

Figure captions in the paper

Figure 1 (**C**hapter **1** **P**aper **1**). Downstream effects of dams on a river sediment budget. (A) Equilibrium in absence of dams and (B) Changes in the sediment transfer: retention in dams and downstream erosion. Both stages show the relation between sediment input (E), sediment output (S) and volume of sediment stored in the channel. Non-temporal sequence illustrates the initial situation with a tendency to aggradation (V1) and the subsequent situation showing incision (V2)

Figure 2 (C1P1). Location of the study area in the Ebro basin (Iberian Peninsula)

Figure 3 (C1P1). Cross section of the Ebro River in Tortosa

Figure 4 (C1P1). Maximum daily discharge in the Lower Ebro (Tortosa, EA27) before and after 1975, including the historical floods of 1907 and 1937 (Novoa, 1984)

Figure 5 (C1P1). Mean discharge and river bedload capacity of the Ebro in Tortosa estimated by means of the Schoklitsh (1950) and Engelund y Hansen (1967) formulae. Full lines indicate mean pre-dam values and dotted lines indicate mean post-dam values

Figure 6 (C1P1). Changes in the Ebro River sediment budget. Sediment input from tributaries is not taken into account. Estimation are based on the assumption that 10% of sediment captured by Mequinenza y Ribarroja dams (Avendaño et al., 1997) is bedload. Downstream transfers are estimations using formulae (E: imput, ΔV:change of volume and S: output). (A) Equilibrium in absence of dams and (B) Changes in the sediment transfer downstream Flix dam

Figure 7 (C1P1). Colonization by vegetation of an active bar in the vicinity of Móra d'Ebre between 1956 and 1995 (air photos: Ejército del Aire 1956 and Institut Cartogràfic de Catalunya (ICC) 1995). Nowadays bar is completely covered by vegetation

Figure 8 (C1P1). Changes in the fluvial pattern downstream Móra d'Ebre (air photos: Ejército del Aire 1956 and ICC 1995)

Figure 9 (C1P1). (A) Colonization of the active channel by riverinne vegetation and reduction of channel width downstream Benissanet and (B) Lateral erosion in the vicinity of Ascó

Table captions (tables in the paper not included)

Table captions in the paper

Table 1 (C1P1). Recurrence intervals for the Lower Ebro before and after 1975, using official flow series and including historical floods of 1907 and 1937

Table 2 (C1P1). Bedload yield (t/y) in the Lower Ebro before and after 1975 from Schoklitsch (1950) and Engelund and Hansen (1967)

1. INTRODUCTION

1.1. State of the art

1.1.1. Transference of water and sediment in rivers

Rivers are basically agents of erosion and transportation, transferring water and sediment supplied to them to seas and oceans (Knighton, 1998). Therefore, they carry water and sediment continuously from headwaters to deposition zones, being responsible for the equilibrium between fluvial and marine processes on beaches and in delta regions.

Only the 0.005 percent of the continental water is stored in rivers, but in terms of their ability to do work (i.e., energy) are the most potent forces operating on the Earth's surface (Knighton, 1998). Overall the world, rivers transport about 19,000 million tonnes of material each year, the 80 per cent as a solid load (i.e., particles transported by the flow), and the 20 percent as a dissolved load (i.e., material transported in solution) (Meybeck, 1987; Millimam and Meade, 1983; Milliman and Syvitski, 1992; Walling and Webb, 1993). Within this context, the movement of water and sediment over the channel and its floodplain is principally the fact that controls its morphology and, consequently, its ecology.

Schumm (1977) divided a river system in three zones according to the sediment and water dynamics. The headwaters are the main source of water and sediment. The main trend of the middle zone is the transfer of water and sediment by mainstems rivers to downstream reaches, while the lowermost zone correspond to the deposition reaches (e.g., deltas). Thus, a mainstem river channel can be seen as a conveyor belt that transports the erosional products downstream to the ultimate depositional sites below sea level (Kondolf, 1997), maintaining its alluvial channel morphology in dynamic quasi-equilibrium, where sediment exported from a specified reach is roughly equal to the supply from upstream reaches (Williams and Wolman, 1984). Dams disturb the continuity of water and sediment to downstream reaches, generating economic and ecological consequences to downstream fluvial and coastline ecosystems.

1.1.2. Effects of dams on fluvial dynamics

Dams interrupt the continuity of water and sediment transfer from upstream reaches along fluvial channels, causing damages of different degree to downstream ecosystems. In most of the cases dams are built to provide water (e.g., agriculture uses), to generate hydropower, and to minimize the risk of flooding overall downstream sections. By the end of the twentieth century there were over 45,000 large dams (i.e., reservoirs with a capacity higher than 3 hm^3, where 1 $hm^3 = 1 \cdot 10^6$ m^3) in over 140 countries, where a worldwide average between 160 to 320 new large dams per year has been estimated. The top five dam-building countries (China, United States, India, Spain and Japan) account for the 80% of large dams worldwide. In particular, Spain owns more than 1,000 dams (2.5% of word dams proportion) (World Commission on Dams, 2000).

Several reviews have been done on downstream effects from dams, for example, by Petts (1984), Williams and Wolman (1994), Carling (1998), and Kondolf (1997). Petts (1987) made a classification of the effects on dammed rivers by grouping in orders (see also Brandt, 2000). The first order changes illustrate the transfer that dams allow, being the alterations in water discharge and sediment transport the main effects. Second order changes will be affected or caused by first order changes; changes on channel form, grain size distributions, and aquatic vegetation populations are clear examples. The third order, not solely linked with the second order, where changes are effects in fish and invertebrate populations (rivers' biota components). Therefore, sediment and water transfer from dams to downstream reaches are ones of most important parameters than determines the changes overall the river sections (Figure 1).

Dams alter the downstream flow regime of rivers (Petts, 1984; Williams and Wolman, 1984), which controls many physical and ecological aspects of river forms and processes, including sediment transport and nutrient exchange (Poff *et al.,* 1997). Principal hydrological alterations caused by dams include changes on flood frequency and magnitude, reduction in overall flows, changes in seasonal flows, and altered timing of releases (Table 1.1). Consequently, the sediment transport capacity of flow will be altered due to the changes on flood magnitude.

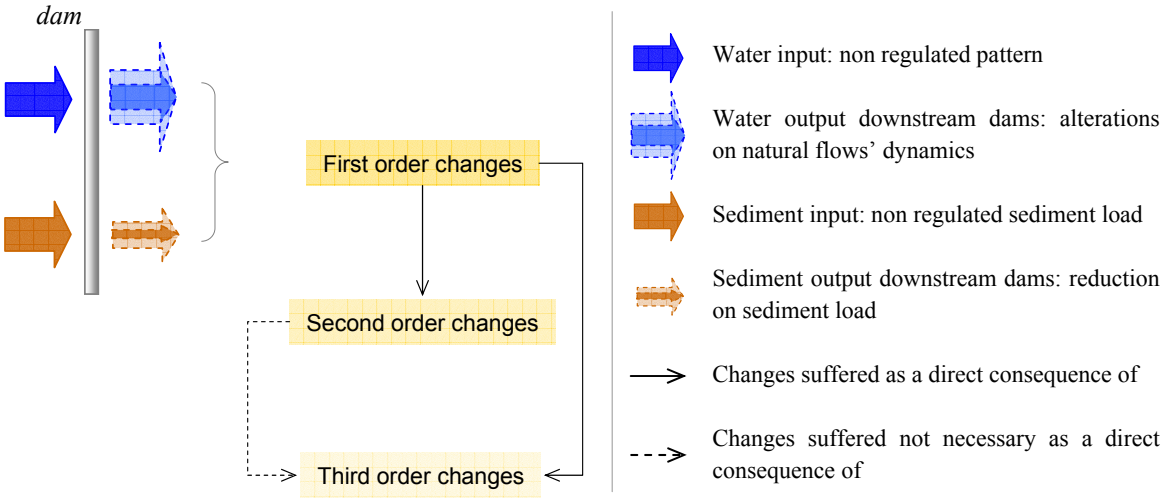

Figure 1.1. Classification of the effects on dammed rivers (after Petts, 1987)

Magnitude of floods can be altered basically in two main ways: a) reduction to a degree in which the energy of the flow still owns capacity to move sediment downstream, and b) peaks dropped by dams' regulation until the boundary in which released flows do not have sufficient competence to do work. Simultaneously, dams disrupt the continuity of sediment transfer in river systems by trapping all bedload and an important part of the suspended load. Under these conditions, changes on sediment budgets downstream dams show two different scenarios:

- Cases in which the exportation of sediment from a river-bed downstream dams is higher than the sediment that is supplied from tributaries. Due to sediment captured in reservoirs the water released becomes starved or *hungry water* (Kondolf, 1997) and main effects are: a) degradation of the fluvial and deltaic ecosystem, b) river bed degradation (e.g., riverbank instability and damage to bridges), c) changes in channel morphology, and d) propagation of riparian vegetation (Table 1.1).
- Cases in which floods do not have sufficient competence to transport sediment from incoming tributaries or other sources, the river bed suffers sedimentation, where the principal effect is the river bed aggradation, and consequently, important changes on biotic components (Table 1.1).

Table 1.1. Main effects of dams on fluvial systems

Order change [1]	Downstream effects from dams [2]	References [3]
First		
	- changes on river regime	- Batalla *et al.* (2004)
	- changes on flows' patterns	- Assani and Petit (2004)
	- reduction of sediment load	- Chen *et al.* (2001)
Second		
	- river bed degradation	- Surian and Rinaldi (2003)
	- river bed aggradation	- Phillips *et al.* (2004)
	- changes on channel morphology	- Grans and Schmidt (2002)
	- changes in aquatic vegetation	- Goes (2002)
	- changes on river-margin vegetation	- Jansson *et al.* (2000)
	- erosion of deltas and beaches	- Vörösmarty *et al.* (2003)
Third		
	- changes in biotic components	- Belaud and Carette (2004)

[1] Petts's (1987) classification, effects on impounded rivers by orders (see figure 1)
[2] Main effects reported on different studies grouped by the Petts's (1987) classification
[3] Only the most recent references are cited

Under such conditions, different management and ecological restoration efforts to compensate the alterations on sediment budgets downstream from dams are conducted in some rivers (e.g., flow releases on Kondolf, 1997). However, the high costs of those operations prevent a general application (e.g., Inman, 1976).

1.2. Objectives and structure

The lack of studies analysing direct effects of dams on fluvial dynamics in largely impounded rivers was the starting point to carry out this research in the lower Ebro River (NE Iberian Peninsula). The study of the sediment transport upstream and downstream dams under different flow conditions, together with the analysis of the effects of dams on rivers are key-elements to define and implement river restoration programs in large dammed rivers as such the Ebro. Within this framework, the objectives of the thesis are:

1. To measure and analyse the **sediment transport** in a highly regulated fluvial system. Sediment transport both suspended and bedload were measured and the **sediment budget** estimated at two monitoring sections upstream and downstream from the largest complex of dams in the Ebro Basin during the period 2002-2004.
2. To study and assesses changes on **river morphology** due to the alterations on sediment supply and water discharge below the dams. Several sections were monitored in active areas (i.e., river bars) downstream from the dams. Sediment processes were observed after floods during the period 2002-2004.

According to the possibility given by the Doctorate Programme of the University of Lleida the thesis is presented in papers format. The document is divided in five chapters containing a total of 8 papers (published, accepted, in press or submitted) (Table 1.2). Each chapter has an introduction in which specific objectives are explained. **Chapter 1** gives a general view in of the changes on fluvial dynamics caused by dams, and describes briefly the Ebro Basin and the study reach, the lower Ebro River. In addition all the papers contain a description of the study reach. **Chapter 2** has the following objectives: a) to describe the fieldwork, b) to describe and discuss the use of bedload samplers in relation to the river-bed material, and c) to assess the temporal and spatial bedload variability as a source of possible bias on annual sediment transport computations. **Chapter 3** describes the sediment transport of the lower Ebro at two different scales: a) during floods and b) on annual scale. **Chapter 4** assesses the changes on river-channel and on river-bed material as a response to the fluvial processes mainly upstream (lack of) sediment supply and downstream sediment transport (reported in chapter 3). Finally, **chapter 5** presents the general discussions and conclusions of the thesis.

Table 1.2. Scheme of the thesis and associated papers

Chapter	Paper (title key words)	Status
1. Introduction	- Bedload, floods, river morphology	- published
2. Methods	- Helley-Smith samplers, sampling bias	- accepted
	- Bedload transport, grain-size, gravel-bed river	- in press
3. Sediment transport and budget	- Sediment transport, river-bed degradation	- published
	- Sediment load, Mediterranean river	- accepted
4. Fluvial adjustments	- Bedload transport, bed material, armouring	- to be submitted
	- River-bed armouring, low floods	- to be submitted
	- Flow regulation, sediment availability, river morphology	- submitted
5. Discussion and conclusions		

2. THE EBRO BASIN

2.1. The catchment

2.1.1. Physical characteristics

The Ebro Basin drains an area of approximately 85,530 km^2 and is located in the north-eastern part of the Iberian Peninsula. Water divides are the southern-facing slopes of the Cantabrian Range and the Pyrenees in the northern part of the basin, the northern-facing slopes of the Iberian Massif in its southern part, and the Catalan Coastal Ranges (i.e., Catalanids) in its south-east (Figure 1.2). The Ebro mainstream drains the sedimentary Depression.

The Ebro Depression is a first order morphostructural unit in the Iberian Peninsula (i.e., geological unit in what structures produced under the same tectonic frame dominate). It forms the foreland of the Pyrenees, having both units a parallel evolution during their development in the Tertiary. The infilling of the Ebro Depression occurred during the orogenic movements between the Cretaceous and the Neogen. The process can be divided into two main stages: a) sea transgressions from the Atlantic (north-west of the

Depression) produced during the Lower and the Upper Eocen, and b) endorreic continental stage in which geological environments were characterized by sedimentation (Oligocen-Miocen), during that period the Depression remained closed to sea transgressions. From the Middle Miocen the Ebro Depression began to drain to the Mediterranean (Enciclopèdia Catalana, 1986).

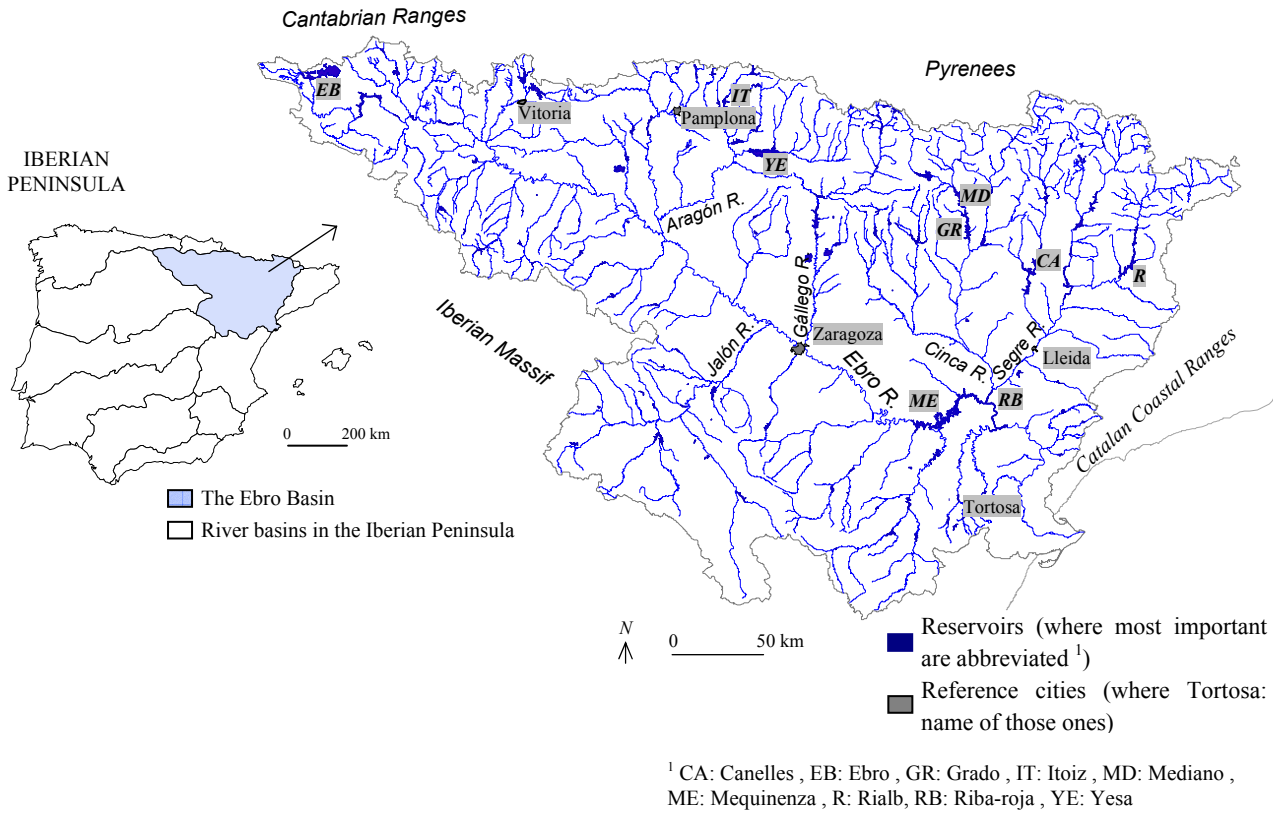

Figure 1.2. The Ebro Basin in the Iberian Peninsula. Water divides, drainage network and main dams and cities are indicated

Figure 1.3 shows the distribution of the main lithologic units of the Ebro Basin. The oldest materials are located in the catchment headwaters, mountain ranges with dominant presence of Paleozoic (e.g., granitoids and metamorphic rocks) and Mesozoics rocks. Central part of the basin is dominated by Tertiary sedimentary materials (i.e., limestones, gypsum, sandstone, clayrocks and conglomerates), where the dominant units are the distals molasses. The lithologic formations get progressively more modern to the west, showing the movement of the basin depocenter to that direction.

The Ebro River flows as a single-thread channel through the central section of the Depression. Mean channel slope is $9 \cdot 10^{-4}$. Channel length (L_r) is 908 km, while the straight-line valley length (L_s) is 580 km. Channel sinuosity, defined as the quotient between L_r and L_s, is 1.6. The Ebro River shows, in most part of its course, a clear meandering pattern (Leopold *et al.* 1964). The degree of meander regularity and the deviation angle between the channel and the downvalley axis can be used as an additional criterion for the channel classification as meandering (e.g., Kellerhals *et al.*, 1976). The Ebro River shows both irregular (i.e., vaguely repeated pattern) and turtuous meanders patterns (i.e., maximum deviation angle >90º) (Figure 1.4).

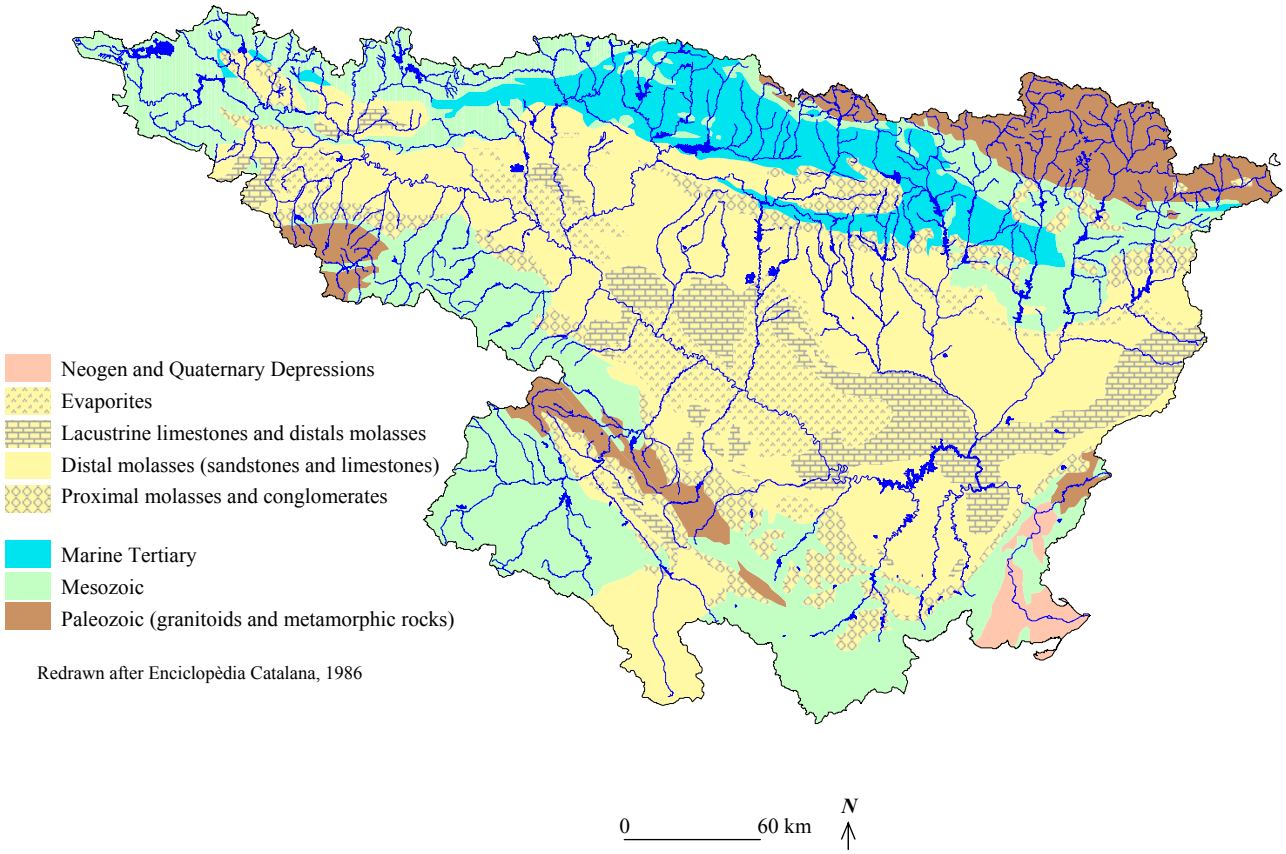

Figure 1.3. Distribution of the main lithologic units of the Ebro Depression

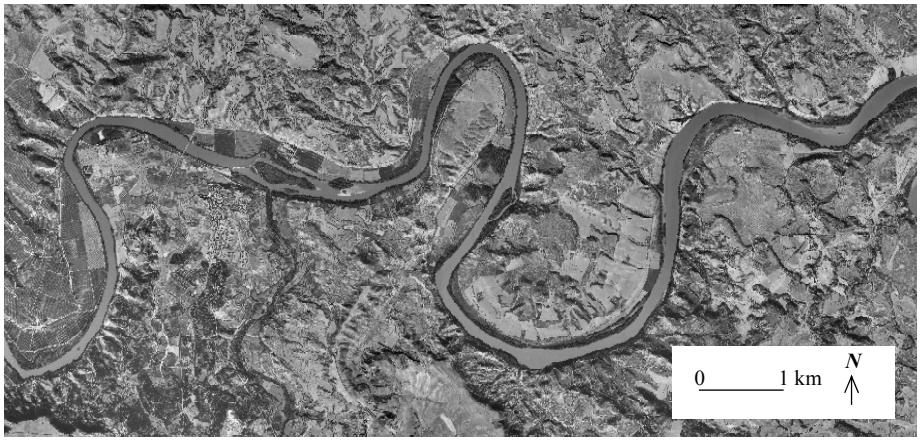

Source: Ebro Water Authorities

Figure 1.4. Irregular and turtuous meanders in the Ebro River near Escatrón. Flow direction is from left to right

Precipitation varies greatly across the basin due to its topographical and climatological heterogenity, and the situation of the Mediterranean Sea and the Atlantic Ocean. Mean annual precipitation ranges from more than 1,500 mm in the mountain ranges (e.g., central Pyrenees) to less than 300 mm in the semi-arid interior. Accordingly the mean annual precipitation can be used to divide the Ebro Basin into four main climatic areas: a) the Atlantic headwaters, with mean annual precipitation of about 900 mm, b) the west-central Pyrenees with about 950 mm, c) the eastern Pyrenees with about 800 mm and d) the southern Mediterranean zone with 500 mm. Mean weighted annual precipitation in the whole of the Ebro Basin during the study years was 590 and 600 mm in 2002-2003 (Figure 1.5) and 2003-2004, respectively (Figure 1.6). Annual data for the different rainfall stations is presented in table 1 in the annex. Annual maximum rainfall was collected in the north sector of the basin (i.e., Cantabrian Ranges and Central Pyrenees) where highest mountains are reached. Annual maximum (>1,800 mm) was recorded in the Beruete rainfall station (Cantabrian Ranges). Minimum values were obtained in the centre of depression (e.g., <240 mm in the Riba-roja Reservoir).

2.1.2. Hydrology and water uses

Annual runoff in the Ebro River (1913-2004) varies across the basin owing to the irregularity of the water supply from the tributaries and as a consequence of the high rainfall variability.

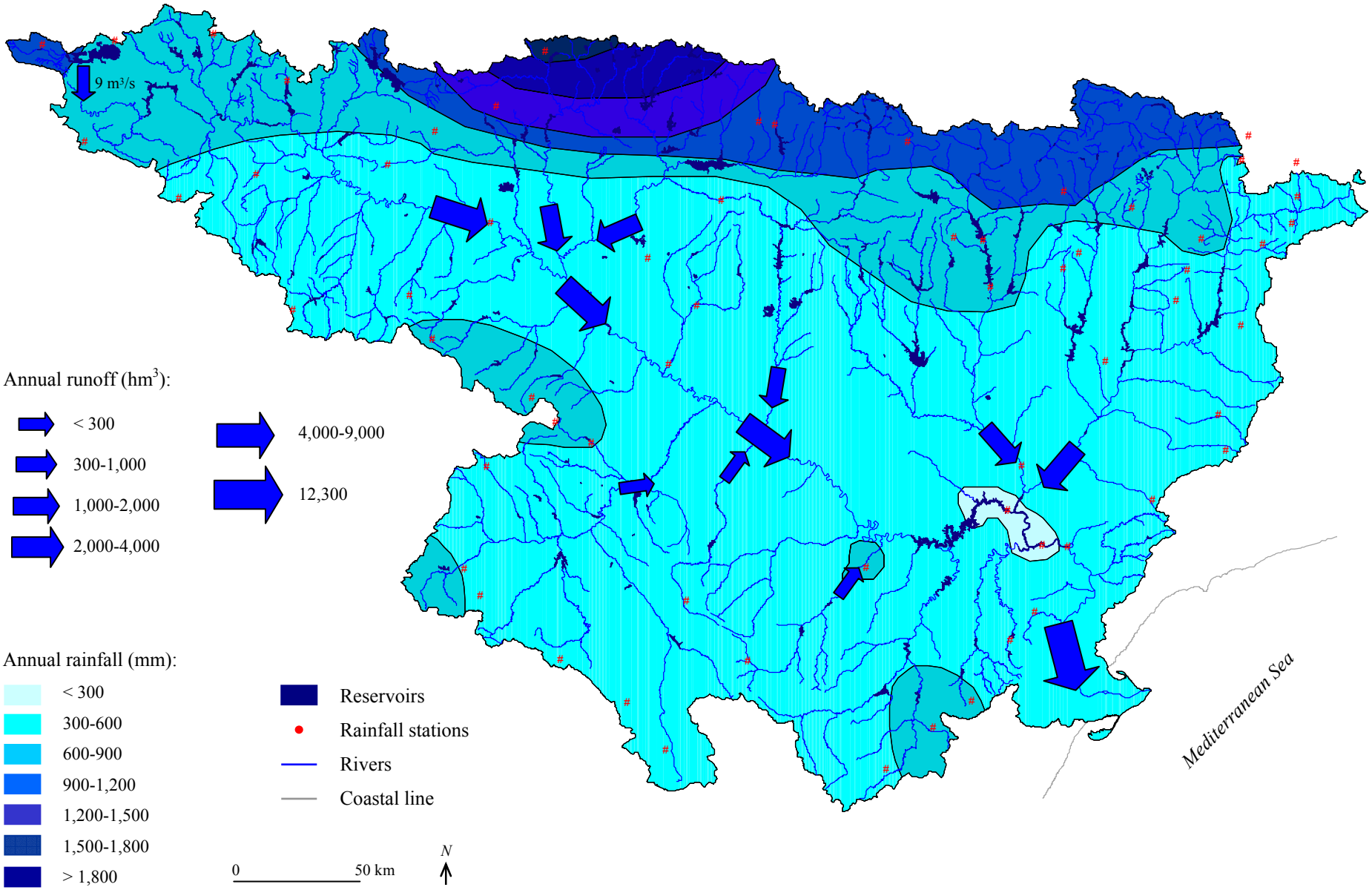

Data source: SAIH, Ebro Water Authorities

Figure 1.5. Annual rainfall and runoff in the Ebro Basin during the 2002-2003 hydrological year

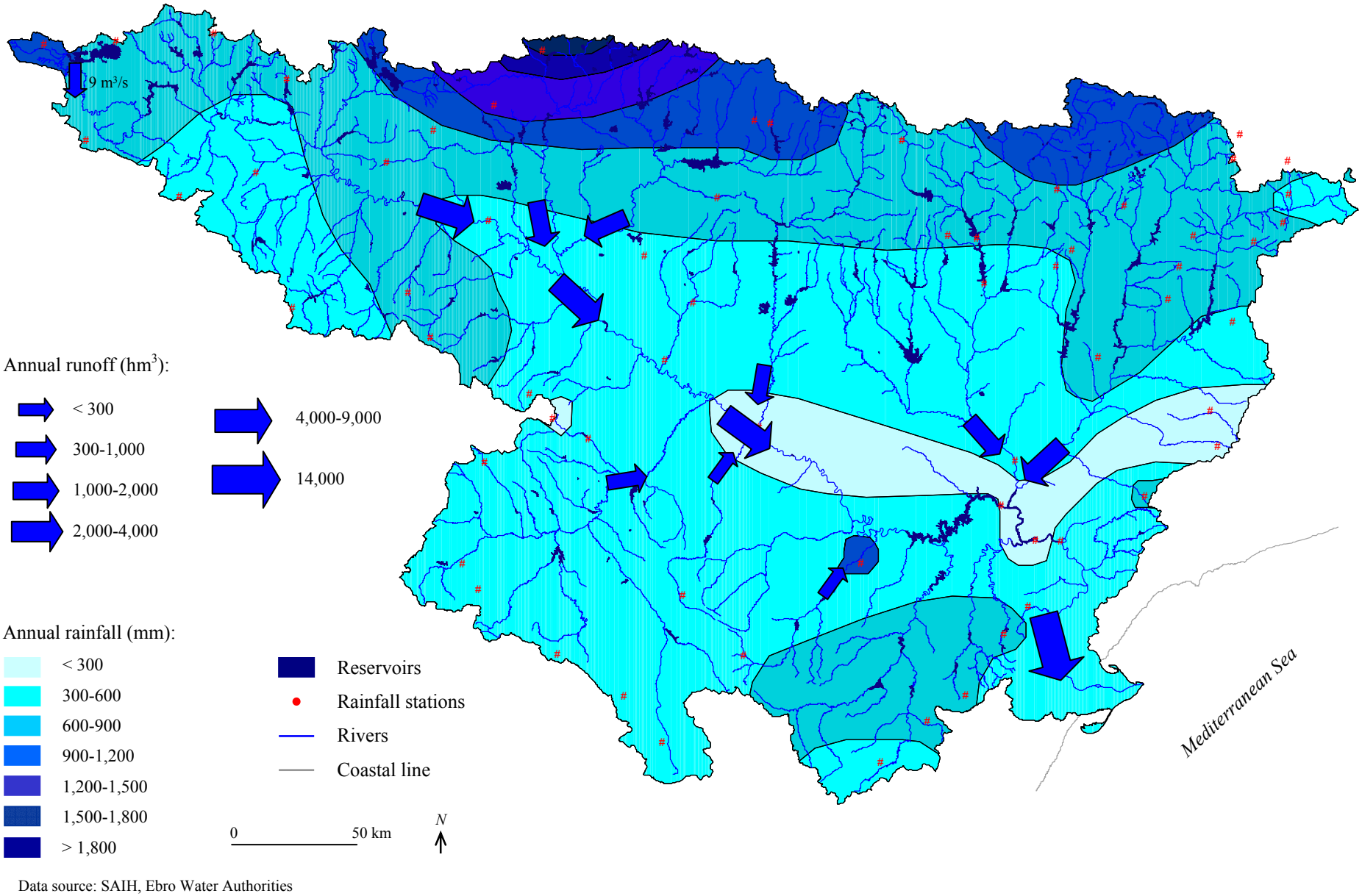

Data source: SAIH, Ebro Water Authorities

Figure 1.6. Annual rainfall and runoff in the Ebro Basin during the 2003-2004 hydrological year

In the Miranda de Ebro gauging station (n.1, located in the Atlantic area) mean annual runoff is around 1,900 hm^3 (60 m^3/s, 346 mm). Further downstream, in Zaragoza (n.11), 335 km downstream from n.1, mean annual runoff is 7,340 hm^3 (233 m^3/s, 179 mm), showing the contribution from large tributaries of the West-Central Pyrenees (e.g., Aragón River). Rivers that drain the Eastern Pyrenees (e.g., Segre River) and the Iberian Massif (e.g., Matarranya River), supply an important volume of water to the lower reaches of the basin. Mean annual runoff in Tortosa (n.27), the lowermost gauging station before the river enters its delta plain, is 14,300 hm^3 (454 m^3/s, 169 mm, and a runoff coefficient of 0.28) (Figure 1.2).

Maximum monthly flow occurs in March, related to snow melt processes. Minimum monthly discharges are recorded in September and January.

Largest estimated flood in the twentieth century succeeded in 1907. Other high magnitude floods occurred in 1937 and 1982 (Table 1.3).

Figure 1.5 and 1.6 also include annual runoff for different gauging stations in the Ebro Basin during both study years (see Table 2 in the annex for data). Maximum discharges recorded during the 2002-2003 hydrological year were higher than those in 2003-2004. For instance, peak flow in the Ebro River in Zaragoza (n.11) was around 3,000 m^3/s in 2002-2003, while maximum discharge only reached 1,200 m^3/s in 2003-2004.

Around 190 dams impound almost 60% of the annual runoff in the Ebro Basin. According to the Ebro Water Authorities, almost 100 of them have a capacity higher than 3 hm^3 (i.e., $1hm^3 = 10^6\ m^3$). Almost, all dams were constructed during the 20^{th} century, with 67% of reservoir capacity built between 1950 and 1975 (Figure 1.7). Most reservoirs are located in the central and the upper reaches of the tributaries at a mean elevation of about 700 meters.

Table 1.3. Main contemporaneous floods in the Ebro River and in its tributaries

River	Gauging station (code)	Year	Peak flow (m^3/s)
Ebro	Tortosa [1]	1907	12,000
Ebro	Zaragoza (n.11)	1937	2,833
Ebro	Miranda de Ebro (n.01)	1938	835
Ebro	Zaragoza (n.11)	1939	3,058
Ebro	Tortosa (n.27)	1960	3,942
Ebro	Castejón (n.02)	1960	4,950
Guadalope	Alcañiz (n.15)	1967	1,002
Ebro	Tortosa (n.27)	1972	6,406
Cinca	Fraga (n.17)	1977	2,587
Aragón	Yesa – CE (n.170)	1977	1,051
Gállego	Santa Eulàlia (n.59)	1979	887
Aragón	Caparroso (n.05)	1979	2,127
Ebro	Zaragoza (n.11)	1982	1,849
Cinca	Fraga (n.17)	1982	2,348
Segre	Seròs (n.25)	1982	3,200 [1]
Ebro	Tortosa (n.27)	1982	3,760
Jalón	Huermeda (n.09)	1986	381
Ebro	Tortosa (n.27)	2000	1,697 [2]
Ebro	Zaragoza (n.11)	2003	2,988
Ebro	Ascó (n.163)	2003	2,602

[1] Maximum peak flow estimated by Novoa (1984)
[2] Maximum daily flow
Data source: Ebro Water Authorities (www.chebro.es)

The Mequinenza Dam, built in 1966, is the largest in the basin with a capacity of 1,534 hm^3. The Ebro Dam in the catchment headwaters was built in 1945 with a capacity of 540 hm^3. The Yesa Dam (446 hm^3) in the Aragon River (Figure 3) was buil in 1959. During the 60s of the twentieth century was built the Canelles Dam in the Noguera Ribagorçana River (tributary that drains the central part of the Pyrenees Mountains) with a capacity of 678 hm^3. The Santa Anna Dam in the Noguera Ribagorçana River was built in 1964 with a capacity of 237 hm^3. The largest large dam was Rialb (402 hm^3) in the Segre River set up in operation in 2000.

Main water uses in the Ebro Basin are hydroelectric generation, irrigation, nuclear power plant refrigeration, industrial demand, urban uses (e.g., potable water), water transfers, and farm needs (Table 1.4).

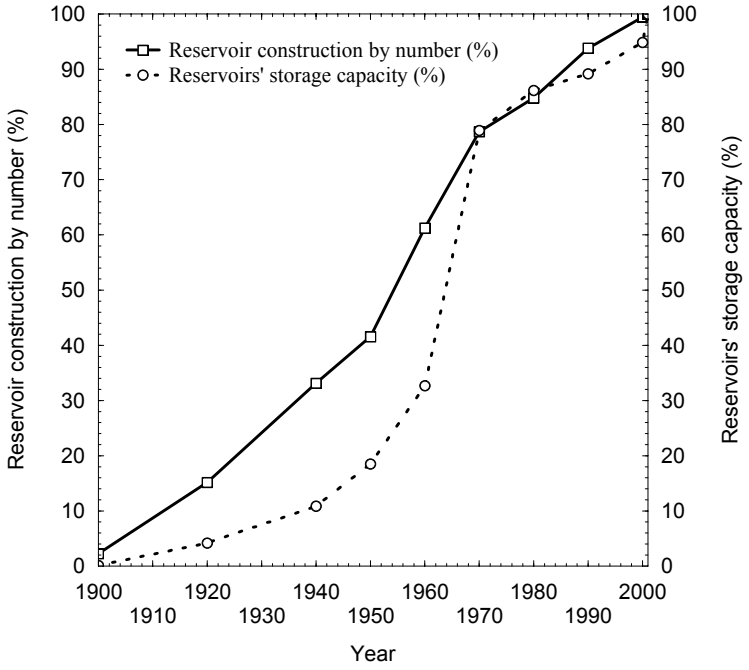

Data source: Ebro Water Authorities (www.chebro.es)

Figure 1.7. Reservoir construction and capacity in the Ebro Basin during the twentieth century

Table 1.4. Theoretical water uses in the Ebro Basin

Water uses	**Annual supply (hm^3)**
Hydroelectric	60,000
Irrigation	6,310
Nuclear	3,354
Industrial	414
Urban	313
Transfers	246
Farm	66

Data source: Ebro Water Authorities (www.chebro.es)

2.1.3. Hydrological and sedimentological alterations due to dams

Reservoirs have produced substantial alterations onto flow regime in many rivers of the Ebro Basin, especially on flood magnitude and monthly flow pattern (Batalla *et al.*, 2004). Twenty-two of the regulated rivers showed reduction in flood magnitude in different degree. For instance, in the Guadalope River downstream from the Santolea Dam, the flood associated with a recurrence interval of 10 years (Q_{10}) have been reduced around 60%, while in the lowermost reach of the Ebro River, in Tortosa, the Q_{10} has been reduced 25%. Flood timing can also be altered as in the Aragón River after the construction of the Yesa Dam (López *et al.*, 2002). Monthly flood frequency has also been altered in different degree in many rivers of the catchment (Figure 1.8). Frequency of floods during November and March has clearly diminished, while in January and June it increased considerable due to dams' operations. The alterations on monthly flows ranged from virtually no change to complete inversion of the seasonal pattern (Figure 1.9a, b).

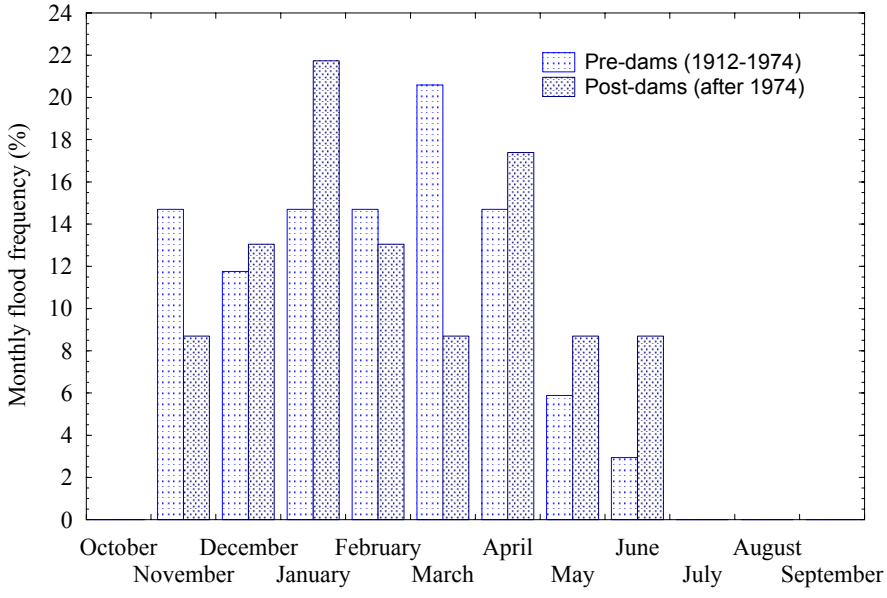

Data source: Ebro Water Authorities

Figure 1.8. Monthly flood frequency during pre and post-dams periods

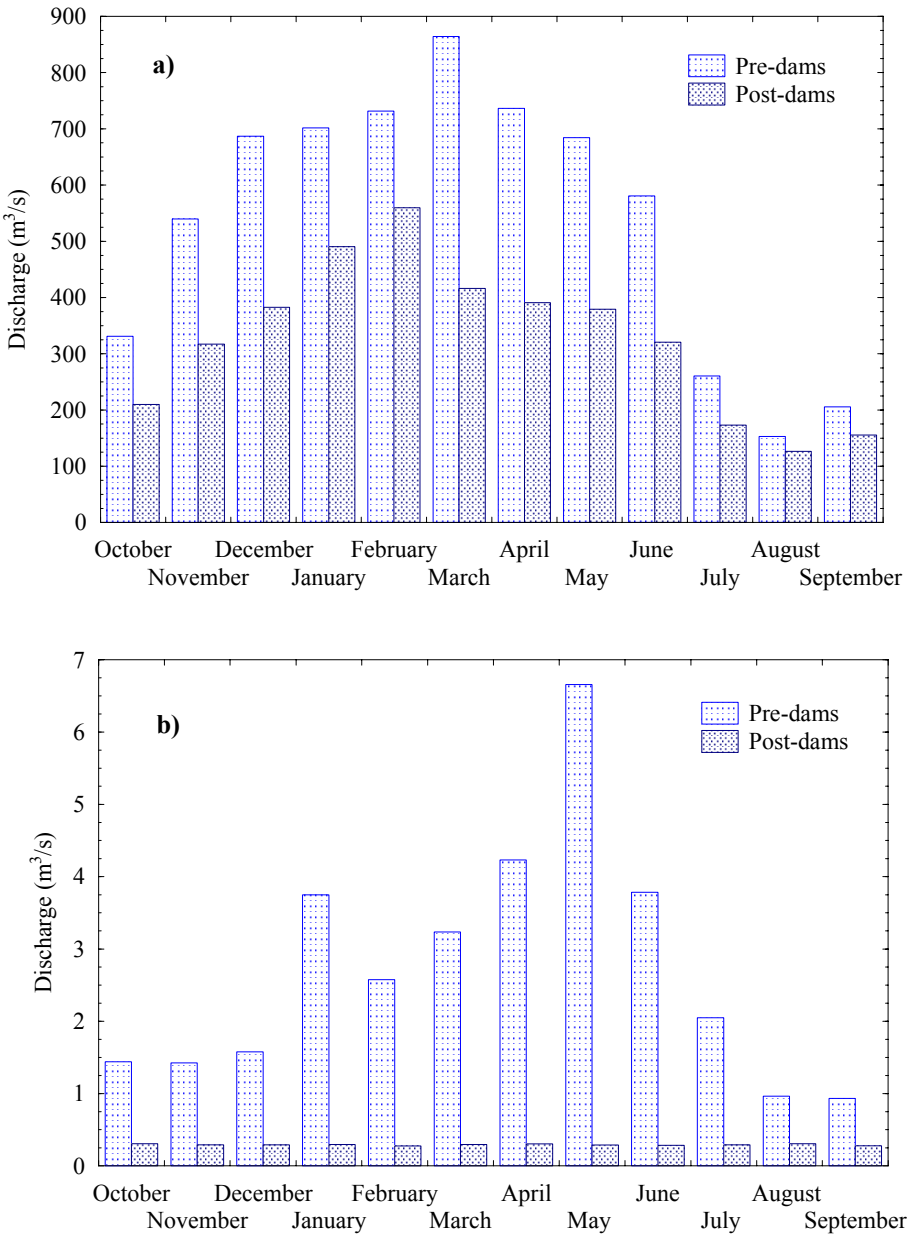

Figure 1.9. (**a**) Mean monthly discharge in the Guadalope River (EA99) during pre (1973-1991) and post (1992-1995) dams periods. (**b**) Mean monthly discharge in the Ebro River (EA27) during pre (1913-1974) and post (1975-2002) dams periods (data source: www.chebro.es)

Dams trap all the sediment moving as bedload (i.e., coarse material) and an important part of the suspended load (i.e., fine material). Sedimentation in reservoirs causes a progressive reduction of dam storage capacity (Avendaño *et al.* 2000), and creates serious problems for water management, especially near dam outlets. Water quality in storage can also be degraded (e.g., eutrophication). Batalla (2003) estimated for the Ebro Basin a mean annual reduction of reservoirs' capacity around 0.2%, giving an estimated total annual

sedimentation of 15 hm^3, which corresponds, approximately, with the annual sediment contribution of the Ebro River to its delta at the beginning of the 20th century (Bayerri, 1934-1935; Nelson, 1990). The same sedimentation rate can be estimated from the data reported by Sanz *et al.* (1999). Sediment retained in reservoirs along the Ebro Basin is composed mainly by silt (62%), clay (25%) and sand (13%) (Sanz, 1998), showing the weight of the suspended load on the sediment yield. Under such conditions, some reservoirs are already full of sediment (e.g., Pignatelli Dam built in 1790 in the Ebro River), and others has a sedimentation problems (e.g., Terradets Dam built in 1935 in the Noguera Pallaressa River).

Different authors have assessed the total annual sediment yield in the Ebro River (Table 1.5). Annual sediment yield in the lowermost reach has suffered a reduction of two orders of magnitude as a consequence, mainly, of the retention of sediment in upstream reaches by dams. The lack of sediment and the reduction of floods magnitude and frequency in the lowermost Ebro River have caused changes in river channel morphology, mainly revegetation of formerly active areas and river-bed armouring (Sanz *et al.,* 1999; Avendaño *et al.,* 2000; Vericat and Batalla, 2004). Moreover, according to Ibáñez *et al.* (1995) the reduction of discharges and the decrement of floods are the main reasons that are causing a progressive water eutrophication and a more permanence of the salt wedge (Sierra *et al.*, 2004), which, nowadays, is extended to 30 km upstream the Ebro's mouth.

2.2. The lower Ebro River

2.2.1. Physical characteristics

We have considered the lower Ebro River as the river reach downstream from Sástago, 2 km upstream from the entering to the Mequinenza Reservoir. Work done in this thesis have been developed between Sástago and Móra d'Ebre, 27 km downstream from the Flix Dam (Figure 1.10a).

Table 1.5. Total annual sediment yield estimated in the lowermost Ebro River

Year	Sediment yield (10^3 t/y)	Reference
1877	30,000 [1]	Gorría (1877) [2]
1900	15,000 [1, 3]	Bayerri (1934-1935), Nelson (1990)
1900	1,000-1,500 [4]	Vericat and Batalla (2004)
1944	22,000 [1]	Ibáñez *et al.* (1996)
1950-1975	400 [5]	Vericat and Batalla (2004)
1961-1963	2,200 [1]	Catalán (1969) [2]
1964	8,700 [1]	Varela *et al.* (1986) [2]
1975-2000	170 [5]	Vericat and Batalla (2004)
1976-1982	320 [1]	Varela *et al.* (1986) [2]
1976-1990	260 [6]	Sanz *et al.* (1999)
1983-86	150 [1]	Palanques (1987) [2]
1986-87	130 [1]	Muñoz (1990) [2]
1988-1990	120 [1]	Guillén and Palanques (1992)
1998-1999	500 [7]	Roura (2004)
1998-1999	30 [8]	Roura (2004)
2002-2003	536 [9]	Vericat and Batalla (2005)
2003-2004	371 [10]	Vericat and Batalla (2005)

[1] Total load downstream Riba-roja Dam (Figure 3)
[2] Source: Ibáñez *et al.* (1996)
[3] Contribution of the Ebro to its delta at the beginning of twentieth century
[4] Bedload, considering the 10% of the total load estimated by Bayerri (1934-1935) and Nelson (1990)
[5] Bedload transport capacity in Tortosa (Figure 3)
[6] Suspended load downstream Flix Dam (Figure 3)
[7] Suspended load upstream from Sástago (Figure 3)
[8] Suspended load below Mequinenza Dam (Figure 3)
[9] Total load in Móra d'Ebre (49 km upstream Tortosa, Figure 3) where the 48 and 52% of this was transported as suspended and bedload, respectively
[10] Total load in Móra d'Ebre (49 km upstream Tortosa, Figure 3) where the 79 and 21% of this was transported as suspended and bedload, respectively

The lower Ebro flows as a single-thread channel through general morphostructural units (Figure 1.10b). Until the Vinebre village, it flows through the SW part of the Catalan Central Depression (Eastend of the Ebro Depression). The Catalan Central Depression is composed by clastic carbonated sediments (e.g., sandstones and conglomerates) of continental origin (Eocene-Oligocene). The fluvial network in this first unit has dissected the continental deposits since early Quaternary times. Downstream Vinebre, the Ebro River crosses the SW bound of the Catalan Coastal Ranges. There the valley is constrained (Pas de l'Ase). The Catalan Coastal Ranges are mainly composed by calcareous rocks (Jurassic) heavily faulted, such as those forming the anticline of the Pàndols-Cavalls and the Tormo Ranges. Between the villages of Garcia and Miravet the river flows across the

Paleo-Neogen Mora Depression, where Quaternary deposits are mainly formed by vast alluvial fans, within which the Ebro River and its terraces (Pleistocene-Holocene) are inserted. Further downstream, the river bends through the Cardó-Boix Range, a thrust sheet structure mostly composed by Jurassic and Cretaceous dolomites over the Triasic (i.e., Muschelkalk-Keuper facies), and into the Baix Ebre Depression, a semi-graben structure limited by a N-S normal fault in its western side, which in turn is masked by vast alluvial fan Quaternary deposits (draining the Ports Massif). Finally, in its lowermost part, the Ebro River flows across the delta plain deposits. The delta is an active modern geological structure (late Pleistocene-Holocene) with an area of 320 km^2 and a volume of 28 km^3 of sediments, the third larger delta in the Mediterranean region, after those in the Nile and the Rhone (Figure 1.10b).

Mean annual precipitation in the lower Ebro valley ranged from 200 to 600 mm, while in the eastern slopes of the Iberian Massif (Ports Massif) it increases to more than 900 mm (e.g., Figure 1.5 and 1.6).

Downstream from the Flix Dam the Ebro River has a mean slope of $8.5 \cdot 10^{-4}$. Its channel length (L_r) is 121 km, while the straight-line valley length (L_s) is 80 km. River-channel sinuosity is 1.5 (L_r/L_s). Similarly to central part of the Ebro (Figure 1.4), the lowermost reach shows a meandering pattern (Leopold *et al.* 1964). The observed river bed stratification below Flix Dam shows that the surface material is coarser than the subsurface. Surface and subsurface sizes distributions shows a dynamic behaviour (see in chapter 4 for analysing) due to the relation between flow's competence and sediment supply from upstream reaches (see in chapter 3 for description). The median surface material ($D_{50\text{-}s}$) in active bars ranged from 9 to 70 mm, characterizing the study reach as a gravel-bed river (e.g., Bunte and Abt, 2001).

2.2.2. Hydrology and water uses

Mean annual discharge in Tortosa (1913-2004, gauging station n.27) is around 450 m^3/s (i.e., 14,200 hm^3/year). Minimum mean monthly discharges are recorded in August and September (150 m^3/s), while maximum mean monthly flows are in March (695 m^3/s), related to the snow melts and spring rains in upstream basin (Figure 1.11). Maximum peak

flow was estimated at around 12,000 m^3/s in Tortosa in 1907 (Novoa, 1984). The river used to experience severe droughts before regulation (<25 m^3/s as summer discharge).

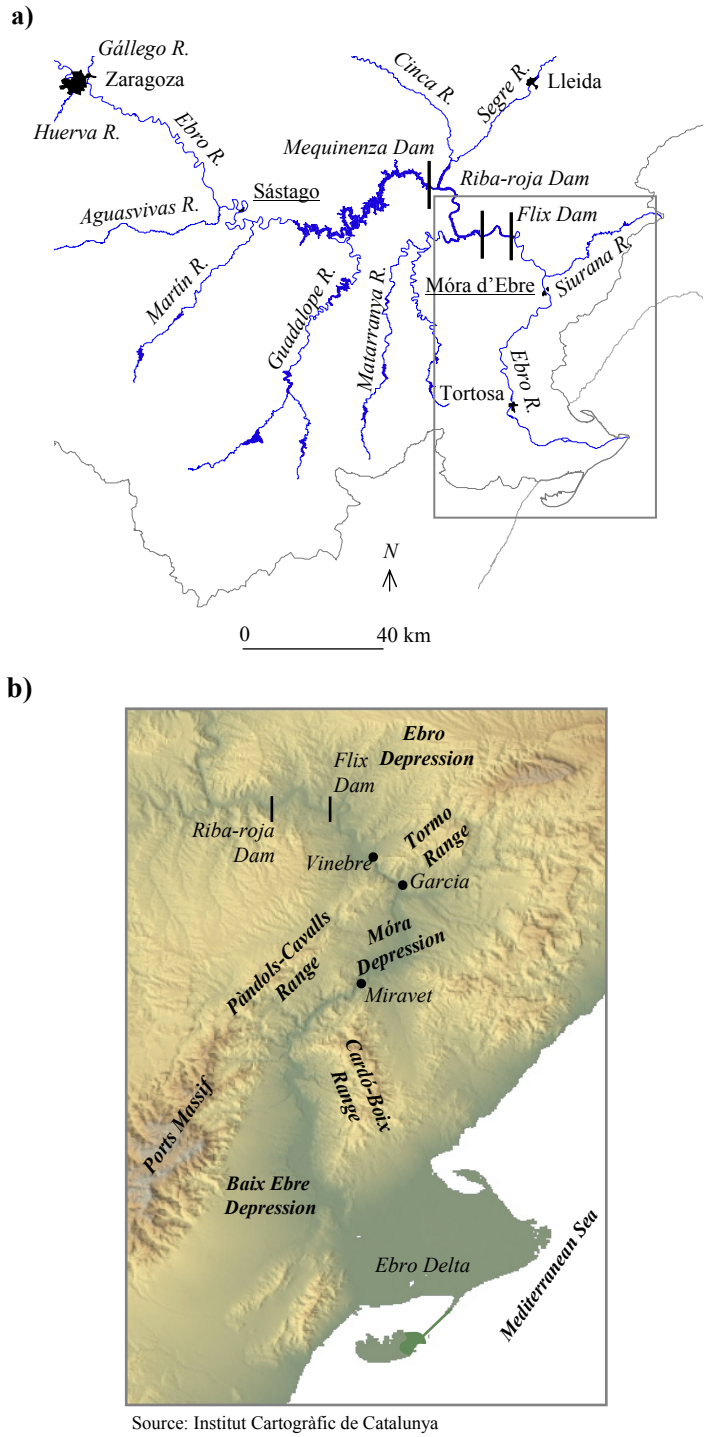

Source: Institut Cartogràfic de Catalunya

Figure 1.10. (**a**) The lower Ebro River: tributaries, dams and villages. Note than Sástago and Móra d'Ebre (underline villages) conform the study reach in this research. (**b**) Morphostructural units downstream Flix Dam. Note than Ribar-roja and Flix dams are plotted as a reference elements in the diagram

The largest complex of reservoirs in the whole Ebro Basin is located in the lower Ebro River. It is formed by the Mequinenza Dam, the Riba-roja Dam, and the Flix Dam, which, together, have a capacity of regulation of 1,752 hm^3 (Table 1.6), the 12% of the mean annual runoff at Tortosa. The most important tributary downstream from the Flix Dam is the Siurana River (Figure 1.10a). However, the potential capacity of this tributary to supply water and sediment into the Ebro River is very samll. The Siurana River is heavily regulated by two large dams, 10 hm^3/year of water are transferred to the Riudecanyes Basin (Table 1.6). In addition suffers from intensive gravel mining since the 1980s.

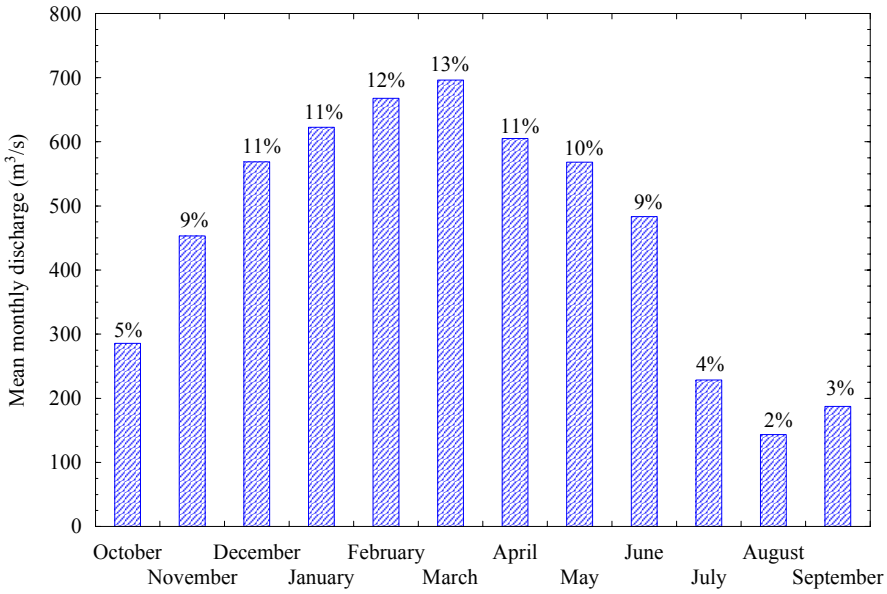

Source: Ebro Water Authorities. Data source from 1912 to 2002 (www.chebro.es)

Figure 1.11. Mean monthly discharges in Tortosa (gauging station n.27). Percentages represent the monthly contributions to the mean annual runoff

Table 1.6. Dams in the lower Ebro River

Dam	Basin	Closured (year)	Capacity (hm^3)	Basin area (km^2)
Mequinenza	Ebro	1966	1,534	58.000
Riba-roja	Ebro	1969	207	80,823
Flix	Ebro	1948	11	82,300
Siurana	Siurana	1972	12	80
Guiamets	Siurana	1975	10	-

Source: Ebro Water Authorities (www.chebro.es)

2.2.3. Hydrological and sedimentological alterations due to dams

The hydrological and sedimentological alterations in the lower Ebro River are described in the paper (see annex for the original hard copy):

Vericat, D. and Batalla, R.J. (2004): Efectos de las presas en la dinámica fluvial del curso bajo del río Ebro. *Cuaternario y Geomorfología* **18**(2): 37-50.

Downstream effects of dams in the fluvial dynamics of the Lower Ebro River

Abstract

The channel of the Lower Ebro River downstream Mequinenza and Ribarroja dams has experienced a series of morphological changes during the second half of the 20th century, mainly: a) lateral erosion, b) colonization of formerly active areas by riverine vegetation and, c) reduction of channel width. Changes have occurred after dam commissioning during the seventies. Dams alter flood frequency and magnitude, which causes a reduction of river capacity to transport sediment. Simultaneously, dams trap most sediment carried by the river from upstream, particularly coarse fractions as bedload, thus the river channel becoming the main downstream sediment source. This study describes the alteration of floods by dams and the subsequent adjustment of the river sediment transport and its morphology, through the analysis of hydrological and geomorphological field data, and historical and recent air photos. Reduction of flood magnitude (up to 25%) is especially important for the small floods in the downstream reaches near to dams. Reduction of flow competence has also diminished river capacity to transport bedload, shifting from a mean annual yield of 400,000 tonnes between 1950 and 1975 to less than 100,000 tonnes afterwards. Morphological changes indicate the river response to such alterations.

Key words: dams, bedload, floods, river morphology

Resumen

La morfología fluvial del cauce del río Ebro aguas abajo de las presas de Mequinenza y Ribarroja ha experimentado una serie de cambios a lo largo de la segunda mitad del siglo XX, entre los que cabe destacar: a) erosión lateral, b) colonización de zonas activas por vegetación de ribera, y c) disminución de la anchura. Dichos cambios se han producido después de la construcción y cierre de las presas en la década de los setenta. Las presas alteran la magnitud y frecuencia de las crecidas, lo que produce una disminución de la capacidad de transporte de sedimento del río. Simultáneamente, retienen la mayor parte del sedimento transportado desde aguas arriba, particularmente material grueso como carga de fondo, convirtiendo al cauce en la principal fuente de sedimento aguas abajo. El trabajo describe la alteración de las crecidas por las presas y el consiguiente ajuste del balance sedimentario y la morfología del río, a partir del análisis de datos hidrológicos, geomorfológicos de campo y de fotografías aéreas. La reducción de la magnitud de las avenidas (hasta un 25%) afecta especialmente a las más pequeñas en el tramo inmediatamente aguas abajo de las presas. La disminución de la capacidad del río para transportar carga de fondo a causa de la reducción de los picos de las avenidas y de los caudales medios es importante, pasando de una media de 400.000 t/a entre 1950 y 1975 a menos de 100.000 t/a durante la década de los noventa. Los cambios morfológicos son la respuesta del río a dichas alteraciones.

Palabras clave: presas, carga de fondo, avenidas, morfología fluvial

1. Introducción

La construcción de presas modifica las condiciones de equilibrio de los ríos generando una serie de cambios en los procesos fluviales. Diversos autores han estudiado los efectos hidrológicos y geomorfológicos de las grandes presas. Cabe destacar los trabajos de Leopold et al. (1964), Petts (1984), Williams y Wolman (1984), y Kondolf (1997), entre otros.

1.1. Cambios hidrológicos aguas abajo de los embalses

Los cambios hidrológicos están relacionados generalmente con las características del embalse, especialmente su tamaño con relación a la aportación hídrica de la cuenca, el funcionamiento de la presa y los usos del agua almacenada.

En algunos casos la aportación hídrica se reduce aguas abajo del embalse (Collier et al., 1996). Sin embargo, en mucho otros la reducción no es drástica pero se produce una alteración importante de la frecuencia de caudales. Por ejemplo, en el río Amarillo aguas abajo de la presa de Sanmexia, el caudal entre 1000 y 3000 m^3/s era igualado o superado 130 días al año durante el periodo anterior a la construcción de la presa (Chien, 1985). Un año después de la entrada en funcionamiento del embalse, dicho caudal se igualaba o superaba 204 días al año, lo que significa un aumento del 57 % en su duración, hecho que indica una mayor regulación de la circulación de agua en el río.

La reducción de las avenidas debido a la construcción de embalses es, no obstante, la modificación hidrológica más importante y significativa por sus implicaciones en la morfología del cauce, el transporte de sedimento, y la ecología del sistema fluvial. Incluso la simple laminación de las avenidas en embalses con poca o nula capacidad de regulación puede reducir los picos de las crecidas hasta el 50% (Moore, 1969). En Estados Unidos, por ejemplo, la reducción del caudal máximo después de la construcción de las presas oscila entre el 3% y el 91 %, aunque en algunos casos puede llegar a ser superior (Williams y Wolman, 1984). En California, las crecidas en la cuenca de los ríos Sacramento y San Joaquín se han reducido considerablemente debido a la construcción de numerosos embalses. El caudal asociado a un periodo de retorno de 2 años (Q_2) ha disminuido entre un 35% y un 95 %. Para periodos de retorno superiores (e.g., Q_{10}), la reducción oscila entre el 2% y el 78 % (Kondolf y Matthews, 1993). En el río Aragón (cuenca del Ebro), aguas abajo de la presa de Yesa, la reducción de las avenidas ha sido considerable. Según López et al. (2002) la capacidad de la presa para regular avenidas está directamente relacionada con el volumen de agua embalsada en el inicio del evento. Al mismo tiempo, la regulación altera el régimen anual de crecidas. En el caso del río Aragón, el número de avenidas en otoño y en primavera ha disminuido desde la construcción de la presa.

1.2. Captura del sedimento por las presas

El sedimento transportado por un río se puede dividir en sedimento en suspensión (arcillas, limos y arenas) y carga de fondo (arenas, gravas y cantos). La carga de fondo, aunque representa un porcentaje generalmente bajo en el total del sedimento transportado, es la responsable del mantenimiento de la estructura morfológica del cauce y de las zonas de ribera en ríos de gravas y/o arenas (Kondolf, 1997). Los embalses retienen la totalidad del material que es transportado como carga de fondo, y porcentajes también importantes de sedimento en suspensión, que en el caso del complejo Mequinenza y Ribarroja en el tramo bajo del río Ebro puede llegar al 90 % del material fino estimado a partir de las curvas de Brune (1953) y de acuerdo con los datos de Sanz et al. (1999).

1.3. Efectos aguas abajo

Las principales modificaciones que sufren los cauces situados aguas abajo de los embalses pueden ser tanto de incisión como de sedimentación (Collier et al., 1996). La mayoría de los cambios ocurren habitualmente en los primeros veinte años después de la construcción de la presa (Williams y Wolman 1984, Petts 1984).

La erosión del cauce se produce porque la presa retiene la mayor parte del sedimento que circulaba por el río en condiciones naturales. El agua que la presa libera durante crecidas erosiona el lecho aguas abajo pero no aporta nuevos sedimentos, por lo que el balance sedimentario del río entra en una fase de desequilibrio (figura 1). La erosión por agua limpia empieza inmediatamente después de la construcción de la presa y va disminuyendo a medida que el lecho del río se va acorazando. Los principales efectos sobre la dinámica del río son a modo de resumen: a) la degradación de los ecosistemas fluviales y deltaicos (Kondolf y Wolman 1993, Day et al. 1989), b) la incisión por erosión del cauce con impactos sobre la estabilidad de infraestructuras (figura 1) (Kondolf 1997, Kondolf y Mathews 1993), c) la disminución de la anchura del cauce (Wilcock et al. 1996, Williams y Wolman 1984), y d) la colonización por la vegetación de ribera de áreas anteriormente activas (Inbar, 1990).

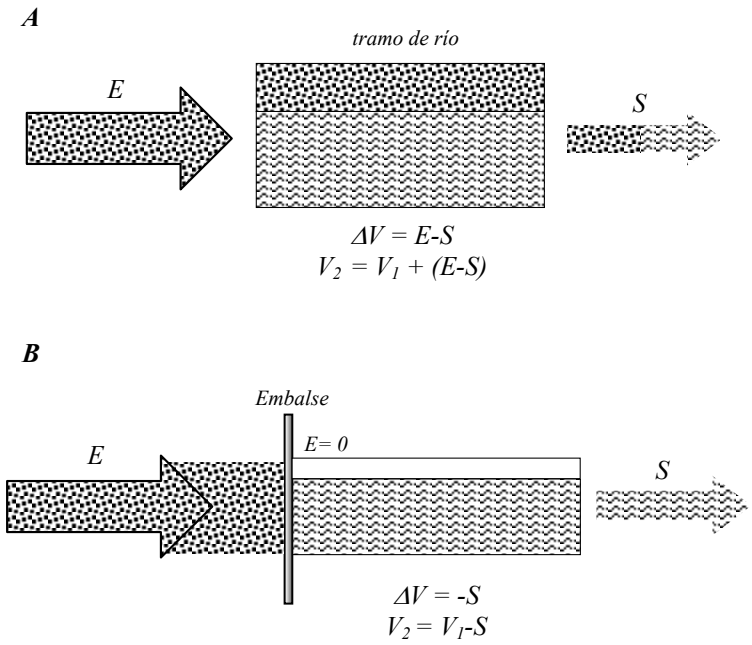

Figura 1 (C1P1). Efectos de una presa sobre el balance de sedimentos de un tramo fluvial. (A) Situación de equilibrio en ausencia de embalses y (B) Cambios en la transferencia de sedimentos aguas abajo de la presa: retención en el embalse y erosión aguas abajo. En ambos escenarios se expresan las relaciones entre las entradas (E), las salidas (S), y el volumen de sedimentos acumulados en el cauce de manera atemporal, partiendo de un estadio inicial (V_1) con tendencia a la acumulación, y transcurrido un periodo de tiempo (V_2) en el que se ha producido incisión

Figure 1 (C1P1). Downstream effects of dams on a river sediment budget. (A) Equilibrium in absence of dams and (B) Changes in the sediment transfer: retention in dams and downstream erosion. Both stages show the relation between sediment input (E), sediment output (S) and volume of sediment stored in the channel. Non-temporal sequence illustrates the initial situation with a tendency to aggradation (V_1) and the subsequent situation showing incision (V_2)

La sedimentación en el cauce se produce cuando los caudales que libera a presa son inferiores a los naturales y no tienen competencia ni capacidad para transportar los sedimentos que llegan al lecho aguas abajo desde: a) materiales provenientes de la misma construcción de la presa, b) aportación de tributarios, c) sedimentos derivados de tramos donde se produce un proceso de erosión, d) aportaciones eólicas, y e) redistribución del sedimento del lecho o de las barras (Petts, 1984). El principal efecto de este proceso es la reducción del volumen de desagüe de la sección del cauce. El material sedimentado en el lecho del río provoca que un caudal de avenida que antes ocupaba la totalidad del cauce se

desborde e inunde áreas próximas a éste. (Collier et al., 1996). En resumen, dicha reducción genera una disminución de la capacidad del cauce para transitar avenidas, perjuicios para la agricultura y otras actividades económicas, y la modificación de las características de los ecosistemas acuáticos y de ribera (Brookes, 1994).

El objetivo de este trabajo es la caracterizarción de los efectos del complejo de presas de Mequinenza, Ribarroja y Flix sobre la dinámica fluvial (hidrológica y geomorfológica) del curso bajo del río Ebro.

2. Área de estudio

La cuenca del Ebro es la más extensa de la Península Ibérica. Drena una área de 85.534 km^2 desde las montañas del Cantábrico y el Pirineo al norte, hasta el Sistema Ibérico al sur (figura 2). La altitud dentro de la cuenca varía entre los 3400 metros del Pirineo Central hasta el nivel del mar en el delta. La precipitación media anual presenta una irregularidad notable, con valores superiores a 2000 mm/año en las zonas pirenaicas hasta valores inferiores a los 400 mm/año en el fondo de la Depresión (www.chebro.es). Las zonas forestales ocupan más del 25% del área, mientras que la agricultura se extiende por el 50% de la cuenca (www.chebro.es).

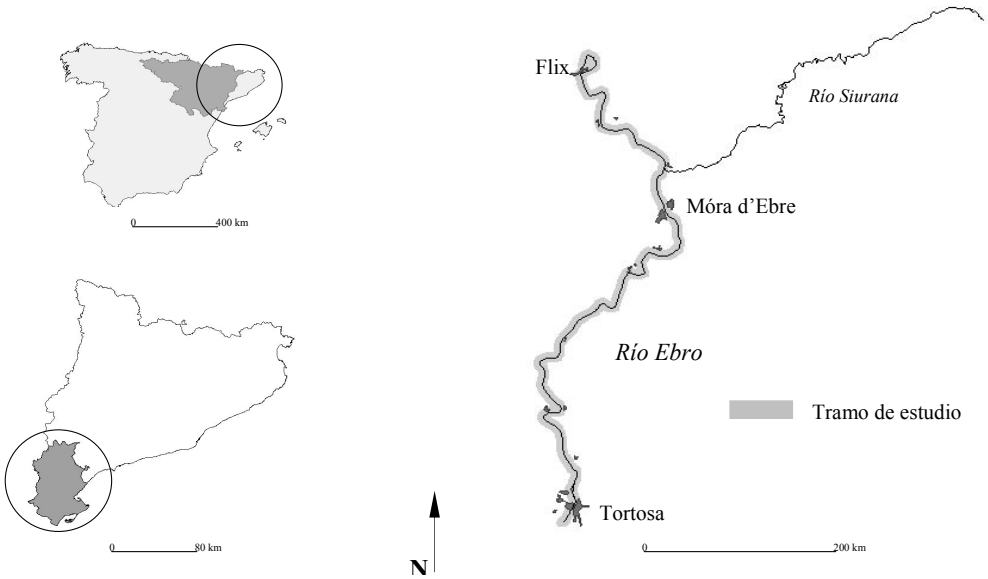

Figura 2 (C1P1). Situación de la cuenca del Ebro en la Península Ibérica y área de estudio

Figure 2 (C1P1). Location of the study area in the Ebro Basin (Iberian Peninsula)

Más de 180 embalses regulan casi el 60% (7700 hm^3) de la escorrentía de la cuenca. El agua embalsada se destina tanto a la producción hidroeléctrica (60000 hm^3/año), como al riego (6310 hm^3/año), a la refrigeración de centrales nucleares (3354 hm^3/año), y al abastecimiento de la población (313 hm^3/año) (www.chebro.es). El embalse de Mequinenza, construido en 1966, es el mayor de la cuenca con una capacidad de 1534 hm^3. El de Ribarroja fue construido en 1969 y tiene una capacidad de 207 hm^3, mientras que el de Flix, que se construyó en 1948, tiene una capacidad de 11,4 hm^3.

El tramo de estudio transcurre a través de 78 km de río desde el municipio de Flix (aguas abajo de la presa de Flix) hasta la ciudad de Tortosa (figura 2). La precipitación media anual en este sector se sitúa entre los 450 mm/a y los 600 mm/a (www.gencat.es). El principal afluente es el río Siurana, que desemboca en el Ebro cerca del municipio de Garcia. Como usos de agua más destacados cabe señalar la central hidroeléctrica de Flix con una capacidad máxima de turbinación de 400 $m^3\ s^{-1}$, la central nuclear de Ascó, así como la presencia de dos canales de riego (*Canal de la Dreta de l'Ebre* y el *Canal de l'Esquerra de l'Ebre*) que, con un caudal medio de 50 m^3/s, abastecen las necesidades de los cultivos del delta y de las poblaciones del área.

Las últimas avenidas importante del Ebro registradas en Tortosa fueron las de octubre de 2000 con un caudal pico de 2609 $m^3\ s^{-1}$ y, recientemente, la de febrero de 2003 con un caudal pico de 2200 $m^3\ s^{-1}$.

3. Metodología

El estudio se basa en el análisis de series de crecidas para comprobar el efecto de las presas sobre la magnitud y frecuencia de las mismas, la aplicación de fórmulas de carga de fondo para estimar la capacidad de los caudales circulantes de transportar sedimentos, y la caracterización de los cambios en la morfología fluvial del tramo final del Ebro como indicadora de cambios en el balance de sedimento.

3.1. Magnitud y frecuencia de las crecidas

El cálculo de los periodos de retorno tiene como objetivo caracterizar la reducción media de las avenidas en el tramo bajo del río Ebro, por lo que se han calculado para dos periodos distintos: anterior a 1975 y posterior a 1975, fecha en la cual todos los grandes embalses en la cuenca, incluidos los de Mequinenza y Ribarroja eran ya operativos. La metodología de análisis empleada no tiene en cuenta los efectos de cambios de tendencia temporal de las avenidas aguas arriba. En la interpretación de los resultados se asume que la regulación de los caudales por parte de las presas constituye el factor más importante de los cambios en la frecuencia y magnitud de las avenidas a partir de 1975.

El tramo de estudio cuenta con los siguientes registros hidrométricos: a) estación de aforos de Flix (EA121) desde 1948 a 1989, b) estación de aforos de Ascó (EA163) con datos desde 1984 a 2000, y c) estación de aforos de Tortosa (EA27) con datos discontinuos desde 1913 a 2000. Para el análisis de las crecidas se han utilizado las series de caudales máximos diarios (Q_c) de dichas estaciones que se encuentran disponibles en la página web de la Confederación Hidrográfica del Ebro (www.chebro.es).

El cálculo de los períodos de retorno en el tramo inicial de la zona de estudio se ha realizado completando la serie de caudales de Flix con los datos de Ascó ponderados por un coeficiente de reducción de caudales de 0,94 obtenido para el periodo de solapamiento de las series entre 1984 a 1989. Las estaciones están separadas 6 km entre sí.

Para el cálculo de los períodos de retorno en el tramo final se ha utilizado la serie de Tortosa (EA27) completada con los caudales máximos diarios de las crecidas históricas de 1907 y de 1937. Para construir las series con caudales oficiales e históricos se han utilizado los siguientes datos y criterios:

a) Serie oficial de caudales que cubre los periodos: 1913 a 1931 y 1951 a 2000, sin incluir las avenidas históricas.
b) Crecidas históricas: 1907 y 1937 a partir de las estimaciones de Novoa (1984). No se ha utilizado en los cálculos el caudal pico (23000 m^3 s^{-1}) de la crecida de 1907 publicado en la Geografia de Catalunya (1958).

c) Relleno de huecos: de 1908 a 1912, de 1932 a 1936 y de 1938 a 1942 con caudales de periodos de retorno de 5, 4, 3, 2 y 1 años; de 1943 a 1950 extrapolando los caudales de la estación de aforos EA11 (Zaragoza) a la estación EA27 (Tortosa), mediante la aplicación de un coeficiente de aumento de cuenca de 1,2 calculado a partir de caudales solapados entre las dos series EA27 y EA11.

El cálculo de periodos de retorno en ríos regulados, especialmente en aquellos en que las presas se han construido para el control de avenidas, se realiza mediante métodos de probabilidad total. La utilización de funciones paramétricas de probabilidad, como la de Gumbel, es menos común (Durrans, 1998). Los métodos de probabilidad total requieren realizar el tránsito de hidrogramas de crecida a través del embalse para comparar las características de la avenida sin regulación con los caudales regulados datos que, históricamente, no están disponibles para la zona de estudio. No obstante, en el caso de que las presas tengan como objetivo el suministro de agua y la producción hidroeléctrica, como ocurre con las de Mequinenza y Ribarroja, la influencia de la regulación del embalse sobre la crecida es habitualmente menor (USACE, 1993), por lo que el uso de funciones como la de Gumbel tiene más fundamento. Se trata, además, de la metodología utilizada generalmente por las Confederaciones Hidrográficas en España (e.g., Junta d'Aigües, 1994). Para el caso del tramo bajo del río Ebro se presentan tanto los periodos de retorno estimados a partir de la función de Gumbel como los datos muestrales (empíricos) sin ningún ajuste.

Los períodos de retorno T(x) = 1/(1-(Fx)) se han calculado utilizando la función de probabilidad Tipo I de Gumbel mediante el método de momentos (Shaw, 1983):

$$F(x) = e^{[-e^{B(x-a)}]}$$

$$a = \mu_{Qc} - (\gamma/b) \qquad [\gamma = 0{,}577]$$

$$b = \pi / \sigma_{Qc} \sqrt{6}$$

donde F(X) es la probabilidad de que un caudal máximo anual (Q_c) iguale o supere X en un año determinado, y *a* y *b* son los dos parámetros relacionados con los momentos de la población de valores Q_c. El primer momento se define como la media (μ_{Qc}) y el segundo como la varianza (σ_{Qc}^2).

Para la aplicación de la función de probabilidad de Gumbel se realizó el ajuste de datos dudosos, que son aquellos valores que se alejan significativamente de la tendencia del conjunto de la serie (Chow et al., 1994):

$$y_h = \mu_{logQc} + (K_n \, \sigma_{logQc})$$
$$y_l = \mu_{logQc} - (K_n \, \sigma_{logQc})$$

donde y_h e y_l son los límites superior e inferior respectivamente, n es el número de datos de caudal (Q_c), μ es la media, σ es la desviación estándar, y K_n es un valor constante asociado al número total de datos de la serie de caudales.

En la serie oficial de la EA27 los limites obtenidos se sitúan entre el rango de caudales utilizados. En las dos series restantes existen valores que exceden el límite superior. Dichos caudales corresponden a datos históricos a partir de las estimaciones de Novoa (1984). De acuerdo con el Water Resources Council (1981) y con Chow et al. (1994), si un dato histórico es dudoso y no puede ser verificado debe ser incluido en el análisis. En el tramo bajo del río Ebro, los datos históricos utilizados que exceden el límite superior calculado no pueden ser verificados. Por consiguiente, han sido utilizados en el análisis.

Además, con el mismo objetivo de mostrar la reducción de la magnitud de las avenidas en el tramo de estudio se han comparado los caudales máximos sin ningún tratamiento estadístico (series muestrales o empíricas). Para ello se ha utilizado la serie de caudales de Tortosa (EA27) a la que se añadieron los datos históricos estimados por Novoa (1984).

3.2. Dinámica geomorfológica y de sedimentos

A lo largo del tramo de estudio se han realizado granulometrías superficiales para la caracterización del material del lecho. Los datos granulométricos se han empleado para la estimación de la carga de fondo mediante fórmulas. El método utilizado para la caracterización del material superficial ha sido el de los transectos lineales mediante el método de Wolman (1954) sobre 400 partículas.

La capacidad actual del río para transportar carga de fondo se ha estimado mediante la utilización de fórmulas, debido a la falta de una base de datos de mediciones directas. Para ello se han empleado datos granulométricos y un perfil transversal en el tramo de Tortosa (figura 3), y se ha estimado la pendiente a partir de mapas topográficos a escala 1:5000.

Las fórmulas utilizadas para el cálculo de las tasas de transporte han sido las de Schoklitsch (1950) y la de Engelund y Hansen (1967):

a) Schoklitsch (1950)

$$i_b = 2500 s^{3/2}(q-q_c)$$

donde s es la pendiente, q es el caudal unitario (m^2/s), q_c es el caudal crítico unitario (m^2/s), e i_b es la tasa de transporte en peso seco ($kg/m \cdot s$)

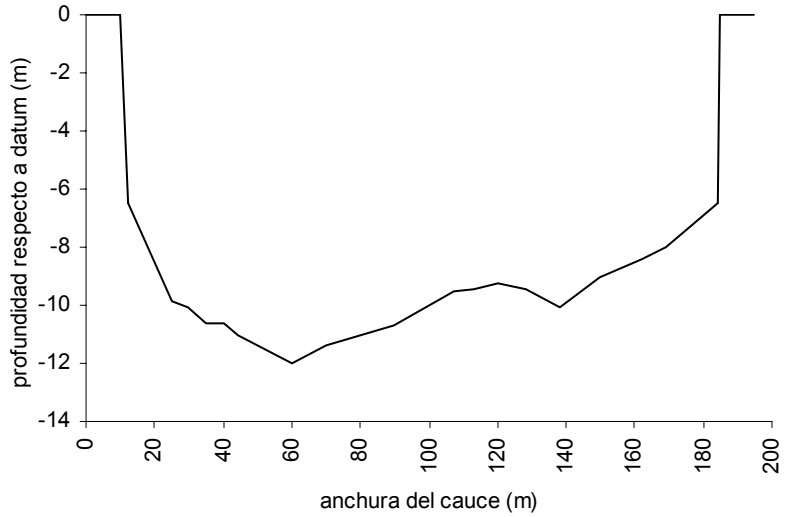

Figura 3 (C1P1). Sección transversal del río Ebro a su paso por Tortosa

Figure 3 (C1P1). Cross section of the Ebro River in Tortosa.

La única limitación de la fórmula de Schoklitsch (1950) hace referencia al diámetro de las partículas. Sólo cuando el tamaño de las partículas no es uniforme se recomienda la

utilización del D_{40} como diámetro representativo para el cálculo del caudal crítico de inicio de movimiento (Maza y García, 1996). Dicho caudal se ha estimado directamente en el campo mediante un muestreador de carga de fondo Helley-Smith, y se ha verificado mediante la ecuación de Shields (1936). La granulometría del tramo de estudio presenta un índice de clasificación (Folk y Ward, 1957) de tipo moderadamente clasificado. Por consiguiente, el uso del D_{50} para el cálculo del caudal crítico de inicio de movimiento en el tramo bajo del río Ebro está plenamente justificado.

b) Engelund y Hansen (1967)

$$i_b = \Phi\ \varphi_s \sqrt{(\varphi'\ g\ D_{50}^3)}$$

$$\Phi = (0{,}1\ \theta^{5/2}) / f_{EH}$$

$$f_{EH} = (2\ g\ d\ S) / U^2$$

$$\theta = \tau_0 / (\varphi\ g\ \varphi'\ D_{50})$$

donde s es la pendiente, φ_s es la densidad del sedimento (2650 kg/m^3), φ es la densidad del agua (1000 kg/m^3), φ' es la densidad relativa del sedimento, D_{50} es el diámetro medio del sedimento (m), g es la aceleración de la gravedad (9,8 m/s^2), d es la profundidad del agua (m), U es la velocidad media (m/s), τ_0 es la tensión de corte (N/m^2), y i_b es la tasa de transporte en peso seco (kg/m·s).

Existen dos limitaciones para la aplicación de la fórmula de Engelund y Hansen (1967) que son $(D_{75}/D_{50})^{0,5} \leq 1{,}6$ y $D_{50} \geq 0{,}15$ mm. Los valores respectivos para el tramo bajo del río Ebro son 0,63 y 19 mm, por lo que queda fundamentado el uso de esta fórmula en el presente trabajo.

Para el cálculo de las tasas de carga de fondo se han utilizado los caudales diarios facilitados por la Confederación Hidrográfica del Ebro. Los caudales utilizados en las fórmulas de transporte sólido corresponden a la energía disponible a partir de un caudal

crítico de inicio de movimiento estimado a partir de muestreos de campo y calculado a partir de Shields (1936).

El estudio de los cambios en la morfología del cauce se realizó mediante la comparación de fotografías aéreas tomadas antes y después de la construcción de las presas, a partir de dos series: a) la de 1956 conocida como vuelo americano y b) la de 1994/1995 que corresponde al vuelo realizado por el Institut Cartogràfic de Catalunya. Las fotos se escanearon y se trataron mediante programas de diseño gráfico (Corel Draw 8.0 y FreeHand 8.0), con el objetivo de analizar los cambios en la morfología del cauce, en base al estudio de la tipología de las barras y a su colonización por vegetación de ribera.

4. Resultados

4.1. Reducción de la magnitud de las avenidas

Las crecidas en el tramo inferior del río han sufrido en general una disminución a partir de los años 70 del siglo XX como consecuencia de la regulación de los embalses de la cuenca y, en particular, de las de Mequinenza y Ribarroja (tabla 1). A partir de la serie de datos oficial, la reducción es, en general, mayor para los caudales de menor magnitud (Q_2) y menor para las crecidas mayores (Q_{25}). Los efectos de la regulación son más evidentes en el tramo cercano a las presas (Flix-Ascó) en el que, por ejemplo, la relación entre Q_{2post} y Q_{2pre} es de 0,73 que en el tramo final (Tortosa) en que la misma relación tiene un valor de 0,89.

La magnitud de las avenidas de 25 años de periodo de retorno en Flix-Ascó se ha reducido un 13%, mientras que en Tortosa ya no se ven afectadas por la regulación. No obstante, si en el cálculo se incluyen las avenidas históricas de 1907 y 1937 la reducción de las avenidas T_{25} en Tortosa alcanza una media del 35%. En este mismo sentido, el análisis de los datos empíricos de los caudales máximos en Tortosa sin ajuste estadístico indica también una clara reducción de los picos de las crecidas después de la construcción de las presas (figura 4).

Tabla 1 (C1P1). Periodos de retorno en el tramo inferior del río Ebro antes y después de 1975, a partir de series de caudales oficiales, incluyendo las crecidas históricas de 1907 y 1937

Table 1 (C1P1). Recurrence intervals for the Lower Ebro before and after 1975, using official flow series and including historical floods of 1907 and 1937

	Q_2		Q_{10}		Q_{25}	
	Q_{cpre} (m^3s^{-1})	Q_{cpost} (m^3s^{-1})	Q_{cpre} (m^3s^{-1})	Q_{cpost} (m^3s^{-1})	Q_{cpre} (m^3s^{-1})	Q_{cpost} (m^3s^{-1})
Series EA121(1) + EA163(2) (CHE)	1585	1160	2653	2235	3261	2846
Cociente Q_{post} / Q_{pre}		0,73		0,84		0,87
Serie oficial EA27(3) (CHE)	1425	1267	2667	2594	3374	3350
Cociente Q_{post} / Q_{pre}		0,89		0,97		0,99
EA27 más 1907 y 1937, con relleno	1603	1267	3632	2594	4787	3350
Cociente Q_{post} / Q_{pre}		0,79		0,71		0,70
EA27 más 1907 y 1937, sin relleno	1620	1267	4149	2594	5589	3350
Cociente Q_{post} / Q_{pre}		0,78		0,63		0,60
Media aritmética (EA27)	1549	1267	3483	2594	4584	3350
Cociente Q_{post} / Q_{pre}		0,82		0,74		0,73

(1) Estación de aforos de Flix (EA121)

(2) Estación de aforos de Ascó (EA163)

(3) Estación de aforos de Tortosa (EA27)

La falta de avenidas importantes en el río Siurana debida a las presas de Siurana (1972), Margalef (1983) y Guiamets (1983), ha contribuido también a la reducción de las avenidas en el tramo bajo del Ebro.

4.2. Efectos sobre la carga de fondo

La aplicación de las fórmulas de Schoklitsch (1950) y de Engelund y Hansen (1967) muestra cómo la capacidad del caudal circulante entre Flix y Tortosa para transportar material como carga de fondo se ha reducido considerablemente después de la construcción de los embalses de Mequinenza y Ribarroja (figura 5). Esta disminución está directamente relacionada con la reducción de la frecuencia y magnitud de las avenidas y, por tanto, con el alcance periódico de los umbrales de movimiento de las fracciones de material presentes en el propio lecho del río. Tal y como se observa en la figura 5, además

de disminuir el aporte de sedimento también lo hace el caudal medio anual. Dicha reducción no tiene porque ser un efecto directo de la construcción de las presas sino del almacenaje y uso posterior del agua. García et al. (2001), en un estudio de los ríos pirenaicos, han llegado a la conclusión de que los procesos que explican la disminución de los recursos hídricos son muy complejos debido a la interacción defactores físicos y humanos. Por su parte Ibáñez et al. (1996) indican que las causas de la disminución de los caudales medios en el tramo bajo del río Ebro son: a) el aumento de la demanda de agua en la cuenca, mayoritariamente para usos agrícolas, lo que equivaldría al 74% de la reducción, b) la evaporación del agua embalsada en el conjunto de la cuenca representaría el 22% de la reducción, en cuyo caso los cambios en la temperatura citados por García et al. (2001) corroborarían esta idea, y c) el 4% restante correspondería a los efectos de las alteraciones climáticas y a las posibles variaciones de los usos del suelo.

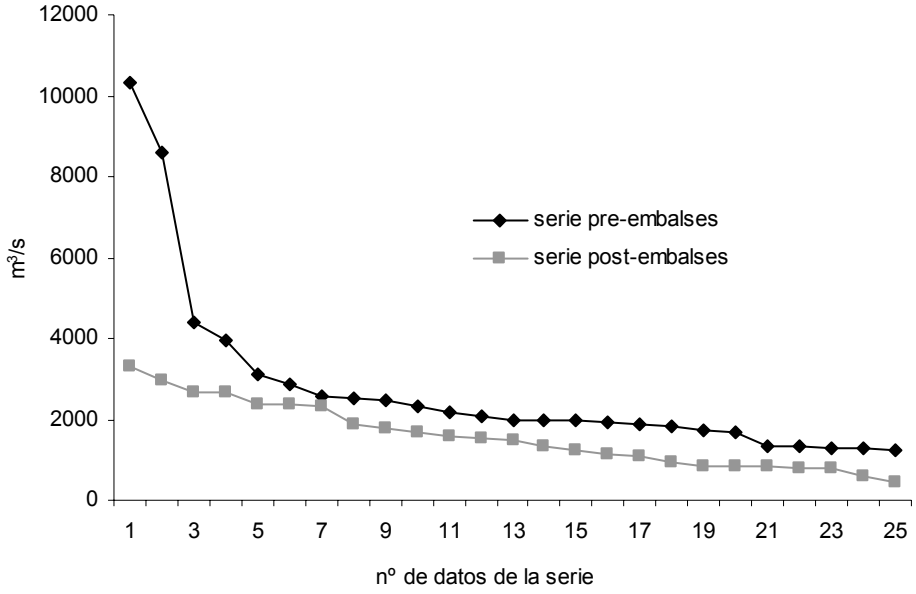

Figura 4 (C1P1). Caudales máximos diarios del río Ebro en Tortosa (EA27) antes y después de 1975, incluyendo los datos de las crecidas históricas de 1907 y 1937 (Novoa, 1984)

Figure 4 (C1P1). Maximum daily discharge in the Lower Ebro (Tortosa, EA27) before and after 1975, including the historical floods of 1907 and 1937 (Novoa, 1984)

El transporte medio anual como carga de fondo para los periodos anterior y posterior a 1975 se muestra en la tabla 2. Aunque la diferencia entre las estimaciones de las fórmulas es notable, el porcentaje de reducción de la carga de fondo es muy similar. El caudal crítico

de inicio de movimiento se ha estimado directamente en el campo mediante un muestreador de carga de fondo Helley-Smith. Caudales alrededor de 680 m^3/s son capaces de movilizar partículas de 25 mm, calibre que corresponde al D_{50} del material superficial del lecho no acorazado del río. Este valor se corroboró mediante la ecuación de Shields (1936):

$$\tau_c = \rho'_s \, g \, D_{50} \, 0{,}056 = 1650 \cdot 9{,}8 \cdot 0{,}025 \cdot 0{,}056 = 22{,}3 \text{ N m}^{-2}$$

$$d = \tau_c / (\rho \, g \, s) \; 22{,}3 / (1000 \cdot 9{,}8 \cdot 0{,}00085) = 2{,}7 \text{ m} \; (680 \text{ m}^3 \text{ s}^{-1} \text{ en EA27})$$

donde τ_c es la tensión de corte crítica (N m^{-2}), ρ'_s es la densidad del sedimento en peso sumergido (g cm^{-3}), D_{50} es el tamaño medio del sedimento (m), g es la aceleración de la gravedad (m s^{-2}), d es el calado medio (m), ρ es la densidad del agua (g cm^{-3}), y *s* es la pendiente (adimensional).

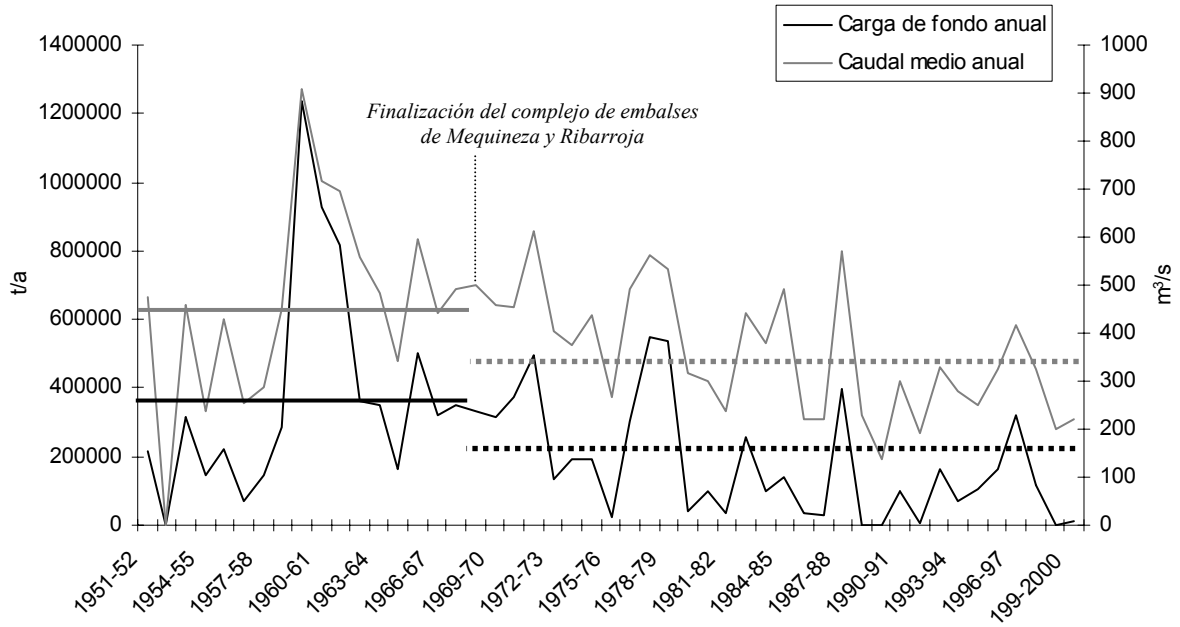

Figura 5 (C1P1). Caudal medio anual y capacidad de transporte del flujo en el bajo Ebro (Tortosa) a partir de las fórmulas de Schoklitsh (1950) y Engelund y Hansen (1967). Las líneas continuas y discontinuas marcan los niveles del caudal medio y la tasa media para el periodo pre-embalses y post-embalses respectivamente

Figure 5 (C1P1). Mean discharge and river bedload capacity of the Ebro in Tortosa estimated by means of the Schoklitsh (1950) and Engelund y Hansen (1967) formulae. Full lines indicate mean pre-dam values and dotted lines indicate mean post-dam values

Tabla 2 (C1P1). Carga de fondo (t/a) en el tramo inferior del río Ebro para los períodos anterior y posterior a 1975, a partir de las fórmulas de Schoklitsch (1950) y Engelund y Hansen (1967)

Table 2 (C1P1). Bedload yield (t/y) in the Lower Ebro before and after 1975 from Schoklitsch (1950) and Engelund and Hansen (1967)

	Schoklitsch (t/a)	**Engelund & Hansen (t/a)**
Anterior a 1975	209171	519551
Posterior a 1975	77801	209855
% reducción	63	60

A principio del siglo XX la contribución total anual de sedimento del río Ebro al mar era de $15 \cdot 10^6$ toneladas (Bayerri 1935, Nelson 1990), la mayor parte del cual era transportado en suspensión, como indican las concentraciones de 10 g l^{-1} obtenidas durante crecidas. Asumiendo que en ríos aluviales la carga de fondo supone un 10% de la carga total de sedimento, la carga de fondo total se estima alrededor de $1 \cdot 10^6$ a $1{,}5 \cdot 10^6$ toneladas anuales. Antes de la construcción de los embalses de Mequinenza y Ribarroja, el río Ebro ya había visto reducido la carga total de sedimento hasta valores entre $3 \cdot 10^6$ y $6 \cdot 10^6$ toneladas anuales debido a la retención en embalses de aguas arriba (Avendaño et al., 1997). De ellas, el 10% (ca. 450.000) serían de carga de fondo. Esta estimación se ajusta a las 400.000 toneladas de capacidad de transporte anual que ofrecen las fórmulas para el periodo 1950-1975. En el periodo posterior a la construcción de las grandes presas el valor medio de carga de fondo se ha reducido a 170.000 toneladas anuales (figura 6). Los resultados obtenidos se ajustan a los de Guillén et al. (1992). Durante la década de los años 90 la capacidad de transporte se ha situado por debajo de las 100.000 toneladas anuales, con algunos años en los que no se alcanzó el umbral de movimiento.

El sedimento que finalmente el río transporta se moviliza del propio cauce, ya que la aportación de aguas arriba es nula. Este hecho junto con los cambios en las crecidas provoca los cambios morfológicos descritos anteriormente, lo que supone un factor clave para la degradación del ecosistema fluvial y un riesgo para el mantenimiento del delta.

4.3. Cambios morfológicos

El análisis de las series fotográficas ha permitido constatar una serie de cambios en el cauce del curso inferior del Ebro. Dichos cambios se pueden resumir en: a) colonización de áreas anteriormente activas del cauce por vegetación de ribera, b) cambios en la anchura del cauce, c) incisión del lecho, y d) cambios en la dinámica y tipología de las barras, y en el patrón de drenaje fluvial. La reducción de la magnitud de las avenidas responsables del modelaje del cauce, y la disminución tanto de la capacidad del caudal para transportar sedimento como al déficit de material causado por los embalses, son las responsables de los cambios morfológicos.

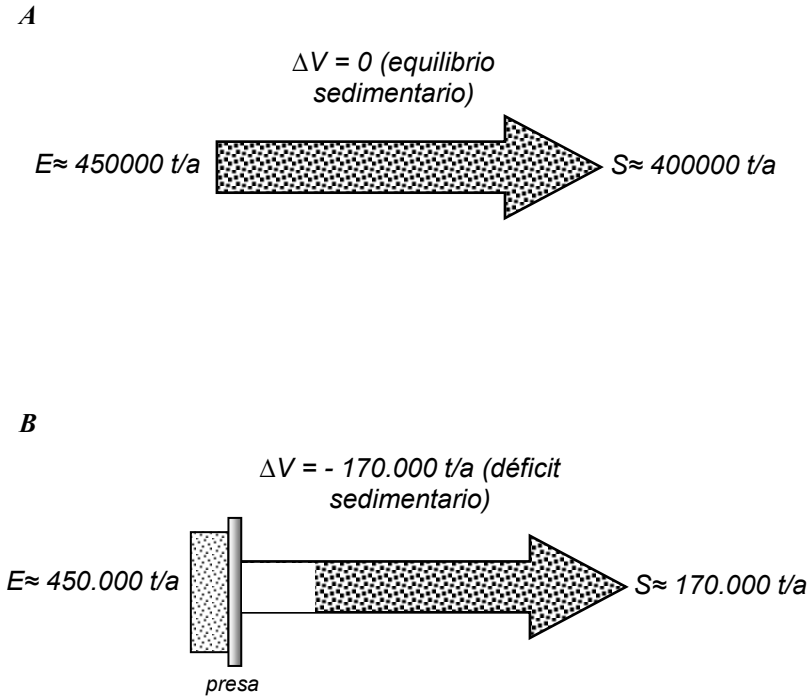

Figura 6 (C1P1). Cambios en el balance de sedimento en el tramo final del río Ebro sin tener en cuenta las aportaciones de los tributarios. Las entradas se han calculado asumiendo que cerca del 10 % del material que retienen las presas de Mequinenza y Ribarroja (Avendaño et al., 1997) es carga de fondo. Las salidas corresponden a los valores medios estimados mediante fórmulas (E: entradas, ΔV: variación del volumen y S: salidas). (A) Situación de equilibrio en ausencia de embalses y (B) Cambios en la transferencia de sedimentos aguas abajo de la presa de Flix

Figure 6 (C1P1). Changes in the Ebro River sediment budget. Sediment input from tributaries is not taken into account. Estimation are based on the assumption that 10% of sediment captured by Mequinenza y Ribarroja dams (Avendaño et al., 1997) is bedload. Downstream transfers are

estimations using formulae (E: imput, ΔV:change of volume and S: output). *(A) Equilibrium in absence of dams and (B) Changes in the sediment transfer downstream Flix dam*

La reducción de la magnitud de las avenidas facilita que la vegetación de ribera pueda colonizar áreas que, con anterioridad a la construcción de las presas, eran habitualmente activas, reduciendo de esta forma, la sección activa del cauce. La figura 7 muestra los cambios en la vegetación de ribera en una barra próxima al municipio de Móra d'Ebre.

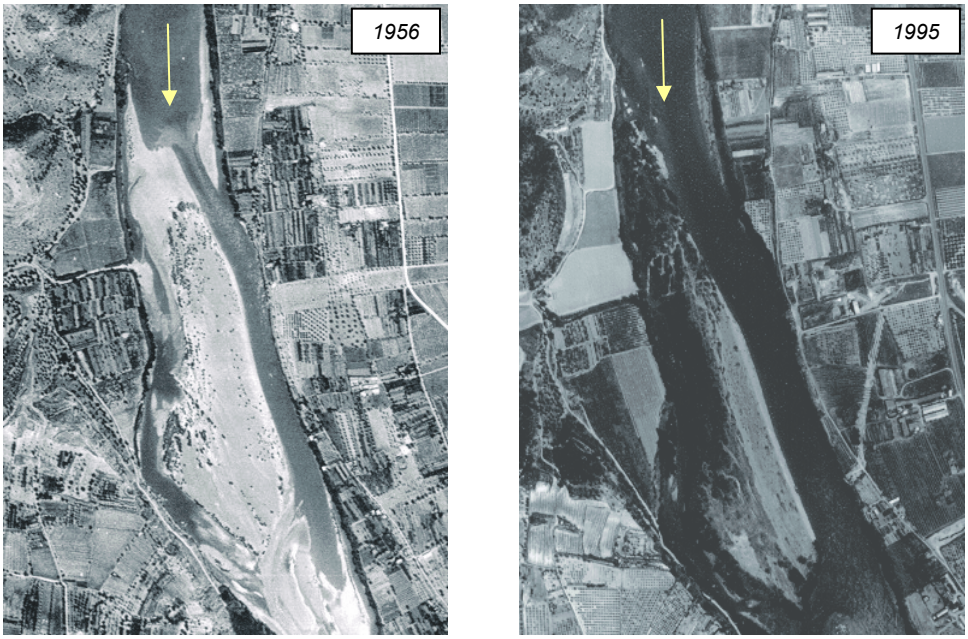

Figura 7 (C1P1). Colonización por vegetación de ribera de una barra en las proximidades de Móra d'Ebre entre 1956 y 1995 (fotografías aéreas: Ejército del aire 1956 e Institut Cartogràfic de Catalunya (ICC) 1995). Actualmente (2003) la barra está totalmente cubierta por vegetación

Figure 7 (C1P1). Colonization by vegetation of an active bar in the vicinity of Móra d'Ebre between 1956 and 1995 (air photos: Ejército del Aire 1956 and Institut Cartogràfic de Catalunya (ICC) 1995). Nowadays bar is completely covered by vegetation

La reducción del suministro de sedimento como carga de fondo provoca también cambios en la morfología del cauce y su patrón de drenaje (Kondolf, 1997). Según Sanz et al. (2001) a partir de la construcción de los embalses de Mequinenza y Ribarroja no se han apreciado nuevos cambios de sedimentación aguas abajo pero, contrariamente, se observan otro tipo de modificaciones que afectan tanto al cauce como a los depósitos. En este

sentido, en el tramo bajo del río Ebro uno de los cambios más destacados ha sido la migración lateral. Numerosas barras que anteriormente eran activas han sido colonizadas por vegetación y han pasado de centrales a laterales, favoreciendo su ocupación por campos de cultivo. Se ha producido también el abandono de cauces secundarios, lo que indicaría una incisión del cauce principal debida a la falta de sedimento y una colonización no sólo de las barras sino de segmentos de cauce anteriormente activos. La figura 8 ilustra los cambios en el cauce con un ejemplo aguas abajo del municipio de Móra d'Ebre. Por lo que se refiere al cauce principal, se ha reducido tanto su sinuosidad como su anchura (-10%).

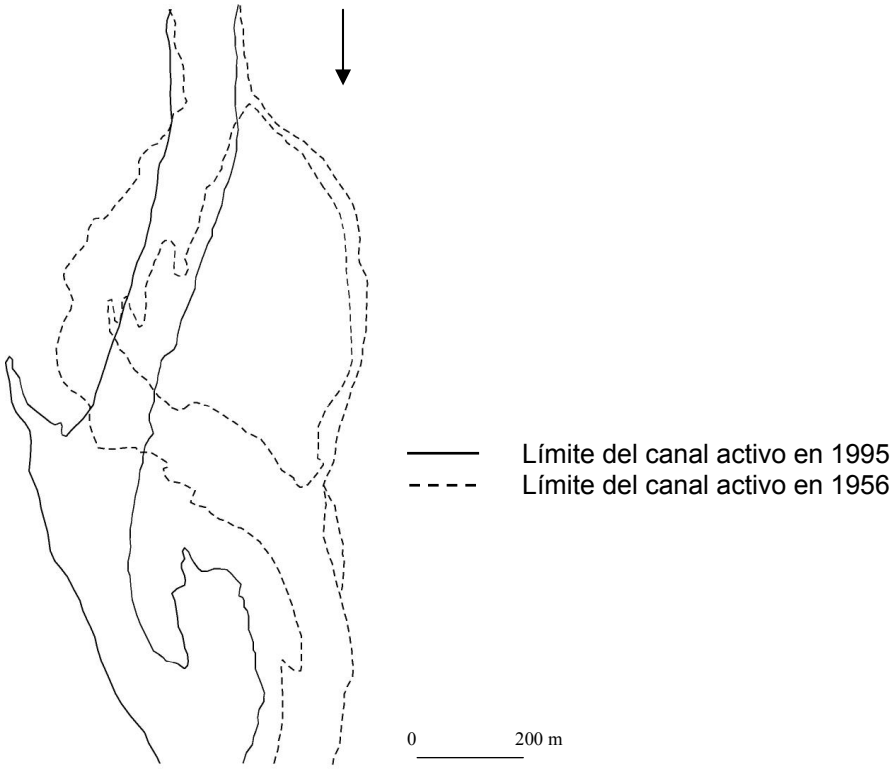

Figura 8 (C1P1). Cambio en el patrón fluvial aguas abajo del municipio de Móra d'Ebre (fotografías aéreas: Ejército del Aire 1956 e ICC 1995)

Figure 8 (C1P1). Changes in the fluvial pattern downstream Móra d'Ebre (air photos: Ejército del Aire 1956 and ICC 1995)

En relación a la anchura del cauce, se han detectado dos tipos de cambios. Parte del cauce que era activo antes de los embalses ha pasado a ser estable debido a la aparición de

vegetación de ribera y, en algunos casos, incluso de nuevos campos de cultivo, que han aprovechado las áreas que se inundaban con frecuencia y que dejaron de hacerlo después de la construcción de las presas. Como consecuencia, en esos sectores se ha producido una reducción de la anchura del cauce, que en algunos casos llega al 20% (figura 9a). En otras zonas, la anchura del cauce se ha incrementado, debido a procesos de erosión lateral que se han convertido en la única fuente relevante de sedimento en el río (figura 9b). En estado natural (sin embalses) los procesos de erosión lateral están compensados a largo plazo por la sedimentación de material, por lo que la anchura del cauce se mantiene estable o en equilibrio dinámico. Después de la construcción de las presas, la erosión lateral continua pero el equilibrio se rompe debido a la reducción de las avenidas y a la falta de suministro de sedimento (Chien, 1985), lo que en el caso del Ebro se ve agravado por la nula aportación del Siurana muy afectado por las extracciones de áridos.

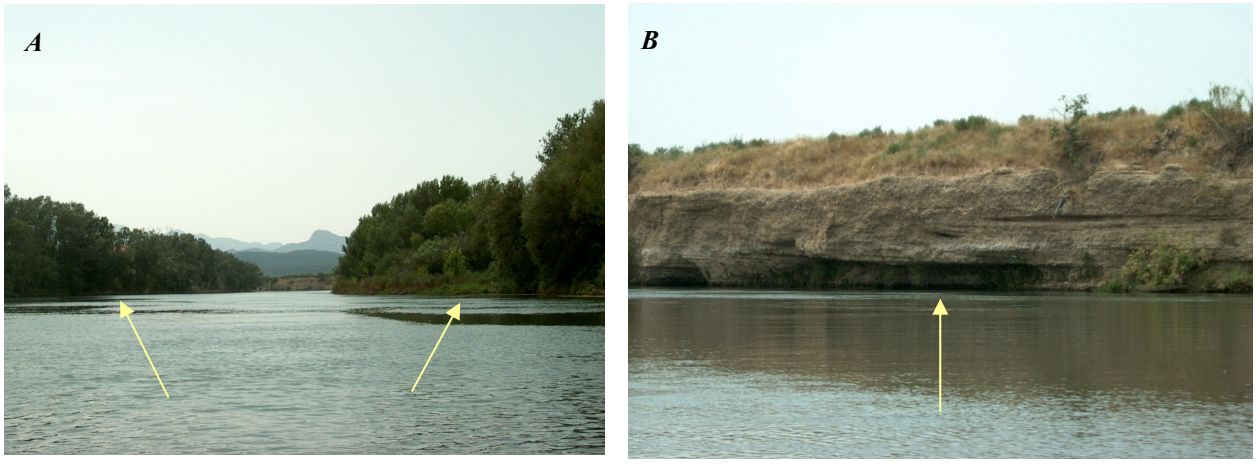

Figura 9 (C1P1). (A) Colonización por vegetación de ribera y reducción de la anchura del cauce aguas abajo del municipio de Benissanet y (B) Erosión lateral cerca del municipio de Ascó

Figure 9 (C1P1). (A) Colonization of the active channel by riverinne vegetation and reduction of channel width downstream Benissanet and (B) Lateral erosion in the vicinity of Ascó

Estos cambios morfológicos han podido ser identificados puntualmente a lo largo del tramo bajo del río Ebro (figura 8 y 9). Aunque podrían sugerir que corresponden a procesos naturales, a lo largo del tramo de estudio todas las evidencias apuntan en la misma dirección, lo que sugiere una clara influencia de los embalses en la dinámica fluvial aguas abajo.

5. Conclusiones

El trabajo ha mostrado los principales cambios que afectan el comportamiento hidrológico y geomorfológico del tramo bajo del río Ebro y los ajustes en el balance sedimentario y su morfología como consecuencia de la acción de las presas aguas arriba, principalmente:

1. Una reducción de la magnitud y frecuencia de las avenidas, con especial incidencia en las crecidas de menor magnitud y mayor frecuencia, en el tramo inmediatamente aguas abajo de las presas.
2. La disminución de la capacidad del río para transportar carga de fondo a causa de la reducción de los picos de las avenidas y de los caudales medios desde los años setenta del siglo XX.
3. Cambios morfológicos como, por ejemplo, la colonización por vegetación de ribera de zonas del cauce anteriormente activas y la disminución de la anchura del mismo.

Estos cambios conllevan el reajuste del cauce fluvial al déficit de sedimento por la escasa o nula aportación de material grueso desde aguas arriba y desde los tributarios, lo que implica la erosión del propio lecho, y a largo plazo, la degradación del ecosistema.

Agradecimientos

Este trabajo se está llevando a cabo gracias a una beca de investigación de Ministerio de Educación, Cultura y Deporte, y en el marco del proyecto (REN2001-0840-C02-01/HID). Los datos hidrológicos han sido subministrados por la Confederación Hidrográfica del Ebro. Los autores agradecen las correcciones de José M. García Ruiz (CSIC) y de un revisor anónimo de la primera versión del trabajo, y a Albert Rovira (UdL) la colaboración en el trabajo de campo.

Bibliografía

Avendaño, C., Cobo, R., Sanz, M.E. y Gómez, J.L. (1997): Capacity situation in Spanish reservoirs. *I.C.O.L.D. Ninenteenth Congress on Large Dams*, 74, 52, 849-862.

Bayerri, E. (1934-35): *Historia de Tortosa y su comarca*. Imprenta Moderna de Alguerri, Tortosa, vol. II, 704 p. And vol. III, 751 p.

Brookes, A. (1994): River chanel change. En: Calow, P. y Petts, G.E. (1994): *The rivers Handbook. Hydrological and ecological principles*. Blackwell Science, Oxford, 55-75.

Brune, G.M. (1953): The trap efficiency of reservoirs. *Transactions of the American Geophysical Union*, 34, 407-418.

Chien, N. (1985): Changes in river regime after the construction of upstream reservoirs. *Earth surface processes and landforms,* 10, 143-159.

Chow, V., Maidment, D.R. y Mays, L.W. (1994): Hidrología aplicada, McGraw-Hill, Santafé de Bogotá, 584p.

Church, M., McLean, D.G. y Wolcott, J.F. (1987): River bed gravels: sampling and analysis. En: Thorne, C. R., Barthurst, J.C. y Hey, R.D. (eds.): *Sediment transport in gravel-bed rivers*. Chichester, John Wiley and Sons, 43-88.

Collier, M.P., Webb, R.H., y Schmidt, J. (1996): *A primer on the downstream effects of dams*. United States Geological Survey Circular 1126, 94 p.

Day, J.W. y Templet, P.H. (1989): Consequences of sea level rise: implications from the Mississippi delta. En: Benkema, J. et al. (eds.): *Expected effects of climate change on marine coastal ecosystems,* 155-165.

Durrans, S.R. (1998): Total probability methods for problems in flood frequency estimation. En: Parent, E., Hubert, P., Bobee, B. and Miquel, J. (eds.): *Statistical and Bayesian methods in hydrological sciences*. UNESCO, Paris, Technical Documents in Hydrology, 20, 299-326.

Engelund, F. y Hansen, E. (1967): *A Monograph on Sediment Transport in Alluvial Chanels*. Danish Technical Press, Copenhagen.

Folk, R.L. y Ward, W.C. (1957): Brazos River Bar: a study in the significance of grain size parameters. *Journal of Sedimentary Petrology,* 27(1), 3-26.

García, J.M., Beguería, S., López, J.I., Lorente, A. y Seeger, M. (2001): *Los Recursos Hídricos Superficiales del Pirineo Aragonés y su Evolución Reciente*, Geoforma Ediciones, Logroño, 192p.

Geografia de Catalunya, Aedos, Barcelona, vol 1, 665 p.

Guillén, J., Díaz, J.I. y Palanques, A. (1992): Cuantificación y evolución durante el siglo XX de los aportes de sedimento transportado como carga de fondo por el río Ebro al medio marino. *Rev. Soc. Geol. España*, 5, 27-37.

Ibáñez, C., Prat, N. y Canicio, A. (1996): Changes in the hydrology and sediment transport produced by large dams on the Lower Ebro River and Its Estuary. Regulated Rivers: Research and Management, 12, 51-62.

Inbar, M. (1990): Effect of dams on montainous bedrock rivers. *Physical Geography*, 11, 4, 305-319.

Junta d'Aigües (1994): *Recomanacions sobre mètodes d'estimació d'avingudes màximes*, Generalitat de Catalunya, 164 p.

Kondolf, G.M. (1997): Hungry Water: Effects of Dams and Gravel Mining on River Channels. *Environmental Management*, 21, 4, 533-551.

Kondolf, G.M. y Matthews, W.V.G. (1993): *Management of coarse sediment in regulated rivers of California*. University of California Water Resources Center, Davis, California.

Kondolf, G.M. y Wolman, M.G. (1993): The sizes of salmonid spawning gravels. *Water Resources Reserach*, 29, 2275-2285.

Leopold, L.B., Wolman, M.G., y Miller, J.P. (1964): *Fluvial processes in geomorphology*. W. H. Freeman, San Francisco, 522 p.

López, J.I., Beguería, S. y García, J.M. (2002): Influence of the Yesa reservoir on floods of the Aragón River, central Spanish Pyrenees. *Hydrology and Earth System Sciences*, 6, 4, 753-762.

Maza, J.M, y García, M. (1996): *Transporte de Sedimentos*, Series del Instituto de Ingeniería, 584.

Moore, C.M. (1969): Effects of small structures on peak flows, En: Moore W.L. and Morgan, C.W. (eds.): *Effects of Watershed Changes on Streamflow*, University of Texas Press, Austin, 101-117.

Nelson, C.H. (1990): Post Messinian deposition rates and estimated river loads in the Ebro sedimentary system. En: Nelson, C.H. y Maldonado, A. (eds.): Marine Geology of the Ebro Continental Margin. *Marine Geology*, 95, 395-418.

Novoa, M. (1984): Precipitaciones y avenidas extraordinarias en Catalunya. *Ponencias y comunicaciones de las Jornadas de Trabajo sobre Inestabilidad de laderas en el Pirineo*, vol. 1., 1-15, Barcelona.

Petts, G.E. (1984): *Impouned Rivers. Perspectives for Ecological Management*. Wiley, New York, 326 p.

Prat, N. y Ibáñez, C. (1995): Effects of water transfers projected in the Spanish Hydrological Plan on the ecology of the Lower River Ebro (N.E. Spain) and Its Delta. *Wat. Sci. Tech.,* 31, 8, 79-86.

Sanz, M.E., Avendaño, C. y Cobo, R. (1999): Influencia de los embalses en el transporte de sedimentos hasta el río Ebro (España). En: *Hydrological and geochemical processes in large-scale river basins*. HIBAM, Manaus.

Sanz, M.E., Avendaño, C. y Cobo, R. (2001): Influencia del complejo de embalses Mequinenza-Ribarroja-Flix (Río Ebro) en la morfología del cauce situado aguas abajo. *Rev. Soc. Geol. España*, 14(1-2), 3-17.

Schoklitsch, A. (1950): *Handbuch des Wasserbaues*. Springer verlag, New York.

Shaw, E. (1983): *Hydrology in Practice*, Van Nostrand-Reinhold, Amsterdam, 322 p.

USACE (1993): *Engineering Manual EM 1110-2-1415*, Chapter 3. Flood Frequency Analysis, US Army Corps of Engineers.

Water Resources Council, *Guidelines for determining flood flor frequency*, Boletín 17B, U.S. Geological Survey, Reston, VA 22092, 1981.

Wilcock, P.R., Kondolf, G.M., Matthews, W.V. y Barta, A.F. (1996): Specification of sediment maintenance flows for a large gravel-bed river. *Water Resources Reserach*, 32, 2911-2921.

Williams, G.P. y Wolman, M.G. (1984): Downstream Effects of Dams on Alluvial Rivers. *US Geological Survey*, 83 p.

Wolman, M.G. (1954): A method of sampling coarse bed material. *American Geophysical Union, Transactions,* 951-956.

3. REFERENCES (references cited in the paper not included)

Assani, A.A., Petit, F. (2003): Impact of hydroelectric power releases on the morphology and sedimentology of the bed of the Warche River (Belgium). *Earth Surface Processes and Landforms* **29**(2): 133-143.

Avendaño, C., Sanz, M.E., Cobo, R. (2000): Embalses en el río Ebro: su influencia en la morfología del cauce y en los sólidos aportados al Delta. *Proceedings of the V Jornadas sobre encauzamientos fluviales*. Centro de Experimentación de Obras Públicas (CEDEX): Madrid; 1-12.

Batalla, R.J. (2003): Sediment deficit in rivers caused by dams and instream gravel mining. A review with examples from NE Spain. *Cuaternario y Geomorfología* **17**(3-4): 79-91.

Batalla, R.J., Kondolf, G.M., Gomez, C.M. (2004): Reservoir-induced hydrological changes in the Ebro River basin, NE Spain. *Journal of Hydrology* **290**: 117-136.

Bayerri, E. (1934-1935): *Historia de Tortosa y su comarca*. Imprenta Moderna de Alguerri: Tortosa.

Belaud, A., Carette, A. (2004): Reseach in the natural Alosa spawning reserve of Agen (Lot-et-Garonne, France). *Revue De Ecologie-La Terre Et La Vie* **59**(1-2): 273-282.

Brandt, S.A. (2000): Prediction of downstream geomorphological changes after dam construction: a stream power approach. *International Journal of Water Resources Development* **16**(3): 343-367.

Bunte, K., Abt, S.R. (2001): *Sampling surface and subsurface. Particle-size distributions in wadable gravel- and cobble-bed streams for analyses in sediment transport, hydraulics, and streambed monitoring*. U.S. Department of Agriculture, Forest Services, Rocky Mountain Research Station.

Carling, P.A. (1998): The concept of dominant discharge applied to two gravel-bed streams in relation to channel stability thresholds. *Earth Surface Processes and Landforms* **13**: 355-367.

Catalán, J.G. (1969): *Química del agua*. Blume, Barcelona.

Chen, Z.Y., Li, J.F., Shen, H.T., Wang, Z.H. (2001): Yangtze River of China: historical analysis of discharge variability and sediment flux. *Geomorphology* **41**(2-3): 77-91.

Enciclopèdia Catalana (1986): *Història Natural dels Països Catalans. 2. Geologia II*. Fundació Enciclopèdia Catalana, Barcelona; 548.

Goes, B.J.M. (2002): Effects of river regulation on aquatic macrophyte growth and floods in the Hadejia-Nguru wetlands and flow in the Yobe River, northern Nigeria; Implications for future water management. *River Research and Applications* **18**(1): 81-95.

Gorría, H. (1877): *Desecación de las marismas y terrenos pantanosos denominados de Los Alfaques*. Imprenta la Giralda, Madrid.

Grams, P.E., Schmidt, J.C. (2002): Streamfow regulation and multi-level flood plain formation: channel narrowing on the aggrading Green River in the eastern Unita Mountains, Colorado and Utah. *Geomorphology* **44**(3-4): 337-360.

Guillén, J., Palanques, A. (1992): Sediment dynamics and hydrodynamics in the lower course of a river highly regulated by dams: the Ebro River. *Sedimentology* **39**: 567-579.

Ibáñez, C., Prat, N., Canicio, A. (1996): Changes in the hydrology and sediment transport produced by large dams on the lower Ebro River and its estuary. *Regulated Rivers* **12**: 51-62.

Ibáñez, C., Rodrigues-Capituolo, A., Prat, N. (1995): The combined impacts of river regulation and eutrophication on the dynamics of the salt wedge and the ecology of the lower Ebro River. In *Ecological Basis for River Management*, John Wiley & Sons, Chichester; 105-114.

Inman D.L. (1976): *Man's impact on the California coastal zone*. Summary Report to California Department of Navigation and Ocean Development: Sacramento.

Jansson, R., Nilsson, C., Dynesius, M., Andersson, E. (2000): Effects of river regulation on river-margin vegetation: A comparison of eight boreal rivers. *Ecological Applications* **10**(1): 203-224.

Kellerhals, R., Church, M., Brai, D.I. (1976): Classification of river processes. *Journal of Hydraulics Division American Society of Civil Engineering* **6**: 18-31.

Knighton, D. (1998): *Fluvial Forms and Processes: a New Perspective*. Arnold, London; 386 p.

Kondolf, G.M. (1997): Hungry Water: Effects of Dams and Gravel Mining on River Channels. *Environmental Management* **21**(4): 533-551.

López, J.I., Beguería, S., García, J.M. (2002): Influence of the Yesa reservoir on floods of the Aragón River, central Spanish Pyrenees. *Hydrology and Earth System Sciences* **6**(4): 753-762.

Meybeck, M. (1987): Global chemical weathering of surficial rocks estimated from river dissolved loads. *American Journal of Science* **287**: 401-428.

Milliman, J.D., Meade, R.H. (1983): World-wide delivery of river sediment to the oceans. *Journal of Geology* **91**: 1-21.

Milliman, J.D., Syvitski, J.P.M. (1992): Geomorphic/tectonic control of sediment discharge to the ocean: the importance of small mountainous rives. *Journal of Geology* **100**: 525-544.

Muñoz, I. (1990): *Limnologia de la part baixa del riu Ebre I els canals de reg: Els factors físico químics, el fitoplancton i els macroinvertebrats bentònics*. PhD thesis, Department of Biology, University of Barcelona.

Nelson, C.H. (1990): Post Messinian deposition rates and estimated river loads in the Ebro sedimentary system. In *Marine Geology of the Ebro Continental Margin,* Nelson C.H., Maldonado A. (eds.). Marine Geology; **95**: 395-418.

Novoa, M. (1984): Precipitaciones y avenidas extraordinarias en Catalunya. *Proceedings of the Jornadas de Trabajo sobre Inestabilidad de laderas en el Pirineo*: Barcelona; 1-15.

Palanques, A. (1987): *Dinámica sedimentaria, meneralogía y microcontaminantes inorgánicos de las suspensiones y de los sedimentos superficiales en el margen continental del Ebro.* PhD Thesis, University of Barcelona.

Petts, G.E. (1984): *Impounded Rivers. Perspectives for Ecological Management*. Wiley, New York; 326 p.

Petts, G.E. (1987) Time-scales for ecological change in regulated rivers. In *Regulated Streams. Advances in Ecology*, Craig, J.F., Kemper, J.B. (eds). Plenum, New York; 257–266.

Phillips, J.D., Slattery, M.C., Musselman, Z.A. (2004): Dam-to-delta sediment inputs and storage in the lower Trinity River, Texas. *Geomorphology* **62**(1-2): 17-34.

Poff, N.L., Allan, J.D., Bain, M.B., Karr, J.R., Prestegaard, K.L., Richter, B.D., Sparks, R.E., Stromberg, J.C. (1997) : The natural flow regime: a paradigm for river conservation and restoration. *Bioscience* **47**(11): 769-784.

Roura, M. (2004): *Incidència de l'embassament de Mequinensa en el transport de sòlids en suspensió i la qualitat de l'aigua del riu Ebre*. PhD Thesis, Facultat de Biologia, Universitat de Barcelona, Barcelona, 145 pp.

Sanz, M.E (1998): Caracterización textural y composi-cional del sedimento en embalses españoles. *Jornada sobre sedimentación en embalses*.

Sanz, M.E., Avendaño, C., Cobo, R. (1999): Influencia de los embalses en el transporte de sedimentos hasta el río Ebro (España). *Proceedings of the Congress on Hydrological and geochemical processes in large-scale river basins*. HIBAM: Shahin, 1985

Sierra, J.P., Sánchez-Arcilla, A., Figueras, P.A., González del Río, J., Rassmussen, E.K., Mösso, C. (2004): Effects of discharge reductions on salt wedge dynamics of the Ebro River. *River Research and Aplications* **20**: 61-77.

Schumm, S.A. (1977): *The fluvial system*. Wiley-Interscience, New York.

Surian, N., Rinaldi, M. (2003): Morphological response to river engineering and management in alluvial channels in Italy. *Geomorphology* **50**: 307-326.

Varela, J., Gallardo, A., López de Velasco, A. (1986): Retención de los sólidos por los embalses de Mequinenza y Ribarroja. Efectos sobre los aportes al Delta del Ebro. In *El Sistema Integrado del Ebro*, M. Mariño (ed.). Gráficas Hermes, Madrid; 203-219.

Vericat, D., Batalla, R.J. (2004): Efectos de las presas en la dinámica fluvial del curso bajo del río Ebro. *Cuaternario y Gemorfología* **18**(1-2): 37-50.

Vericat, D., Batalla, R.J. (2005): Sediment transport in a highly regulated fluvial system during two consecutive floods (Lower Ebro River, NE Spain). *Earth Surface Processes and Landforms* **30**.

Vörösmarty, C.J., Meybeck, M., Fekete, B., Sharma, K., Green, P., Syvitski, J.P.M. (2003): Anthropogenic sediment retention: major global impact from registered river impoundments. *Global and Planetary Change* **39**(1-2): 169-190.

Walling D.A., Webb, B.W. (1983): Patterns of sediment yield. In: *Background to Paleohydrology,* K.J. Gregory (ed.). John Wiley and Sons: Chichester; 69-100.

Williams, G.P., Wolman, M.G. (1984): *Downstream Effects of Dams on Alluvial Rivers*. US Geological Survey Professional Paper 1986.

World Commission on Dams (2000): *Dams and development. A new framework for decision making*. Earthscan, London; 322.

CHAPTER 2

METHODS

INDEX CHAPTER 2: METHODS

Figure captions (figures in the papers not included)

Figure 2.1. Sediment transport monitoring sections: (a) Sástago, upstream from the Mequinenza Dam (b) Móra d'Ebre, below Flix Dam. The dashed blue line represents the mean water depth in each section. See figure 3 in chapter 1 for the location of the sections

Figure 2.2. (a) Location of the monitoring sections downstream the Flix Dam (the inserted table indicates the distance between the Flix Dam and each section), and the location of the Móra d'Ebre sediment transport monitoring section (see Figure 2.1b). (b) Painted pebbles placed in the monitored section n.1. (c) Scour chains after the 2002-2003 hydrological year: left photo shows sedimentation, while right photo shows erosion in n.4 and n.2, respectively . (d) Bed-material sampling. (e) River cross-sections in n.7

Figure captions in the papers

Vericat, D., Church, M., Batalla, R.J. (2005): Bedload bias: Comparison of measurements obtained using two Helley-Smith samplers in a gravel-bed river. *Water Resources Research* (accepted)

Figure 1 (**C**hapter **2** **P**aper **1**). Location of the study section in the lower Ebro River (NE Iberian Peninsula)

Figure 2 (C2P1). Ebro River bed surface and subsurface grain-size distributions at *Móra d'Ebre B* (Figure 1). Bulk grain-size distribution in the East Fork River [*Emmett*, 1980]. Grain- size distribution for bed surface (obtained in riffles) and subsurface material in Harris Creek [*Sterling and Church*, 2002]

Figure 3 (C2P1). (a) Cable suspended Helley-Smith sampler 76-mm intake and (b) Cable suspended Helley-Smith sampler 152-mm intake at the Móra d'Ebre Monitoring Section

Figure 4 (C2P1). (a) Load-rating curve for all bedload samples obtained during the hydrological year 2003-2004. Gray dashed lines show the envelope of data for each device (HS76 and HS152). (b) Mean load-rating curve corresponding to each Helley-Smith sampler bedload database, obtained by averaging all samples at 1 m^2/s wide bins from 4 to 11 m^2/s. Note that: i) error ranges represent 95% confidence intervals about the individual averages, and ii) positive and statistically significant relations with specific discharge (q) ($p<0.01$) for each device are calculated, and iii) solid and dashed lines define the relation for the HS152 and HS76, respectively

Figure 5 (C2P1). Relation between stream power (ω) and bedload transport rate (i_b) for different fluvial environments

Figure 6 (C2P1). (a) River bed surface material at MEMS (*Móra d'Ebre B*) *bar* and scaled plan of the two Helley-Smith samplers (76-mm and 152-mm intakes). Note the difference between the sampler nozzles (A_s) in relation to the bed material. Possible sources of errors

related to the bed material size and the Helley-Smith samplers' nozzles sizes are: (b) blockage of the HS nozzle when the sampler is located behind a coarse particle (front view). Note that the mouth of the HS152 is less covered than that of the HS76 under the same conditions; and (c) samplers not deposited flush with the bed surface due to the bed roughness (front view). Note that the samplers can adjust (dashed lines): 'tilting of the samplers'

Figure 7 (C2P1). (a) Line-by-frequency distributions: cumulative density functions at East Fork River, Harris Creek and Ebro River. Theoretical probabilities of interference with the sampler: a) blockage (right *y* axis), and b) hanging (left *y* axis); (b) as (a) scaled for sampler nozzle width (76 mm opening on the lower abscissa; 152 mm opening on the upper abscissa)

Figure 8 (C2P1). (a) Load-rating relation for all paired bedload samples obtained with HS152 and HS76 samplers (Table 1). Gray straight and dashed lines show the envelopes of the data for the HS152 and HS76 respectively (and are the same as those in figure 4a). (b) Correlation of each pair of samples in group A and B. (c) Estimated median efficiency by grain size for the HS76 bedload samples in group A and B. Median efficiency has been calculated by dividing each collection rate by size obtained with the HS76 by the rate by size collected with the HS152

Figure 9 (C2P1). (a) Relation between $R_{Dmax\text{-}bl}$ and specific discharge (q) for the samples in group A, where $R_{Dmax\text{-}bl} = D_{max\text{-}bl}/A_s$, $D_{max\text{-}bl}$ is the maximum particle collected and A_s is the sampler's nozzle width of each sampler. Note that the grey dashed line shows the expected relation for equivalent grain size (two times the relation for the HS152 —). (b) Relation between $R_{Dmax\text{-}bl}$ and specific discharge (q) for the samples in group B. Note that the grey dashed line shows the relation between $R_{Dmax\text{-}bl}$ and specific discharge (q) for the HS152 in group A

Figure 10 (C2P1). (a) Paired samples obtained with the HS152 and maximum potential load-rating curve. The dashed line delimits the rest of samples in group A. (b) Paired samples taken with the HS76 and maximum potential load-rating curve defined with HS152 samples (as in figure 10a). The dashed line delimits the rest of samples in group A

Vericat, D. and Batalla, R.J. (2004): Bedload variability under low sediment transport conditions in the lower Ebro River (NE Spain). En: Batalla, R.J. and Garcia, C. (eds.): *River/Catchment Dynamics: Natural Processes and Human Impacts*, IAHS Red Book (in press)

Figure 1 (**C**hapter **2** **P**aper **2**). Location of the monitoring section in the lower Ebro River (NE Iberian Peninsula)

Figure 2 (C2P2). Bed load sampling section in Móra d'Ebre (Fig. 1). Sampling verticals and water stage at 900 $m^3 s^{-1}$ are indicated

Figure 3 (C2P2). Mean fractional bed load transport rate as a function of relative size. The mean fractional transport rate (i_{bi} in g $m^{-1}s^{-1}$) has been scaled by the proportion of each size fraction in the surface bed material ($f_{i\text{-}s}$). Relative size has been calculated scaling each size (D_i) by the median bed surface size ($D_{50\text{-}s}$) in 2004. Vertical lines represent the standard deviation around the mean ($\varepsilon=\sigma/\sqrt{N}$, where σ is the standard deviation and N the number of data)

Figure 4 (C2P2). Mean bed load transport rate at each vertical during the 5 transects. Vertical lines represent the standard deviation around the mean

Table captions (tables in the papers not included)

Table 2.1. Fieldwork design in the lower Ebro River

Table captions in the papers

Vericat, D., Church, M., Batalla, R.J. (2005): Bedload bias: Comparison of measurements obtained using two Helley-Smith samplers in a gravel-bed river. *Water Resources Research* (accepted)

Table 1 (C2P1). Paired samples collected successively with both HS76 and HS152 devices

Table 2 (C2P1). Probability that samples collected with each device are biased, not biased, or insufficient evidence to classify

Table 3 (C2P1). Annual load (2003-2004) estimated for the mean load-rating curve for each Helley Smith sampler (see mean load-rating curves in the Figure 4b), and for the maximum potential load-rating curve for the HS152 (in Figure 10)

Vericat, D. and Batalla, R.J. (2004): Bedload variability under low sediment transport conditions in the lower Ebro River (NE Spain). En: Batalla, R.J. and Garcia, C. (eds.): *River/Catchment Dynamics: Natural Processes and Human Impacts*, IAHS Red Book (in press)

Table 1 (C2P2). Bed load transport rates collected during the five transects at each vertical

Table 2 (C2P2). Vertical variance in each transect (v_n, where v_n is the variance of each vertical *n* at a given transect *t* around the sampling mean)

1. INTRODUCTION

This chapter describes the fieldwork designed and carried out to measure sediment transport and to monitore river morphology during 2002-2004 in the lower Ebro River. Special emphasis is devoted to the explanation of bedload transport sampling. For this purpose we present two papers in the analysis of the bedload sampling procedures. Papers are presented maintaining their original format. The first paper is accepted in the journal *Water Resources Research* (Vericat *et al.*, 2005). The work shows how the size of the Helley-Smith bedload sampler nozzle affects the accuracy of bedload sampling. Two different Helley-Smith samplers have been compared in the lower Ebro, and the trend indicate that the use of the biggest sampler (152-mm intake), has a probability of the samples collected to be interfered by the device less than the 10%. The second paper is accepted for publication (in press) in the IAHS Red Book: *River/Catchment Dynamics: Natural Processes and Human Impacts* (edited by Batalla, R.J. and Garcia, C.). The paper describes the bedload transport regime observed under low sediment transport conditions and constant discharge; it studies the temporal and spatial bedload transport variability under steady flow conditions. This is an important element to estimate errors on calculation of annual sediment loads.

2. FIELDWORK DESIGN

A complete sediment transport and fluvial processes monitoring program has been undertaken between 2002 and 2004 in the lower Ebro River. The sampling programme was established to obtain reliable data on sediment transport and to study on-going morphological effects downstream from the Flix Dam. The monitoring programme includes sampling of suspended and bedload transport at the Sástago Monitoring Section upstream from the Mequinenza Dam (Figure 2.1a), and at the Móra d'Ebre Monitoring Section below the Flix Dam (Figure 2.1b). Special attention has been devoted to the measurement of sediment transport during floods. A total of 551 samples of water were collected during floods and subsequently analysed to obtain the suspended sediment concentrations. Bedload transport was characterized using 304 samples. Largest clasts were measured in all the samples and subsequently dried, sieved and weighted in order to obtain the bedload transport rates and their grain-size distributions. A total of 21 velocity

profiles were obtained in a range of flows from 750 to 2,200 m^3/s. At the same time water depth and channel width were measured. In addition, nine sections (river-bars) below Flix Dam were monitored to study sedimentary processes (Figure 2.2). Bars are mainly central and have several degrees of vegetation cover. In each bar we have placed painted cobbles (Figure 2.2b) and installed two scour chains (Figure 2.2c). Moreover, grain-size distributions (Figure 2.2c) for both the surface and subsurface river-bed material and topographic cross-sections (Figure 2d) were done before and after floods (Table 2.1). Measurements has been done within the research project *Elaboración de una metodología de base física para la preparación de crecidas generadoras aguas abajo de embalses: Aplicación al tramo inferior del río Ebro (REN2001-0840-C02-01/HID)*coordinatde by the University of Lleida.

Table 2.1. Fieldwork design in the lower Ebro River

Tasks	
Monitored sections	11
Sediment transport	2
River-bed processes	9
Hydraulic measurements	21
Bedload samples	
Number	304
Total weight (kg)	624
Suspended load samples	
Number	551
Total volume (l)	140
Bed-material samples	
Number	27
Total weight (kg)	2,997
Particles measured	4,100

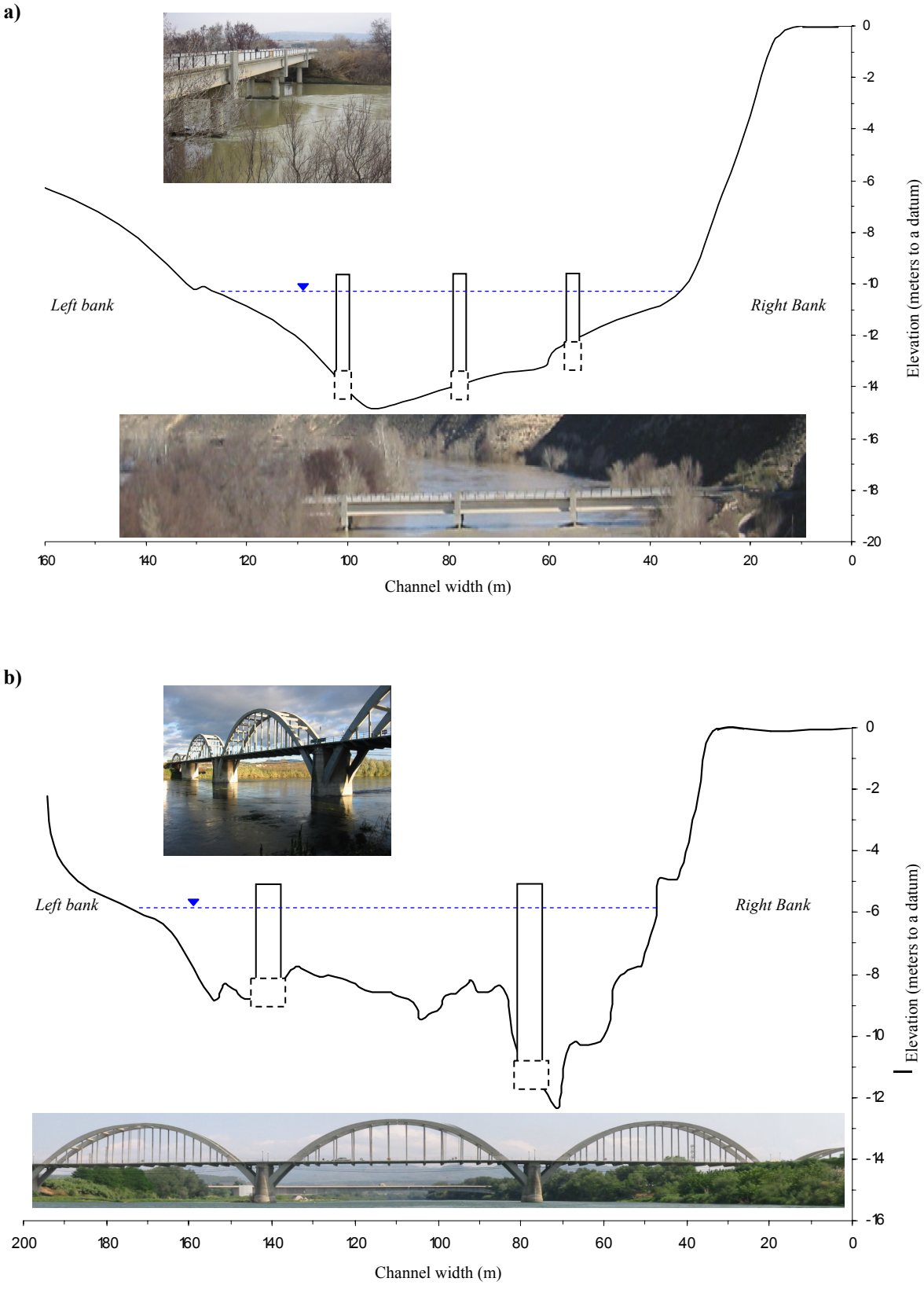

Figure 2.1. Sediment transport monitoring sections: (**a**) Sástago, upstream from the Mequinenza Dam (b) Móra d'Ebre, below Flix Dam. The dashed blue line represents the mean water depth in each section. See figure 3 in chapter 1 for the location of the sections

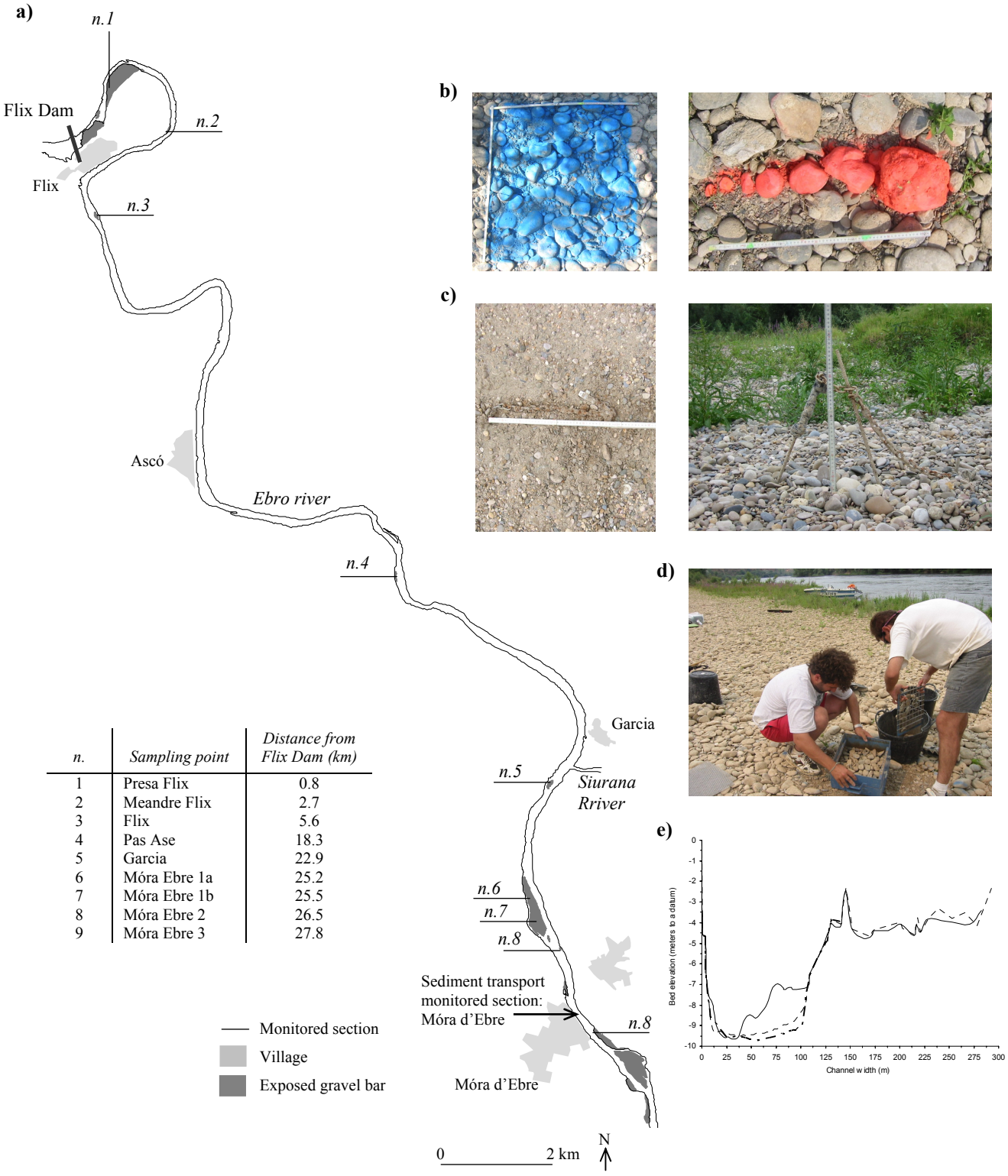

n.	*Sampling point*	*Distance from Flix Dam (km)*
1	Presa Flix	0.8
2	Meandre Flix	2.7
3	Flix	5.6
4	Pas Ase	18.3
5	Garcia	22.9
6	Móra Ebre 1a	25.2
7	Móra Ebre 1b	25.5
8	Móra Ebre 2	26.5
9	Móra Ebre 3	27.8

Figure 2.2. (**a**) Location of the monitoring sections downstream the Flix Dam (the inserted table indicates the distance between the Flix Dam and each section), and the location of the Móra d'Ebre sediment transport monitoring section (see Figure 2.1b). (**b**) Painted pebbles placed in the monitored section n.1. (**c**) Scour chains after the 2002-2003 hydrological year: left photo shows sedimentation, while right photo shows erosion in n.4 and n.2, respectively . (**d**) Bed-material sampling. (**e**) River cross-sections in n.7

3. SAMPLING OF BEDLOAD TRANSPORT

Vericat, D., Church, M., Batalla, R.J. (2005): Bedload bias: Comparison of measurements obtained using two Helley-Smith samplers in a gravel-bed river. *Water Resources Research* (accepted)

Bedload bias: comparison of measurements obtained using two Helley-Smith samplers in a gravel-bed river

Abstract

This paper assesses how the size of the Helley Smith (HS) bedload sampler nozzle affects the accuracy of bedload sampling. The work analyses the equivalence of the sediment trapped by two HS samplers (76-mm and 152-mm intake) during floods in the lower Ebro gravel-bed river. Results show that: a) the bias of the HS76 with respect to the HS152 increases with discharge, b) most bedload rates were higher when the sampling was done with the HS152 than with the HS76 and c) the probability of a bedload sample collected with the HS152 to be biased is less than the 10%, whereas more than 60% of samples are biased when they are obtained with the HS76. The analysis demonstrates that the use of samplers with intake size that interfere less with sampling, will both increase the accuracy of particle entrainment determination and hence the precision of annual loads estimation in gravel-bed rivers.

Key words: bedload transport, Helley-Smith sampler, sampling bias, gravel-bed rivers

1. Introduction

Bedload transport can be highly variable [*Einstein*, 1937; Gomez et al., 1989]. This circumstance presents important problems for the calibration and use of bedload samplers [*Emmett*, 1980; *Hubbell*, 1987]. Bedload measurement remains a major obstacle to understanding sediment transport in gravel-bed rivers.

The most widely deployed bedload samplers are the basket types, in which the moving sediment enters a nozzle and is trapped in a bag or basket. *Helley and Smith* [1971] designed a pressure-difference bedload sampler for use in natural streams carrying fine gravels. First tests in a flume transporting sand showed that the sampler might consistently overregister by about 50%, a result confirmed in a field test by *Sterling and Church* [2002]. *Helley and Smith* observed that, when the sampler was raised from the bed, it tended to scoop additional material, and reported that the performance of the sampler would be dependent on the bed material size. *Johnson et al.* [1977] reported clogging of the sampler's bag as another source of bias for the Helley-Smith (hereafter HS) design. In the East Fork River, Wyoming, *Emmett* [1980] completed the first field calibration of the original device. He reported for the 76-mm intake HS sampler an efficiency of 1 (i.e., the real bedload rate tends to be the same as that collected with the sampler) for particles between 0.5 and 16 mm, approximately the range of sizes for which the sampler was designed. *Hubbell* [1987] determined in a laboratory flume that the device's efficiency decreases as grain size and bedload rates increase. Changes in the efficiency of modified HS samplers have also been reported. For instance, in Goodwin Creek, central Mississippi, *Kuhnle* [1992] estimated an efficiency of 1 for a device with a trapezoidal nozzle modified from a 76-mm intake HS sampler, while *Ryan and Porth* [1999] reported, on the basis of measurements in two cobble-bed streams, that slight modifications of three HS samplers of 76-mm intake generated substantially different collections of bedload.

Various attempts have been made to asses the efficiency of this sampler in gravel-bed rivers. In the Drau River of Austria, a coarse gravel channel, *Habersack and Laronne* [2002] calculated for a 152-mm intake HS sampler an efficiency close to unity by comparing the device's bedload rates and slot sampler bedload rates. However, in Harris Creek (median surface material between 45 mm and 75 mm), British Columbia, *Sterling*

and Church [2002], by comparing magnitude and grain size distributions of sediment samples collected by a pit trap and by a standard HS sampler (76-mm intake), reported a clear bias of the bedload samples collected with the HS device. *Bunte et al.* [2004] tested bedload transport measurements in two gravel and cobble bedded rivers and concluded that the HS measurements were biased as bedload ratings were well defined and steeper using bedload traps than those obtained with an HS sampler (76-mm intake). Even so, and as a consequence of the lack of choices, this sampler has often been deployed in coarse gravel-bed rivers [e.g., *Andrews*, 1994], and even on cobble-beds [e.g., *Ryan and Porth*, 1999], without attempt to reassess the sampler's efficiency or accuracy. In particular, no assessment has been made of the relation between sampler intake dimension, river bed material size, and the probability that the samples will be biased. These concerns motivate our efforts to understand how the relative size of the HS sampler's nozzle might affect the accuracy of the sampling and the precision of bedload measurements or loads. A significant goal in this paper is the field evaluation of the equivalence of the sediment trapped by two HS samplers respectively with 76-mm and 152-mm intake. We subsequently compare the bedload yields predicted by the load-rating curves elaborated by the two devices.

2. Methods

2.1. Study site

Bedload was sampled in the lower Ebro River (NE Iberian Peninsula) at Móra d'Ebre Monitoring Section (**MEMS**) (Figure 1 (C2P1)). Mean annual runoff at Tortosa, 49 km downstream from MEMS, is 13,400 hm^3 (1 $hm^3 = 10^6 m^3$), where maximum peak flow was estimated by *Novoa* [1984] to be around 12,000 m^3/s in 1907. Today, close to 190 reservoirs impound almost 60% of the catchment's annual runoff, most of them constructed between 1950 and 1975, reducing magnitude and frequency of floods in the lowermost reaches of the basin [*Batalla et al*., 2004]. The maximum discharges recorded at Tortosa in the post-dams period has been 3,300 m^3/s in 1982, much lower than that estimated for 1907. The median slope at the sampling section is $8.5 \cdot 10^{-4}$ [*Vericat and Batalla*, 2004]. Bed material was characterized before the samples were taken. Surface and

subsurface materials were sampled at the two exposed bars closest to MEMS. *Móra d'Ebre A* bar is located about 1 km upstream, while *Móra d'Ebre B* is just one-hundred meters downstream (Figure 1 (C2P1)). Surface and subsurface size distributions show small differences between both bars (less than 5%), therefore, the closest bar (*Móra d'Ebre B*) has been chosen to characterize the river bed material at MEMS (Figure 2 (C2P1)). The median surface material size is 39 mm ($D_{50\text{-}s}$), and maximum surface particle almost 90 mm ($D_{95\text{-}s}$= 86 mm). However, subsurface bed material size is 21 mm ($D_{50\text{-}ss}$), while $D_{95\text{-}ss}$ is 62 mm (Figure 2 (C2P1)). The bed armour ratio (A_r), measured as the ratio of median surface ($D_{50\text{-}s}$) to median subsurface ($D_{50\text{-}ss}$) bed material size [e.g., *Church et al., 1987*] is 1.8.

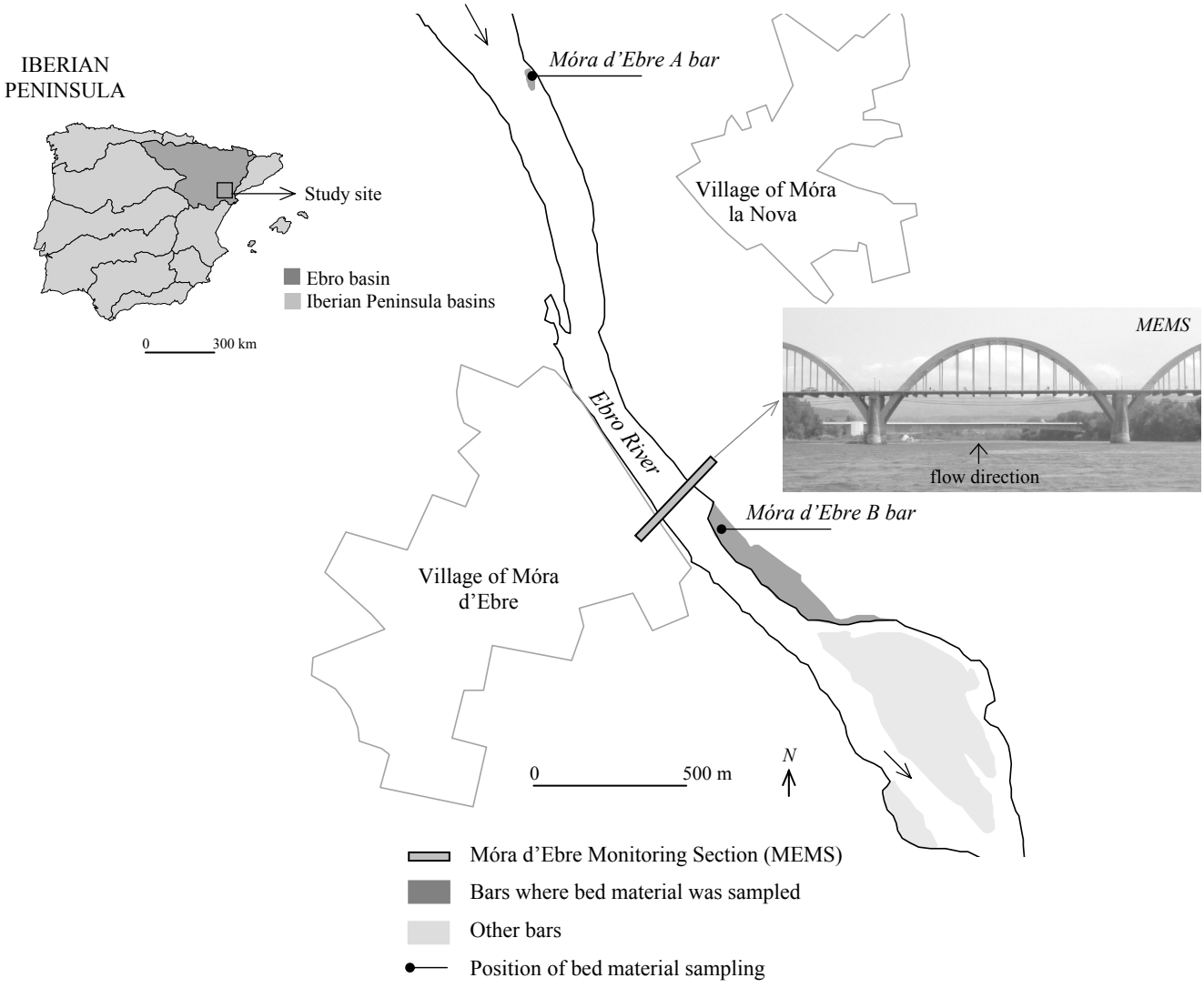

Figure 1 (C2P1). Location of the study section in the lower Ebro River (NE Iberian Peninsula)

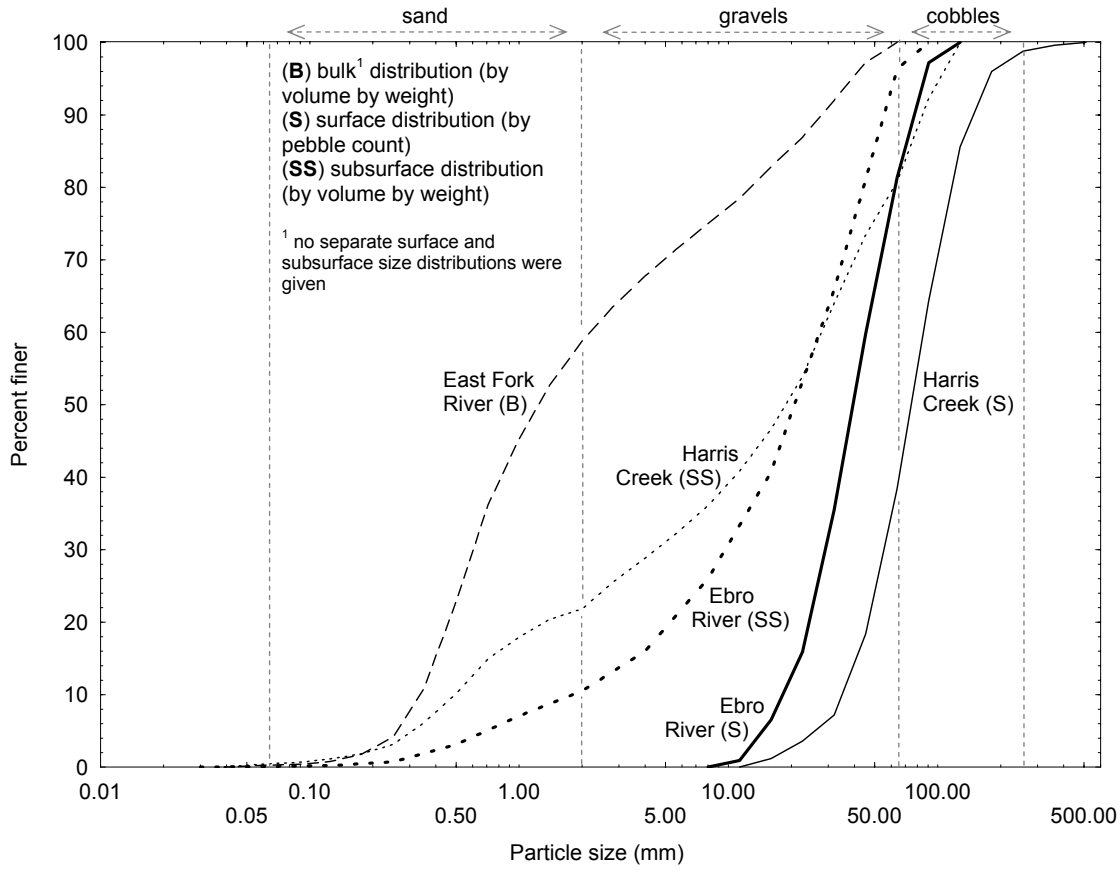

Figure 2 (C2P1). Ebro River bed surface and subsurface grain-size distributions at *Móra d'Ebre B* (Figure 1 (C2P1)). Bulk grain-size distribution in the East Fork River [*Emmett*, 1980]. Grain- size distribution for bed surface (obtained in riffles) and subsurface material in Harris Creek [*Sterling and Church*, 2002]

2.2. Sampling program

Bedload transport was sampled from a bridge at a single vertical (MEMS, Figure 1 (C2P1)) during 2003-2004 using a 29-kg cable-suspended HS sampler with a 76-mm intake (**HS76**) (Figure 3a (C2P1)), and a 76-kg cable suspended HS sampler with a 152-mm intake (**HS152**) (Figure 3b (C2P1)). Fifty-four bedload samples were obtained with the HS76, while forty-seven were taken with the HS152. Twenty-three of these samples were paired; that is, they were obtained with only few minutes difference in time (the difference being the recovery and deployment time for the samplers). The sampling time for both devices was 5 minutes. Water depth at the place where bedload was sampled ranged from 3 to 5 meters, while mean velocity varied from 1.5 to 2 m/s. The samples were taken to the laboratory, where they were dried, sieved and weighed. The samples were

truncated at 1 mm (excluding in any case no more than 5% of the total sample weight) before obtaining the total mass and grain size distribution in order to avoid including particles that could be transported in suspension. Discharge during sampling ranged from 500 to 1,350 m^3/s, while specific discharge at the vertical where samples were obtained varied from 4.5 to 10.6 m^2/s.

Figure 3 (C2P1). (**a**) Cable suspended Helley-Smith sampler 76-mm intake and (**b**) cable suspended Helley-Smith sampler 152-mm intake at the Móra d'Ebre Monitoring Section

2.3. General comparison between the HS samplers

Load-rating relations between specific discharge at the vertical where samples were collected (q in m^2/s) and bedload transport rates (i_b in g/ms) differentiated by sampler have been constructed for the samples collected. Figure 4a (C2P1) shows that the envelope of each load-rating curve is, practically the same. However, for a given specific discharge the

bedload rate collected by each device can vary over one order of magnitude. For instance, for a specific discharge of 10.4 m^2/s the bedload transport rate collected with the HS152 was 340 g/ms, while with the HS76 it was 48 g/ms. This difference could be attributed to: a) bias between samplers, or b) different conditions the when samples were taken (i.e., the samples were not obtained at the same time, so that river bed features and transport could be different in each sampling). Furthermore, it is evident that each sampler can individually return as wide a range of catches at essentially the same flow. Temporal variations in bedload transport under near-steady conditions have been reported by various authors [e.g., *Hamamori*, 1962; Gomez et al., 1989] and also could influence the comparison of samples.

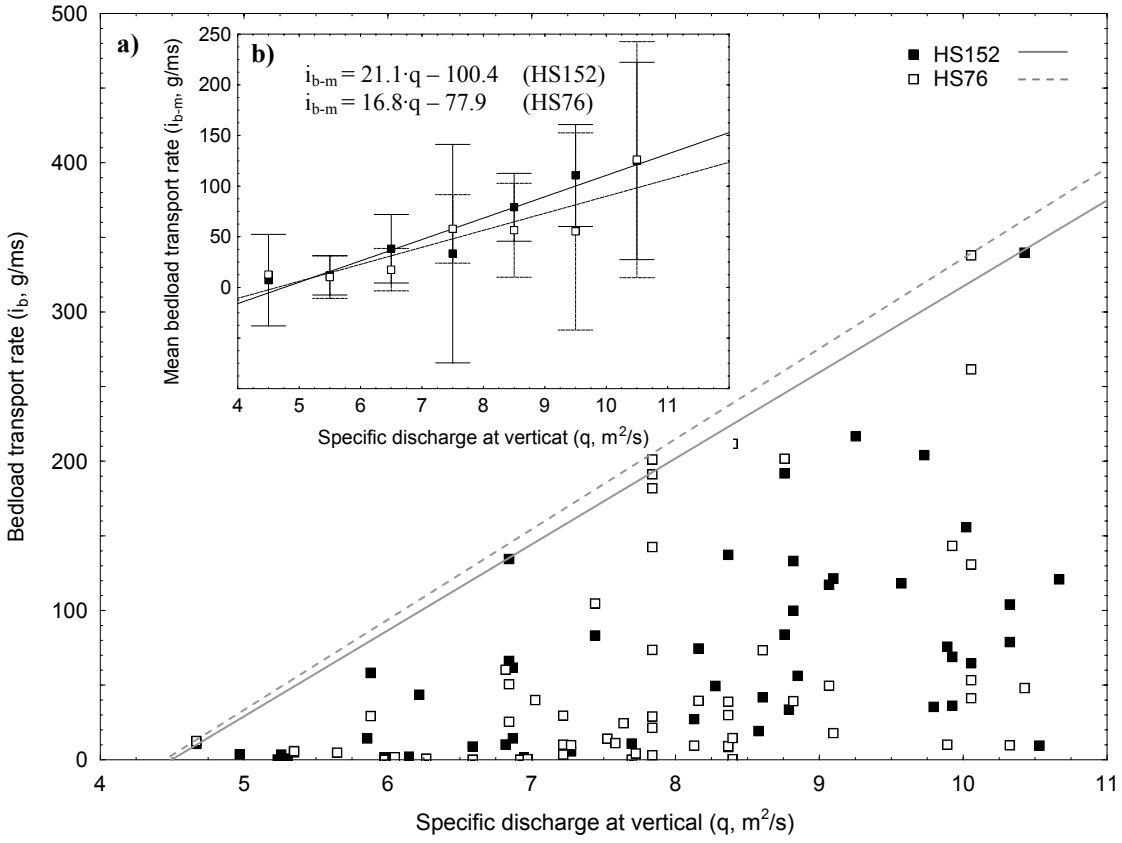

Figure 4 (C2P1). (**a**) Load-rating curve for all bedload samples obtained during the hydrological year 2003-2004. Gray dashed lines show the envelope of data for each device (HS76 and HS152). (**b**) Mean load-rating curve corresponding to each Helley-Smith sampler bedload database, obtained by averaging all samples at 1 m^2/s wide bins from 4 to 11 m^2/s. Note that: i) error ranges represent 95% confidence intervals about the individual averages, and ii) positive and statistically significant relations with specific discharge (q) ($p<0.01$) for each device are calculated, and iii) solid and dashed lines define the relation for the HS152 and HS76, respectively

Figure 5 (C2P1) shows that, in different rivers, bedload transport presents high temporal variability which has been attributed to the stochastic behaviour of the sediment transport. The data from Goodwin Creek [*Kuhnle*, 1992] were obtained with a modified HS76, for which, due the sampling procedure, sampler efficiency was 100%. Under such conditions, the high variability of bedload rates under similar stream power would be attributed to the natural behaviour of the bedload transport rates rather than to bias during the sampling. Moreover, various laboratory experiments corroborate the high bedload variability [e.g., *Kuhnle and Southard*, 1988]. The rest of the data in figure 5 (C2P1) show that the MEMS data are typical of bed load transport observed in gravel bed channels and exhibit similar variability. There is no obvious reason to conclude that MEMS data are biased.

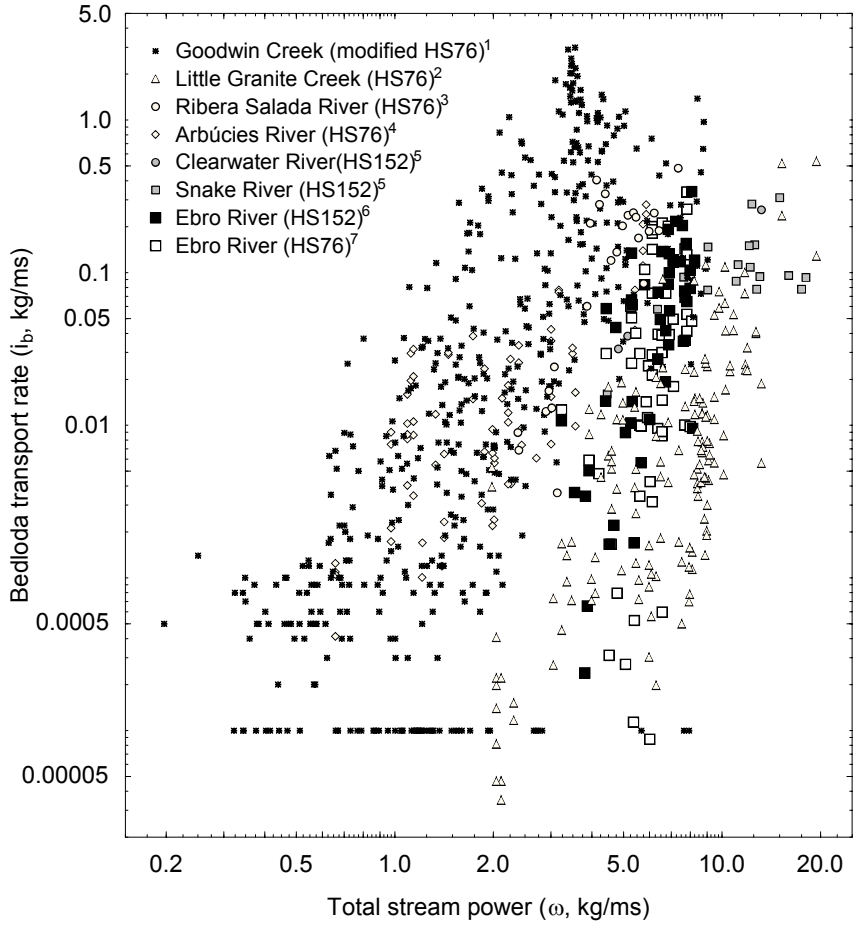

[1]data from *Kuhnle* [1992]
[2]data from *Ryan and Emmett* [2002]
[3]data from *Batalla et al.* [2004]
[4]data from *Batalla* [1997]
[5]data from *Jones and Seitz* [1980]
[6]data from this study (HS152)
[7]data from this study (HS76)

Figure 5 (C2P1). Relation between stream power (ω) and bedload transport rate (i_b) for different fluvial environments

A mean load-rating curve for the data of each sampler was defined by averaging the samples in 1 m^2/s wide bins from 4 to 11 m^2/s (Figure 4b (C2P1)) in order to eliminate the temporal variability of the bedload transport cited above, hence to define the mean bedload transport rate ($i_{b\text{-}m}$ in g/ms) given specific flow (i.e., q) for each device [e.g., *Kuhnle*, 1992]. Figure 4b (C2P1) shows that there is an apparent bias between the two samplers and that the bias of the HS76 with respect to the HS152 increases with specific discharge. The scatter of the mean rates is also higher for the HS76 than for the HS152 and, as a consequence, the correlation with specific discharges is greater for the HS152 (r^2= 0.58) than for the HS76 (r^2= 0.24).

3. Sources of bias

3.1. Sampler efficiency

The relation between bed material size and the sampler intake width (Figure 6a (C2P1)) must be an important determinant of sampler efficiency, which may not be constant for all sediment sizes (Figure 6a (C2P1)). According to *Emmett* [1980] the efficiency of the HS76 is close to unity for particle sizes between 0.5 and 16 mm, but decreases when the particles transported are larger than 16 mm. The nozzle width of his sampler (A_{HS76}) was 76 mm. The ratio between the *b* axis of the largest size for which the efficiency was considered by *Emmett* [1980] to be close to 100% (D_i= 16 mm) and the sampler's nozzle width is 0.2. Emmett also reported that the efficiency decreased to 70% for particles between 16 and 32 mm (D_i/A_{HS76} = 0.42, where D_i is equal to 32 mm). Trap efficiency obviously goes to zero when the particle size is the same as the sampler's nozzle. According to the movement of particles during their transport, the *a*-axis of the particles may actually be the critical axis to be compared with the sampler's width, especially in rivers with low particle roundness, which is not the case of the Ebro (Figure 6 (C2P1)). Nevertheless, *a*-axis values are not often available. This first observation from *Emmett's* [1980] calibration gives some indication, then, of the propensity of the moving grain D_i to fit into the nozzle opening, which will become a more severely limiting factor as $D_i \rightarrow A$.

Sterling and Church [2002], by comparing magnitude and grain size distributions of sediment samples collected by a pit trap and a standard HS sampler (76-mm intake), reported efficiencies higher than 1 for particles smaller (*b* axis) than 0.5 mm, presumably because the sampler was catching suspended sand, while efficiencies declined for particles between 0.5 and 16 mm (D_i/A_{HS76} = 0.2, where D_i is equal to 16 mm). They estimated a median efficiency of 0 for particles larger than 8 mm, while the pit trap collected particles up to 32 mm. Compared with *Emmett's* [1980] calibration, in spite of using the same HS sampler, there is a large difference in the sampler's apparent grain size dependent efficiency. In the study by *Sterling and Church*, the trapping efficiency declined for all sizes larger than coarse sand and approached zero when the *b* axis exceeded 10% of the sampler's width, while in *Emmett's* [1980] study the efficiency decreased when the particle size exceeded 20% of the sampler's width, or some modestly larger proportion.
Comparing bed material grain size distributions from both study sections (Figure 2 (C2P1)) we can see that the relation between the bed material size and the sampler intake is greatly different. The largest particles in East Fork River [*Emmett*, 1980] attain 64 mm, while the median surface material in Harris Creek [*Sterling and Church*, 2002] is 75 mm. Thus, in Harris Creek half of the surface material exceeds in size the sampler's width; however, in East Fork River bed particles do not attain a size equivalent to the sampler's width. Two principal sources of interference with the collection of bedload using the HS sampler can be invoked to explain the differences between the outcomes: a) 'blockage' of the sampler's nozzle (Figure 6b (C2P1)), and b) 'hanging' of the sampler's intake (Figure 6c (C2P1)).

3.2. Sources of interference

When the sampler is positioned immediately downstream from a coarse clast (Figure 6b (C2P1)), the flow may be competent to move the clast, or it may not be competent and the clast will remain to block the entrance of the sampler. In the first case, as we have explained above, the propensity of that clast to pass through the nozzle opening will be related to the ratio D_i/A_s. However, when the flow strength is not high enough to move it, it will block the entrance of the sampler, reducing the sampler's operative width and decreasing the probability to catch the moving sizes. For any grain size D_i, the ratio D_i/A_s indicates the capacity of the grain to interfere with bedload sampling by decreasing the sampler's effective nozzle width (A_s).

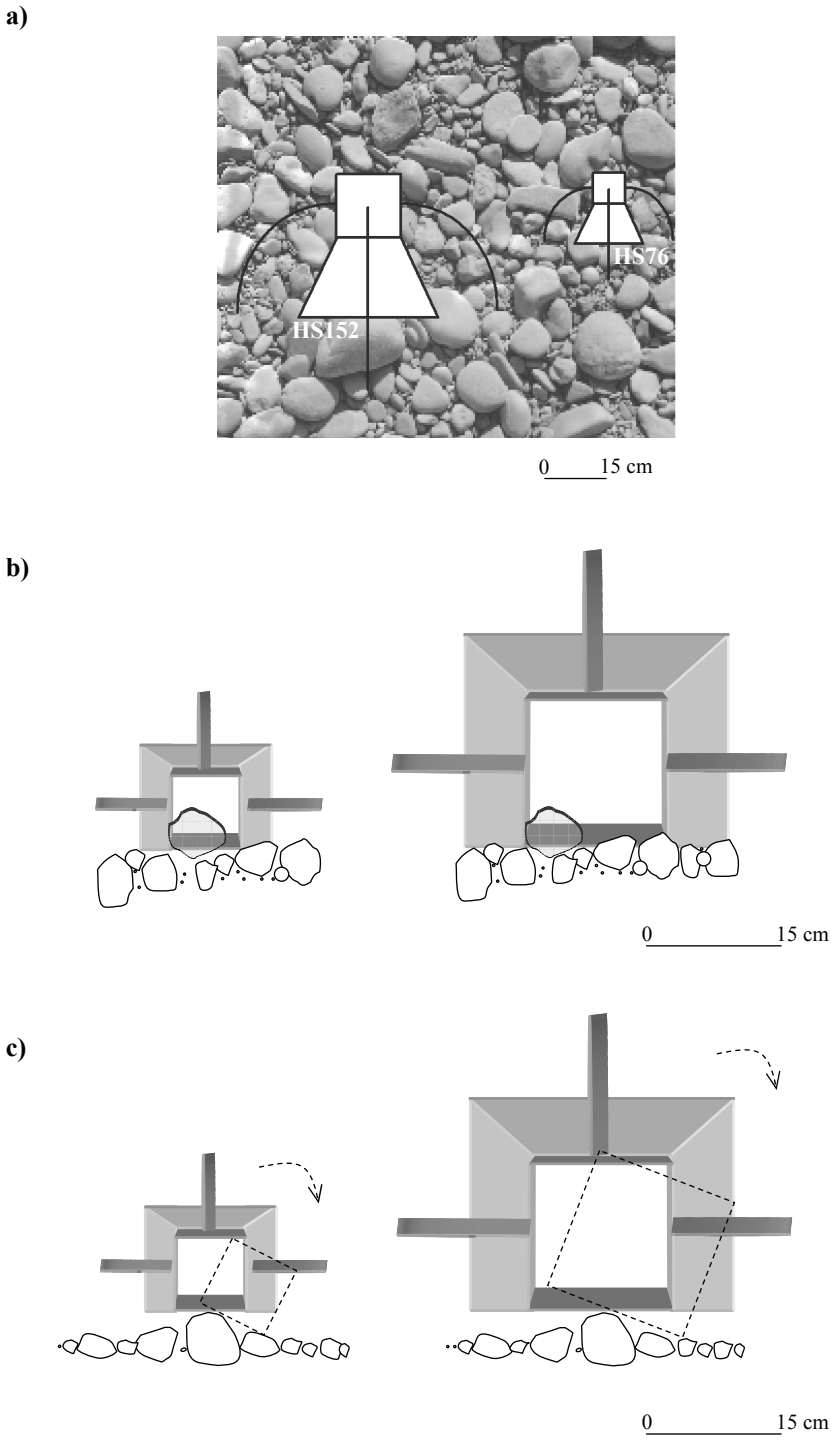

Figure 6 (C2P1). (**a**) River bed surface material at MEMS (*Móra d'Ebre B*) *bar* and scaled plan of the two Helley-Smith samplers (76-mm and 152-mm intakes). Note the difference between the sampler nozzles (A_s) in relation to the bed material. Possible sources of errors related to the bed material size and the Helley-Smith samplers' nozzles sizes are: (**b**) blockage of the HS nozzle when the sampler is located behind a coarse particle (front view). Note that the mouth of the HS152 is less covered than that of the HS76 under the same conditions; and (**c**) samplers not deposited flush with the bed surface due to the bed roughness (front view). Note that the samplers can adjust (dashed lines): 'tilting of the samplers'

Bedload size distributions obtained during the field calibration in East Fork River [*Emmett*, 1980] show that maximum sizes transported were between 32 and 45.3 mm. Consequently, only a small proportion of the bed material (Figure 2 (C2P1)) remained immobile during *Emmett's* calibration. An immobile clast of 45.3 mm could decrease the sampler's effective opening width by about 60%, decreasing the propensity of the moving particles to pass through the nozzle opening. However, the small proportion of these sizes in the river bed material yields only a small probability that the sampler might be positioned immediately downstream from a coarse immobile clast. On the other hand, in Harris Creek [*Sterling and Church*, 2002] all the material apparently transported was much smaller than the median size of the bed surface material. Maximum sizes in the bedload samples collected by the pit trap attained 45.3 mm, while the HS sampler collected maximum sizes of 16 mm. Large immobile particles might decrease the sampler's effective opening width. Indeed, the bed surface grain size distribution shows that the entire sampler opening might be blocked. The sampler's efficiency by grain size will be decreased as the effective opening decreases, so that fine particles travelling in saltation or suspension can still pass through the remaining nozzle opening, while many or all rolling clasts will be excluded.

The sampler also may not repose squarely on the bed (i.e., it may 'hang' on a large clast: see figure 6c (C2P1)), in which case moving sediment may pass beneath the sampler's mouth. If the sampler settles onto a clast of diameter D_i, smaller material is almost certain not to be sampled. Indeed, one might easily assume that it will require a clast with $D > 2D_i$ to achieve the necessary elevation to surmount the step. This assumption may not be strictly true because the sampler may be tilted (dashed lines in Figure 6c (C2P1)) so that part of the smaller material can be trapped while, on the other hand, clasts larger than $2D_i$ may not be able to surmount the step that is encountered. Together with b-axis, the particle *c*-axis may be also important in this instance. Our knowledge of the situation remains rudimentary at best.

3.3. Probability of interference

The bulk grain size distribution in East Fork River (no separate surface size distribution was given) and the surface distribution in Harris Creek (Figure 2 (C2P1)) were converted to line-by-frequency distributions following a conversion factor of -1 [after *Kellerhals and*

Bray, 1971]. The line-by-frequency distribution represents the collection of all clasts falling under a straight line across a sampling plane [*Muir*, 1969; *Kellerhals and Bray*, 1971]. Thus, the distribution can be interpreted as the probability for the sampler to encounter a clast of given size D_i. The probability is the same for the sampler to be positioned immediately downstream from such a clast (source of blockage, Figure 6b (C2P1)), or for the sampler to settle onto it (source of hanging, Figure 6c (C2P1)). Therefore, the integral of the probability density function (i.e., cumulative density function) quantifies: a) the probability of the sampler's nozzle to be blocked by a clast coarser than D_i, and b) the probability for a moving stone, D_i, not to be sampled because the sampler's nozzle is hung.

Figure 7a (C2P1) shows the cumulative density function at East Fork River and at Harris Creek. In East Fork River the sampler's nozzle has probability 0.5 (50%) to be blocked by clasts coarser than 0.5 mm, while sizes larger than 60 mm have probability 0.5 to block the entrance of the sampler in Harris Creek, reducing the sampler's effective nozzle in much greater degree than in East Fork River. Again, as we have explained above, when the sampler is positioned immediately downstream from a particular clast the flow may or not be competent to move it, so that the interference with the bedload sample by blockage of the sampler nozzle will be determined jointly by the flow competence and the size of the particle that is positioned in front of the nozzle. The probability for the sampler to be blocked by a size coarser than the largest size trapped during the field calibrations is around 0.1% in East Fork (D_i= 45.3 mm) and 80% in Harris Creek (D_i= 32 mm); a clear source that helps to explain the differences between the calibrations. Considering an immobile clast of 45.3 mm blocking the sampler's nozzle in both rivers, the effective sampler intake (i.e., 76-45.3=30.7 mm) remains larger than 99% of bed material in East Fork River and 63% of bulk bed material, but only 7% of surface material, in Harris Creek (Figure 2 (C2P1)). Moreover, at Harris Creek the sampler has probability 0.38 to be blocked by a particle size coarser than 76 mm; that is, a probability to block the sampler's entire nozzle. Thus, large, immobile particles might decrease the sampler's effective opening width at both rivers, affecting the propensity of a moving grain to enter to the effective nozzle in different degree according to the relation between river bed material and the sampler's nozzle.

Figure 7a (C2P1) also quantifies the probability for a moving stone, D_i, not to be sampled because of hanging of the sampler's nozzle, tilt not being considered. The probability to be excluded should be higher for the small particles and decreases as their sizes increase. A moving size of 1.0 mm has a probability to be excluded at East Fork River of 0.5 (considering a doubling of sizes to overcome the hung elevation), while the efficiency of the HS sampler for this size reported by *Emmett's* [1980] calibration was 1.0. This suggests that the relative weight of the HS76 compared with the compactability of the relatively fine river bed might allow a readjustment of the sampler attitude so that the probability will be less than that assessed in figure 7a (C2P1); indeed, hanging must become a negligible problem in sufficiently fine gravel. The coarsest river bed distribution at Harris Creek is apt to be much more refractory. A moving D_i of 6.5 mm (again, doubling D_i to overcome the step) has a probability to be excluded of 1. However, *Sterling and Church* [2002] reported efficiencies close to 100% for particles as fine as 0.5 mm. This discrepancy may be related to the configuration of the upstream approach that may steer the fine material into the sampler, and to fine particles travelling in saltation or suspension, or may merely reflect the circumstance that the sampler (visually placed) was not normally hung.

These assessments show that coarse bedded rivers potentially more strongly interfere with sampler performance, and this can explain part of the difference between sampler efficiency calculated for the Harris Creek observations [*Sterling and Church*, 2002] and for East Fork River [*Emmett*, 1989]. Figure 7b (C2P1) shows rescalings of figure 7a (C2P1) for the two sampler sizes discussed in this paper, and defines the regions of limited efficiency [*Emmett*, 1989, see 3.1.] for each sampler. In practice, of course, it is not possible to partition the sources of impaired sampler efficiency discussed above. Therefore, we turn to empirical results.

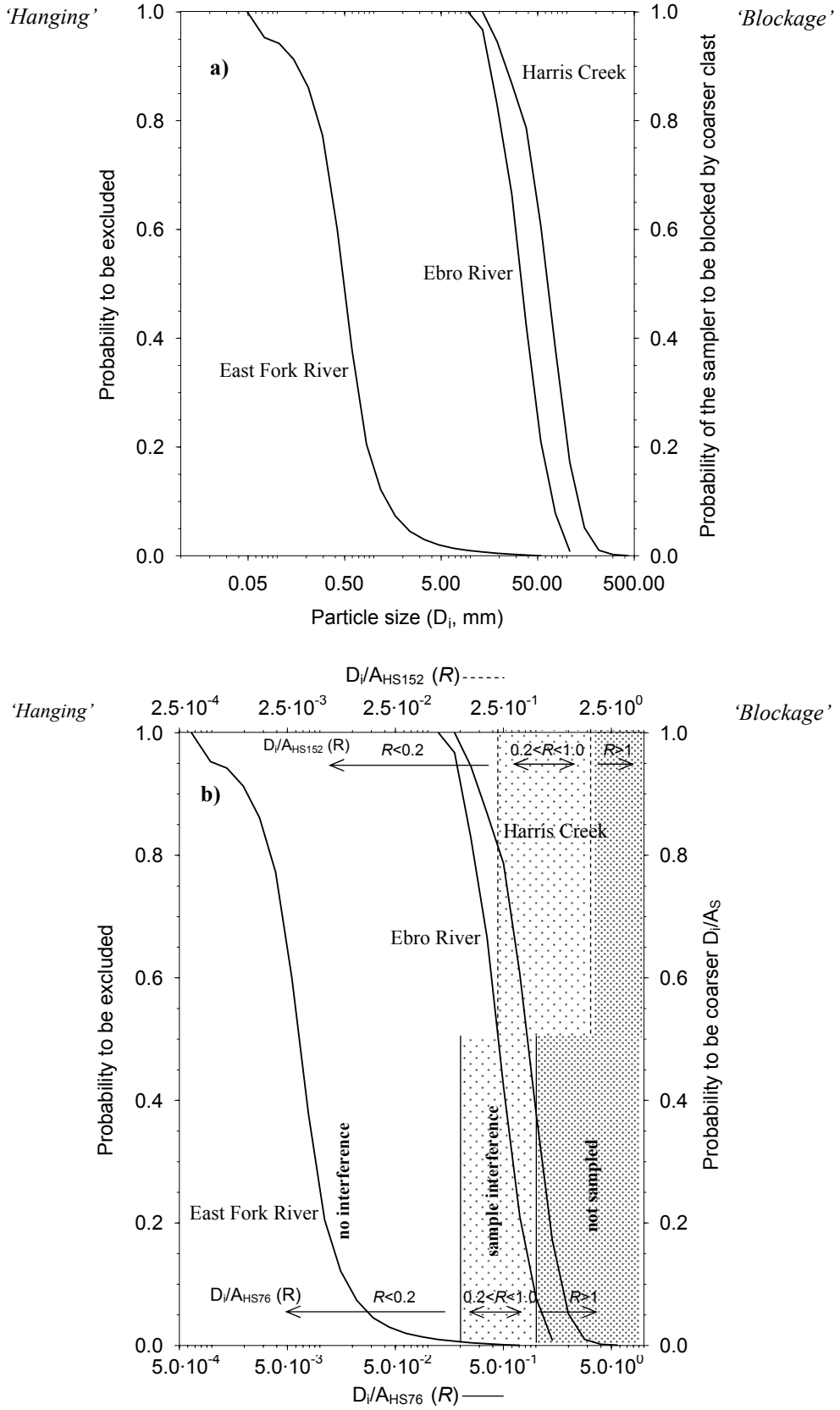

*Figure 7 (C2P1). **(a)** Line-by-frequency distributions: cumulative density functions at East Fork River, Harris Creek and Ebro River. Theoretical probabilities of interference with the sampler: a)*

*blockage (right y axis), and b) hanging (left y axis); (**b**) as (a) scaled for sampler nozzle width (76 mm opening on the lower abscissa; 152 mm opening on the upper abscissa)*

4. Analysis of the Ebro paired samples

Twenty three pairs of bedload samples were obtained successively on the same vertical at the MEMS station (Table 1 (C2P1)). The samples plotted against the discharge show, again, that the envelope of the general load-rating curve for each device is similar (Figure 8a (C2P1)). However, clear differences can be observed for samples collected at the same time. We sometimes obtained similar bedload rates using both devices but, on the other hand, bedload rates can be up to one order of magnitude different. For instance, at 8.8 m^2/s the bedload rate sampled by the HS152 is 192 g/ms, while by the HS76 it is 202 g/ms. Yet with a specific discharge of 10.4 m^2/s, the bedload rate for the HS152 is 340 g/ms and 46 g/ms for the HS76 (Table 1 (C2P1)). Comparing bedload grain size distributions and surface bed grain sizes distribution, it appears that river bed material was only partially mobilized during the sampling. The coarsest bedload samples collected with both HS samplers cover only the finer 80% of the river bed surface distribution.

Analysing the largest particles collected in the samples ($D_{max\text{-}bl}$) we can define the first bias between samplers (Table 1 (C2P1)). The HS152 sampler generally catches larger stones than the HS76 device. We represent the difference using the ratio $R_{Dmax\text{-}bl}$, calculated as the quotient between the size of the *b* axis of the maximum particle caught and the sampler's intake. For the samples collected with the HS152 $R_{Dmax\text{-}bl}$ ranged from 0.2 to 0.5, but the maximum particle sampled never rose above the half-size of the sampler's intake width, possibly because such material was not moving. However, for the samples obtained with the HS76 $R_{Dmax\text{-}bl}$ varied from 0.1 to 0.9. Assuming that the maximum particles collected with the HS152 were moving when the HS76 was sampling, these sizes, in many of the cases, would have been excluded from the HS76 intake (figure 7b (C2P1)) and, consequently, could not be collected. If we compare these ratios with the ratio (D_i/A_{HS76}) derived from *Emmett's* [1980] calibration, the values obtained with the HS152 are closer to Emmett's full efficiency limit than those obtained with the HS76. Consequently, it appears

that the largest particles collected with the HS76 may be subject to bias than those obtained with the HS152.

Three general groups of samples have been identified by comparing the bedload rates in table 1 (C2P1). In group A, bedload rates are similar (i.e., do not differ more than 25%) for both devices; in group B, bedload rates are higher (i.e., differ more that 25%) when the sampling was done with the HS152 than with the HS76; and in group C, bedload rates are higher (i.e., differ more than 25%) when the sampling was done with the HS76 than with HS152.

Table 1 (C2P1). Paired samples collected successively with both HS76 and HS152 devices

Sample number	**Specific discharge**	**Standardized collection rate**		**Maximum particle size**		**Classification**
	m^2/s	*g/ms*		*mm*		*group*
		HS76	*HS152*	*HS76*	*HS152*	
1	5.35	5.8	4.5	22	29	A
2	6.08	29.5	58.2	46	47	B
3	7.99	37.6	73.7	52	58	B
4	9.85	50.4	64.4	47	58	A
5	9.97	9.8	75.9	38	45	B
6	9.74	143.2	68.7	44	49	C
7	9.07	17.9	121.6	31	49	B
8	8.13	9.6	27.3	33	41	B
9	7.69	0.1	10.9	11	35	B
10	5.98	0.3	1.7	9	24	B
11	4.67	12.6	10.7	34	36	A
12	7.44	104.4	83.1	48	53	A
13	9.07	43.7	116.6	53	54	B
14	10.42	46.5	338.8	36	55	B
15	10.32	9.3	103.7	23	54	B
16	8.76	201.7	191.9	51	75	A
17	8.82	39.4	99.9	43	55	B
18	8.61	73.5	41.8	52	46	C
19	7.27	9.9	5.7	36	32	A
20	6.59	0.3	9.0	13	43	B
21	6.84	50.3	65.9	67	40	A
22	6.84	25.4	134.2	32	45	B
23	6.82	17.6	30.0	45	51	B

4.1. Group A

The first group was composed of 7 paired samples (Table 1 (C2P1)) in which the difference between the samples collected at the same time with each device does not vary more than 25%. The specific discharge ranged from 4.7 m^2/s to 9.8 m^2/s, which covers most of the sampled range of flows. To compare the pairs of bedload rates, we have plotted

each rate against the rate collected at the same time with the other sampler (Figure 8b (C2P1)). Under this condition, considering that the HS152 has a higher probability to collect unbiased bedload samples or, at least, to collect a wider range of sizes without bias, a *relative efficiency* estimated by dividing the individual sample collection rate with the HS76 by the rate collected with the HS152, was used to compare the devices. Thence, median efficiency by grain size has been calculated over all samples and is found not to diverge dramatically from 100% (Figure 8c (C2P1)). No consistent and clear bias was found, although the relative efficiency of the HS76 falls off at both extremes of the size range, perhaps indicating various problems with both blockage and hanging. The upper fall in efficiency, however, is consistent with the expected limit of 100% efficiency of the device.

The grain size distributions of corresponding samples have been compared in order to examine whether or not the measurements provide similar frequency distributions of grain sizes collected by each device. Four of the seven paired samples have practically equivalent grain size distributions. However, in two samples the HS152 distributions are coarser, while in one case the HS76 grain size distribution is coarser. Again, no consistent bias between grain size distributions of paired samples in group A was found, whence we conclude that sampling was not significantly biased.

4.2. Group B

The second group was composed of 14 samples (Table 1 (C2P1)), in which bedload rates were more than 25% higher with the HS152 than with the HS76. Specific discharge ranged from 6.0 m^2/s to 10.4 m^2/s. Pairs of bedload rates plotted in figure 8b (C2P1) show a clear and consistent discrepancy between the rates. The divergence of the rates for the HS76 compared with those for the HS152 ranged from 40% to one order of magnitude, and is not correlated with the specific discharge.

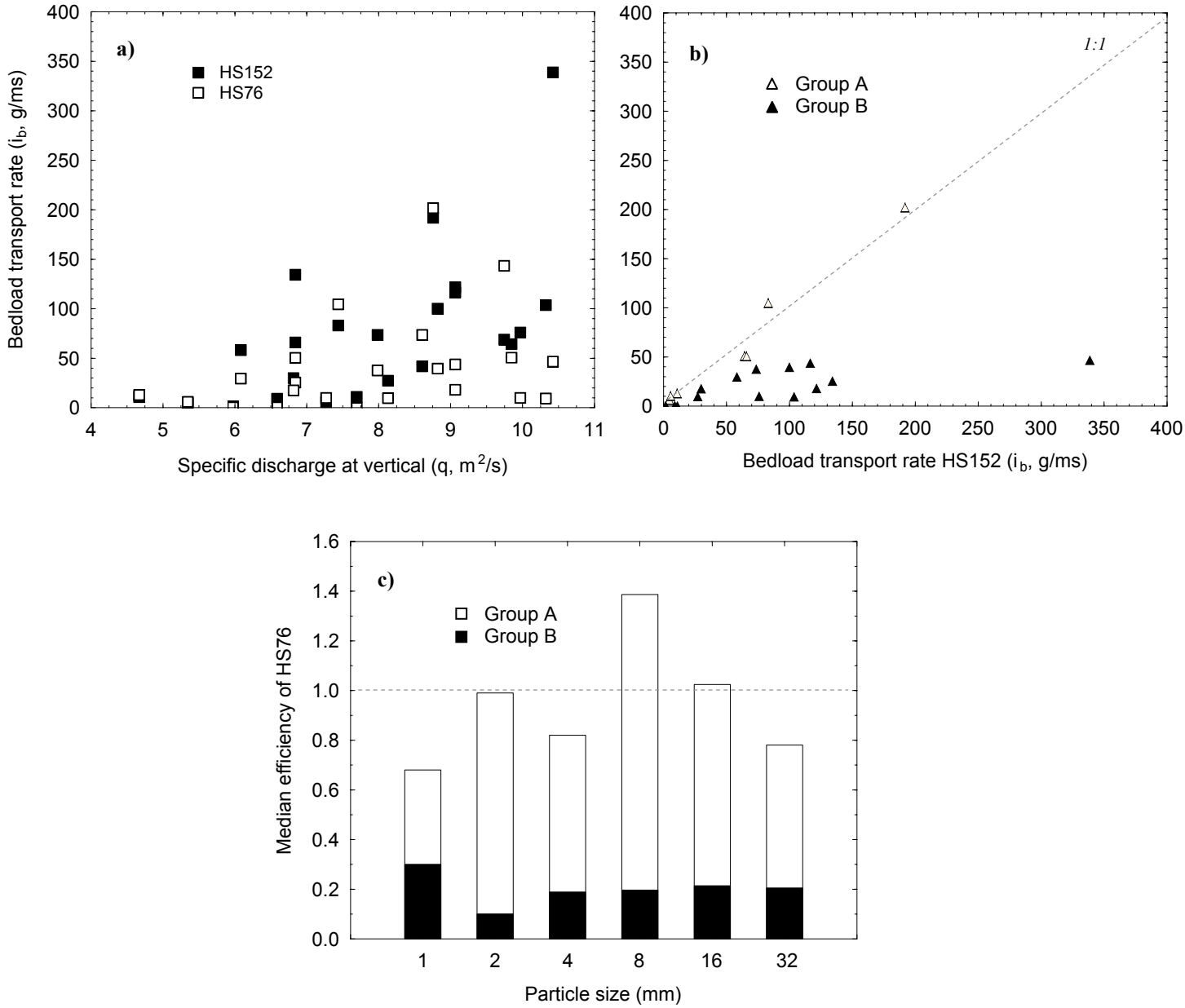

Figure 8 (C2P1). (**a**) Load-rating relation for all paired bedload samples obtained with HS152 and HS76 samplers (Table 1 (C2P1)). Gray straight and dashed lines show the envelopes of the data for the HS152 and HS76 respectively (and are the same as those in figure 4a (C2P1)). (**b**) Correlation of each pair of samples in group A and B. (**c**) Estimated median efficiency by grain size for the HS76 bedload samples in group A and B. Median efficiency has been calculated by dividing each collection rate by size obtained with the HS76 by the rate by size collected with the HS152

Median efficiency by grain size shows that the HS76 undercatches material in all the fractions (Figure 8c (C2P1)). The maximum efficiency is 0.3 for particles between 2 mm and 1 mm, while the minimum efficiency is 0.1 for particles between 4 mm and 2 mm. All sizes exhibit similar bias.

Bedload grain size distributions show variable indications of bias. Four of the fourteen paired samples present similar grain size distributions for both devices; in these cases, we cannot be sure that we are not observing real fluctuations in the bedload transport rate. In 3 of the fourteen, the HS76 distributions are coarser than the HS152 ones. This outcome is possible, but seems unlikely; scooping of bed material upon recovery is a possible cause of the result. The remaining 50% of the paired grain size distributions are coarser when the sample was obtained with the HS152. In these samples, maximum particles sizes obtained with the HS76 were around 30 mm (D_i/A_s = 0.4) while, for the samples collected by the HS152, maximum sizes were in some cases close to 60 mm (D_i/A_s = 0.4). This outcome appear to represent sampling bias, although it is possible that the performance of the individual samplers might represent the limit of their individual catching range. We conclude that many of the samples obtained with the HS76 were interfered with during sampling.

4.3. Group C

Group C is composed of only two samples (Table 1 (C2P1)), in which bedload rates are clearly higher when the sampling was done with the HS76 than with the HS152. The specific discharges were 9.7 m^2/s (#6) and 8.6 m^2/s (#18), and the underestimation by the HS152 was 52% and 43% of the rates for the HS76, respectively. These two samples suggest that the material trapped with the HS152 can be more biased than with the HS76. Maximum collected sizes for each device do not show clear differences. However, bedload grain size distributions are coarser when the samples were obtained with the HS76 (i.e., ratios $D_{50\text{-bl HS76}}/D_{50\text{-bl HS152}}$ are 1.3 and 1.1, respectively). Therefore, scooping by the lighter sampler remains an alternate possibility, decreasing the apparent bias between samples.

5. Sources of bias in the Ebro paired samples

Figure 9a (C2P1) shows the relation between specific discharge (q, m^2/s) and the ratio $R_{Dmax\text{-}bl}$ for the samples in group A. A statistically significant relation ($p < 0.01$) has found for each sampler, but substantially stronger for the HS152. $R_{Dmax\text{-}bl}$ increases as specific

discharge increases; that is, the higher the flow strength the larger the maximum particles potentially moved and trapped. The difference between $D_{max\text{-}bl}$ collected with each sampler is not large, nor are the bedload transport rates (Table 1 (C2P1)). Under the same specific discharge the ratio $R_{Dmax\text{-}bl}$ is always higher for the HS76 than for the HS152, reflecting the smaller nozzle width of the HS76. However, the maximum size does appear to fall off, in comparison with that expected, for the HS76 at the highest flows.

Different behaviour is found if we analyze the samples in group B (Figure 9b (C2P1)). In this case a similar, though less strong, relation than in figure 9a (C2P1) was found for the HS152, but no statistical relation is found for the HS76. Thus, samples obtained with the HS76 may be more variably affected by blockage and hanging. In group C, $R_{Dmax\text{-}bl}$ for the HS152 remains consistent with the other results. This again suggests that scooping by the HS76 sampler remains a possibility.

The coarsest 20% of the bed surface material at MEMS, that is, sizes larger than 64 mm, were not sampled and probably mostly not entrained. Those sizes cover 42% or more of the HS152 opening width and 84% or more of HS76 width. Assuming that the samplers were blocked by an immobile clast of D_i = 64 mm, the opening width would remain sufficient to catch particles up to 88 mm (*b* axis) in the case of the HS152, but only sizes around 12 mm with the HS76. Three samples in group B for the HS76 indeed have $D_{max\text{-}bl}$ close to 12 mm (Table 1 (C2P1)) while, at the same time, the HS152 collected sizes almost three times larger, reflecting the possibility that the HS76 was highly blocked during sampling. The other samples in group B show that $D_{max\text{-}bl}$ obtained with the HS76 is generally finer (in varying degree) than that for the HS152.

According to figure 7 (C2P1), the samplers at MEMS have probability 0.5 to be blocked by a particle larger than 32 mm, while some of those sizes were moving when the samplers were operated. Thus, considering again an immobile size D_i= 64 mm, the probability that the HS samplers may be placed just below a clast coarser than 64 mm is 0.2, a probability much higher than that estimated for immobile particles in East Fork River and lower than that in Harris Creek during the field calibration (Figure 7 (C2P1)). Change of the sampler's nozzle width influences the probability of a moving grain D_i to fit into the effective nozzle opening. On the other hand, while the probability for the each sampler to

be hung is the same, the greater width of the HS152 may increase its propensity to be tilted so that it may catch more material and yield less biased samples.

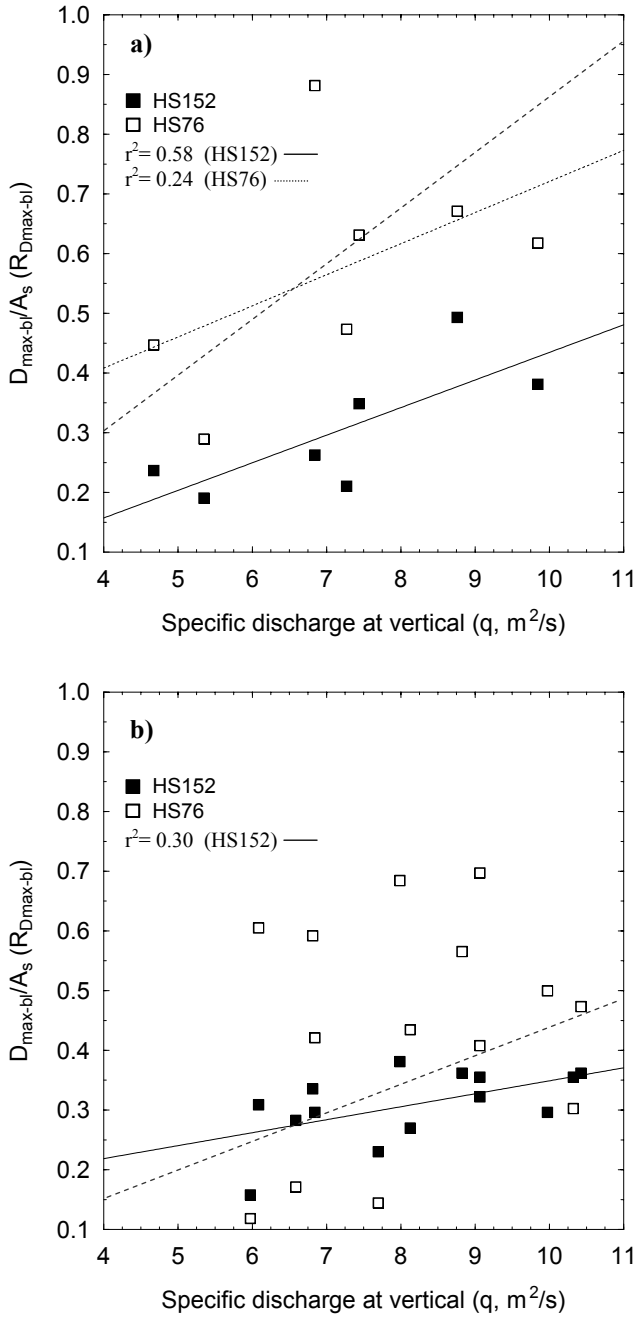

Figure 9 (C2P1). (**a**) Relation between $R_{Dmax\text{-}bl}$ and specific discharge (q) for the samples in group A, where $R_{Dmax\text{-}bl} = D_{max\text{-}bl}/A_s$, $D_{max\text{-}bl}$ is the maximum particle collected and A_s is the sampler's nozzle width of each sampler. Note that the grey dashed line shows the expected relation for equivalent grain size (two times the relation for the HS152 —). (**b**) Relation between $R_{Dmax\text{-}bl}$ and specific discharge (q) for the samples in group B. Note that the grey dashed line shows the relation between $R_{Dmax\text{-}bl}$ and specific discharge (q) for the HS152 in group A

6. Probability of bias in the Ebro paired samples

The objective for this section is to compare transport rates between devices and sample groups in order to assess the probability for each sampler to be interfered with during sampling in the Ebro River. In order to do this we have to define a reference relation, the maximum potential load-rating for the HS152 (Figure 10a (C2P1)). The relation is defined by 7 samples taken with the HS152, of which 4 belong to group A and 3 to group B. They were selected simply on the basis of their self-consistent plot positions near the envelope of all observations. The rest of the samples plotted in figure 10a (C2P1) are differentiated according to the group in which are classified. The remaining three samples in group A delimit a minimum potential load-rating curve (i.e., lower envelope) that encloses all the samples plotted against specific discharge (dashed line in figure 10a (C2P1)). These three samples, yielding consistent transport estimates, probably are the consequence of a bedload transport reduction. For the samples in group B the departure from the maximum potential transport trend can be attributed to bias of the samples, temporal bedload variability, or both. Individual HS152 samples may or may not be biased. However, some HS76 samples clearly are biased. The presence of all the samples between the maximum and minimum potential load-rating relations defined by the samples in group A shows that, although the samples in group B obtained with the HS152 could be biased, the degree of interference is never higher than the difference between two samples in which the low rate of one is the consequence of a natural bedload transport reduction. Hence, bias of the HS152 samples is not clearly established.

Figure 10b (C2P1) shows the maximum potential load-rating relations in comparison with the HS76 transport rates. As in figure 10a (C2P1), the samples are differentiated according to the group in which they are classified. The best data (all from group A) approach the maximum potential relation for specific discharges up to 7.5 m^2/s. However, when the rest of samples are plotted, not all of them fall above the minimum potential load-rating relation. Bias in some samples seems clearly to be established.

We can estimate the probability of bias of the samples collected by each device during the sampling (Table 2 (C2P1)). The most important uncertainty is associated with the samples in group B that were not used to construct the maximum potential load-rating relation. In

this case, the discrepancy can be attributed either to sample bias or to intermittency of the process of bedload transport. Therefore, the balance of the HS152 samples in group B may not be biased and, consequently, the distribution of the probabilities reported in table 2 (C2P1) would change. The probability of a sample collected by the HS152 to be biased may be less than the 10% whereas 61% of the HS76 samples appear certainly to be biased (Table 2 (C2P1)).

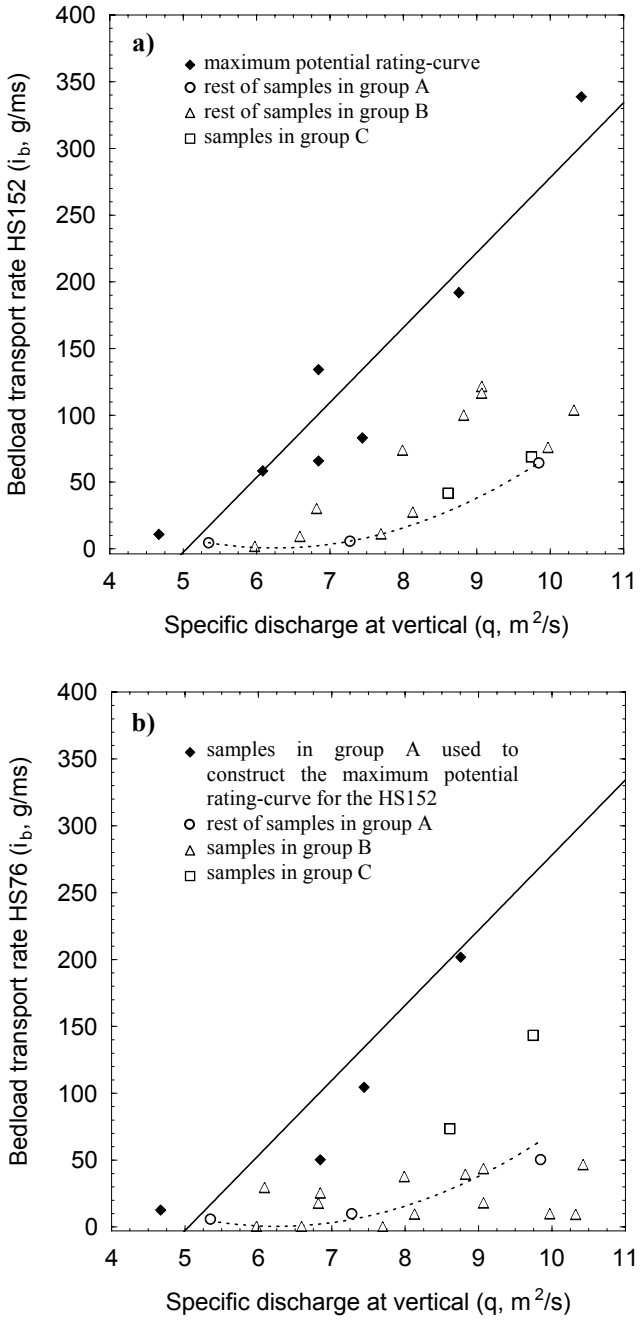

Figure 10 (C2P1). (**a**) Paired samples obtained with the HS152 and maximum potential load-rating curve. The dashed line delimits the rest of samples in group A. (**b**) Paired samples taken with the

HS76 and maximum potential load-rating curve defined with HS152 samples (as in figure 10a (C2P1)). The dashed line delimits the rest of samples in group A

7. Bias in annual bedload yield for the Ebro samples

The samples collected during the 2003-2004 hydrological year using each HS sampler were used in order to compare the sediment load computations using individual mean load-rating curves. For that purpose, the relations in figure 4b (C2P1) have been used, where the data for each device were averaged to define the mean transport rate for each Helley-Smith device given specific discharge according to the flow duration curve method [*Walling*, 1984]. The sediment load has also been calculated using the maximum potential load-rating curve defined in figure 10 (C2P1).

Table 2 (C2P1). Probability that samples collected with each device are biased, not biased, or insufficient evidence to classify

Helley-Smith sampler	***Probability of the samples collected to be***		
	biased	*not biased*	*undecided*
HS76	0.61	0.30 [1] / 0.39 [2]	0.09 [1] / 0.00 [2]
HS152	0.09	0.43 [3]/ 0.91 [4]	0.48 [3] / 0.00 [4]

[1] assuming that samples in group C collected with the HS76 are undecided
[2] assuming that samples in group C collected with the HS76 are not biased
[3] assuming that the rest of the samples in group B collected with the HS152 (see figure 10a (C2P1)) are biased
[4] assuming that the rest of the samples in group B collected with the HS152 (see figure 10a (C2P1)) are not biased (see text for discussion)

The sediment load estimated for the 2003-2004 hydrological year changes by about 10% between the two load-rating curves, the load estimated from HS76 measurements being lower than that for the HS152 (Table 3 (C2P1)). However, the annual load computed with the maximum potential load-rating curve for the HS152 is much higher than the other loads (Table 3 (C2P1)). Therefore, adopting the assumption that the difference between rates collected under the same flow strength is a consequence of natural bedload temporal variability, could change the computed annual load in greater degree than the possible errors in samples due to varying sampler efficiency (i.e., 10%). It is clear, as shown in figure 5 (C2P1) and in flume experiments [e.g., *Kuhnle and Southard*, 1988], that high variability in bedload rates under a similar threshold would be more likely attributed to the

natural behaviour of the bedload transport than to bias during the sampling; consequently, assessing the efficiency of samplers, or trying to use samplers with characteristics (i.e., intake size) that interfere less with sampling, will increase the precision of annual loads estimated in gravel-bed rivers. Moreover, an adequate sampler opening is strictly necessary, as shown by the results of the paired sampling, in order to assess accurately the grain size distributions of bedload samples.

Our results show that two further issues necessary to take in to account when a sampling program is defined. It is necessary to collect a significant number of samples under steady conditions in order to define accurate mean bedload rates for different flow strengths, and to asses the error around the load estimates due to the bedload temporal variability [e.g., *Gomez and Troutman*, 1997). Furthermore, the possibility for sampler bias, and the sediment size related limit of sampler efficiency mean that it may be difficult to determine flow competence from sample catch. In this respect, it appears that sample nozzle opening should remain greater than 5x the diameter (conservatively the *a*-axis) of the largest stones apt to move in the stream.

Table 3 (C2P1). Annual load (2003-2004) estimated for the mean load-rating curve for each Helley Smith sampler (see mean load-rating curves in the Figure 4b (C2P1)), and for the maximum potential load-rating curve for the HS152 (in Figure 10 (C2P1))

Helley-Smith sampler	***Annual load (tonnes)***
HS76 [1]	$84 \cdot 10^3$
HS152 [2]	$77 \cdot 10^3$
envelope load-rating [3]	$183 \cdot 10^3$

[1] mean load-rating curve for the HS76 in figure 4b (C2P1)
[2] mean load-rating curve for the HS152 in figure 4b (C2P1)
[3] maximum potential load-rating curve for the HS152 in figure 10 (C2P1)

8. Conclusions

Field calibrations of the standard HS sampler (76-mm) by *Emmett* [1980] and by *Sterling and Church* [2002] have been compared. Two principal sources of interference with the collection of bedload using the HS sampler are invoked to explain the differences between the calibrations:

a) *Blockage* of the sampler's nozzle: during the field calibration by *Emmett* [1980] the small size and the low proportion of coarser immobile clasts in East Fork River yields only a small probability to block the sampler's nozzle (e.g., 0.1%), while in Harris Creek [*Sterling and Church*, 2002] the probability to block the sampler's nozzle by immobile coarser stones attained 0.9 (clasts being in some cases larger than the nozzle).
b) *Hanging* of the sampler's intake: the relative weight of the HS compared with the fine sizes of the East Fork River bed might decrease the interference of bedload samples due hanging of the sampler, whereas the coarse clasts in Harris Creek might prevent effective contact with the bed.

Because of complexities in the possible juxtaposition of the samplers and clasts resident on the streambed, a quantitative model of probabilities for these biases remains elusive. The size distributions of samples obtained in Harris Creek strongly suggest, however, that blockage was the major problem encountered in that work.

The bedload samples obtained in the gravel-bedded Ebro River using two HS samplers of different size show that the bias of the HS76 with respect to the HS152 increases with specific discharge. Twenty-three of the bedload samples were paired, and their analysis leads to the following main conclusions:

1. The largest clasts collected with the HS76 are apt to be more biased, in comparison with the maximum actually moving, than those obtained with the HS152.
2. In 30% of the paired samples, the difference between the loads collected with each device does not vary more than 25%, while in the 61% the bedload rates were higher when the sampling was done with the HS152 than with the HS76. In 9% the bedload rates were lower when samples were obtained with the HS152.
3. Comparing samples and samplers' intakes we assessed the probability of interference of both HS76 and HS152 samplers: the probability of a bedload sample collected with the HS152 to be biased would be less than the 10%, whereas 61% of samples would be biased when they are obtained with the HS76.
4. Although annual loads assessed with the both samplers do not differ by more than 10% an adequate sampler opening is firmly necessary in order to estimate accurately the grain size distributions of the bedload samples.

Finally, this work demonstrates both that it is necessary to obtain repeated samples at similar flows in order to define mean bedload transport rates for rating purposes, and that it may be difficult to determine, from sampler measurements, what is the competence limit of the stream for a given flow. Sampler nozzle size needs to be adapted to the expected size of the largest material likely to move in the streambed.

Acknowledgements

This study was undertaken while the first author was a Visiting Research Fellow at The University of British Columbia, Vancouver, Canada, thanks to a grant of the Spanish Ministry of Education. The research was carried out within the framework of the research project REN2001-0840-C02-01/HID (Spanish Ministry of Science and Technology). Hydrological data were supplied by the Ebro Water Authorities. The Móra d'Ebre Town Council provided logistical support during fieldwork. We thank Albert Rovira at the University of Lleida for assistance during fieldwork, and Marwan Hassan at the University of British Columbia for helpful comments on the first data analysis and for furnishing some of the data used in this study.

Notations

A_{HS152}	Helley-Smith sampler's nozzle width of 152 mm
A_{HS76}	Helley-Smith sampler's nozzle width of 76 mm
A_r	Armouring ratio (ratio between $D_{50\text{-}s}$ and $D_{50\text{-}ss}$, e.g., *Church et al.,* 1987).
A_s	Bedload sampler's nozzle width (mm)
d	Water depth at vertical where the samples were collected (m)
$D_{50\text{-}s}$	Median surface grain size (mm)
$D_{50\text{-}ss}$	Median subsurface grain size (mm)
$D_{95\text{-}s}$	Percentile 95 of the surface grain size distribution (mm)
$D_{95\text{-}ss}$	Percentile 95 of the subsurface grain size distribution (mm)
D_i	Particle size i (mm)
$D_{max\text{-}bl}$	Maximum bedload grain size (mm)
i_b	Bedload transport rate (g/ms or kg/ms)
$i_{b\text{-}m}$	Mean bedload transport rate (g/ms)
q	Specific discharge ($q= d \cdot v$) at the vertical where the samples were collected (m^2/s)
$R_{Dmax\text{-}bl}$	Ratio between the $D_{max\text{-}bl}$ in each Helley-Smith sampler and its width (A_s)
v	Mean velocity at vertical where the samples were collected (m/s)
ω	Total stream power (kg/ms) [i.e., *Bagnold*, 1980]

References

Andrews, E. D., Marginal bed load transport in a gravel bed stream, Sagehen Creek, California, *Water Resour. Res., 30*, 2241-2250, 1994.

Bagnold, R.A., An empirical correlation of bedload transport rates in flumes and natural rivers, *Proceedings of the Royal Society*, *372A*, 453-473, 1980.

Batalla, R.J., Evaluating bed-material transport equations from field measurements in a sandy gravel-bed river, *Earth Surf. Process. Landforms*, *21*, 121-130, 1997.

Batalla, R.J., C. Garcia, and J.C. Balasch, Total sediment load in a Mediterranean mountainous catchment (the Ribera Salada River, Catalan Pre-Pyrenees, NE Spain), *Zeitschrift für Geomorphologie* (submitted), 2004.

Batalla, R.J., G.M. Kondolf, and C.M. Gomez, Reservoir-induced hydrological changes in the Ebro River basin, NE Spain, *J. Hydrol., 290*, 117-136, 2004.

Bunte, K., S.R. Abt, J.P. Potyondy, and S.E. Ryan, Measurement of coarse gravel and cobble transport using portable bedload traps, *J. Hydraul. Eng.*, *130*, 879-893, 2004.

Church, M., D.G. McLean, J.F. Wolcott, River bed gravels: sampling and analysis. In *Sediment transport in gravel-bed rivers*, edited by C. R. Thorne *et al.*, pp. 43-88, John Wiley & Sons Ltd, New York, 1987.

Einstein, H. A., Bedload transport as a probability problem. PhD Dissertation published in *Sedimentation*, edited by H.W. Shen, Colorado State University, 1937.

Emmett, W. W., A Field Calibration Of The Sediment Trapping Characteristics Of The Helley-Smith Bedload Sampler, *US Geological Survey Professional Paper*, *1139*, 44p., 1980.

Gomez, B., and B.M. Troutman, Evaluation of process errors in bed load sampling using a dune model, *Water Resour. Res.*, *33*, 2387-2398, 1997.

Gomez, B., Naff, R. L., and Hubbell, D. W. 1989. Temporal variations in bedload transport rates associated with the migration of bedforms. *Earth Surf. Process. Landforms, 14,* 135-156.

Habersack, H. M., and J.B. Laronne, Evaluation and improvement of bed load discharge formulas based on Helley-Smith sampling in an alpine gravel bed river, *J. Hydraul. Eng.-Asce*, *128*, 484-499, 2002.

Hamamori, A., A theoretical investigation on the fluctuations of bedload transport, in *Report R4,* Delft Hydraul. Lab., Delft, Netherlands, 1962.

Helley, E. J., and W. Smith, Development and calibration of a pressure-difference bedload sampler, *Open-file report United States Department of the Interior Geological Survey, Water Resources Division*, Menlo Park, California, 1971.

Hollingshead, A. B., Sediment transport measurements, Elbow River at Bragg Creek, Research Council of Alberta, Edmonton. *Open File 1968-14*, 1968.

Hubbell, D. W., Apparatus and techniques for mesuring bed-load, U.*S. Geological Survey Water-Suplply Paper*, *1784*, 74p., 1964.

Hubbell, D. W., Bed load sampling and analysis, in *Sediment Transport in Gravel-bed Rivers,* edited by C. R. Thorne *et al.*, pp. 89-118, John Wiley & Sons Ltd, New York, 1987.

Johnson, C. W., R.L. Engleman, J.P. Smith, and C.L. Hanson, Helley-Smith bed load samplers, *J. Hydraul. Div. Am. Soc. Civ. Eng*., 103, 1217-1221, 1997.

Jones, M.L., and M.R. Seitz, Sediment transport in the Snake and Clearwater Rivers in the vicinity of Lewiston, Idaho, *United States Geological Survey Open-File Report*, 80-690, 1980.

Kellerhals, R., and D.I. Bray, Sampling procedures for coarse fluvial sediments, *J. Hydraul. Div., ASCE97(HY8),* 1165-1180, 1971.

Kuhnle, R. A., Fractional transport rates of bedload on Goodwin Creek, in *Dynamics of Gravel-bed Rivers*, edited by P. Billi *et al.*, pp. 141-155, John Wiley & Sons Ltd., New York, 1992.

Kuhnle, R. A., and J.B. Southard, Bed load transport fluctuations in a gravel bed laboratory channel, *Water Resour. Res.* 24, 247-260, 1988.

Muir, T.C., Sampling and analysis of coarse riverbed sediments, in *Proceedings, Mississipi Water Resources Conference*, Water Resources Research Institute, Mississipi State University, State College, Mississipi, 1969.

Novoa, M., Precipitaciones y avenidas extraordinarias en Catalunya, pages 1-15 in *Proceedings Jornadas de Trabajo sobre Inestabilidad de laderas en el Pirineo*, Barcelona, 1984.

Ryan, S. E., and W.W. Emmett, *The nature of flow and sediment movement in Little Granit Creek near Boundurant, Wyoming*, Gen. Tech. Rep. RMRS-GTR-90, Ogden, UT: U.S. Department of Agriculture, Forest Service, Rocky Mountain Research. 48p., 2002.

Ryan, S. E., and L. S. Porth, A field comparison of three pressure-difference bedload samplers, *Geomorphology,* 30, 307-322, 1999.

Sterling, S. M., and M. Church, Sediment trapping characteristics of a pit trap and the Helley-Smith sampler in a cobble gravel bed river, *Water Resour. Res.*, *38*, 2002.

Vericat, D. and R.J. Batalla, Sediment transport in the lower Ebro River (NE Spain), *Geomorphology* (submitted), 2004.

Walling, D.E., Dissolved loads and their measurements, in *Erosion and sediment yield: Some methods of measurements and modelling*, edited by Hadley R.F., and D.E. Walling, pp. 111-177, Geo Books, London, 1984.

Vericat, D. and Batalla, R.J. (2004): Bed load under low sediment transport in a large regulated river: the lower Ebro, NE Spain. In: Batalla, R.J. and Garcia, C. (eds.): *River/Catchment Dynamics: Natural Processes and Human Impacts*, IAHS Red Book (in press)

Bed load under low sediment transport in a large regulated river: the lower Ebro, NE Spain

Abstract

This study describes the bed load transport regime observed under low sediment transport conditions and constant discharge in the gravel-bedded lower Ebro River (NE Iberian Peninsula). The data show a tendency toward size-selective transport during bed load sampling. The maximum bed load transport rate was lower (35%) than average rates previously obtained under similar discharges. This decline is related to the development of an armour layer during winter floods, which has reduced sediment availability and, consequently, influenced the bed load transport rate and grain-size during the sampling period. Bed load transport observed at individual sampling verticals varied up to 3.7 times the mean rate computed at the same vertical. The highest transport rates and highest variance around the sampling mean occurred in mid-channel, with both the variance and rate diminishing towards the channel margins.

Key words: bed load transport, grain-size, gravel-bed river, Ebro River

1. Introduction

Sediment transport is a key component of catchment and river processes. Information on the sediment load of a river can be used for a variety of purposes. It can be used to estimate erosion rates, to assess effects of land use changes on the sediment yield and river dynamics and to evaluate downstream geomorphic effects of instream human activities, such as dam construction and removal, and gravel mining. Bed load is an essential element of a river's sediment transport regime but accurate assessment of bed load transport rates is difficult because of the inherent variability of the transport process (Einstein, 1937). This variability posses important problems for the calibration and use of bed load samplers (Emmett, 1980; Hubbell, 1987), and must be taken into account when estimating the precision of bed load measurements (e.g. Gomez *et al.*, 1989; McLean & Tassone, 1987 in Hubbell, 1987). The temporal variability has been linked to the movement of dunes in sandy rivers (Gomez *et al*., 1990) and with cyclic slugs of sediment in coarser beds (Ehrenberger, 1931; Hamamori, 1962). Bed load rates vary across a given river section too. All or most of the bed load transport can occur in a narrow part of the channel width, which does not always correspond with the area with the highest velocity or shear stress. Moreover, distribution of bed load transport in a cross section can shift with changes in hydraulic conditions or sediment characteristics (Emmett, 1980). The objective of this study is to report the variance of bed load transport rates observed during sampling at almost constant discharge in the Ebro River. The samples analysed are part of a sediment transport monitoring programme carried out in the University of Lleida since 2002 in order to obtain direct field data on river processes, both to assess the magnitude of the reservoir-induced sediment deficit and to inform on-going fluvial restoration projects (Vericat & Batalla, 2005a).

2. Study area

The Ebro watershed (85,530 km^2) is located in the north-eastern part of the Iberian Peninsula (Figure 1 (C2P2)). Mean annual runoff at Tortosa is about 12,700 hm^3 (i.e. 150 mm, Q_{mean}=430 $m^3 s^{-1}$), of which almost 60% is stored in reservoirs (Batalla *et al.*, 2004). Maximum peak flow at Tortosa, near the watershed outlet, was estimated at around 12,000

m^3s^{-1} in 1907 (Novoa, 1984). Dams have reduced the magnitude of frequent floods (Q_2-Q_{25}) by 25% (Batalla *et al.*, 2004) and trap most sediment transported from upstream reaches (Batalla, 2003), and have caused morphological and ecological adjustments to the lowermost reaches of the river (Vericat & Batalla, 2004, 2005a). The lower Ebro River is a gravel-bed river with a mean slope of $8.5 \cdot 10^{-4}$. It flows as a single thread meandering channel, but is constrained by bedrock outcrops when the River crosses the Coastal Range (Figure 1 (C2P2)). The bed material consists mainly of gravel and sand. The median grain-size of the surface is 58 mm at the Móra d'Ebre monitoring section, where bed load measurements are taken (Figure 1 (C2P2)). The median subsurface grain-size is 21 mm. An armour layer tends to develop under partly competent flows such as the small floods occurred during winter 2004, just before bed load samples reported here were taken (Vericat & Batalla, 2005a).

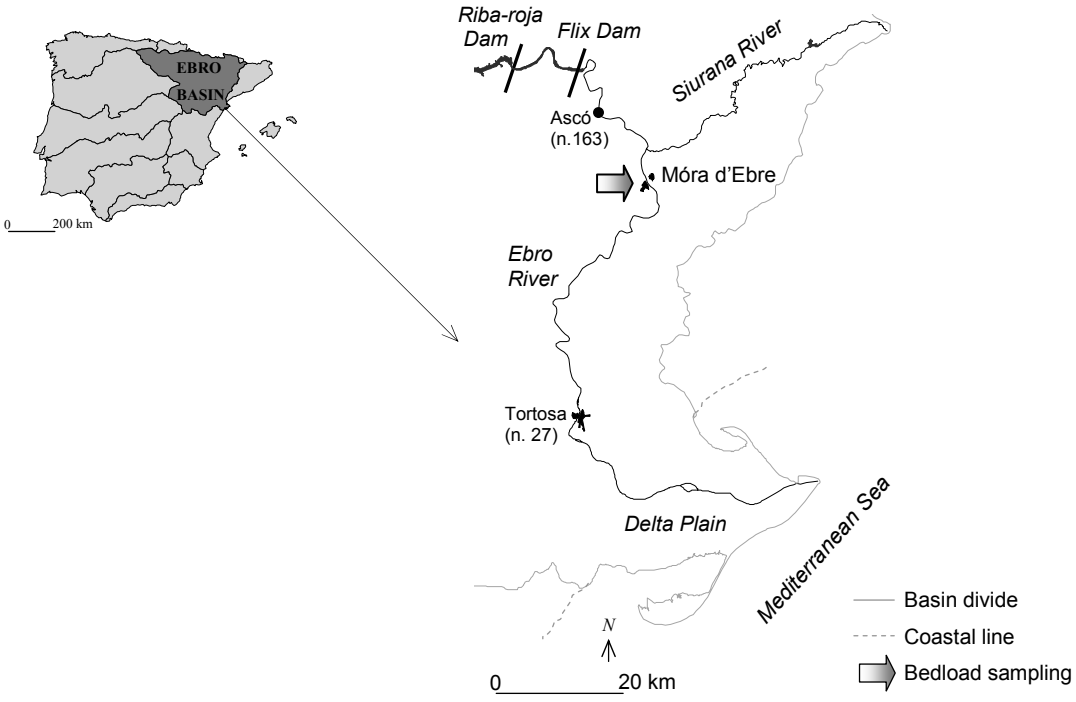

Figure 1 (C2P2). Location of the monitoring section in the lower Ebro River (NE Iberian Peninsula)

3. Methodology

Bed load transport was measured on two consecutive days at the Móra d'Ebre monitoring section, 27 km downstream from the lowermost dam (Figure 1 (C2P2)). Bed load was sampled at 7 equally spaced verticals (Figure 2 (C2P2)) using a 29 kg cable-suspended Helley-Smith sampler with a 76-mm intake (Helley & Smith, 1971). Bed load was sampled for a nearly constant discharge of 900 $m^3 s^{-1}$. Median bed load sizes collected ranged from 8 mm to 16 mm, implying that a 76-mm opening Helley-Smith sampler is adequate for most grain-size classes that may be encountered during sampling (Emmett, 1980). The bed load sampler was deployed using a manual crane. The sampling time was five minutes which prevented the sampler bag (0.25 mm mesh) from becoming more than 50% full, thereby maintaining adequate sampling efficiency (Vericat & Batalla, 2005a,b). The sampling interval between verticals was fifteen minutes. A total of thirty-five measurements were taken but, only eighteen samples collected bed load. They were taken to the laboratory, where they were dried, sieved and weighed to obtain the total mass and the grain-size distribution.

Discharge was estimated by routing hydrographs from the upstream gauging station in Ascó (n.163) using the Muskingum method (Shaw, 1983), and further compared with discharges recorded at the downstream station in Tortosa (n.27) (Figure 1 (C2P2)). The actual discharges tended to be systematically overestimated by around 3% (Vericat & Batalla, 2005a).

4. Results and discussion

The relatively high flows during 1-2 June 2004 were the consequence of unusually water releases from the Riba-roja Dam (Figure 1 (C2P2)), due to dam maintenance operations. Maximum discharge at Móra d'Ebre was 925 $m^3 s^{-1}$ and the mean discharge during the period when bed load sampling was undertaken was 910 $m^3 s^{-1}$, ranging from 890 to 925 $m^3 s^{-1}$ (i.e. according to flow duration curve, discharges equalled or exceeded 13% of time). Maximum water depth during sampling was close to 8 m and the maximum variation was 0.1 m. According to Shields' (1936) equation, the mean discharge during the sampling period was competent (26.7 N m^{-2}) to entrain at most the D_{20} (35 mm) of the bed surface

distribution. Discharge dropped to 200 $m^3 s^{-1}$ (and transport ceased) immediately after the sampling period ended, and the bed-material was sampled at this point in time.

4.1. Bed load transport

The mean bed load transport rate on 1 June was 1.2 g $m^{-1}s^{-1}$, with a maximum of 10.7 g $m^{-1}s^{-1}$ observed in vertical n.3 (V_3) near to the mid-section of the channel (Figure 2 (C2P2)). On 2 June the mean bed load transport rate was 4.5 g $m^{-1}s^{-1}$. Again V_3 showed the highest rate (33.4 g $m^{-1}s^{-1}$); which was much lower than the mean bed load transport rate obtained under same discharge at the same vertical during 2003 and 2004 (51.4 g $m^{-1}s^{-1}$, N=30). Median bed load size varied from 1 to 39 mm, and the maximum sampled particle size was 45 mm. The coarsest median bed load size (39 mm) was sampled at V_4 (mid with), while the lowest median (1 mm) was sampled at verticals close to channel margins (Figure 2 (C2P2)). Largest grain-sizes were close to the maximum theoretically movable size (35 mm) at the available discharge.

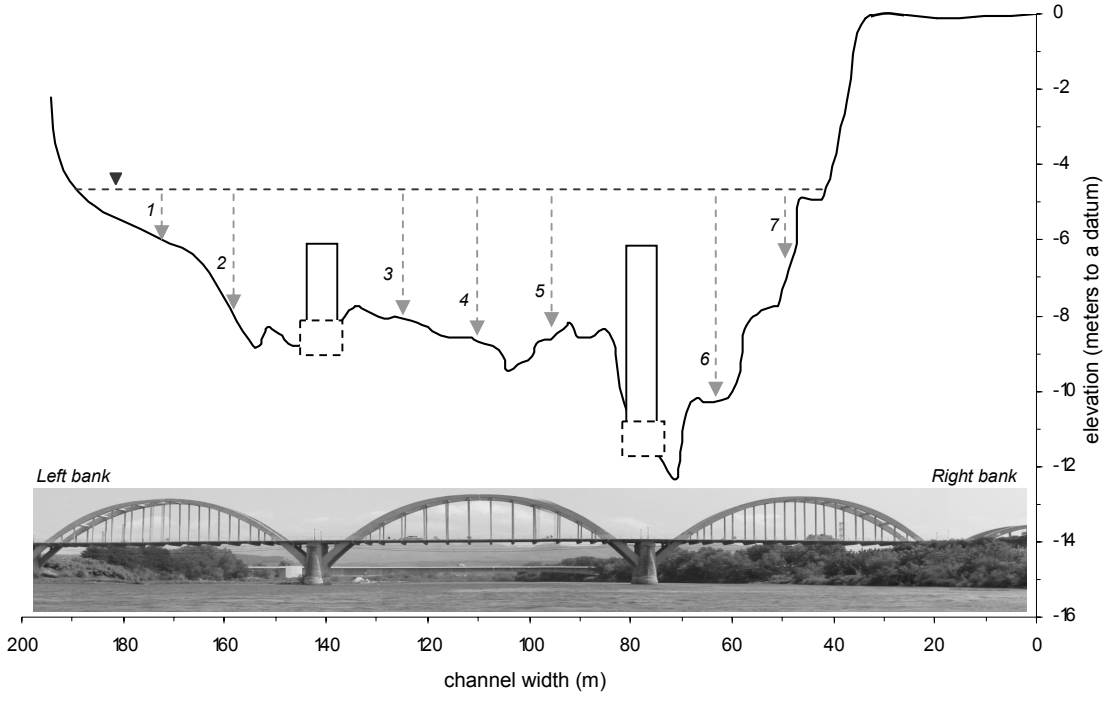

Figure 2 (C2P2). Bed load sampling section in Móra d'Ebre (Figure 1 (C2P2)). Sampling verticals and water stage at 900 $m^3 s^{-1}$ are indicated

The mean fractional bed load transport rate (i_{bi}) scaled by the proportion of each size fraction in the surface bed material was calculated (Figure 3 (C2P2)). Relative size was calculated by scaling each size (D_i) by the median bed surface size ($D_{50\text{-}s}$) (e.g. Gomez, 1995). Figure 3 (C2P2) suggests a tendency towards size-selective transport during bed load sampling. On one hand, particles around 16 mm were the main contributors to bed load, indicating that an active phase of winnowing of such fine surface size-fractions was still taking place during sampling. On the other hand, the low mobility of finest particle sizes (<4 mm), both from the surface and the subsurface, might be attributed to the lack of movement of the coarse particles (>16 mm) that shelter them (e.g. Kirchner *et al.*, 1990). The coarse riverbed surface (i.e. armour layer) created during small winter floods likely reduced surface sediment availability and, consequently, determined bed load rate and grain-size during the sampling period.

4.2. Variance of bed load transport

The bed load samples collected in this study were not numerous enough to accurately assess the temporal variability around the true bed load mean (e.g. Carey & Hubbell, 1986; Gomez *et al.*, 1990; Gomez & Troutman, 1997). However, the standard deviation for each sampling vertical provides an indication of bed load temporal variance, and we use it to compare sampled values at given locations with the cross-section mean for the entire sampling period. Using this approach, it is clear that the larger the bed load transport the larger is the variance around the sampling mean (Figure 4 (C2P2)). Similar results were obtained from the Fall River, Colorado (Pitlick, 1987, in Hubbell, 1987). In the lower Ebro River, the maximum variation occurred in vertical located situated around the mid channel width (V_3 and V_4), where the coarsest bed load was collected. The maximum bed load transport rate at each vertical exceeded almost 2.4 times the mean rate at the same point, on average, while the maximum discrepancy was 3.7 at V_4 (Table 1 (C2P2)), suggesting that temporal variability is also present in this large gravel-bed river. Comparable results were obtained in the Fraser River, Canada (McLean *et al.*, 1999).

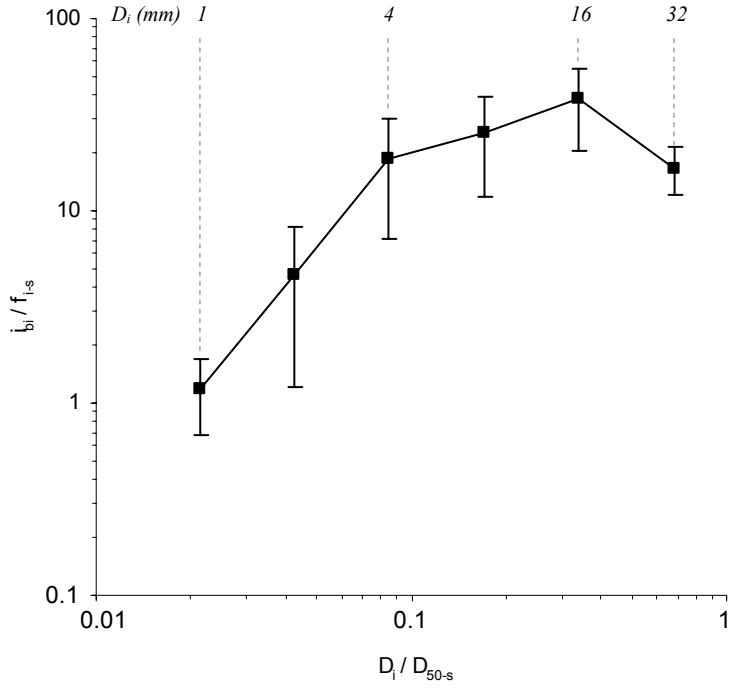

Figure 3 (C2P2). Mean fractional bed load transport rate as a function of relative size. The mean fractional transport rate (i_{bi} in g $m^{-1}s^{-1}$) has been scaled by the proportion of each size fraction in the surface bed material (f_{i-s}). Relative size has been calculated scaling each size (D_i) by the median bed surface size (D_{50-s}) in 2004. Vertical lines represent the standard deviation around the mean ($\varepsilon=\sigma/\sqrt{N}$, where σ is the standard deviation and N the number of data)

Table 1 (C2P2). Bed load transport rates collected during the five transects at each vertical

Vertical[1]	**Bed load rate (i_b in g $m^{-1}s^{-1}$)**					**Mean bed load rate (i_{bm} in g $m^{-1}s^{-1}$)**	**Maximum bed load rate (i_{bmx} in g $m^{-1}s^{-1}$)**	**Dimensionless bed load rate (i_{bmx} / i_{bm})**
	t_1[2]	t_2	t_3	t_4	t_5			
1	0.00	0.00	0.00	0.00	0.00	0.00	0.00	-
2	0.00	0.07	0.05	0.11	0.00	0.05	0.11	2.40
3	0.45	3.65	10.65	33.45	0.10	9.66	33.43	3.50
4	3.25	0.00	5.40	26.00	0.65	7.06	25.98	3.70
5	0.55	0.00	0.60	2.52	0.11	0.76	2.52	3.30
6	0.02	0.01	0.00	0.00	0.00	0.01	0.02	2.90
7	0.00	0.00	0.00	0.00	0.00	0.00	0.00	-

[1] Sampling vertical along the cross-section (Figure 2 (C2P2))

[2] Transect number

The mean bed load transport rate also varied from vertical to vertical. Maximum bed load transport rates were recorded in the channel centre (Table 2 (C2P2)), as were the largest variances in transport rates (Figure 4 (C2P2)). In all the transects the maximum bed load transport rate was observed in the section between the two piles of the bridge (V_3, V_4, V_5, Figure 2 (C2P2)); a 50 m long sub-section that is not the deepest in the river channel. In contrast, V_6 is deeper but, there the bed load transport rate did not exceed 0.02 g $m^{-1}s^{-1}$, that is, three orders of magnitude lower than those obtained in the centre of the channel. Marginal sections V_1 and V_7 did not move bed load at any time during the sampling period (Table 2 (C2P2), Figures 2 and 4 (C2P2)).

The variance of bed load transport rates at a single vertical around the mean (v_n) was been calculated as follows,

$$v_n = G_n/G_m$$

$$G_m = \sum_{n=1}^{7} i_{b,\,n} \times w_n$$

$$w_n=(w_{n,\,n-1} / 2)+(w_{n,\,n+1} / 2)$$

where, G_n is the bed load transport rate (g s^{-1}) at a given vertical, G_m is the mean bed load transport rate (g s^{-1}) for the entire cross-section, w_n is the interpolated width, and $w_{n,\,n\pm1}$ is the distance between verticals. The variance of each vertical (v_n) was calculated for each of the five transects (Table 2 (C2P2)). Once again, V_3 and, particularly, V_4 showed the highest variance around the sampling mean. These results confirm that during the sampling period bed load transport was concentrated in the centre of the channel, within section V_5. The transport rate in sections V_3 and V_5 during transects (1 and 5) showed the best overall agreement with the mean bed load transport rate ($v_n \approx 1$). The high discrepancy between verticals and cross-sectional measurements (v_n) prevents us from deriving a factor to correct for spatial variability when measuring bed load at a single point.

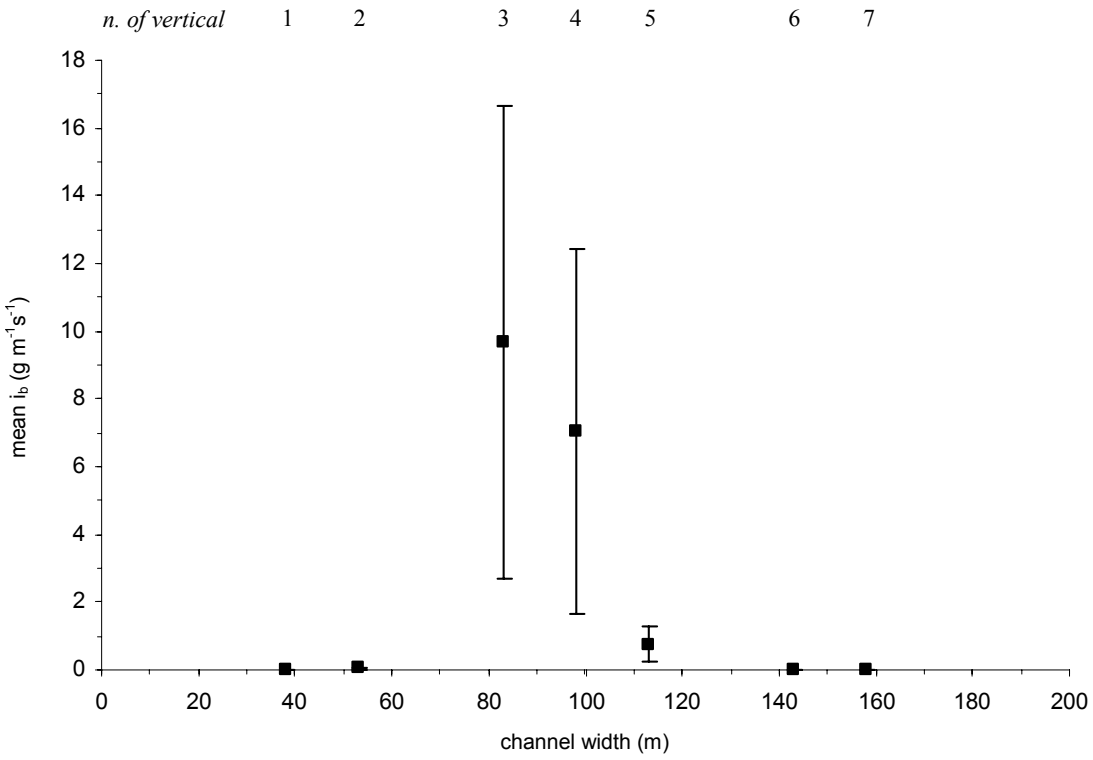

Figure 4 (C2P2). Mean bed load transport rate at each vertical during the 5 transects. Vertical lines represent the standard deviation around the mean

Table 2 (C2P2). Vertical variance in each transect (v_n*)

t[1] / **n**[2]	**1**	**2**	**3**	**4**	**5**	**Mean v_n**
1	0.0	0.0	0.0	0.0	0.0	0.0
2	0.0	0.1	0.0	0.0	0.0	0.03
3	0.9	6.1	4.4	3.9	1.1	3.3
4	6.4	0.0	2.2	3.0	6.2	3.6
5	1.1	0.0	0.3	0.3	1.0	0.5
6	0.0	0.0	0.0	0.0	0.0	0.0
7	0.0	0.0	0.0	0.0	0.0	0.0

[1] Transect number

[2] Vertical along the cross-section (Figure 2 (C2P2))

[*] v_n is the variance of each vertical *n* at a given transect *t* around the sampling mean

5. Final remarks

This paper reports on bed load transport observed during five transects (each consisting of seven equally-spaced sample verticals), of the lower Ebro River (a large gravel-bed river located in the NE Iberian Peninsula) made under low sediment transport conditions and constant discharge. Results indicate that:

a. There was a tendency towards size-selective transport during bed load sampling. The armour layer created during winter floods reduced sediment availability and, consequently, determined the bed load transport rate and grain-size observed during the sampling period.
b. The bed load transport rate at individual sampling verticals varied up to 3.7 times the mean rate computed for the same vertical.

c. The highest bed load transport rates and highest variance around the sampling mean were observed in mid-channel and the transport rate and variance both diminished toward the channel margins.

Our results provide a first glimpse of the variability of bed load transport in the lower Ebro River under near-steady flow and low sediment transport conditions. The data will help refine the measurement programme that is underway in this river. However, the characteristics of bed load transport must be investigated over a wider range of flow conditions, utilizing a greater number of transects to obtain an accurate assessment of the bed load transport regime of the River Ebro.

Acknowledgements
This experimental study was carried out within the framework of the research project REN2001-0840-C02-01/HID, funded by the Spanish Ministry of Science and Technology. The first author received a grant from the Spanish Ministry of Education. Hydrological data was supplied by the Ebro Water Authorities. Albert Rovira at the University of Lleida assisted during fieldwork. Michael Church and Brett Eaton at the University of British Columbia reviewed various versions of the manuscript. Basil Gomez at the University of Indiana did the paper review and provided constructive critiques that helped us to substantially improve the paper.

References

Batalla, R. J. (2003) Sediment deficit in rivers caused by dams and instream gravel mining. A review with examples from NE Spain. *Cuaternario y Geomorfología* **17**(3-4), 79-91.

Batalla, R. J., Kondolf, G. M., Gomez, C. M. (2004) Reservoir-induced hydrological changes in the Ebro River basin, NE Spain. *J. Hydrol.* **290**, 117-136.

Carey, W. P. & Hubbell, D. W. (1986) Probability distributions for bedload transport. In: *Proc. 4th Fed. Inter-Agency Sediment. Conf. 4th,* **2***,* 131-140.

Ehrenberger, R. (1931) Direkte geschiebemessungen an de Donau bei Wien und deren bisherige ergebnisse. *Die Wasserwirtschaft* **34**, 1-9.

Einstein, H. A. (1937) Bedload transport as a probability problem. PhD Dissertation published in *Sedimentation* (ed. By H.W. Shen), Colorado State University, 1972.

Emmett, W. W. (1980) A Field Calibration Of The Sediment Trapping Characteristics Of The Helley-Smith Bedload Sampler. *US Geol. Survey Professional Paper 1139*.

Gomez, B. (1995) Bedload transport and changing grain-size distributions. In: *Changing rivers channels* (ed. by A. Gurnell & G. Petts), 177-199. John Wiley & Sons, Chichester.

Gomez, B., Naff, R. L. & Hubbell, D.W. (1989) Temporal variations in bedload transport rates associated with the migration of bedforms. *Earth Surf. Processes and Landforms* **14**, 135-156.

Gomez, B., Hubbell, D. W. & Stevens, H. H. (1990) At-a-point bedload sampling in the presence of dunes. *Water Resour. Res.* **26**, 2717-2731.

Gomez, B. & Troutman, B. M. (1997) Evaluation of process errors in bed load sampling using a dune model. *Water Resour. Res.* **33**(10), 2387-2398.

Hamamori, A. (1962) *A theoretical investigation on the fluctuations of bedload transport*. Report R4, 14 p., Delft Hydraul. Lab., Delft, Netherlands.

Helley, E. J. & Smith, W. (1971) Development and calibration of a pressure-difference bedload sampler. *US Geol. Survey Open-file Report*, Water Resources Division, Menlo Park, California.

Hubbell, D.W. (1987) Bed load sampling and analysis. In: *Sediment transport in gravel-bed rivers* (ed. by C. R. Thorne, J. C. Barthurst & R. D. Hey), 89-118. John Wiley and Sons, Chichester.

Kirchner, J. W., Dietrich, W. E., Iseya, F. & Ikeda, H. (1990) The variability of critical shear stress, friction angle, and grain protrusion in water-worked sediments. *Sedimentology* **37**, 647-672.

McLean, D. G., Church, M. & Tassone, B. (1999) Sediment transport along lower Fraser River 1. Measurements and hydraulic computations. *Water Resour. Res.* **35**(8), 2533-2548.

Novoa, M. (1984) Precipitaciones y avenidas extraordinarias en Catalunya. In: *Proc. Jornadas de Trabajo sobre Inestabilidad de laderas en el Pirineo*, Barcelona; 1-15.

Shaw, E. M. (1983) *Hydrology in Practice*. Van Nostrand Reinhold, London.

Shields, A. (1936) *Answendung Ahnlichkeitsmechanik und der Turbulenzforschung auf die Geschiebebewegung*. Mitt. Preussichen Versuchsanstalt Wasserbau Schiffbau, Berlin.

Vericat, D. & Batalla, R. J. (2004) Efectos de las presas en la dinámica fluvial del curso bajo del río Ebro. *Cuaternario y Gemorfología* **18**(1-2), 37-50.

Vericat, D. & Batalla, R. J. (2005a) Sediment transport in the lower Ebro River (NE Iberian Peninsula). *Geomorphology* (submitted).

Vericat, D.& Batalla, R. J. (2005b) Sediment transport in a highly regulated fluvial system during two consecutive floods (Lower Ebro River, NE Spain). *Earth Surf. Processes and Landforms* (in press).

CHAPTER 3
SEDIMENT TRANSPORT

INDEX CHAPTER 3: SEDIMENT TRANSPORT

Figure captions in the papers

Vericat, D. and Batalla, R.J. (2005): Sediment transport in a highly regulated fluvial system during two consecutive floods (lower Ebro River, NE Iberian Peninsula*). Earth Surface Processes and Landforms* **30**(4): 385-402.

Figure 1 (**C**hapter **3** **P**aper **1**). Location of the study reach on the lower Ebro River

Figure 2 (C3P1). Field equipment to measure discharge and sediment transport from bridges: a) OTT C31 current metre attached to a cable suspended US DH74 sediment sampler, b) cable suspended 76 kg Helley Smith Sampler, c) automatic crane for suspension of sampling equipment, and d) intake (152 mm) of the Helley Smith Sampler, showing bedload material captured on February 11th 2003. Photos by the authors (February 2003)

Figure 3 (C3P1). Grain size distribution of bed-materials at SMS reach, upstream dams, and MEMS reach, downstream from the dams. The sorting coefficient (σ) was calculated from the Folk and Ward (1957) formulae: $[(\phi_{95}-\phi_5)/6.6] + [(\phi_{84}-\phi_{16})/4]$, when $-\phi_x$ is a given percentile of the particle size distribution in the phi scale

Figure 4 (C3P1). Storm hyetograph (at one representative station, A-260, located in the centre of the Ebro basin), flood hydrographs (upstream and downstream dams), and flow frequency curves (upstream and downstream dams), corresponding to the February 2003 flood on the Lower Ebro River. Note that precipitation is represented only for 29th and 30th of January, when almost all rainfall took place

Figure 5 (C3P1). Sediment load rating curves at the monitoring sections on the lower Ebro River upstream (SMS) and downstream from the dams (MEMS) during the February 2003 flood: a) a significant statistical relation between suspended sediment concentration and discharge ($p<0.01$) and b) a significant statistical relation between bedload rates and discharge ($p<0.01$). Note that at the MEMS, the bedload rates were averaged for the same discharges in order to obtain the highest possible correlation with discharge

Figure 6 (C3P1). Storm hyetograph (at one representative station, A-260, in the centre of the Ebro basin), flood hydrographs (upstream and downstream dams), and flow frequency curves (upstream and downstream dams), corresponding to the March 2003 flood on the Lower Ebro River. Note that precipitation is represented only for 25th and 26th of February, when almost all rainfall took place

Figure 7 (C3P1). The sediment load rating curves at the monitoring sections on the lower Ebro River upstream (SMS) and downstream from the dams (MEMS) during the March 2003 flood. Significant statistical relations between (a) suspended sediment concentration and discharge ($p<0.01$) and (b) bedload rates and discharge ($p<0.01$)

Figure 8 (C3P1). Suspended sediment and bedload on the lower Ebro River during the February and March 2003 floods, expressed as percentages of the total solid load

Figure 9 (C3P1). Representative cross sections of the lower Ebro River before and after February and March 2003. First section (above) is located at the beginning of the study reach, immediately downstream from the Flix Dam. Second section (below) is located at the lowermost end of the study reach at MEMS. Both show evidences of river-bed net erosion

Figure 10 (C3P1). Scour chain in the Flix Meander section, showing its position in the river-bed before February and March 2003 floods (left diagram), and illustrating the net scour after the two events floods (right, photo by the authors, June 2003)

Vericat, D. and Batalla, R.J. (2005): Sediment transport in a large impounded river: the lower Ebro, NE Iberian Peninsula. *Geomorphology* (accepted)

Figure 1 (**C**hapter **3** **P**aper **2**). Location of the study area in the Ebro basin (NE Iberian Peninsula).

Figure 2 (C3P2). Flow hydrographs at the monitoring sections (upstream and downstream from the dams) for the 2002-2004 hydrological years. Note that hydrographs finish on 1st June 2004.

Figure 3 (C3P2). (**a**) Flow duration curves calculated for the pre and post-dam discharge series at the Zaragoza gauging station, and for the study years (2002-2004) at SMS. Mean monthly discharges are also presented. (**b**) Flow duration curves calculated for the pre and post-dam discharge series at the Tortosa gauging station, and for the study years (2002-2004) at MEMS. Mean monthly discharges are also presented.

Figure 4 (C3P2). Suspended sediment load rating curves at the monitoring sections (**a** and **b** at SMS and **c** and **d** at MEMS) in the lower Ebro River for the hydrological years 2002-2003 and 2003-2004. Dashed lines represent the 0.95 confidence limits above and below the regression line (solid line) (see table 2 (C3P2) for equations). Data represented by empty squares have not been included in the analysis.

Figure 5 (C3P2). Hysteretic behaviour during April 2004 flood at Sástago Monitoring Section (upstream from the dams). Relation between discharge and suspended sediment concentrations shows a well defined clock-wise hysteresis, indicating progressive exhaustion of sediment during flood. Each point represent a single measurement.

Figure 6 (C3P2). Frequency of suspended load at the two monitoring sections (upstream and downstream dams) during the hydrological years 2002-2003 and 2003-2004.

Figure 7 (C3P2). Seasonal variation of suspended sediment concentration at SMS and MEMS during the two hydrological years (2002-2004).

Figure 8 (C3P2). Bedload variability at a single vertical (MEMS, 2002-2003).

Figure 9 (C3P2). Frequency of bedload upstream and downstream from the dams during the hydrological years 2002-2003 and 2003-2004.

Figure 10 (C3P2). Bedload rating curves downstream from the dams at the Móra d'Ebre Monitoring Section for the hydrological years 2002-2003 and 2003-2004. Dashed lines represent the 0.95 confidence limits above and below the regression line (solid line) (see table 2 for equations).

Figure 11 (C3P2). Sediment budget in the lower Ebro River for the period 2002-2004.

Table captions in the papers

Vericat, D. and Batalla, R.J. (2005): Sediment transport in a highly regulated fluvial system during two consecutive floods (lower Ebro River, NE Iberian Peninsula*). Earth Surface Processes and Landforms* **30**(4): 385-402.

Table 1 (C3P1). Mean daily discharges and the associated mean sediment loads obtained during sampling campaigns during February and March 2003 floods in the lower Ebro River, upstream and downstream from the large Mequinenza and Ribarroja dams

Table 2 (C3P1). Water and sediment yield of the lower Ebro River during the floods of February and March 2003

Table 3 (C3P1). Changes in the river bed in representative sections of the lower Ebro River after the two consecutive floods (February-March 2003)

Vericat, D. and Batalla, R.J. (2005): Sediment transport in a large impounded river: the lower Ebro, NE Iberian Peninsula. *Geomorphology* (accepted)

Table 1 (C3P2). Flow regime in the monitoring sections of the lower Ebro River during the study years 2002-2004 in relation to long-term flow records. See also Figure 3 (C3P2).

Table 2 (C3P2). Rating curves between discharge and sediment transport in the lower Ebro with error estimates (see Figure 4 (C3P2) and 10 (C3P2) for data).

Table 3 (C3P2). Sediment yield of the lower Ebro River for the period 2002-2004.

Table 4 (C3P2). Scour and fill in the riverbed and maximum particles mobilised in 7 experimental sections of the lower Ebro River for each hydrological year (2002-2004).

1. INTRODUCTION

This chapter describes the sediment transport processes in the lower Ebro River at two different temporal scales. For this purpose we present two papers on the analysis of the sediment transport at the two monitoring sections upstream and downstream from the dams. Papers are presented maintaining their original format.

The first paper was accepted for publication in July 2004 in the journal *Earth Surface Processes and Landforms* and it is currently published. This paper reports on sediment transport, both in suspension and as bedload, during two consecutive floods (February and March 2003) and gives a general description of the on-going morphological changes due to the retention of sediment by the large chain of dams Mequinenza-Riba-roja-Flix. Both floods were the largest monitored and analysed events during the thesis. Paper evaluation helped to revise the objectives of the thesis, especially the firm need of measuring transport upstream and downstream the reservoirs, and to refine fieldwork practices, particularly in relation to the bedload sampling.

The second paper was accepted for publication in February 2005 in the journal *Geomorphology* and it is currently accepted. In this second paper we present sediment dynamics on annual scale. Both suspended and bedload sediment transport modes are analysed for the two hydrological years 2002-2003 and 2003-2004. In this work we present: i) a quantitative budget based on the annual sediment loads at the monitoring sections upstream and downstream from the dams, ii) a description of the patterns of sediment transport at both monitoring sections, and iii) an assessment of the reduction of sediment supply downstream the lowermost Flix Dam. Finally, the paper presents data from scour chains to contextualize the order of magnitude of the riverbed incision and to show that the tendency observed in the study reach is consistent with the appearance that degradation is actually occurring.

2. SEDIMENT TRANSPORT DURING FLOODS

Vericat, D. and Batalla, R.J. (2005): Sediment transport in a highly regulated fluvial system during two consecutive floods (lower Ebro River, NE Iberian Peninsula). *Earth Surface Processes and Landforms* **30**(4): 385-402.

Sediment transport in a highly regulated fluvial system during two consecutive floods (lower Ebro River, NE Iberian Peninsula)

Abstract

The sediment transfer through a highly regulated large fluvial system (lower Ebro River) was analysed during two consecutive floods by means of sediment sampling. Suspended sediment and bedload were measured upstream and downstream of large reservoirs. The dams substantially altered flood timing, particularly the peaks, which were advanced downstream from the dams for flood control purposes. The suspended sediment yield upstream from the dams was 1,700,000 tonnes, which represented nearly 99% of the total solid yield. The mean concentrations were close to 0.5 g/l. The sediment yield downstream from the dams was an order of magnitude lower (173,000 tonnes), showing a mean concentration of 0.05 g/l. The dams captured up to 95% of the fine sediment carried in suspension in the river channel, preventing it from reaching the lowermost reaches of the river and the delta plain. Total bedload transport upstream from the dams was estimated to be about 25,000 tonnes, only 1.5% of the total load. The median bedload rate was 100 g/ms. Below the dams, the river carried 178,000 tonnes, around 51% of the total load, at a mean rate of 250 g/ms. The results of sediment transport upstream and downstream from the large dams illustrates the magnitude of the sediment deficit in the lower Ebro River. The river mobilised a total of 350,000 tonnes in the downstream reaches, which were not replaced by upstream coming sediment. Therefore, sediment was necessarily entrained from the riverbed and channel banks, causing a mean incision of 33 mm over the 27 km-long study reach below the dams, altogether a significant step towards the long-term degradation of the lower Ebro River.

Keywords: sediment transport, dams, riverbed degradation, large Mediterranean river

1. Introduction

The transfer of sediment through the catchment and along the natural river system is continuous, thus the river channel can be seen as a conveyor belt that transports the erosional products downstream to the ultimate depositional sites below sea level (Schumm 1977, Kondolf 1994). Dams disrupt the continuity of sediment transfer in river systems by trapping all bedload and an important part of the suspended load. For instance, in the Colorado River, after the construction of the Hoover Dam, the annual suspended sediment load was reduced from 150 million tonnes to 100,000 tonnes. (Meade and Parker, 1985).

Sedimentation in reservoirs causes a progressive reduction of dam impoundment capacity and creates serious problems for water management, especially near dam outlets. Dams release sediment-starved or 'hungry water' to downstream reaches, which may transport sand and gravel downstream without replacement from upstream, resulting in coarsening of the surface layer (armouring) (Williams and Wolman, 1984), and may erode the bed, resulting in incision, and can undercut banks, thereby causing widening (Kondolf, 1997). The channel changes caused by hungry water can cause dramatic alterations in river ecology as well as damage to bridges and other infrastructures. Downstream from the Davis Dam, in the Colorado River, the channel has incised up to 6 metres (Williams and Wolman, 1984). In the Green River, downstream from the Flaming George Dam, the rate of change in sediment storage along the channel is negative and the flow systematically scours the riverbed and banks (Collier *et al.*, 1996). The situation worsens when gravel mining takes places downstream from dams, and the incision in the riverbed can reach up to 10 metres, as has been described for some Italian rivers (Surian and Rinaldi, 2003). For instance, in the Arno River, the deficit of sediment in the channel has produced an incision of between 2 and 5 metres on average, and up to 9 metres in some places. The consequence of that is riverbank instability, upstream erosion in tributaries, loss of groundwater, reduction of sediment supply to beaches, and damage to bridges, embankments and levees (Rinaldi and Simon, 1998).

In addition, dams diminish the magnitude of floods, which transport the majority of sediment, and reduce the sand supply to the coastline and deltas. In different rivers of the Sacramento-San Joaquin River system of California, the discharge with a 2-year recurrence

interval (Q_2), was reduced below dams from 35% to 95% of pre-dam values, while the Q_{10} was reduced from 2% to 78%, depending on the reservoir size and operating rules (Kondolf and Mathews, 1993). In the Aragón River (Ebro Basin), the magnitude of the floods was reduced after the construction of the Yesa Dam (López *et al.*, 2002). Similar results have been reported for the whole Ebro basin (Batalla *et al.*, 2004). In contrast, if the floods are reduced and the flow released from dams cannot transport the sediment supplied by tributaries, sedimentation might occur in the river channel as well. For instance, in the Rio Grande, below Elephant Butte Dam, the material carried by tributaries has caused important aggradation in the channel (Howard and Dolan, 1981). In the Colorado River, downstream from the Glen Canyon Dam, the sedimentation had reached 2.6 metres in the river-bed during the 1980s. Beginning on March 26, 1996, Glen Canyon Dam spilled 1,285 m^3/s for 8 days to remobilise sand accumulated downstream. It was the first time that a flood was used as a management tool (Collier *et al.*, 1996).

Under all such conditions, the balance between fluvial and marine processes on beaches and in delta regions is disrupted. There, sediment deposition is no longer in balance with coastal erosion. The erosion of the Nile Delta (150 m/y), 1,000 km downstream of the Aswan High Dam demonstrates the importance of sediment supply from the upper catchment. Other examples can be seen elsewhere (e.g. Brownlie and Taylor 1981, Milliman and Meade 1983, Shahin, 1985). To compensate for this, beach nourishment with imported sediment dredged from reservoirs and harbours has been implemented along many beaches in southern California, although the high costs of extraction and transportation prevent the generalisation of this system (Inman 1976, Allayaud 1985, Everts 1985).

In Mediterranean-climate regions, water availability and demand are out-of-phase. Precipitation and runoff occur (almost exclusively) in the autumn and winter, while plants are dormant and demand for irrigation (and often hydroelectric generation) is lowest. Thus, seasonal and inter-annual water storage is needed to meet the basic needs of human populations and to support industrial-scale agriculture. As a result, Mediterranean-climate rivers tend to be more heavily regulated than humid climate rivers of comparable size. Within this context, the objective of this paper is to analyse the sediment transport through a highly regulated fluvial system, the lower Ebro River (NE Spain), 100 km upstream

from its delta. Sediment transport (both as bedload and in suspension) was measured during two consecutive floods (T_{5-10}), upstream and downstream of the largest dams in the Ebro valley. We are aware of no systematic attempt to directly assess the sediment transfer through reservoirs in a large river during frequent floods. The results from the Ebro River can be of use for the design and implementation of restoration programmes in large highly degraded fluvial ecosystems, especially in Mediterranean environments through, for instance, the artificial injection of sediment to mitigate sediment deficit and the release of flushing flows downstream from big dams.

2. Study area

The Ebro basin is the largest in the Iberian Peninsula. It drains 85,530 km^2 along the southern-facing slopes of the Cantabrian Range and Pyrenees, and the northern-facing slopes of the Iberian Massif, and debouches into the Mediterranean downstream from Tortosa, 180 km south of Barcelona (Figure 1 (C3P1)). Mean annual precipitation varies from over 2000 mm in the Pyrenees to less than 400 mm in the arid interior. Mean annual runoff at Tortosa is 13,400 hm^3 (e.g. 1 hm^3 = 1 x 10^6 m^3). Maximum peak flow on the Ebro River was around 12,000 m^3/s in 1907 in Tortosa (Novoa, 1984).

One hundred and eighty-seven reservoirs regulate 57% (7,700 hm^3) of the Ebro River's total annual runoff. This is a much higher rate of impoundment than that typically encountered in more humid regions and for catchments of similar size (e.g. 5% to 18% in the Rhine, Elba and Wesser rivers, P. Ergenzinger and C. de Jong, Freie Universität Berlin, personal communication). Virtually all dams were constructed during the 20^{th} century, with 67% of reservoir capacity built in the 1950-1975 period. Mequinenza (1966) is the largest dam in the basin with a capacity of 1,534 hm^3 (11% of annual runoff). The Riba-roja Dam (1969) has a capacity of 207 hm^3 and impounds the two largest tributaries of the Ebro (the Segre and the Cinca rivers). The confluence of the two rivers occurs 5 km upstream the reservoir. It completes the 110 km-long reservoir chain in the lower Ebro (Figure 1 (C3P1)). The influence of the lowermost Flix Dam (1948), with a capacity of 11 hm^3, is less significant.

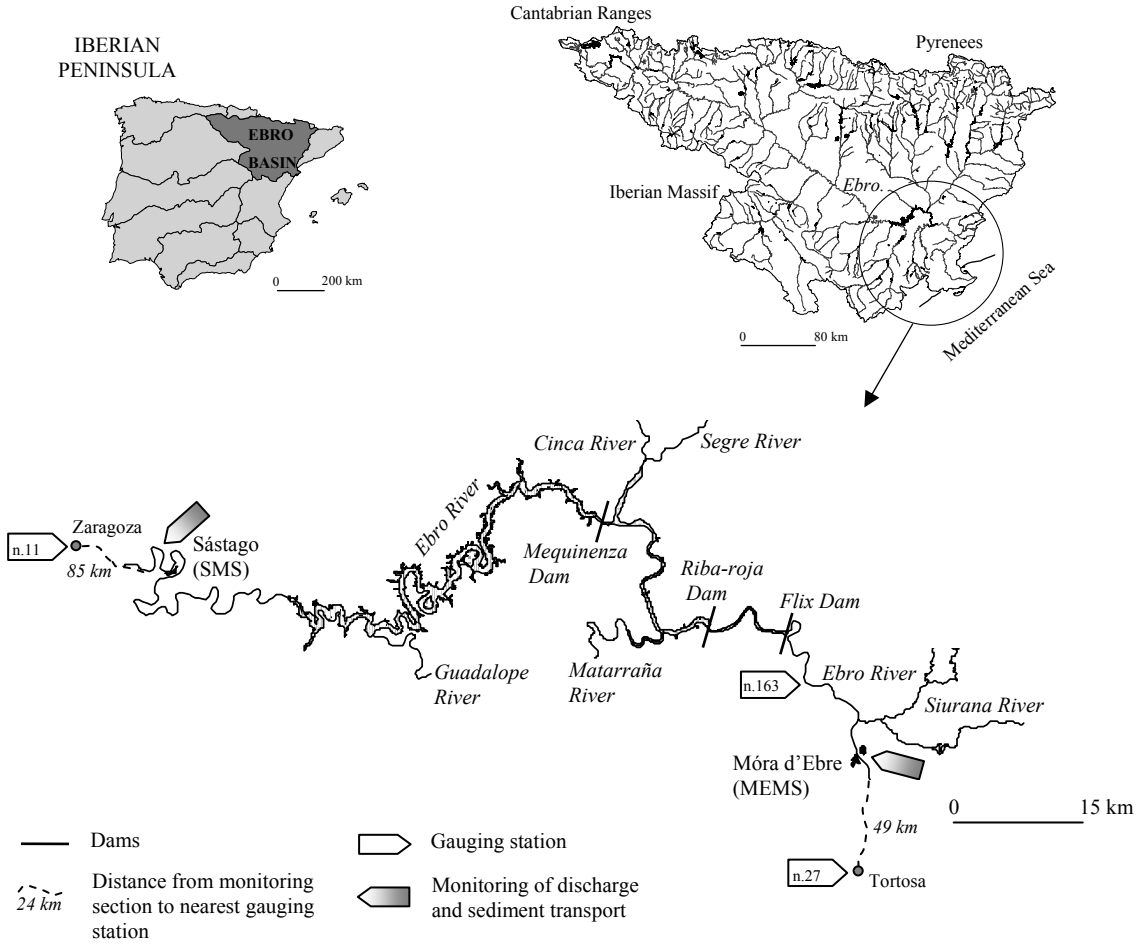

Figure 1 (C3P1). Location of the study reach on the lower Ebro River

Dams have altered the downstream hydrology of the lower Ebro River. Downstream from the Mequinenza and Riba-roja dams, frequent floods (e.g. Q_2 to Q_{25}) have been reduced by around 25%, on average (Batalla *et al.*, 2004). Moreover, dams trap most of the sediment transported in the basin and in the river mainstem. Estimated total annual sedimentation in the basin is 15 hm^3 (Sanz *et al.* 1999, Batalla 2003). According to data from Bayerri (1934-1935) and further estimates by Nelson (1990) the annual sediment contribution of the Ebro to its delta at the beginning of the 20^{th} century was around 15 x 10^6 tonnes. Most of that sediment was carried in suspension as indicated by mean concentrations of around 1 g/l, rising to 10 g/l during floods. Sediment trapping efficiency for suspended sediment in the Mequinenza and Riba-roja reservoirs has been estimated at around 90%, following the method of Brune (1953). Sanz *et al.* (1999) reported a current mean release of sediment in suspension of 263,000 t/y. This value represents less than 10% of the mean upstream

sedimentation in the Mequinenza and Riba-roja reservoirs reported by Avendaño *et al.* (1997). In addition, all bedload is trapped by reservoirs. The lower Ebro River does not receive coarse fractions from upstream dams. However, the river partially maintains its bedload transport capacity since floods have not been dramatically reduced. Current bedload capacity has been estimated at around 150,000 t/y (Vericat and Batalla, 2004). This was an estimation, based on bedload formulae, of the annual average capacity made over a 30-yr period, while data presented in this paper have been directly obtained in the field and are analysed at flood scale. Since dams were constructed, and according to field observations, sediment is typically entrained from the riverbed and from lateral deposits, and deposited in the lowermost reaches of the river, already in the delta plain (Vericat and Batalla, 2004).

Lack of sediment nourishment due to large dams and reduction in sediment transport capacity can be identified as the main reason for the retreat of the Ebro delta, which has been observed since the 1970s. Moreover, the lack of sediment and the reduction of floods have caused changes in river channel morphology, mainly revegetation of formerly active areas, riverbed coarsening, and increasing erosion of channel banks (Sanz *et al.* 1999, Avendaño *et al.* 2000, Vericat and Batalla, 2004).

3. Methodology

Discharge and sediment transport were measured during two consecutive floods (4 to 8 years of return period) that occurred during February and March 2003. Measurements and samples were taken upstream from the Mequinenza and Riba-roja dams, at the Sástago Monitoring Section (SMS), and downstream from the dams, at the Móra d'Ebre Monitoring Section (MEMS) (Figure 1 (C3P1)).

3.1. Measurement and computation of flood discharges

Flow velocity was measured from a bridge during floods by means of an OTT C31 current meter attached to a cable-suspended US DH74 sampler (Figure 2a (C3P1)). Five velocity profiles were compiled at the SMS for instantaneous discharges between 750 m^3/s and

2,135 m^3/s. Eight velocity profiles were undertaken at the MEMS for instantaneous discharges between 750 m^3/s and 2,160 m^3/s (Table 1 (C3P1)). Mean velocities were calculated from velocity profiles and subsequently used to calculate flood discharges. Simultaneously, we measured channel width by means of a laser telemeter and flow depth from the corrected vertical of the crane cable.

Figure 2 (C3P1). Field equipment to measure discharge and sediment transport from bridges: a) OTT C31 current metre attached to a cable suspended US DH74 sediment sampler, b) cable suspended 76 kg Helley Smith Sampler, c) automatic crane for suspension of sampling equipment, and d) intake (152 mm) of the Helley Smith Sampler, showing bedload material captured on February 11th 2003. Photos by the authors (February 2003)

Complete flood hydrographs at the monitoring sections were obtained by routing hydrographs from upstream official gauging stations operated by the Ebro Water Authorities. Discharges for the SMS were obtained from the gauging station located in Zaragoza (n.11, 85 km upstream), and discharges at the MEMS were estimated from the gauging station located in Ascó (n.163, 15 km upstream) and further compared with discharges in Tortosa (n.27, 49 km downstream). At-a-section discharge measurements

were used to calibrate flood hydrographs. The Muskingum method (Shaw, 1983) was used to route hydrographs from upstream to downstream sections:

$$O_2 = (C_1 \cdot I_1)+(C_2 \cdot I_2)+(C_3 \cdot O_1)$$
$$C_1 = [\Delta T+(2 \cdot k \cdot X)] / \{[(\Delta T+[(2 \cdot k)-(2 \cdot k \cdot X)]\}$$
$$C_2 = [(\Delta T-(2 \cdot k \cdot X)] / \{[(\Delta T+(2 \cdot k)-(2 \cdot k \cdot X)]\}$$
$$C_3 = 1- (C_1+C_2)$$

where, k is time (in hours), ΔT is the increment of time from point 1 to point 2, $I_{1 \text{ and } 2}$ are flow inputs in 1 and 2, $O_{1 \text{ and } 2}$ are flow outputs in 1 and 2, and X is the relative importance of I and O in determining water storage in the river reach. The limits of X are 0 and 0.5. X=0.2 was used to best fit the hydrographs using the field data at SMS, and X=0.1 at MEMS.

3.2 Sampling and computation of sediment transport

Suspended sediment was point sampled at the two measuring sections, the SMS and MEMS. For that purpose, we used a 28 kg cable-suspended depth-integrating US DH78 sampler (Figure 2a (C3P1)). Approximately, ¾ litres of water were collected in every sample. A total of one hundred and thirty-seven samples were carried to the laboratory and filtered using 1.2 μm cellulose filters. Subsequently, the suspended sediment concentration for each sample was calculated.

Bedload was sampled at the same vertical at the SMS using a 29-kg cable-suspended Helley-Smith sampler with a 76 mm intake. The median size of riverbed sediments is 17 mm and maximum particles attain 55 mm (Figure 3 (C3P1)), thus this type of Helley-Smith sampler provides an efficient sampling for most grain size classes that may entrain in motion during floods. The bedload sampler was operated using a manual crane. At the MEMS, bedload was sampled by means of a 76-kg cable suspended Helley-Smith sampler with a 152-mm intake (Figure 2b and 2d (C3P1)). The bedload sampler was operated from the bridge using an automatic crane (Figure 2c (C3P1)). In this section, the median size of bed-material is 50 mm and maximum particles in the surface reache 117 mm (Figure 3 (C3P1)), thus this type of Helley-Smith ensures an efficient sampling of bedload for almost

all grain size classes. In both sections, sampling time ranged from 1 to 5 minutes, to ensure that the sampler bag was not filled to more than 50% and thus to keep sampling efficiency as high as possible (Emmett, 1980). The sampling interval was thirty minutes. A total of one hundred and three samples were collected and taken to the laboratory, where they were dried, sieved and weighed to obtain the total mass and grain size distribution.

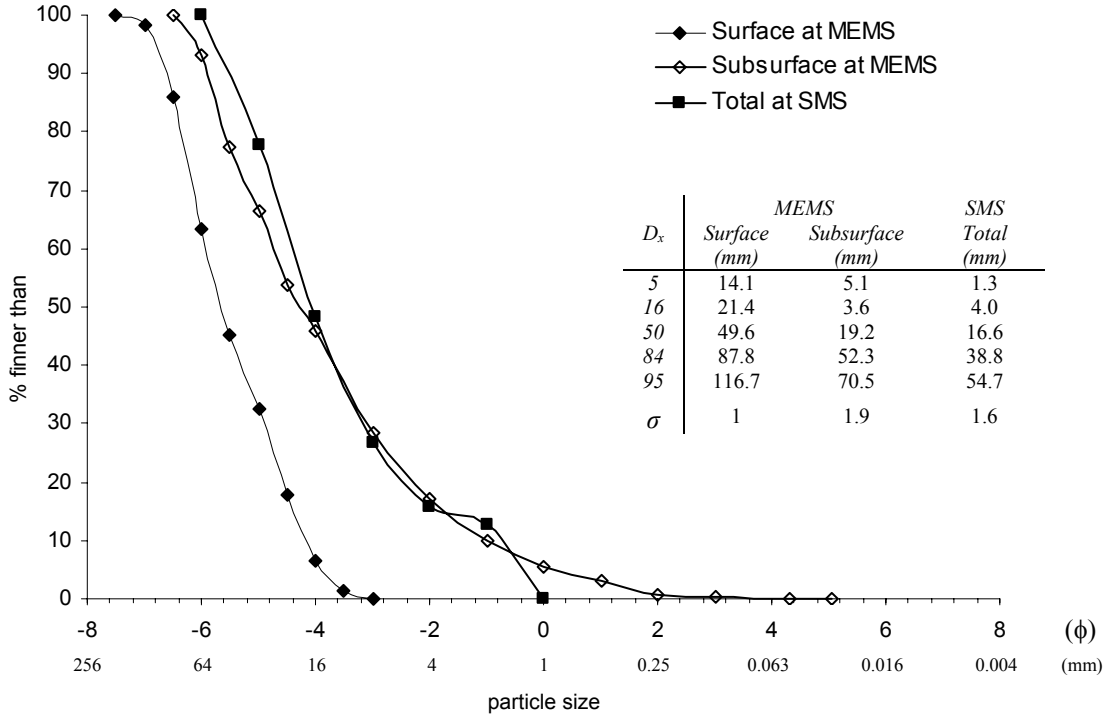

D_x	MEMS Surface (mm)	MEMS Subsurface (mm)	SMS Total (mm)
5	14.1	5.1	1.3
16	21.4	3.6	4.0
50	49.6	19.2	16.6
84	87.8	52.3	38.8
95	116.7	70.5	54.7
σ	1	1.9	1.6

Figure 3 (C3P1). Grain size distribution of bed-materials at SMS reach, upstream dams, and MEMS reach, downstream from the dams. The sorting coefficient (σ) was calculated from the Folk and Ward (1957) formulae: $[(\phi_{95}-\phi_5)/6.6] + [(\phi_{84}-\phi_{16})/4]$, when $-\phi_x$ is a given percentile of the particle size distribution in the phi scale

On February 10th 2003, we lost the 29-kg Helley-Smith sampler at the SMS, when floating woody debris broke the crane cable and dragged the sampler downstream. Up to that moment, fifteen samples had been obtained, all of them under discharges higher than 1,900 m^3/s. In order to calculate bedload rates for discharges below that value, we applied the bedload transport formula by Meyer Peter *et al.* (1934) and Schoklitsch (1950), both fully applicable to the physical characteristics of the river reach (slope and particle size). In order to obtain the degree of adjustment (ε) between computed and observed bedload rates, the following ratio was used:

$$\varepsilon = i_{bc}/i_{bo}$$

where i_{bc} is the mean computed bedload transport rate using the formula and i_{bo} is the mean observed bedload in the field, both in g/ms. A value of 1 would indicate a perfect match between the two data sets. Except for this particular case, sediment yield at the two monitoring sections was calculated using load-rating relations between discharge and suspended sediment and between discharge and bedload (Walling, 1984).

A series of experimental reaches were selected in order to assess the response of the river-bed after floods. Seven cross sections were made by means of an ecosound Lowrance LCX-15 (decimetric resolution) and a total station; in addition and, in order to verify changes observed after surveying cross sections, pairs of scour chains (e.g. Hassan, 1988) and painted pebbles (e.g. Sala and Gallart, 1988) were placed in each section.

Riverbed material was sampled upstream from the two monitoring sections in order to characterise its grain size distribution. Upstream from the SMS, and due to the absence of armouring, we took a volumetric sample of 46 kg, in which the D_{max} of 70 mm did not exceed 1% of sample weight (Church *et al.*, 1987) (Figure 3 (C3P1)). Upstream from the MEMS, we sampled surface and subsurface material separately. The surface layer was characterised using the pebble count method measuring the b axis of 400 particles (Wolman 1954, Rice and Church 1996). The subsurface material was sampled using the volumetric technique, in which the D_{max} of 72 mm did not exceed 1% of sample weight (Church *et al.*, 1987) (Figure 3 (C3P1)).

4. Results and discussion

The flood events of February and March 2003 were basically mainstem Ebro River floods, with most runoff contributed from the basin headwaters in the Cantabrian Ranges, the Western Pyrenees and the Western Iberian Massif. The main tributaries, such as the Gállego, the Cinca and the Segre, did not play a major role in those two events.

4.1 Flood of February 2003

The 'February 2003 flood' began on January 31st and finished on February 20th. It was produced by a mean precipitation of 15 mm (Figure 4 (C3P1)), calculated for the period 29th January to 1st February 2003 from 65 stations distributed over the whole catchment. Maximum precipitation over the same period was 135 mm. It occurred in the north-west end of the Ebro basin (Cantabrian Ranges). Flood caused widespread damage in the central Ebro Valley, especially in small riverine villages upstream from the city of Zaragoza. The return period for the peak flow is 10 years, estimated from the flow series at the gauging station in Zaragoza (upstream from the large dams), and 8 years estimated from the regulated flow series of the gauging station at Tortosa (downstream from the dams) (Batalla *et al.*, 2004).

4.1.1. Flood peaks and water yield

Mean discharge at the SMS was 995 m^3/s (calculated between 31st January 2003 and 20th February 2003) (Figure 4 (C3P1)). In terms of flow duration, a discharge of 360 m^3/s was equalled or exceeded 90% of the time during the flood, while a discharge of 780 m^3/s was equalled or exceeded 50% of the time (Figure 4 (C3P1)). The flood yielded 1,785 hm^3 of water, which represents 26% of the mean annual water yield of the Ebro River in Zaragoza (85 km upstream from the SMS).

The mean discharge at the MEMS was 1,180 m^3/s (31st January 2003 to 20th February 2003) (Figure 4 (C3P1)). In terms of flow duration, a discharge of 800 m^3/s was equalled or exceeded 90% of the time during the flood, while a discharge 1,050 m^3/s was equalled or exceeded 50% of the time (Figure 4 (C3P1)). The flood yielded 2,120 hm^3 of water, which represents 16% of the mean annual water yield of the Ebro River in Tortosa (49 km downstream from the MEMS), close to the river mouth.

The reservoirs modified the flood timing. The volume of water in storage was close to 100% before the event. For this reason, the Mequinenza and Riba-roja dams started to release water before the flood peak reached Sástago (SMS), at the tail of the Mequinenza reservoir. As a result, the flood hydrographs are similar in both sections, but the main peak

discharge was advanced 3 days downstream from the dams. Overall, the dams released more water downstream in comparison with the upstream contribution. The water budget after the flood showed a net loss of 330 hm^3 of water in storage, mainly in the Mequinenza reservoir.

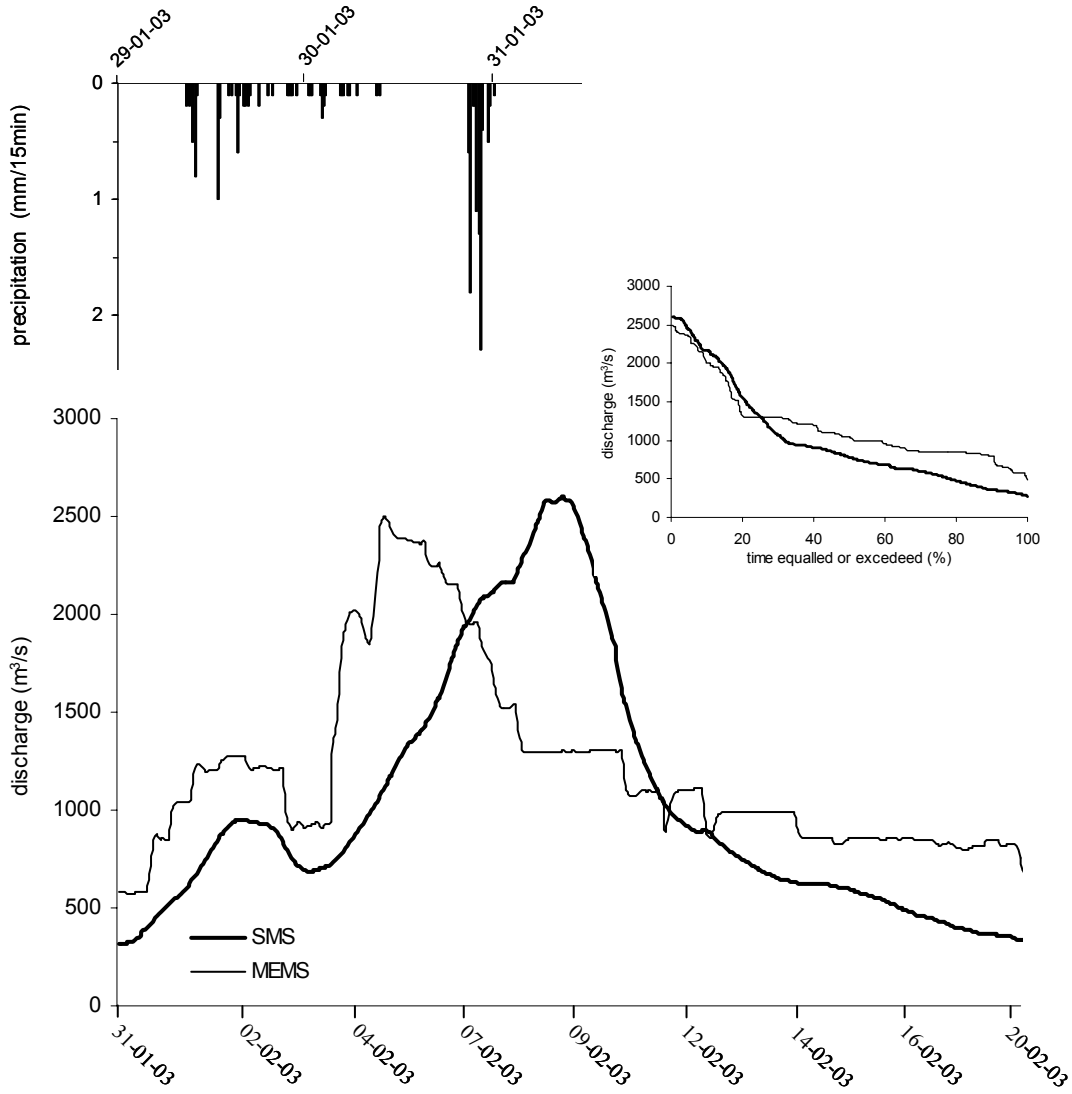

Figure 4 (C3P1). Storm hyetograph (at one representative station, A-260, located in the centre of the Ebro basin), flood hydrographs (upstream and downstream dams), and flow frequency curves (upstream and downstream dams), corresponding to the February 2003 flood on the Lower Ebro River. Note that precipitation is represented only for 29th and 30th of January, when almost all rainfall took place

4.1.2. Suspended sediment load

During the February flood, a total of twenty-five samples of water and suspended sediment were taken at the SMS, upstream from the dams (Table 1 (C3P1)). The mean suspended concentration was 460 mg/l with a coefficient of variation of 130%. The statistical relation between discharge and suspended sediment concentration is best fitted by an equation of the type $y = a \cdot x^b$ with $r^2 = 0.91$ (Figure 5a (C3P1)). The total sediment yield due to suspended load at the SMS was 885,000 tonnes.

Table 1 (C3P1). Mean daily discharges and the associated mean sediment loads obtained during sampling campaigns during February and March 2003 floods in the lower Ebro River, upstream and downstream from the large Mequinenza and Riba-roja dams

Measuring section by flood	Sampling date	Discharge (m^3/s)	Depth (m)	Velocity (m/s)	Suspended load		Bedload	
					Concentration (mg/l)	Number of samples	Transport rate (g/ms)	Number of samples
February flood								
SMS[1]	07/02/2003	1,980	6.3	2.2	981.7	10	79.2	10
	10/02/2003	2,060	6.5	2.4	258.9	5	124.3	5
	13/02/2003	765	3.8	1.9	111.3	4	-[3]	-
	20/02/2003	280	2.8	-[4]	1.9	6	-[3]	-
MEMS[2]	02/02/2003	1,280	4.7	-[4]	9.7	12	52.4	12
	03/02/2003	1,125	4.4	-[4]	3.3	12	56.3	12
	05/02/2003	2,250	7.0	3.1	286.2	8	250.8	4
	11/02/2003	1,090	4.3	1.5	11.3	8	218.8	25
	13/02/2003	990	4	1.7	9.0	6	108.5	6
March flood								
SMS	28/02/2003	1,440	5.2	-[4]	1,200	6	-[3]	-
	03/03/2003	1,125	4.6	2.1	142.8	6	-[3]	-
	05/03/2003	730	3.7	2.0	79.7	5	-[3]	-
MEMS	28/02/2003	1,740	5.8	-[4]	47.1	10	-[4]	-
	02/03/2003	1,760	5.8	2.3	52	4	-[4]	-
	03/03/2003	1,630	5.5	2.5	38.2	6	-[4]	-
	05/03/2003	1,480	5.2	2.1	28.7	5	842.4	5
	10/03/2003	1,170	4.5	1.6	17.7	12	333.3	12
	12/03/2003	823	3.6	1.7	12.8	12	149.8	12

[1] **S**ástago **M**onitoring **S**ection, upstream Mequinenza and Riba-roja dams
[2] **M**óra d'**E**bre **M**onitoring **S**ection, downstream Mequinenza and Riba-roja dams
[3] Estimated by means of the Meyer-Peter et al., (1936) formulae
[4] Not measured

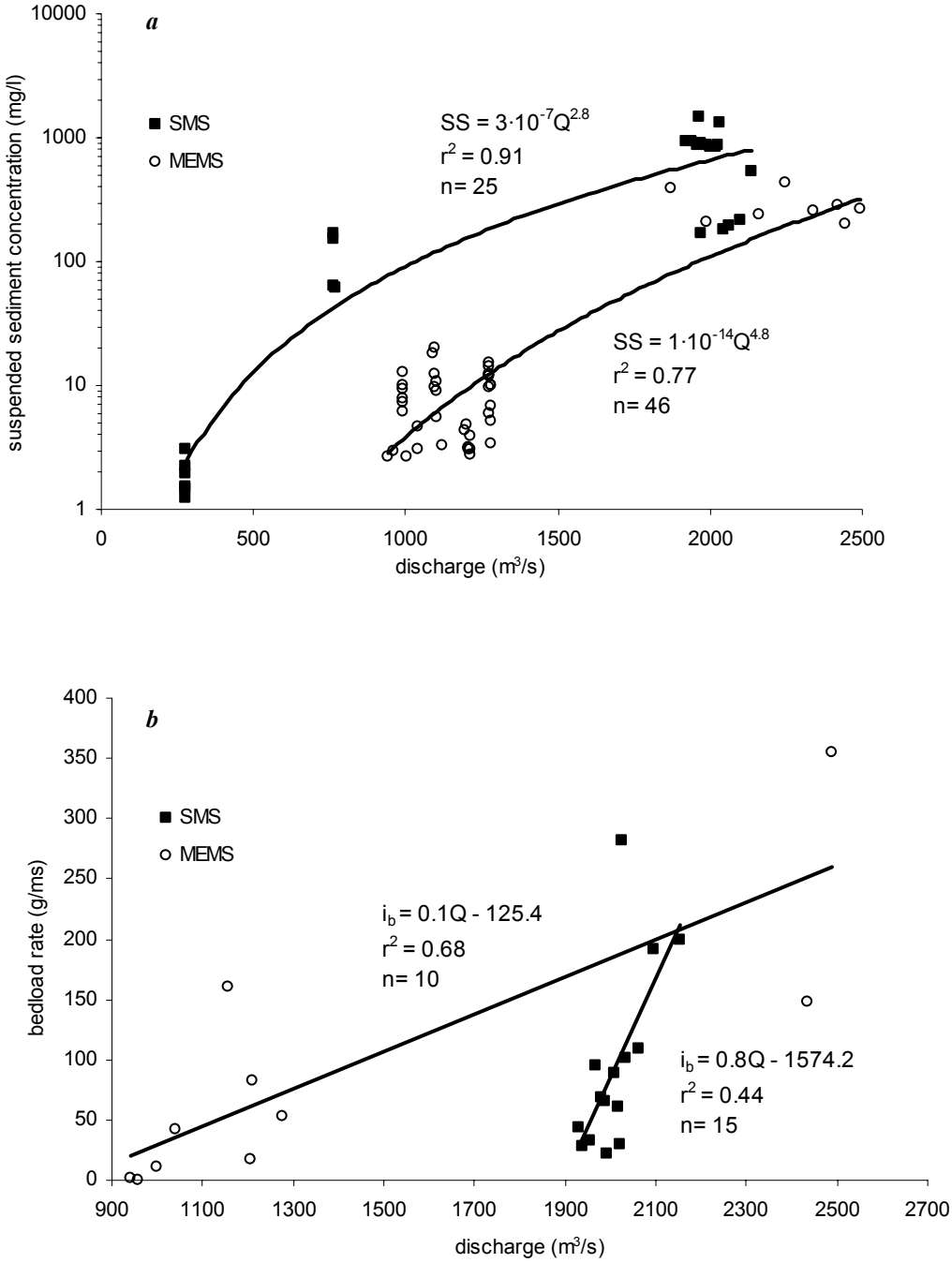

Figure 5 (C3P1). Sediment load rating curves at the monitoring sections on the lower Ebro River upstream (SMS) and downstream from the dams (MEMS) during the February 2003 flood: **a**) a significant statistical relation between suspended sediment concentration and discharge ($p<0.01$) and **b**) a significant statistical relation between bedload rates and discharge ($p<0.01$). Note that at the MEMS, the bedload rates were averaged for the same discharges in order to obtain the highest possible correlation with discharge

At the MEMS, forty-six samples of water and suspended load were obtained (Table 1 (C3P1)). The mean suspended concentration was 64 mg/l with a coefficient of variation of 195%. This concentration is one order of magnitude lower than the average (700 mg/l to 1,700 mg/l) value calculated by Bayerri (in Guillén and Palanques, 1992) for the Ebro River under pre-dam conditions. The maximum value was obtained during sampling on February 5th, with a concentration of 435 mg/l for a discharge of 2,250 m^3/s. This value is twenty-five times less than the maximum concentration during floods (10 g/l) reported by Bayerri (in Guillén and Palanques, 1992). The statistical relation between discharge and suspended sediment concentration is best fitted by a potential regression with $r^2 = 0.77$ (Figure 5a (C3P1)). The total sediment yield due to the suspended load at the SMS was 100,000 tonnes.

The dams deeply altered the transfer of fine sediment in suspension between the two monitoring sections and, hence, between the upper Ebro basin and the downstream reaches and the delta. Concentrations of suspended sediment were significantly reduced by almost an order of magnitude. A total of 785,000 tonnes of fine sediment was trapped in the two reservoirs, but especially in the upstream and largest one, Mequinenza. The trapping efficiency of the reservoirs during this event was 90%.

4.1.3 Bedload

At the SMS, upstream from the dams, fifteen bedload samples were obtained before the loss of the 29-kg Helley Smith sampler (Table 1 (C3P1)). The mean bedload rate was 94 g/ms (5 g/m^3) under a mean discharge of 2,000 m^3/s with a coefficient of variation of 80%. McLean *et al.* (1999) reported similar bedload rates for the Fraser River in British Columbia, under non-regulated conditions, such as in the Ebro at the SMS. The statistically significant relation between discharge and bedload for discharges above 1900 m^3/s is best fitted by an equation of the type $y = a+bx$ with $r^2 = 0.44$ (Figure 5b (C3P1)), although the plot shows a considerable degree of data point scatter. The maximum median bedload size (D_{50}) was 40 mm. Bedload for discharges lower than 1,900 m^3/s was not sampled, but estimated using the Meyer Peter *et al.* (1934) formulae. The mean degree of adjustment (ε) between the computed bedload rates and the observed rates was 0.94. The degree of adjustment between the computed values from the Schoklitsch (1950) formulae and the

observed values in the field was 1.3, and, therefore, it was not used in the calculation. The mean computed bedload rate for discharges lower than 1900 m^3/s was 120 g/ms. The bedload yield from the observed and computed values were added to yield a total bedload transport in the section of around 13,000 tonnes (1.5% of the total sediment load). This proportion of bedload in relation to total load is similar to values reported for other large fluvial systems, such as the Fraser River (McLean *et al.*, 1999).

At the MEMS, downstream from the dams, fifty-nine samples of bedload were collected (Table 1 (C3P1)). The mean bedload rate was 143 g/ms (19 g/m^3) for a mean discharge of 1,220 m^3/s. Wohl and Cenderelli (2000) reported maximum bedload rates of around 20 g/ms following a reservoir sediment release in north-central Colorado. The maximum median bedload size (D_{50}) was 72 mm. The minimum value was 0.3 g/ms, which is still one order of magnitude higher than the rates reported by Guillén *et al.* (1992) at the lower end of the Ebro River (estuary) for the same range of discharges. The mean coefficient of variation was 100%. The bedload shows a remarkable degree of variability. Even under similar discharges variability of bedload rates was important: on February 11th, with a discharge 1,095 m^3/s, the bedload had a maximum variability of 800% between samples under the same discharge. The bedload yield was calculated separately, both for the rising and the falling limbs of the hydrograph. During the rising limb of the flood (from January 31st to the flood peak on February 5th), the bedload rates were low (80 g/ms, on average) and showed a notable correlation with discharges, as indicated by $r^2 = 0.68$ (Figure 5b (C3P1)). The bedload still reflected the role of riverbed armouring not releasing subsurface sediment after a long period of non bed-material entrainment. For that part of the flood, the bedload yield was 4,830 tonnes. In contrast, bedload rates increased substantially around and after the flood peak, but they no longer showed no statistically significant relation with the discharge. Thus, bedload yield during flood recession was calculated as the product of the mean bedload rate measured in the field (207 g/ms) and the mean discharge. For the second part of the flood, the bedload yield was 42,725 tonnes, yielding a total of 47,555 tonnes for the whole event (42% of the total solid load downstream from the dams).

One of the most important characteristics of regulated rivers is that dams trap 100% of coarse sediment, generally moving as bedload. On the lower Ebro, the dams break the continuum of bedload. Under these conditions, the channel of the lower Ebro should be

itself the main bedload source in the river channel, at least in the monitored reach between Flix dam and the MEMS. The major tributary in the whole reach, the Siurana River, suffers from a large sediment deficit due to dams and instream gravel mining. River incision due to bedload entrainment and non-replacement during this flood would have been about 9 mm. Field evidences of riverbed incision are presented in section 4.5. Bank erosion was previously described by Batalla (2003). This value was calculated from a sediment density of 1.65 t/m^3 (in submerged weight), a porosity of the riverbed deposits of 0.26, an average channel width of 155 metres (corresponding to 7 representative instrumented cross-sections), and a distance of 27 km from the lowermost dam at Flix to the measuring site in Móra d'Ebre. Bouno *et al.* (1999) reported important riverbed degradation after a high-magnitude flood in the Saru River downstream from the Nibutani dam in Japan.

4.2 Flood of March 2003

The 'March 2003 flood' began on February 26th and finished on March 17th. It was produced by a mean precipitation of 35 mm (Figure 6 (C3P1)), calculated for the period 22nd February to 28th February 2003 from 65 stations distributed over the whole catchment. Maximum precipitation over the same period was 122 mm. It occurred in the Western Ebro headwaters, between the Iberian Massif and the Cantabrian Ranges. Flood again caused problems in the central Ebro Valley, but fewer than those produced by the February flood. The return period for the peak flow was 4 years, estimated from the flow series at the gauging station in Zaragoza (upstream from the dams), and 4.5 years estimated from the regulated flow series at the gauging station in Tortosa (downstream from the dams).

4.2.1. Flood peaks and water yield

The mean discharge at the SMS was 810 m^3/s (calculated between 25th February 2003 and 16th March 2003) (Figure 6 (C3P1)). In terms of flow duration, a discharge of 280 m^3/s was equalled or exceeded 90% of the time during the flood, while a discharge of 720 m^3/s was equalled or exceeded 50% of the time (Figure 6 (C3P1)). The flood yielded 1,350 hm^3 of water, which represents 20% of the mean annual water yield of the Ebro in Zaragoza (85 km upstream from the SMS).

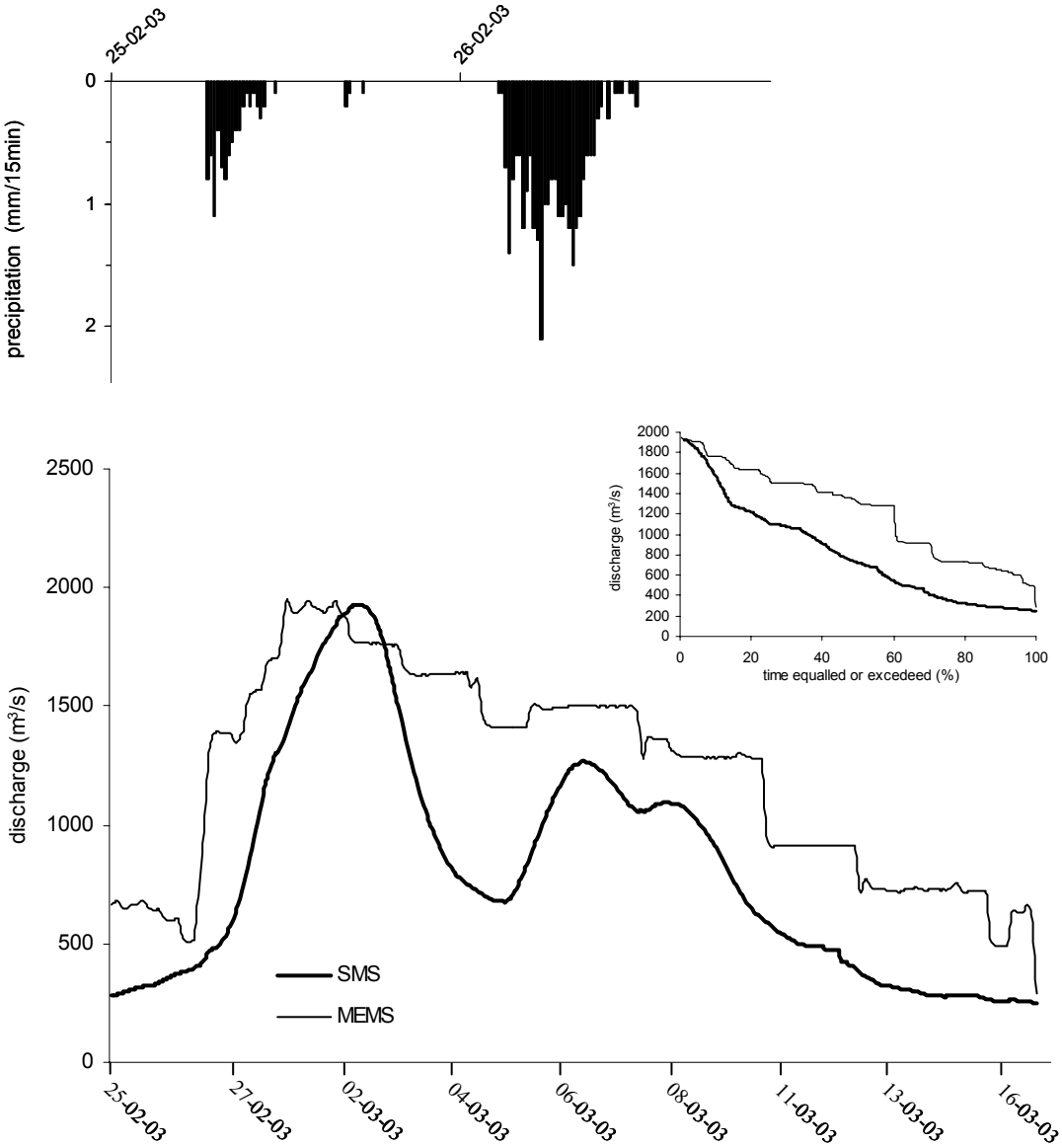

Figure 6 (C3P1). Storm hyetograph (at one representative station, A-260, in the centre of the Ebro basin), flood hydrographs (upstream and downstream dams), and flow frequency curves (upstream and downstream dams), corresponding to the March 2003 flood on the Lower Ebro River. Note that precipitation is represented only for 25th and 26th of February, when almost all rainfall took place

The mean discharge at the MEMS was 1,220 m^3/s (25th February 2003 to 16th March 2003) (Figure 6 (C3P1)). A discharge of 650 m^3/s was equalled or exceeded 90% of the time, while a discharge of 1,300 m^3/s was equalled or exceeded 50% of the time (Figure 6 (C3P1)). Flood yielded 2,030 hm^3 of water (Table 1 (C3P1)), which represents 15% of the mean annual water yield of the Ebro in Tortosa (49 km downstream from the MEMS).

As in the case of the February flood, the reservoirs substantially altered the flood timing. The water volume in storage in the Mequinenza and Riba-roja reservoirs was again high before the flood (>90%). For this reason, the two dams started to release water before the flood peak reached Sástago, where the river enters the Mequinenza reservoir. The main peak discharge downstream the dams was advanced by 36 hours. Overall, the dams released more water downstream from the dams than the upstream flow contribution. This fact is clearly reflected by the relative duration of given discharges (for instance, a discharge of 1,000 m^3/s was exceeded 35% of the time at the SMS but 60% at the MEMS). The water budget after the flood indicated a net loss of 680 hm^3 of stored water, double that of the February flood and mainly from the Mequinenza dam.

4.2.2. Suspended sediment load

During the March flood, a total of seventeen samples of water and suspended sediment were taken at the SMS, upstream from the dams (Table 1 (C3P1)). The mean suspended concentration was 495 mg/l with a coefficient of variation of 110%. The statistical relation between discharge and the suspended sediment concentration was best fitted by an equation of the type $y = a \cdot x^b$ with $r^2 = 0.76$ (Figure 7a (C3P1)). The total sediment yield due to suspended load at the SMS was 803,000 tonnes, slightly lower than that carried by the February flood.

At the MEMS, forty-nine samples of water and suspended load were obtained (Table 1 (C3P1)). The mean suspended concentration was 29 mg/l (with a coefficient of variation of 195%), relatively higher than those reported by Guillén and Palanques (1992) for the Ebro downstream from MEMS for the same range of discharges. The statistical relation between discharge and the suspended sediment concentration is best fitted by an equation of the type $y = a \cdot x^b$ with a $r^2 = 0.84$ (Figure 7a (C3P1)). The total sediment yield due to suspended load at the MEMS was 73,000 tonnes, slightly lower than that carried by the February flood, as was the case at the SMS.

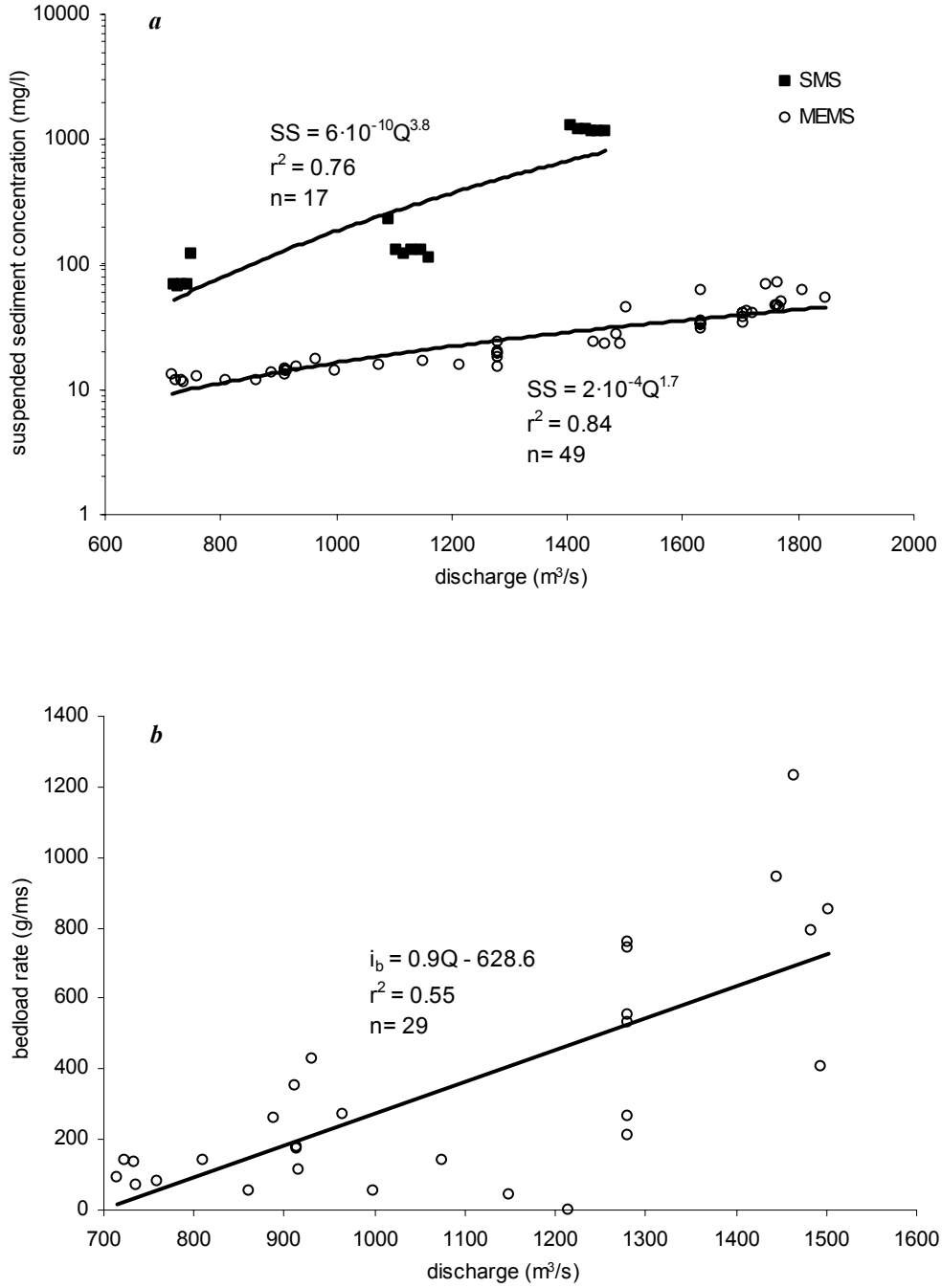

Figure 7 (C3P1). The sediment load rating curves at the monitoring sections on the lower Ebro River upstream (SMS) and downstream from the dams (MEMS) during the March 2003 flood. Significant statistical relations between (**a**) suspended sediment concentration and discharge ($p<0.01$) and (**b**) bedload rates and discharge ($p<0.01$)

As occurred during the February flood, suspended sediment transport and yield was much higher at the SMS, upstream from the dams, than at the MEMS, downstream from the

dams. The suspended sediment load was significantly reduced by the dams by an order of magnitude. A total of 730,000 tonnes of fine sediment was trapped in the two reservoirs, especially in the upstream one, Mequinenza. The trapping efficiency of the reservoirs during this event was again 90%. The results of the Ebro River confirm that most of the sedimentation in reservoirs on large rivers occurs as fine-sediment load (e.g. Bouno *et al.*, 1999).

4.2.3 Bedload

The mean computed bedload rate at the SMS using the Meyer Peter *et al.* (1934) formulae was 120 g/ms for a mean discharge of 1,460 m^3/s. The estimated amount of sediment entering the Mequinenza reservoir as bedload was 11,800 tonnes, which means 1.5% of the total sediment load, a very similar ratio to that in the February flood.

At MEMS, downstream from the dams, twenty-nine samples of bedload were collected (Table 1 (C3P1)). The mean bedload rate was 350 g/ms (52 g/m^3) for a mean discharge of 1,080 m^3/s. The maximum median size (D_{50}) of the bedload was 34 mm. The mean coefficient of variation is 93%. Even under similar discharges, the variability of bedload rates was important (up to 350% during consecutive samples). A significant statistical relation between bedload rates and discharge ($r^2 = 0.55$) was used to calculate the bedload yield on the downstream section (Figure 7b (C3P1)). Overall, around 130,000 tonnes of coarse bed-material moved as bedload, almost $^2/_3$ of the total sediment load. This fact can be related, on one side, to the lack of fine sediment supplied from the catchment to the river and, on the other, to the capacity of the water to entrain coarse material (sand and gravels) from the riverbed. It can be described as a river situation by which bedload transport occurs under almost clear water.

As in the case of the February flood, the dams on the lower Ebro broke the continuum of bedload. Therefore, the channel of the lower Ebro River again acted as the main source of the bedload passing the downstream MEMS. River incision due to bedload entrained but not replaced was estimated at around 24 mm, three times higher than the estimated riverbed degradation during the February flood.

4.4. Water and sediment transfer

During the two large floods of February and March 2003 on the lower Ebro, a total of 3,135 hm^3 of water entered the Mequinenza reservoir and 4,150 hm^3 was released downstream from the Riba-roja dam, yielding a negative water balance for the reservoir system of around 1,015 hm^3. This fact was especially important after the March flood (Table 2 (C3P1)). At the SMS, upstream from the dams, water yield was higher during the February flood (57%) than during the March flood (43%), and it was almost in balance at the MEMS, downstream from the dams. The two floods together represents 46% of the mean annual water yield at SMS (estimated from the gauging station series in Zaragoza) and 31% of the mean annual water yield at the MEMS (estimated from the gauging station series in Tortosa, near the river mouth).

Table 2 (C3P1). Water and sediment yield of the lower Ebro River during the floods of February and March 2003

	February flood				**March flood**				**February and March floods**			
	Water yield (hm^3)	**Sediment yield (1×10^3 t)**			**Water yield (hm^3)**	**Sediment yield (1×10^3 t)**			**Water yield (hm^3)**	**Sediment yield (1×10^3 t)**		
		In suspension	*Bedload*	*Total load*		*In suspension*	*Bedload*	*Total load*		*In suspension*	*Bedload*	*Total load*
SMS[1]	1,785	885	13	898	1,350	803	12	815	3,135	1,688	25	1,713
MEMS[2]	2,120	100	48	148	2,030	73	130	203	4,150	173	178	351

[1] **S**ástago **M**onitoring **S**ection, upstream Mequinenza and Riba-roja dams
[2] **M**óra d'**E**bre **M**onitoring **S**ection, downstream Mequinenza and Riba-roja dams

During the two floods, the river transported a total of 1,713,000 tonnes into the upstream Mequinenza reservoir at the SMS, almost all as suspended load (98.6%) (Table 2 (C3P1) and Figure 8 (C3P1)). The suspended sediment yield after the two floods was higher than the annual average (690,000 tonnes) and the annual maximum (1,445,000 tonnes) reported by Sanz *et al.* (1999) from intermittent suspended sediment sampling at the SMS between 1975 and 1992. The reservoir system may have captured around 90% of suspended sediment during the two floods, as the 173,000 tonnes still transported downstream from the dams would suggest. However, assuming that some erosion of fine materials occurred in the river channel (banks and bed) downstream from the dams, the trapping efficiency of

the reservoir could have reached even higher values. At least 1.6 x 10^6 tonnes of fine sediment carried by the river to the Mequinenza reservoir did not reach the lowermost part of the basin and the delta. Similar values of reservoir sediment retention (>95%) were reported for the Nile (Milliman and Meade 1983, Shahin 1985).

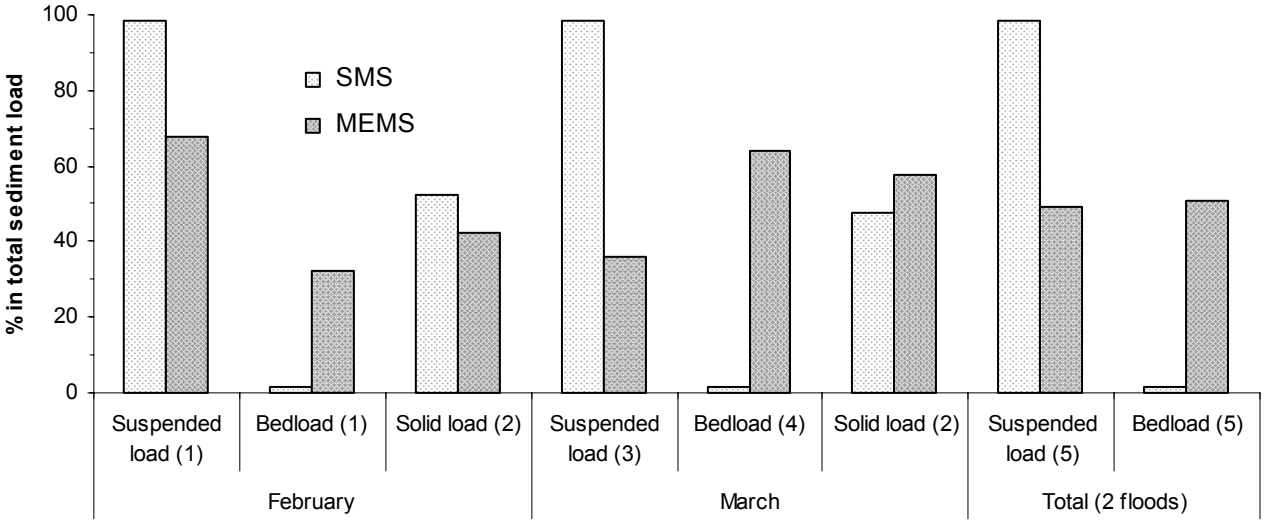

SMS: **S**ástago **M**onitoring **S**ection, upstream dams
MEMS: **M**óra d'**E**bre **M**onitoring **S**ection, downstream dams

(1) Suspended load or bedload in relation to total load during February flood
(2) Total load during February or March floods in relation to total load during the the two floods
(3) Suspended load in relation to total load during March flood
(4) Bedload in relation to total load during March flood
(5) Suspended load or bedload in relation to total load during the two floods

Figure 8 (C3P1). Suspended sediment and bedload on the lower Ebro River during the February and March 2003 floods, expressed as percentage of the total solid load

The bedload yield at the SMS was very small in comparison with the suspended load, although it reached 25,000 tonnes, a significant transport of sand and especially gravels, taking into account the low gradient of the river channel between Zaragoza and Sástago (0.0006).

Downstream from the dams at the MEMS, the river carried a total load of 350,000 tonnes during the two consecutive floods, with the higher load reached during the March flood (almost 60%) (Table 2 (C3P1) and Figure 8 (C3P1)). As indicated above, a total of 173,000 tonnes of sediment in suspension passed the downstream section at the MEMS. This value is lower than the annual average of 263,000 tonnes estimated by Sanz *et al.*

(1999) just downstream from the Flix dam, upstream from the MEMS. The average value by Sanz *et al.* (1999) includes frequent sediment contributions from the main tributaries of the Ebro, the Cinca and Segre Rivers, debouching directly into Riba-roja reservoir (Figure 1 (C3P1)). In contrast, the February and March 2003 floods occurred mainly in the mainstem Ebro River, thus with most sedimentation occurring in the large Mequinenza reservoir and with no significant contribution from the tributaries.

Bedload played a major role in comparison with the suspended load distribution in the downstream reaches, especially during the March flood, accounting for 51 % of the flood's total load. This fact could be related to the breaking of the armour layer after the flood peak on February the 28th, which effectively caused a sudden increase in the bedload rates registered at the MEMS (e.g. Ryan *et al.*, 2002). This fact is illustrated, on one side, by the different nature of the hydraulic relation between discharge and bedload before and after the peak discharge, as it has been explained in section 4.1.3. and, on the other, by the increase of the grain size of bedload after the peak discharge (D_{50} increased from an average of 15 mm to an average of 20 mm, while D_{max} increased from an average of 47 mm to an average of 55 mm).

4.5. Sediment deficit and riverbed response

The dams capture all bedload, creating an important downstream sediment deficit of coarse fractions. In the case of the lower Ebro River, a total of 178,000 tonnes of sediment may have been entrained from the riverbed downstream from the dams and transported during the two consecutive floods. This fact caused a mean incision of 33 mm as a consequence of the action of the 'hungry water' during the events. This value was confirmed after surveying cross sections, scours chains and painted pebbles at 7 experimental sites along the study reach. Cross sections, both at the beginning of the study reach (immediately downstream from the Flix Dam) and at the lowermost end of the study reach (MEMS) show evidences of river-bed net erosion (Figure 9 (C3P1)). Average incision in the armoured section ($D_{50surface}/D_{50subsurface}$ = 2.7) of the Flix Dam was 8 mm. In contrast, average incision in the loose section ($D_{50surface}/D_{50subsurface}$ = 1.6) of MEMS was 200 mm, after the two consecutive floods. No data for other cross sections is yet available, but tendency to net erosion in the whole study reach (downstream dams) is also suggested by

scour chains (Figure 10 (C3P1)), although with high variability from section to section. Average net incision from scour chains is 22 mm (Table 3 (C3P1)). Maximum mobilised particles point out to the same order of magnitude in terms of river-bed remobilization (Table 3 (C3P1)).

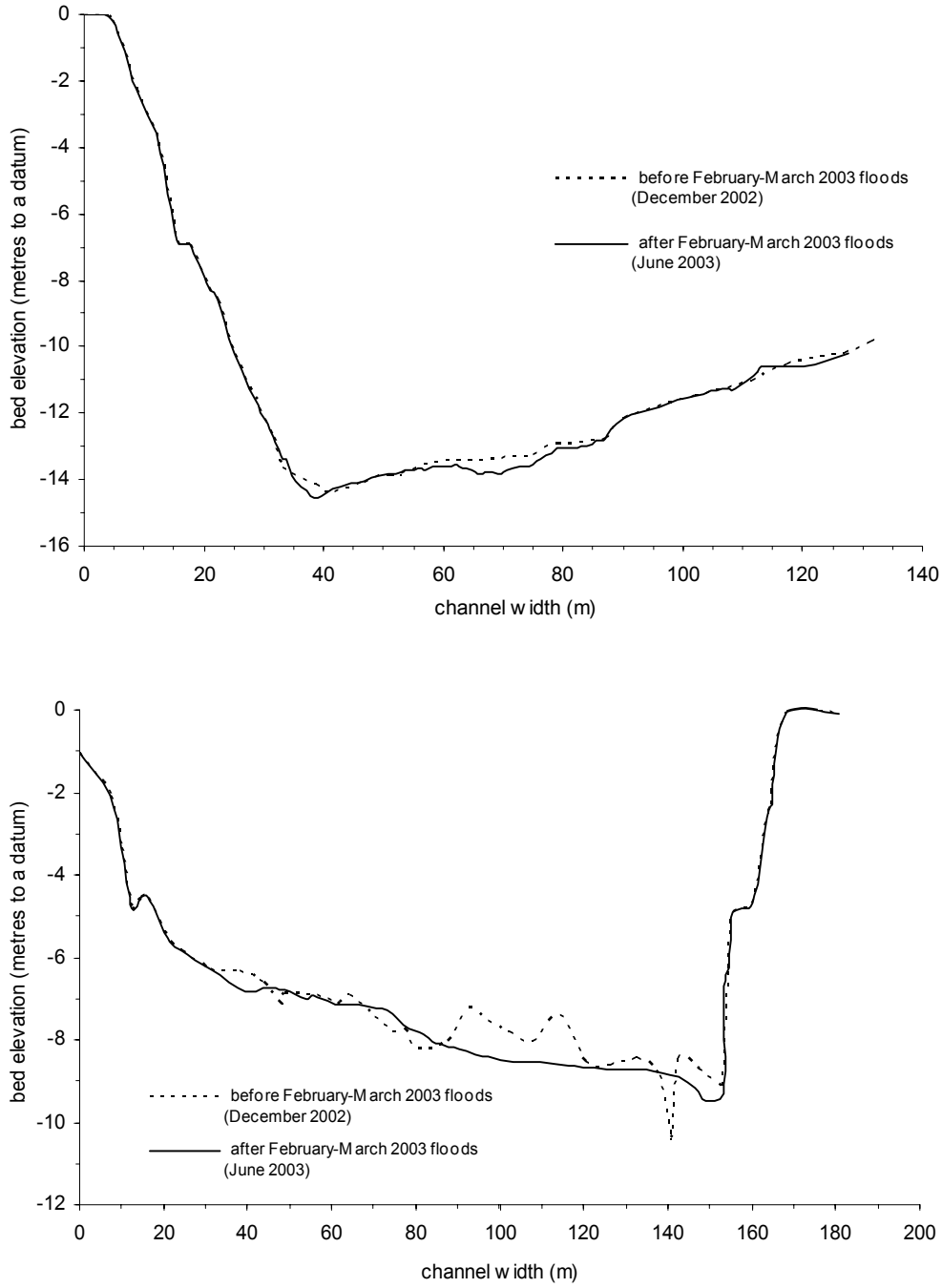

Figure 9 (C3P1). Representative cross sections of the lower Ebro River before and after February and March 2003. First section (above) is located at the beginning of the study reach, immediately downstream from the Flix Dam. Second section (below) is located at the lowermost end of the study reach at MEMS. Both show evidences of river-bed net erosion

Table 3 (C3P1). Changes in the riverbed in representative sections of the lower Ebro River after the two consecutive floods (February-March 2003)

Section	**Distance from Flix Dam (km)**	**Net scour/fill (mm)[1]**	**D_{max} mobilised (mm)[2,3]**
Flix Dam	0.850	-18	151
Flix Meander	2.700	-202	70
Flix	5.600	+523	64
Pas d'Ase	18.300	-46	78
Móra d'Ebre 1	25.200	-116	115
Móra d'Ebre 2	25.500	-38	70
Móra d'Ebre 3 (MEMS)	27.000	-151	113
Weighted mean		-23	94

[1] Scour chains (e.g. Hassan, 1988) / - net scour, + net fill
[2] Painted pebbles (e.g. Sala and Gallart, 1988)
[3] Mean slope 0.00085

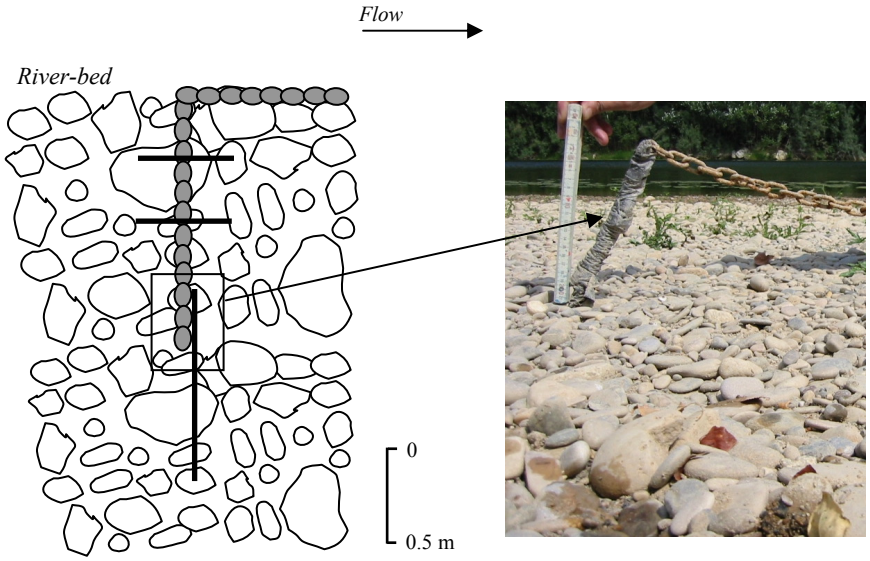

Figure 10 (C3P1). Scour chain in the Flix Meander section, showing its position in the river-bed before February and March 2003 floods (left diagram), and illustrating the net scour after the two events floods (right, photo by the authors, June 2003)

Guillén and Palanques (1992) estimated an average of 120,000 t/y of sediment discharged for the Ebro River into the sea after dam construction (most in suspension and measured when the river was already in the delta plain). That load would include 50,000 t/y to 100,000 t/y released from the reservoirs plus sediment eroded from the river channel and banks. Current sediment yield is around 1% of what was delivered at the beginning of the 20th century. The total solid yield (351,000 tonnes) after the winter 2003 floods agrees, in order of magnitude, with the average annual estimations by Guillén and Palanques (1992).

However, results presented in this paper are higher probably due to the magnitude of the floods and the sedimentation that may occur along the 80 km of river between the MEMS and the beginning of the delta plain. Therefore, and considering that the two floods were relatively frequent (with recurrence periods of between 4 years and 8 years), our estimation of incision gives the order of magnitude of the long-term rate of degradation of the lower Ebro River downstream dams.

5. Conclusions

This paper analysed the sediment transfer through a highly regulated fluvial system during two consecutive frequent floods that occurred in February and March 2003. The data on discharge and sediment transport was obtained upstream and downstream from the large dams on the lower Ebro River (NE Spain). The results indicated that:

1. In spite of the similar flood hydrographs, the dams substantially altered flood timing. In particular, peaks were advanced downstream from the dams in order to create a buffer to store the incoming upstream water yield. The water budget after floods yielded a net loss of around 1000 hm^3 of water in storage.

2. Upstream from the dams (at the SMS), both floods had a similar suspended sediment yield (ca. 850,000 tonnes), with mean concentrations of around 0.50 g/l. The load in suspension represented nearly 99% of the total solid yield. Downstream from the dams (at the MEMS) the suspended sediment yield was slightly different during the two floods (100,000 tonnes as against 75,000 tonnes), and an order of magnitude lower than that measured upstream dams at SMS. The mean concentration was 0.05 g/l. The results show the ability of the reservoirs to retain fine sediments (up to 95%), which otherwise would have reached the delta plain.

3. Upstream from the dams, both floods again had a similar bedload yield (ca. 12,500 tonnes), with mean rates of around 100 g/ms. Bedload represents approximately 1.5% of the total solid yield. Downstream from the dams, the bedload showed different behaviour during the two floods. During the February flood, the mean bedload rate (ca. 150 g/ms) was less than half than that obtained during March (ca. 350 g/ms). In terms of bedload

yield, the February flood carried 48,000 tonnes (32% of the total load) and the March flood transported 130,000 tonnes (64% of the total load). Taking into account that the tributaries did not supply sediment during the two events, the increment in transport may be attributed to the breaking of the armour layer, which produced a substantial increase in bedload rates.

4. The reservoirs trapped most of the fine sediment and all the coarse bed-material load. Therefore, the 350,000 tonnes of sediment mobilised downstream from the dams during the two floods was necessarily entrained from the riverbed and eroded from the channel banks. This phenomenon caused a mean incision of 33 mm over the 27 km-long study reach, which means a significant step towards the long-term degradation of the lower Ebro River.

Results show how important the sediment deficit is downstream from the dams on the lower Ebro River. However, further analysis on a broader and updated Ebro sediment transport database is needed to test whether the patterns of sediment yield observed during the winter 2003 floods can be extrapolated to a broader time scale, and the extent to which data can be of use for management and ecological restoration efforts in this and other large regulated river systems.

Acknowledgements

This research was carried out within the framework of the research project REN2001-0840-C02-01/HID, which is funded by the Spanish Ministry of Science and Technology. The first author received a grant from the Spanish Ministry of Education. Hydrological data was supplied by the Ebro Water Authorities. The Móra d'Ebre Town Council provided logistic support. Albert Rovira at the University of Lleida provided assistance during field and labwork. Alan Werritty at the University of Dundee undertook a helpful review of the first version of the manuscript. Reviews by two anonymous reviewers greatly improved the final version of the manuscript. The authors are indebted to all of them.

REFERENCES

Allayaud, W.K. 1985. Innovations in non-structural solutions to preventing coastal damage. In: *California's battered coast, Proceedings from a Conference on Coastal Erosion*, McGrath J. (ed.). California Coastal Commission: 260-280.

Avendaño, C., Cobo, R., Sanz, M.E., Gómez, J.L. 1997. Capacity situation in Spanish reservoirs. *I.C.O.L.D. Proceedings of the Nineteenth Congress on Large Dams* **74**(52): 849-862.

Avendaño, C., Sanz, M.E., Cobo, R. 2000. Embalses en el río Ebro: su influencia en la morfología del cauce y en los sólidos aportados al Delta. *Proceedings of the V Jornadas sobre encauzamientos fluviales*. Centro de Experimentación de Obras Públicas (CEDEX): Madrid; 1-12.

Batalla, R.J. 2003. Sediment deficit in rivers caused by dams and instream gravel mining. A review with examples from NE Spain. *Cuaternario y Geomorfología* **17**(3-4): 79-91.

Batalla, R.J., Kondolf, G.M., Gomez, C.M. 2004. Reservoir-induced hydrological changes in the Ebro River basin, NE Spain. *Journal of Hydrology* **290**: 117-136.

Bayerri, E. 1934-35. *Historia de Tortosa y su comarca*. Imprenta Moderna de Alguerri: Tortosa.

Bouno, S., Shimizu, Y., Saitou, D. 1999. Sediment transport in the Saru River and Nibutani Dam. In *River sedimentation*, Jayawardena M., Lee L. Wang Y. (eds.). Balkema: Rotterdam; 409-414.

Brownlie W.R., Taylor, B.D. 1981. Sediment management for southern California mountains, coastal plains, and shoreline. Part C. Coastal sediment delivery in major rivers in southern California. Report 17-C, Environmental Quality Lab., California Institute of Technology: Pasadena.

Brune, G.M. 1953. The trap efficiency of reservoirs. *Transactions of the American Geophysical Union* **34:** 407-418.

Church, M., McLean, D.G., Wolcott, J.F. 1987. River bed gravels: sampling and analysis. In *Sediment transport in gravel-bed rivers*, Thorne C. R., Barthurst J.C., Hey R.D. (eds.). Chichester: John Wiley and Sons; 43-88.

Collier, M.P., Webb, R.H., Schmidt, J. 1996. Dams and Rivers. *A primer on the downstream effects of dams*. United States Geological Survey Circular 1126.

Emmett, W.W. 1980. *A Field Calibration Of The Sediment Trapping Characteristics Of The Helley-Smith Bedload Sampler*. US Geological Survey Professional Paper 1139.

Everts, C.H. 1985. Effects of small protective devices on beaches. In: *California's battered coast, Proceedings from a Conference on Coastal Erosion*, McGrath J. (ed.). California Coastal Commission; 127-138.

Folk, R.L., Ward, C. 1957. Brazos River bar: a study in the significance of grain size parameters. *Journal of Sedimentary Petrology* **27**(1): 3-26.

Guillén, J., Palanques, A. 1992. Sediment dynamics and hydrodynamics in the lower course of a river highly regulated by dams: the Ebro River. *Sedimentology* **39**: 567-579.

Guillén, J., Díaz, J.I., Palanques, A. 1992. Cuantificación y evolución durante el siglo XX de los aportes de sedimento transportado como carga de fondo por el río Ebro al medio marino. *Revista de la Sociedad Geológica de España* **5**: 27-37.

Hassan, M. (1988): *The movement of bedload particles in a gravel stream and its relation to the transport mechanism of the scour layer*. PhD Thesis, Jerusalem, The Hebrew University of Jerusalem.

Howard, A., Dolan, R. 1981. Geomorphology of the Colorado River in Grand Canyon. *Journal of Geology* **89**: 269-297.

Inman D.L. 1976. *Man's impact on the California coastal zone*. Summary Report to California Department of Navigation and Ocean Development: Sacramento.

Kondolf, G.M. 1994. Geomorphic and environmental effects of instream gravel mining. *Landscape and Urban Planning* **28**: 225-243.

Kondolf, G.M. 1997. Hungry Water: Effects of Dams and Gravel Mining on River Channels. *Environmental Management* **21**(4): 533-551.

Kondolf, G.M., Matthews, W.V.G. 1993. *Management of coarse sediment in regulated rivers of California*. University of California Water Resources Center: Davis, California.

López, J.I., Beguería, S., García, J.M. 2002. Influence of the Yesa reservoir on floods of the Aragón River, central Spanish Pyrenees. *Hydrology and Earth System Sciences* **6**(4): 753-762.

McLean, D.G., Church, M., Tassone, B. 1999. Sediment transport along lower Fraser River 1. Measurements and hydraulic computations. *Water Resources Research* **35**(8): 2533-2548.

Meade, R.H., Parker, R.S. 1985. *Sediment in rivers of the United States*. U.S. Geological Survey Water-Supply Paper 2275.

Meyer-Peter, E., Favre, H., Einstein, H.A. 1934. Neuere versuch-sresultate über den geschiebetrieb. *Schweiz Bauzeitung* **103**.

Milliman, J.D., Meade, R.H. 1983. World-wide delivery of river sediment to the oceans. *Journal of Geology* **91**: 1-21.

Nelson, C.H. 1990. Post Messinian deposition rates and estimated river loads in the Ebro sedimentary system. In *Marine Geology of the Ebro Continental Margin,* Nelson C.H., Maldonado A. (eds.). Marine Geology; **95**: 395-418.

Novoa, M. 1984. Precipitaciones y avenidas extraordinarias en Catalunya. *Proceedings of the Jornadas de Trabajo sobre Inestabilidad de laderas en el Pirineo*: Barcelona; 1-15.

Rice, S., Church, M. 1996. Sampling surficial fluvial gravels: the precision of size distribution percentile estimates. *Journal of Sedimentary Research* **66**(3): 654-665.

Rinaldi, M., Simon, A. 1998. Bed-level adjustments in the Arno River, Central Iyaly. *Geomorphology* **22**: 57-71.

Ryan, S.E., Porth, L.S., Troendle, C.A. 2002. Defining phases of bedload transport using piecewise regresión. *Earth Surface Processes and Landforms* **27**, 971-990.

Sala, M. and Gallart, F. (1988): *Métodos y técnicas para la medición de campo de procesos geomorfológicos*. Sociedad Española de Geomorfología, Zaragoza, Monograph 1.

Sanz, M.E., Avendaño, C., Cobo, R. 1999. Influencia de los embalses en el transporte de sedimentos hasta el río Ebro (España). *Proceedings of the Congress on Hydrological and geochemical processes in large-scale river basins*. HIBAM: Manaus.

Schoklitsch, A. 1950. *Handbuch des Wasserbaues*. Springer: Viena.

Schumm, S.A. 1977. *The fluvial system*. John Wiley and Sons, New York.

Shahin, M. 1985. *Hydrology of the Nile basin*. Developments in Water Science 21, Elsevier: Amsterdam.

Shaw, E.M. 1983. *Hydrology in Practice*, Van Nostrand Reinhold: London.

Surian, N., Rinaldi, M. 2003. Morphological response to river engineering and manegement in alluvial channels in Italia. *Geomorphology* **50**: 307-326.

Vericat, D., Batalla, R.J. 2004. Efectos de las presas en la dinámica fluvial del curso bajo del río Ebro. *Cuaternario y Gemorfología* **18**(1-2), 37-50.

Walling, D.E. 1984. Dissolved loads and their measurements. In *Erosion and sediment yield: Some methods of measurements and modeling*. Hadley R.F., Walling D.E (eds.). Geo Books: London; 111-177.

Williams, G.P., Wolman, M.G. 1984. *Downstream Effects of Dams on Alluvial Rivers*. US Geological Survey Professional Paper 1986.

Wohl E.E., Cenderelli, D.A. 2000. Sediment deposition and transport patterns following a reservoir sediment release. *Water Resources Research* **36**(1): 319-333.

Wolman, M.G. 1954. A method of sampling coarse bed material. *American Geophysical Union Transactions*, **35**: 951-956

3. TOTAL SEDIMENT TRANSPORT

Vericat, D. and Batalla, R.J. (2005): Sediment transport in a large impounded river: the lower Ebro River (NE Iberian Peninsula). *Geomorphology* (accepted)

Sediment transport in a large impounded river: the lower Ebro River (NE Iberian Peninsula)

Abstract

The sediment transport of the highly regulated lower Ebro River is estimated on the basis of a sediment transport measuring programme that has been carried out between 2002 and 2004. Total sediment transport, including both suspended load and bedload was measured upstream and downstream from the Mequinenza and Riba-roja reservoirs, with special attention to the transport during floods. Annual total load upstream from the dams is estimated at around 1.64•106 tonnes, of which at least 99% is transported in suspension. Annual total load downstream from the dams is estimated at around 0.45•106 tonnes, of which the 60% is transported in suspension and the remain 40% as bedload (mean D50-bl in the range of 32 mm). Total load represents 3% of what was transported at the beginning of the 20th century. Sediment yield is three to four times lower below the dams, a fact that is caused by the trapping of sediment within the reservoirs (around 90% in the case of suspended sediment and 100% in the case of bedload). As a consequence, sediment that is transported downstream from the dams is all entrained from the riverbed and eroded from the banks. The lack of sediment (sediment deficit) causes a mean riverbed incision of 30 mm per year. This value has been estimated from bedload measurements and the order of magnitude corroborated by means of scour chains and painted pebbles located between the lowermost dam and the measuring section 27 km downstream. Since floods have been reduced on average by 25% but sediment supply from upstream has been reduced to almost nothing, the river channel of the lower Ebro River will continue exporting sediment both during floods (>2,000 m3/s, mostly bedload) and frequent high flows (1,000 m3/s to 2,000 m3/s), making the incision progressive, unless restoration steps are taken.

Key words: sediment load, dams, riverbed incision, Mediterranean river

1. Introduction

Rivers carry sediment continuously from headwaters to deposition zones, being responsible for the equilibrium between fluvial and marine processes on beaches and in delta regions. Alluvial channel morphology is, over long-time scale, maintained in dynamic quasi-equilibrium where sediment exported from a specified reach is roughly equal to the supply from upstream (Williams and Wolman 1984). Within this context, the sediment budget in a fluvial system could be expressed as $I_n - O_n = \Delta S_n$, where I_n is the sediment coming into the nth reach, O_n is the exportation of sediment from the reach, and ΔS_n is the change in sediment storage in that reach.

Dams interrupt the continuity of the sediment transfer along fluvial channels, causing morphological changes to downstream fluvial and coastline ecosystems (e.g., Kondolf and Mathews 1993). Sediment deficit is not only an environmental issue but also is, in some cases, a socio-economic problem, for instance due to loss of reservoir capacity (e.g., Fan and Springer 1993). In the Trinity River, California, after the construction of the Lewiston Dam, desirable instream alluvial features such as gravel bars were gradually lost during periods of sediment transport (Trinity River Flow Evaluation 1999). In the Colorado River the annual suspended load was reduced more than three orders of magnitude after the construction of the Hoover Dam, Nevada-Arizona (Meade and Parker 1985). A general sediment deficit downstream from dams is generated under such conditions. In addition, dams alter the downstream flow regime of rivers (Williams and Wolman 1984), which controls many physical and ecological aspects of river form and processes, including sediment transport and nutrient exchange (Poff *et al.* 1997).

Hydrological alterations caused by dams include changes in flood frequency and magnitude, reduction in overall flows, changes in seasonal flows, and altered timing of releases (Ward and Stanford 1979, Petts 1984, Ligon *et al.* 1995, Ward and Stanford 1995, Kondolf 1997). In different rivers of the Sacramento-San Joaquin River system of California, frequent floods (Q_2-Q_{10}) were reduced below dams from 2% to 95% in comparison with pre-dam values (Kondolf and Mathews 1993). Batalla *et al.* (2004) reported reduction of the flood magnitude as the most important flow alteration in the

whole of the Ebro basin (NE Iberian Peninsula). Geomorphological consequences of flood reduction on downstream reaches are two fold:

On one hand, if flows released from dams have sufficient capacity to move coarse sediment, water becomes 'hungry water' (Kondolf 1997), which may transport sediment downstream without replacement from upstream ($I_n<O_n$). Main effects of the 'hungry water' on the fluvial dynamics are: a) ecological degradation of the fluvial and deltaic systems (e.g., Day and Templet 1989, Kondolf and Wolman 1993), b) geomorphological degradation of the river channel (e.g., Kondolf and Mathews 1993, Kondolf 1997, Shields *et al.* 2000) that includes riverbed incision, riverbank instability, upstream erosion in tributaries, groundwater overdrafting, damage to bridges, embankments and levees (e.g., Kondolf 1997, Rinaldi and Simon 1998, Batalla 2004), and changes in channel width (e.g., Williams and Wolman 1984, Wilcock *et al.* 1996, Shields *et al.* 2000), and c) propagation of riparian vegetation into previously unvegetated or lightly-vegetated areas (e.g., Inbar 1990, Church 1995, Vericat and Batalla 2004).

On the other hand, if floods do not have sufficient competence to transport sediment from incoming tributaries or other sources, the river bed suffers sedimentation ($\Delta S_n>0$) (Howard and Dolan 1981). In the Trinity River downstream from Trinity Dam, the capacity of the river to transport sand was maintained to a greater degree than the sand supplied by tributaries downstream, resulted in a channel aggradation and a decline of invertebrate and salmonid spawning habitat (Wilcock *et al.* 1996).

River sedimentary processes are thus disrupted after the dam set in operation ($I_n \approx 0$). Furthermore, at the outlet of the basin the balance between fluvial and marine processes on beaches and in delta regions is altered (e.g., Brownlie and Taylor 1981, Milliman and Meade 1983, Shahin 1985). The erosion of the Nile Delta (150 m/y), 1,000 km downstream of the Aswan High Dam, Egypt, is one of the examples that illustrates the effects at the delta as a consequence of the reduction of sediment yield downstream from dams.

Different management and ecological restoration efforts to compensate the sediment deficit downstream from dams are conducted in some rivers (Kondolf 1997). For instance,

controlled flow releases (*flushing flows*) and beach nourishment with imported sediment dredged from reservoirs and harbours have been implemented along many rivers (Inman 1976, Allayaud 1985, Everts 1985). However, the high costs of these operations prevent the general application of such restoration techniques (Inman 1976). In spite of the amount of literature on geomorphic effects of dams on downstream channels, we are aware of no attempt to quantitatively assess the sediment deficit caused by large dams on a large river system, based upon regular, systematic and extensive direct measurements of total load (both in suspension and as bedload) upstream and downstream the reservoirs.

The objective of this paper is, therefore, to analyse the sediment transport through a highly regulated fluvial system, the lower Ebro River, during two consecutive hydrological years (2002-2004). Total sediment transport was measured upstream and downstream from the largest complex of dams in the Ebro basin. Results establish the sediment deficit in the lower Ebro River and may assist in assessing which are the main consequences on fluvial dynamics in the lowermost part of the river.

2. Study area

2.1. The Ebro basin

The Ebro basin drains an area of around 85,530 km^2 and is located in the north-eastern part of the Iberian Peninsula. Water divides are the southern-facing slopes of the Cantabrian Range and the Pyrenees in the northern part of the basin, and the northern-facing slopes of the Iberian Massif in its southern part. The Ebro River debouches into the Mediterranean Sea downstream from the city of Tortosa, which is located 180 km south of Barcelona (Figure 1 (C3P2)). Precipitation varies greatly across the basin due to its topographical and climatological diversity. Mean annual precipitation ranges from more than 2,000 mm in the Pyrenees to less than 300 mm in the arid interior. Mean annual discharge in Tortosa is 450 m^3/s, which means an average annual water yield of 14,300 hm^3 (data from 1913, where 1 $hm^3 = 1 \cdot 10^6\ m^3$). Runoff varies substantially from year to year: maximum annual runoff was 30,821 hm^3 in the hydrological year 1914-1915, whereas the minimum was 4,284 hm^3

during the year 1989-1990. Maximum peak flow was estimated at around 12,000 m^3/s in Tortosa in 1907 (Novoa 1984).

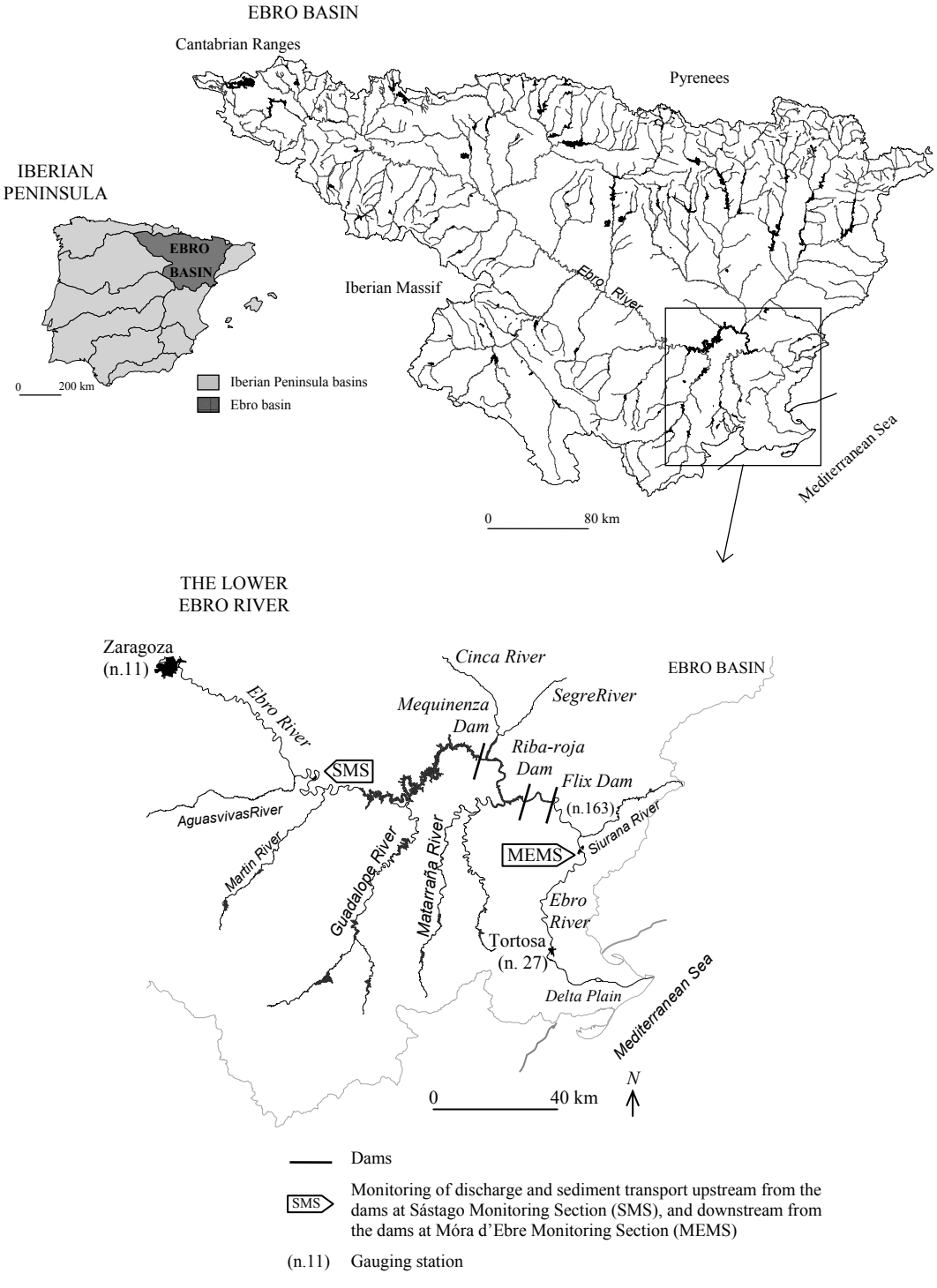

Figure 1 (C3P2). Location of the study area in the Ebro basin (NE Iberian Peninsula)

Close to 190 dams impound 60% of the annual runoff in the Ebro basin. In more humid regions and for basins of similar size, the impoundment calculated is much lower (Batalla *et al.* 2004). Almost all the main tributaries of the Ebro River are dammed (Figure 1 (C3P2)). In the Ebro basin water is mainly used for hydropower production (60,000 hm^3/year), followed by irrigation (6,300 hm^3/year) and to cool a nuclear power plant (3,350 hm^3/year). Virtually all of the dams were constructed during the 20th century. In particular, a total of 5,200 hm^3 of water were impounded during the period 1950-1975 (67% of the current reservoirs' capacity). Only 25 of the dams in the whole of the basin have a capacity larger than 50 hm^3, but they possess a storage capacity of 90% the total basin storage (Batalla *et al.* 2004). Maximum discharge in the post-dams period has been 3,300 m^3/s in 1982 in the Tortosa gauging station.

2.2. The lower Ebro River

For the purpose of this study, we have considered the lower Ebro River as the river reach between Sástago, 2 km upstream from the Mequinenza reservoir, to Móra d'Ebre, 27 km downstream from the Flix Dam (Figure 1 (C3P2)). In this reach, the river flows as a single thread meandering channel through the Ebro depression, which is constrained by bedrock outcrops where it crosses the Coastal Ranges (e.g., Pas de l'Ase). The largest complex of reservoirs in the whole Ebro Basin is located in this area. Mequinenza (1966) is the largest reservoir in the basin with a capacity of 1,534 hm^3, while Riba-roja reservoir (1969) has a capacity of 207 hm^3 and impounds the two largest tributaries of the Ebro, the Segre and the Cinca rivers. The lowermost dam is Flix (1948) with a capacity of 11 hm^3 (Figure 1 (C3P2)). The most important tributary downstream from the Flix Dam is the Siurana River, which in turn is heavily regulated by three dams and suffers from intensive gravel mining since the 1980s.

In Sástago (upstream dams) the median size of riverbed material (D_{50}) is 17 mm (no difference between surface and subsurface were observed). Riverbed material is bimodal (B= 2.6, where B is the bimodality index reported by Wilcock 1993) with well defined modes, one fine mode at the coarse sand fraction and one coarse mode at medium gravel. Below Flix Dam surface material (s) is coarser than the subsurface (ss) material. Surface material is unimodal coarse gravel (B≈1). Mean $D_{50\text{-}s}$ measured in active bars is 32 mm,

and varies from 16 mm to 70 mm. Subsurface deposits are predominantly bimodal sandy-gravel materials (B>2). Mean $D_{50\text{-}ss}$ is 17 mm, ranging from 8 mm to 34 mm. The sand fraction comprises between 20% and 30% of subsurface deposits, in which the median size of the sand ($D_{50\text{-}sand}$) is 1 mm (i.e., coarse sand). Mean channel slope is $8.5 \cdot 10^{-4}$, channel length (L_r) is 307 km, while the straight-line valley length (L_s) is 190 km. Therefore, the lower Ebro shows in most part of its course a clear meandering pattern (L_r/L_s= 1.6, Leopold *et al.* 1964). Channel width ranges from 50 metres to more than 160 metres along the study reach.

Estimated total annual sedimentation in the reservoirs of the Ebro basin is 15 hm^3 (Sanz *et al.* 1999, Batalla 2004) which corresponds, approximately, with the annual sediment contribution of the Ebro River to its delta at the beginning of the 20th century (Bayerry 1934-1935, Nelson 1990). The lack of sediment delivery downstream from the dams has caused changes in river channel morphology, mainly vegetation of formerly active areas (Sanz *et al.* 1999, Avendaño *et al.* 2000, Vericat and Batalla 2004, 2005a), and can be identified as the main reason for the retreat of the Ebro delta. In addition, over 4 years, the riverbed has been continuously dredged downstream from Móra d'Ebre to Tortosa to ensure the navigability of the river for tourism purposes (Figure 1 **(C3P2)**), eventually affecting fish habitat and contributing to the disequilibrium of the river's sedimentary system (Batalla 2004).

3. The lower Ebro River Sediment Sampling Programme

3.1. The hypothesis

The degree of alteration of river processes downstream from the dams depends upon the relation between the original and altered flow regimes, especially floods, and the sediment load. In the case of the lower Ebro River dams have reduced relatively frequent floods (e.g., Q_2 to Q_{25}) by around 25%, on average (Batalla *et al.* 2004). The alteration of flow regime (i.e., competent discharges for sediment transport) due to dams is much lower than that affecting the downstream sediment transfer (dams capture all bedload and most of the suspended load). Changes in the frequency of competent flows can be assessed by means

of the dimensionless ratio T*, calculated as the quotient between the pre-dam and post-dam frequency of sediment transporting flows (Grant *et al.* 2003). The ratio calculated for the lower Ebro River is 0.97, reflecting almost the same flow competence during both pre and post-dams periods. The flow data have been taken from Batalla *et al.* (2004). Changes on sediment supply can also be analysed by the dimensionless ratio $S^* = S_B/S_A$, where S_B is the sediment supply below-dam and S_A is the sediment supply above-dam (Grant *et al.* 2003). In the lower Ebro, sediment supply downstream from the dams has been remarkably reduced. The low S* ratio should confirm this. The combination of high T* and low S* leads to a number of riverbed adjustment such as riverbed scour, bank erosion and channel degradation as probable dominant fluvial processes.

3.2. The measurements

Between 2002 and 2004, a research group from the University of Lleida has undertaken a sediment sampling programme in the lower Ebro River in order to determine the sediment load upstream and downstream from the large Mequinenza and Riba-roja reservoir complex. The sampling programme includes monitoring of suspended and bedload transport at the Sástago Monitoring Section (**SMS**, channel width 110 m) upstream from the dams and at the Móra d'Ebre Monitoring Section (**MEMS**, channel width 160 m) downstream from the dams (Figure 1 (C3P2)). Special attention has been devoted to the measurement of sediment transport during floods. The sampling programme was established to obtain reliable data on sediment transport, both to assess the magnitude of the changes on sediment supply in the river and to inform on-going restoration projects in the river and in its delta plain.

4. Discharge

4.1. Measurements

Flow was calculated at the two monitoring sections by routing hydrographs from upstream gauging stations operated by the Ebro Water Authorities (Vericat and Batalla 2005a). Discharges for the SMS were obtained from the gauging station located in Zaragoza (n.11,

85 km upstream), and discharges at MEMS were estimated from the gauging station located in Ascó (n.163, 15 km upstream) and further compared with discharges in Tortosa (n.27, 49 km downstream) (Figure 1 (C3P2)). The Muskingum method (Shaw 1983) was used to route hydrographs to the monitoring sections (Figure 2 (C3P2)).

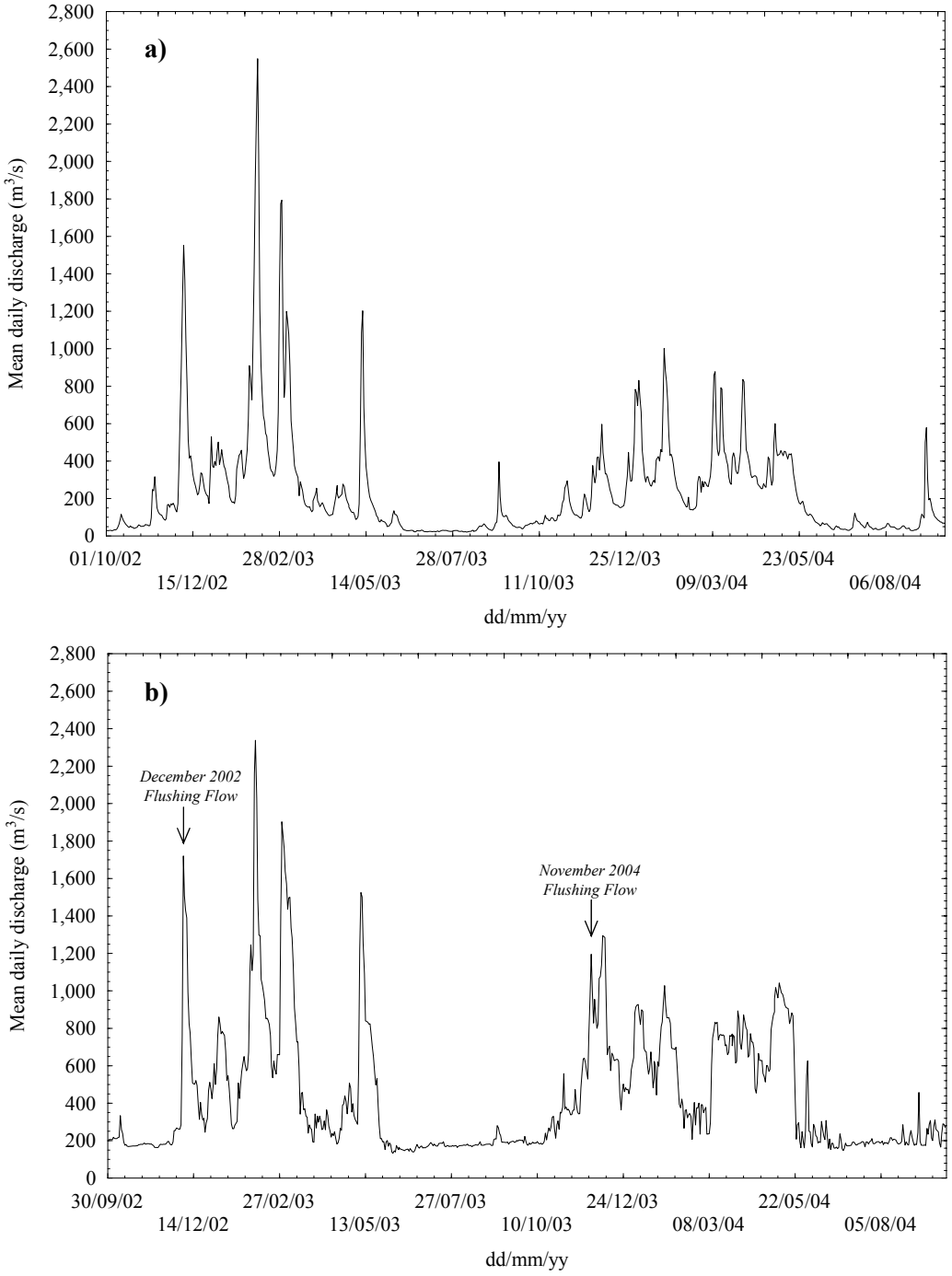

Figure 2 (C3P2). Flow hydrographs at the monitoring sections (upstream and downstream from the dams) for the 2002-2004 hydrological years

At a single vertical discharge measurements were used to calibrate flood hydrographs. Velocity of the flow was measured from a bridge by means of an OTT C31 current meter, which was attached to a cable-suspended US DH74 sampler. Six velocity profiles were compiled at SMS for instantaneous discharges between 750 m^3/s and 2,135 m^3/s. Eleven velocity profiles were undertaken at MEMS for instantaneous discharges between 750 m^3/s and 2,160 m^3/s. Mean velocities were calculated from velocity profiles and subsequently used to verify routed discharges from upstream gauging stations. Simultaneously, we measured channel width by means of a laser telemeter and flow depth from the corrected vertical of the crane cable. The Muskingum method tended to systematically overestimate discharges at the monitoring sections, especially for low flows. Mean overestimation is about 10% (σ= 3%, where σ is the standard deviation) at SMS and 3% at MEMS (σ= 1%).

4.2. Flow regime

The study years 2002-2003 and 2003-2004 were average hydrological years at the two monitoring sections compared to both, the pre-dam and the post-dam flow records (Table 1 (C3P2)). At SMS the year 2002-2003 showed similar mean discharge and water yield than the pre-dam mean value. Values of the year 2003-2004 were slightly lower than the mean pre-dam and higher than the post-dam discharges. In contrast, at MEMS, both years show slightly lower mean discharge and water yield than the pre-dam mean values, and slightly higher than the post-dam observations. Overall differences are small between study years and flow series at the two monitoring sections, as the flow duration curves indicate (Figure 3a, b (C3P2)). More than 99.5% of the flows were sampled for suspended sediment and 96.5% for bedload during the study years. Mean monthly discharges of the study period present similar distribution pattern than the pre and post-dams series at both monitoring sections (Figure 3a, b (C3P2)). Peak discharges in both sections and years are lower than the annual maximum daily discharges of the whole flow series. Maximum discharge at SMS during the study period (2,604 m^3/s) had a recurrence interval of 10 years (Q_{10}), estimated from the post-dam flow series at the Zaragoza gauging station, while at MEMS maximum discharge was 2,498 m^3/s (Q_8), estimated from the post-dam flow series at the Tortosa gauging station. Overall seven floods occurred during the study period and all of them were monitored for sediment transport.

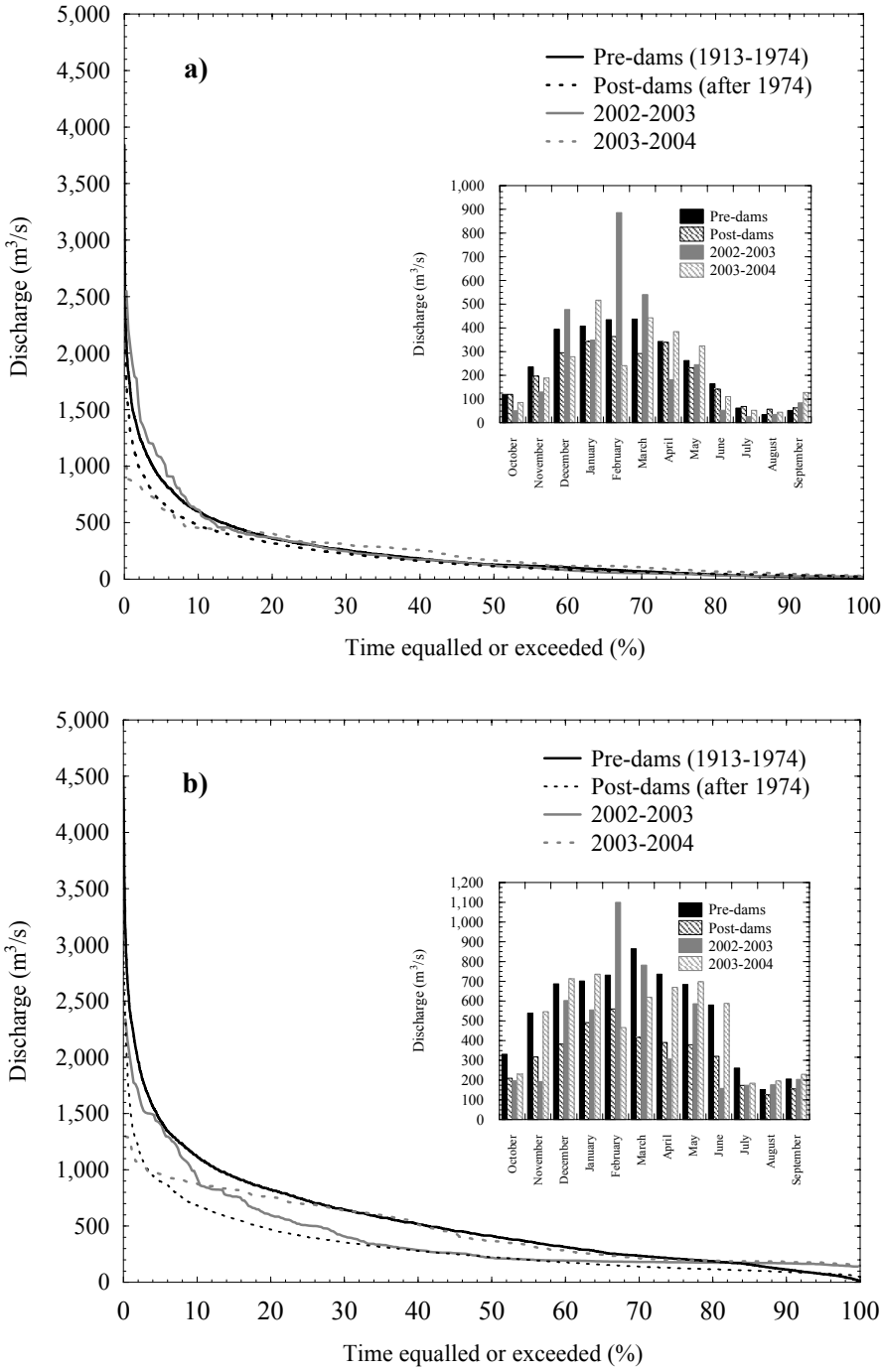

Figure 3 (C3P2). (**a**) Flow duration curves calculated for the pre and post-dam discharge series at the Zaragoza gauging station, and for the study years (2002-2004) at SMS. Mean monthly discharges are also presented. (**b**) Flow duration curves calculated for the pre and post-dam discharge series at the Tortosa gauging station, and for the study years (2002-2004) at MEMS. Mean monthly discharges are also presented

Table 1 (C3P2). Flow regime in the monitoring sections of the lower Ebro River during the study years 2002-2004 in relation to long-term flow records. See also Figure 3 (C3P2)

Monitoring section	**Mean discharge** (m^3/s)				**Median discharge** (m^3/s)			
	Pre-dam [1]	Post-dam [2]	2002-03	2003-04	Pre-dam	Post-dam	2002-03	2003-04
Sástago bridge - SMS [3] *(Section upstream dams)*	244	208	251	235	129	115	125	166
Móra d'Ebre bridge - MEMS [4] *(Section downstream dams)*	581	332	415	465	413	224	217	382
	Water yield (hm^3/y)				**Peak discharge** [5] (m^3/s)			
	Pre-dam	Post-dam	2002-03	2003-04	Pre-dam	Post-dam	2002-03	2003-04
Sástago bridge - SMS [3] *(Section upstream dams)*	7,708	6,576	7,913	7,263	3,843	3,065	2,604	1,035
Móra d'Ebre bridge - MEMS [4] *(Section downstream dams)*	16,664	10,473	13,080	14,656	12,000	3,303	2,498	1,355

[1] Pre-dam period: 1913-1974; 1974 was the year when most reservoirs were already constructed and in operation (Batalla *et al.* 2004)
[2] Post-dam period: 1974-2004 (Batalla *et al*. 2004)
[3] Pre and post-dam values from the flow series of the upstream gauging station of Zaragoza; values of 2002-2003 and 2003-2004 routed from the upstream section of Zaragoza (see text for discussion). No major tributaries are located between Zaragoza and Sástago
[4] Pre and post-dam values from the flow series of the downstream gauging station of Tortosa; values of 2002-2003 and 2003-2004 routed from the upstream section of Ascó (see text for discussion). No major tributaries are located between Ascó and Tortosa
[5] Maximum daily discharges of the flows series, except for the pre-dam peak discharged of 12,000 m^3/s estimated by Novoa (1984) in Tortosa. Values of 2002-2003 and 2003-2004 are maximum instantaneous discharges routed from related gauging stations

5. Suspended load

5.1. Measurements

Calculation of suspended sediment load at the two lower Ebro River monitoring sections has been based on the analysis of 434 depth integrating water and suspended sediment samples collected between 2002-2003 (154 samples) and 2003-2004 (280 samples). The samples were regularly obtained during floods, in which most sediment load is transported, and sparsely collected during low flows (i.e., below mean discharge). As indicated, almost the whole range of discharges for each of the two hydrological years was sampled. Samples were obtained at a single vertical section by means of a 28 kg cable-suspended depth-integrating US DH74 sampler. The vertical were located at the centre of both monitored sections, the same vertical where flow measurements were done. Around ¾ litres of water were collected in every sample. Samples were carried to the laboratory and filtered using 1.2 μm cellulose filters.

Single vertical samples were compared with the mean cross-section samples according to the ratio $k = C_s/C_1$, wherein C_s is the mean concentration of suspended sediment determined from three vertical samples at SMS, and six vertical samples at MEMS, and C_1 is the mean concentration determined at the same time from the usual single vertical section (e.g., McLean *et al.* 1999). Six and three sets of vertical samples were collected to assess the *k* ratio at SMS and MEMS, respectively. The *k* ratio varied randomly with discharge at the two monitoring sections and values ranges from 1.02 to 1.12. Hassan and Church (in McLean *et al.* 1999) found that small spatial bias is offsetting and has no significant effect on the computation of the annual load. Due to the restricted number of simultaneous samples and the low bias observed between C_s and C_1, the variation was not explicitly incorporated in the analysis of this paper.

5.2. Precision of the measurements

A measure of relative precision of a single instantaneous load is given by the coefficient of variation of the estimates (CV_i), which can be expressed as (modified from McLean *et al.* 1999)

$$CV_i = [(\sigma_C/C)^2 + (\sigma_Q/Q)^2]^{1/2}$$

wherein σ_C/C and σ_Q/Q represent the relative error terms for the concentration measurements and discharge, respectively. Determination of measurement precision was done by analysing instantaneous concentration obtained from replicate single vertical samples collected at the two monitoring sections for each of the two sampling years 2002-2003 and 2003-2004, and the flow measurements precision by estimating the RMSE deviations from stage-discharge rating curves. At SMS replicate single vertical samples included eight (2002-2003) and twelve (2003-2004) sets of samples of at least two samples each over almost all the range of flows. At MEMS vertical samples were composed by ten sets of samples (in both years), of at least two samples each over all the range of discharges. The results yielded estimates of CV_C ($=\sigma_C/C$) = 0.06 at SMS and 0.19 at MEMS, and CV_Q ($=\sigma_Q/Q$) = 0.09 at MEMS (no data is available at SMS, so we have adopted also 0.09), so the relative precision of a single instantaneous load would be CV_i = 0.11 at SMS (i.e., ±10%) and 0.21 at MEMS (i.e., ±20%).

Sediment load estimation can also be biased by technical measurement errors. For instance, depth integrating sampling misses a portion of the suspended load near the bed (e.g., Nordin and Richardson 1971). In this study, the original data of both sections have been used and no adjustment has been made.

The 0.95 confidence limits have been calculated above and below the regression lines (rating loads) for each year. The RMSE of both limits have been subsequently calculated to determine the mean error estimates. At SMS the mean error estimates of suspended sediment measurements is ±14% for the year 2002-2003 and ±7% for the year 2003-2004. At MEMS the mean error estimates is ±23% for the year 2002-2003 and ±6% for the year 2003-2004.

5.3. Computation of sediment yield

Annual suspended sediment yield at the monitoring sections was calculated from load-rating relations between discharge (Q in m^3/s) and suspended sediment concentration (C_1 in mg/l), using the Flow Duration Curve method (Walling 1984). Annual statistically significant relations were used to estimate suspended sediment concentrations, and thus loads, during periods or discharges for which measurements were unavailable. Since sediment-rating curves are based on instantaneous measurements of discharge, they possibly underestimate the sediment loads (Walling 1984), especially for the very high flows. In the case of the lower Ebro River, unsampled discharges were equalled or exceeded 0.5% of time at SMS and 0.1% of time at MEMS in both years. Therefore, the suspended load was probably not underestimated.

In order to compare results from the Flow Duration Curve method, annual sediment was also estimated as the product of the 15-min interval discharge and the suspended sediment concentration obtained from the annual Q-C_1 rating curve. The results by this method show loads similar for those obtained with the Flow Duration Curve method (i.e., -10% difference, on average).

5.4. Patterns of suspended sediment transport and yield at SMS

Suspended sediment concentrations (C_1) of the Ebro River at the Sástago Monitoring Section (SMS) showed a positive and statistically significant relation with discharge (Q) ($p<0.01$) for the two study years, 2002-2003 and 2003-2004 (Table 2 (C3P2), Figure 4a, b (C3P2)). The degree of scatter is, however, very high, indicating important temporal variability which can be related both to seasonal effects and to hysteretic effects during floods (Figure 5 (C3P2)). The relatively high values of suspended sediment concentration during 2002-2003 suggest that suspended sediment dynamics are not extremely affected by upstream regulation. The main tributaries draining the Central Pyrenees (e.g., Gállego) and, especially, the Iberian Massif (e.g., Jalon) contribute large quantities of fine sediment to the Ebro mainstream. As an example maximum concentration observed in the Jalon during the February 2003 flood attained 4 g/l (unpublished field data collected by the authors). Lower concentrations and less variability during 2003-2004 could be related to a comparably smaller sediment availability and presumably to less contribution of fine sediment from the tributaries.

Table 2 (C3P2). Rating curves between discharge and sediment transport in the lower Ebro with error estimates (see Figure 4 (C3P2) and 10 (C3P2) for data)

Monitoring section	Sediment transport	Rating curve	r^2	N	ε
Sastago bridge - SMS (*Section upstream dams*)	in suspension	[1] $C_1 = 0.42 \cdot Q + 1.01$	0.23	80 (3*)	0.08
		[2] $C_1 = 0.37 \cdot Q - 61.50$	0.24	65 (6*)	0.08
	as bedload	[3] $i_b = 0.35 \cdot Q - 660.70$	0.34	15	0.13
		[4]	-	-	-
Mora d'Ebre bridge - MEMS (*Section downstream dams*)	in suspension	[1] $C_1 = 0.09 \cdot Q - 89.12$	0.40	175	0.008
		[2] $C_1 = 0.06 \cdot Q - 25.48$	0.20	94 (9*)	0.01
	as bedload	[5] $i_b = 0.34 \cdot Q - 210.31$	0.15	130	0.07
		[6] $i_b = 0.17 \cdot Q - 103.10$	0.32	49	0.03

C_1 = Suspended sediment concentration (mg/l)
Q = Discharge (m^3/s)
ε = Standard error of the coefficient
i_b = Specific bedload rate (g/ms)
(#*) Samples excluded from the analysis (see text for details)
[1] Q- C_1 best fit rating curve for 2002-2003 (statistically significant at $p<0.01$)
[2] Q- C_1 best fit rating curve for 2003-2004 (statistically significant at $p<0.01$)
[3] Q-i_b best fit rating curve for 2002-2003 for discharges higher than 1900 m^3/s (statistically significant at $p<0.01$, see text for details)
[4] The relation between Q and i_b is not statistically significant. Bedload yield has been calculated as the product of discharge times average bedload rate (see text for details)
[5] Q- i_b best fit rating curve for 2002-2003 (statistically significant at $p<0.01$)
[6] Q- i_b best fit rating curve for 2003-2004 (statistically significant at $p<0.01$)

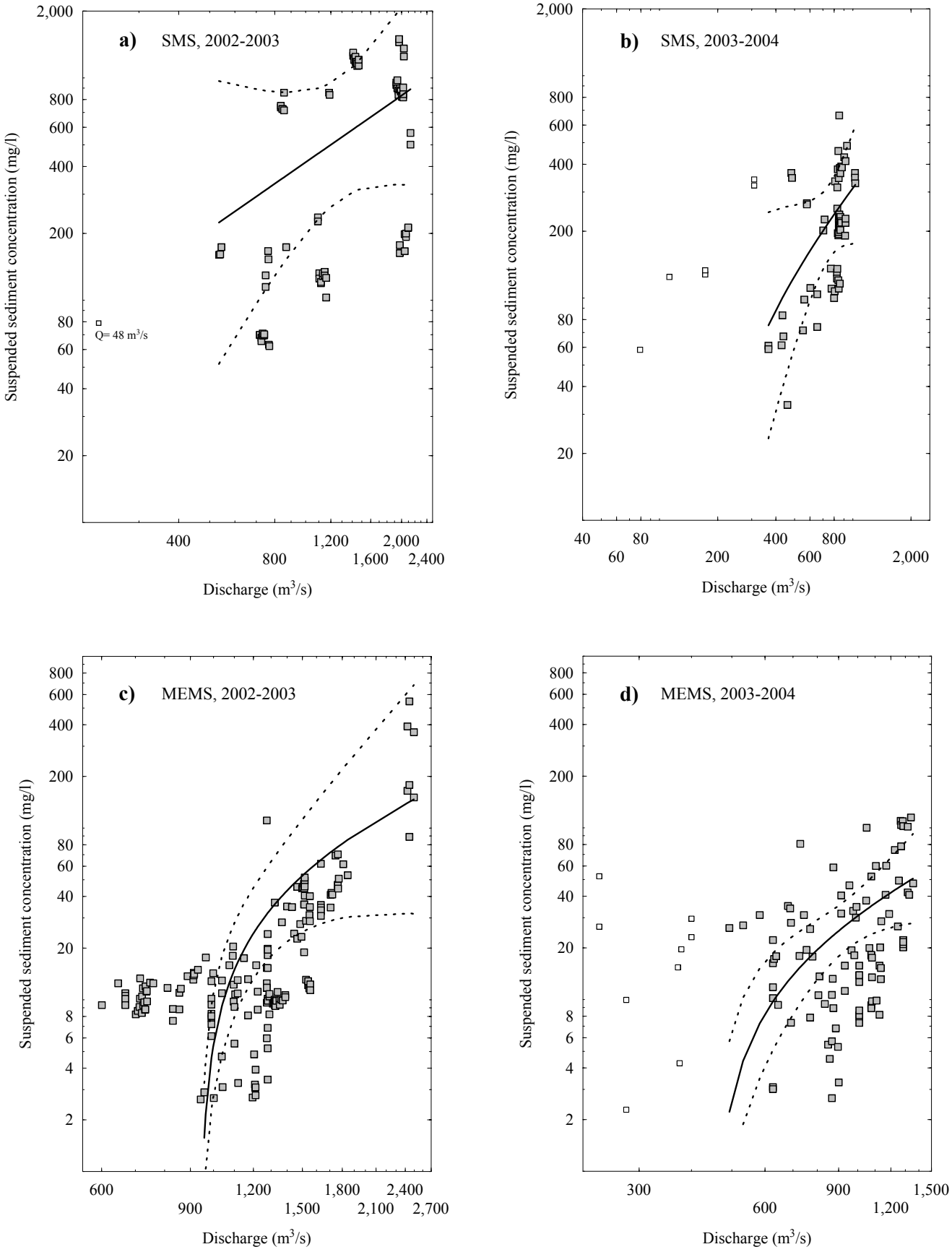

Figure 4 (C3P2). Suspended sediment load rating curves at the monitoring sections (**a** and **b** at SMS and **c** and **d** at MEMS) in the lower Ebro River for the hydrological years 2002-2003 and

2003-2004. Dashed lines represent the 0.95 confidence limits above and below the regression line (solid line) (see table 2 (C3P2) for equations). Data represented by empty squares have not been included in the analysis

The mean suspended concentration (estimated as the mean of the measured concentrations) was 530 mg/l for a mean sampled discharge of 1,280 m^3/s in 2002-2003, and 215 mg/l for a mean sampled discharge of 725 m^3/s in 2003-2004. The maximum concentrations were recorded during 2002-2003 (1.5 g/l) under discharges close to 2,000 m^3/s.

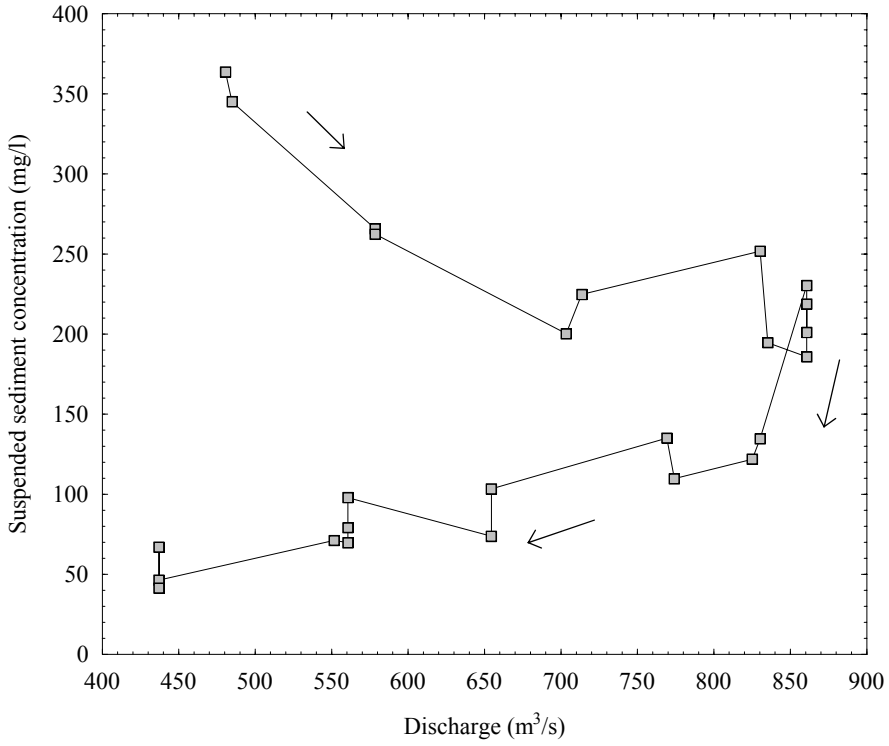

Figure 5 (C3P2). Hysteretic behaviour during April 2004 flood at Sástago Monitoring Section (upstream from the dams). Relation between discharge and suspended sediment concentrations shows a well defined clock-wise hysteresis, indicating progressive exhaustion of sediment during flood. Each point represent a single measurement

The mean annual suspended sediment load passing the upstream section of SMS and entering the Mequinenza reservoir was calculated at around $2.30 \cdot 10^6$ tonnes ($\pm 0.32 \cdot 10^6$ tonnes) for the year 2002-2003 and $0.97 \cdot 10^6$ tonnes ($\pm 0.07 \cdot 10^6$ tonnes) for the year 2003-2004, which represents a specific sediment yield of approximately 47 $t/km^2 \cdot y$ and 19 $t/km^2 \cdot y$ (Table 3 (C3P2)). This value is lower than others reported for smaller basins in the

Mediterranean region (Walling and Webb 1983, Lvovich *et al.* 1991, Inbar 1992, Batalla *et al.* 1995, Walling and Webb 1996). According to data from Bayerri (1934-1935) and further estimates by Nelson (1990), specific sediment yield at the beginning of the 20th century before most dams were constructed was of the order of 200 t/km^2·y. Reduction may reflects upstream sediment retention. Suspended sediment loads show a different pattern between the two years (Figure 6 (C3P2)). Suspended load was transported in less time during 2002-2003 (e.g., 10% of time carried 90% of the load) than during 2003-2004 (10% of time carried 60% of the load). This fact is a reflection of the different hydrological behaviour of the two study years (Figure 2 (C3P2)). During 2002-2003 higher magnitude events occurred in comparison to 2003-2004, so that most of the load was transported by less frequent discharges (e.g., 50% of the load was transported by discharges equalled or exceeded only 1.5% of the time).

Table 3 (C3P2). Sediment yield of the lower Ebro River for the period 2002-2004

Monitoring section	**Sediment transport**	**2002-2003**	**2003-2004**	**2002-2004**
Sastago bridge - SMS (*Section upstream dams*)	Suspended load (t) [1]	(99)2,297,000	(99.8)972,200	(99.5)3,269,200
	Bedload (t)	(1)15,300 [2]	(0.02)155 [3]	(0.5)15,455
	Total load (t)	2,312,300	972,355	3,284,655
Mora d'Ebre bridge - MEMS (*Section downstream dams*)	Suspended load (t) [1]	(48)257,580	(79)294,500	(60) 552,080
	Bedload (t) [1]	(52)279,000	(21)77,000	(40)356,000
	Total load (t)	536,580	371,500	908,080

(#) Percentage of sediment load within total load
[1] Calculated by means of the Flow Duration Method (Walling 1984)
[2] Estimated using the Meyer Peter *et al.* (1934) bedload transport formula
[3] Calculated as the product of the discharge times the average bedload rate (see text for details)

The seasonal variation in suspended sediment load is illustrated in figure 7 (C3P2). Seasonal variation is expressed as the relation between mean discharge (Q in m^3/s) and mean suspended sediment concentration (C_1 in mg/l) for each season. Suspended sediment samples covered almost the whole range of discharges in each season. Within the year 2002-2003 there is a clear anticlockwise hysteresis, reflecting the progressive supply of sediment from the catchment and the upstream tributaries, which mostly arrived at SMS and entered the Mequinenza reservoir during February-March and May high magnitude floods (Vericat and Batalla 2005a). Mean suspended sediment concentration in winter is more than two orders of magnitude higher than in summer. The year 2003-2004 shows a visible clockwise hysteresis, indicating that the supply of sediment was still higher during

autumn and winter, possibly due to reworking of sediment remaining from the previous year, which became limited at the end of spring season.

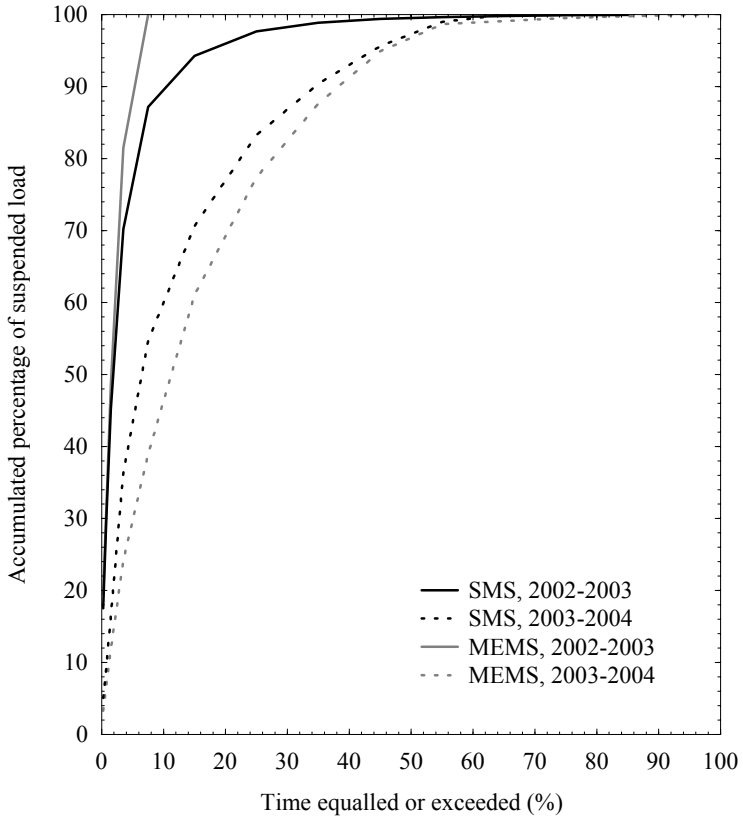

Figure 6 (C3P2). Frequency of suspended load at the two monitoring sections (upstream and downstream dams) during the hydrological years 2002-2003 and 2003-2004

5.5. Patterns of suspended sediment transport and yield at MEMS

Suspended sediment concentrations (C_1) in the Ebro River at the Móra d'Ebre Monitoring Section (MEMS) downstream from the dams showed a positive and statistically significant relation with discharge (Q) ($p<0.01$) for the two study years, 2002-2003 and 2003-2004 (Table 2 (C3P2), Figure 4c, d (C3P2)). The positive relation of the load rating curves indicates that the increment of the suspended load is related to the increase of discharge during floods (i.e., hydraulically dependent). Taking into account that almost all fine sediment supplied from the upstream catchment gets trapped in the large Mequinenza and Riba-roja reservoirs (120 km-long), the riverchannel would act as the main source during high flows. Concentrations may be the consequence of the unusual sediment supply from the riverbed and banks after two years of intense drought (2000-2002).As in the case of

SMS, the degree of scatter is very high, indicating a notable temporal variability. This again can be related mainly to seasonal effects. In contrast to SMS, no hysteresis has been observed during floods.

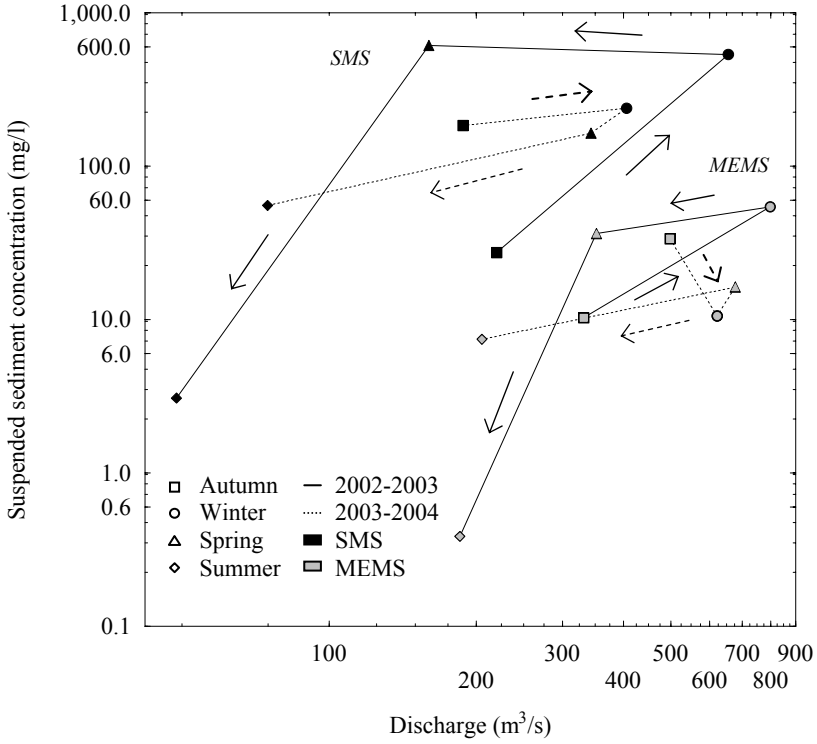

Figure 7 (C3P2). Seasonal variation of suspended sediment concentration at SMS and MEMS during the two hydrological years (2002-2004)

The mean suspended concentration (estimated as the mean of the measured concentrations) was 38 mg/l for a mean sampled discharge of 1,284 m^3/s in 2002-2003, and 27 mg/l for a mean sampled discharge of 910 m^3/s. The maximum concentrations were recorded during 2002-2003 (0.55 g/l) under discharges close to 2,440 m^3/s. Mean and maximum concentrations are an order of magnitude lower than those obtained at SMS under similar discharges. This fact reflects clearly the influence of reservoirs in trapping fine sediment that otherwise would circulate downstream.

The mean annual suspended sediment load passing the downstream section of MEMS was calculated at around $0.26 \cdot 10^6$ tonnes ($\pm$ $0.06 \cdot 10^6$ tonnes) for the year 2002-2003 and $0.29 \cdot 10^6$ tonnes ($\pm$ $0.02 \cdot 10^6$ tonnes) for the year 2003-2004, which represents a specific sediment yield of approximately 3 $t/km^2 \cdot y$ and 3.4 $t/km^2 \cdot y$, respectively (Table 3 (C3P2)).

These values are much lower than the ones obtained at SMS, indicating the major role of the 120-km reservoirs chain on trapping the river's solid load. No flood occurred in the Siurana River during the study period and, consequently, the sediment supply was negligible. Suspended sediment load shows a different pattern between the two years, very similar to the one described for SMS. Suspended load was transported in much less time during 2002-2003 (e.g., 10% of time carried around 99% of the load) than during 2003-2004 (10% of time carried 45% of the load) (Figure 6 (C3P2)). This fact is a reflection of the different hydrological behaviour between study years one and two (Figure 2 (C3P2)). On one hand, during 2002-2003 several floods occurred and they were responsible for most of the load (e.g., 50% of the load was transported by discharges equalled or exceeded only 2% of time). On the other, during 2003-2004 sediment was more constant through time and relatively frequent discharges achieved most of the transport (e.g., 50% of the load was transported by discharges equalled or exceeded 20% of time). Similarities between sediment transport patterns for both years and between sections would suggest that the river downstream from the dams keeps most of its capacity to transport suspended sediment, an observation that can be of interest to inform on-going restoration measurements in the river, including the possibility of carrying out artificial feeding and transport of fine sediment into the delta plain and the delta front. This conclusion is supported by the hydrological analysis of Batalla *et al.* (2004).

In the year 2002-2003 seasonal variation (Figure 7 (C3P2)) shows an anticlockwise hysteresis, reflecting the progressive supply of sediment from the river channel which passed the MEMS during February-March high magnitude floods (Vericat and Batalla 2005a). Mean suspended sediment concentration in winter is more than one order of magnitude higher than in summer. The year 2003-2004 shows a poorly defined clockwise hysteresis, indicating that the availability of sediment was still very high during autumn and winter, possibly due to sediment remaining from the previous year, and became limited during summer. Concentrations during periods of low sediment transport (i.e., summer months) are relatively similar between the two sections, while maximum concentrations occurring in winter are clearly higher at SMS than at MEMS.

6. Bedload

6.1. Measurements

Bedload was sampled during floods at the same vertical as suspended sediment load. Bedload analysis has been based upon 274 samples, 149 during 2002-2003 and 125 during 2003-2004. At SMS we used a 29-kg cable-suspended Helley-Smith sampler with a 76-mm intake and an expansion ratio (i.e., ratio of nozzle exit area to entrance area) of 3.22. Bedload has been measured at MEMS by means of a 76-kg cable suspended Helley-Smith sampler with a 152-mm intake and an expansion ratio of 3.22. The bedload samplers were operated from a bridge using a manual crane and an automatic crane at SMS and MEMS, respectively. In both sections and, in order to keep sampling efficiency as high as possible, sampling time did not exceed 5 minutes, thus preventing the sampler bag being filled to more than 50% (Emmett 1980, Habersack and Laronne 2001). Sample catches typically ranged from few grams to 13 kg. The sampling interval was thirty minutes. Samples were collected and taken to the laboratory, where they were dried, sieved and weighed to obtain the total mass and grain size distribution.

Using a suspension criterion based on the particle settling velocity (Dietrich 1982), the grain size distributions of the bedload were truncated at 0.5 mm in order to exclude the suspended load (Emmett 1980). Efficiency of the Helley-Smith sampler is known not to be constant. Calibrations are certain not to be applicable to all situations in which this sampler is being used. Emmett (1980) reported for the 76 mm intake Helley-Smith sampler an efficiency of 1 (100%) for particles between 0.5 and 16 mm. Efficiency decreases as grain size and bedload rates increase. Similar results were found by Hubbell (1987) for different Helley-Smith type samplers. In the Drau River, Austria, a coarse gravel channel, Habersack and Laronne (2002) calculated for the 152 mm intake Helley-Smith an efficiency close to unity by comparing the Helley-Smith bedload rates and slot sampler bedload rates. The median size (D_{50}) of the Ebro River bed sediments at SMS is 17 mm and maximum particles (D_{max}) attain 55 mm, thus the 76 mm Helley-Smith sampler provides, in principle, an efficient sampling for most grain size classes that may be entrained upstream from the dams. At MEMS the median size of surface bed-material (D_{50-s}) is close to 50 mm and maximum particles on the surface reach (D_{max-s}) 117 mm, thus the

152 mm Helley-Smith ensures an efficient sampling of bedload for almost all grain size classes downstream from the dams.

6.2. Precision of the measurements

Bedload transport can be highly variable (e.g., Gomez *et al.* 1989), circumstance that poses important problems for the calibration and use of bedload samplers (Emmett 1980, Hubbell 1987). Several authors have attempted to estimate such errors (e.g., Gibbs and Neill 1972, Csoma 1973) in relation to the minimum number of samples needed to obtain an estimate of the mean bedload transport rate under given confidence levels. Hamamori (1962) described temporal variations in relation to the movement of bedforms. The maximum relative bedload transport rate that may result from the Hamamori probability distribution function is 4, that is, the actual maximum bedload transport rate cannot exceed four times the mean rate. In the case of the Ebro River at MEMS, the maximum measured bedload rate exceeds by almost 3.5 times the mean rate, indicating that temporal variability is expectedly high, possibly in relation to the movement of primary and secondary waves of sand and gravel on the river bed. Similar results have been obtained in other large rivers, such as the Fraser River, British Columbia, Canada (McLean *et al.* 1999).

Bedload variability in the Ebro River increases with discharge (Figure 8 (C3P2)). Discharges were grouped in to regular intervals of 200 m^3/s and accumulated frequency of bedload transport rates was calculated for each group of discharges. As an example, discharges between 600 m^3/s and 800 m^3/s showed bedload rates between 0 g/ms and 143 g/ms, while discharges between 1,400 m^3/s and 1,600 m^3/s showed bedload rates between 1.5 g/ms and 1,230 g/ms. These facts can be related to the progressive entrainment of bed-material of coarser sizes as flow increases and, eventually, to the breaking up of the armour layer that releases large quantities of subsurface fine materials to be transported. For instance, during the first flood occurred at MEMS (December 2002) the first finite bedload sample was collected under 1,525 m^3/s. The ratio τ_o/τ_c was 1.7, where τ_o is the estimated mean bed-shear stress at the flow peak and τ_c is the critical bed shear stress according to Shields's (1936) equation. This ratio is much lower than the estimated by Powell *et al.* (2001) ($\approx$ 4.5) in which equal mobility was arisen in an ephemeral river-bed with loose sediment, but close to the estimations done in flume experiments with armoured beds (e.g.,

Wilcock 1992). Riverbed material was set in motion 6 hours after critical shear stress was reached. Delay of bedload can be then attributed to the strength of the armour (i.e., stable armour) after almost two years with no competent flows.

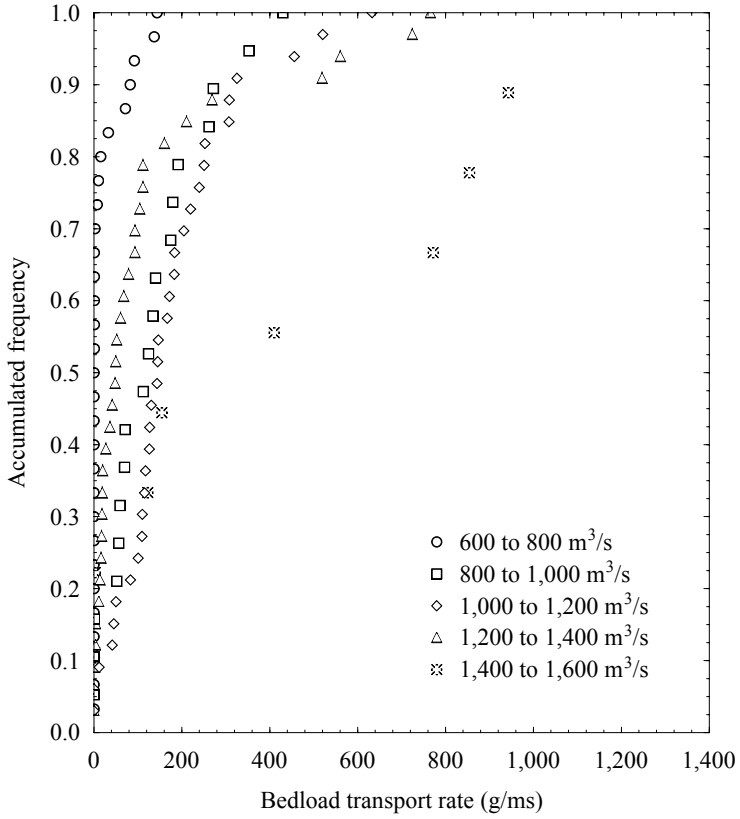

Figure 8 (C3P2). Bedload variability at a single vertical (MEMS, 2002-2003)

Sources of variability are believed to be both actual fluctuations in bedload transport (e.g spatial and temporal variability) and operational effects caused by misalignment of the sampler on the river bed and sampler dragging during raising and lowering (McLean *et al.* 1999). In order to have a first-order estimation of the spatial variability of bedload transport and to assess the deviation of samples taken at the usual vertical in relation to the mean bedload rate at the section, five sets of seven equally-spaced vertical samples were taken at MEMS under constant discharges between 800 and 900 m^3/s (discharges equalled or exceeded between 13% and 25% of time) (Vericat and Batalla 2005b). Sampling interval between verticals was 15 minutes and sampling time was 5 minutes for all the flows. A ratio between the bedload rate at the vertical where samples in this study were obtained and the weighted mean bedload of the channel cross-section, composed by the 7 equally-spaced verticals, was calculated to assess the spatial variability (e.g., *k* factor for

the suspended sediment explained above). The ratio was close to 1 in two of the experiments (i.e., bedload sampling at the single vertical represents exactly the mean bedload of the section), and ranged from 4 to 6 in the other three sets (Vericat and Batalla 2005b). Cross-sectional measurements in the Ebro River at MEMS are not sufficient to allow us to establish a factor to correct the spatial bedload variability. We have no information on the actual cross-channel variation at SMS.

The 0.95 confidence limits have been calculated above and below the regression lines (rating loads). The RMSE of both limits have been subsequently calculated to determine the mean error estimates. The mean error estimates of bedload measurements for the year 2002-2003 and for discharges higher than 1,900 m^3/s at SMS is ±29%. At MEMS the estimated annual load for the year 2002-2003 could be specified within ±110%, which reflects the high bedload variability under similar discharges. The estimated annual load for the year 2003-2004 could be specified within ±50%, which reflects a better fit regression line (Table 2 (C3P2)).

6.3. Computation of bedload yield

As for the suspended sediment load, annual sediment yield at the monitoring sections was intended to be calculated from load-rating relations between discharge (Q in m^3/s) and bedload transport rates (i_b in g/ms), using the Flow Duration Curve method (Walling 1984). However, due to technical problems only 15 bedload samples were obtained at SMS during 2002-2003, all of them under discharges higher than 1,900 m^3/s. In order to calculate bedload rates for discharges below that value, we applied the Meyer Peter *et al.* (1934) bedload transport formula, which is fully applicable to the physical characteristics of the river reach (slope and particle size). Samples were used to check the accuracy of the model (Vericat and Batalla 2005a). The adjustment between the computed bedload rates by the Meyer Peter *et al.* (1934) bedload transport formula and the observed rates had an average value of 0.94 (94%) (Vericat and Batalla 2005a). No statistically significant relation was found between discharge and bedload transport rates at SMS during the year 2003-2004. Bedload yield was thus calculated as the product of the discharge times the

average bedload rates. Bedload rates were very small (<5 g/ms) and can be within the range of error due to, for example, scooping.

At MEMS, annual statistically significant relations were used to estimate bedload rates, and thus loads, during periods or discharges for which measurements were unavailable. Unsampled discharges were equalled or exceeded 3.5% of time in 2002-2003 and all discharges were sampled in 2003-2004. Therefore, bedload was sampled under most discharges and probably bedload yield was not underestimated. As for the suspended sediment load, annual bedloads calculated from the Flow Duration Curve method are compared with the annual loads estimated as the product of the 15-min interval discharge and with the bedload rate obtained from the annual Q-i_b rating curve. Results are similar in both methods (i.e., -20% difference, on average).

6.4. Patterns of bedload transport and yield at SMS

Bedload rates of the Ebro River at the Sástago Monitoring Section (SMS) showed a positive and statistically significant relation with discharge (Q) ($p<0.01$) for the study year 2002-2003 and for discharges higher than 1,900 m^3/s. The degree of scatter is, however, very high, indicating expected fluctuations in gravel transport (see 6.2) and operational effects caused by misalignment of the sampler on the river bed and sampler dragging during raising and lowering. As was previously indicated in section 6.3, no statistically significant relation was found between discharge and bedload transport rates at SMS during the year 2003-2004 (Table 2 (C3P2)).

The mean bedload rate (estimated as the mean of the measured rates) was 41 g/ms for a mean sampled discharge of Q=2,012 m^3/s in 2002-2003, and 2 g/ms for a mean sampled discharge of 894 m^3/s in 2003-2004, which represents a daily transport of 389 t/day and 19 t/day, respectively. For comparison, in the Clearwater River, Idaho, bedload rates close to 40 g/ms were estimated for discharges around 2,000 m^3/s (Jones and Seitz 1980). Median bedload size ($D_{50\text{-bl}}$) at SMS ranged from 21 mm to 40 mm in 2002-2003 and from 11 mm to 22 mm during 2003-2004, which represents the D_{60} and the D_{84} of the bed grain size distribution (in absence of surface layer) for the sizes collected in the first year, and the D_{40}

and the D_{60} for the sizes collected in the second year. The mode of the bedload $D_{50\text{-bl}}$ was 21 mm in both years.

The mean annual bedload carried downstream from SMS and entering the Mequinenza reservoir was calculated at around 15,300 tonnes (± 4,440 tonnes) for the year 2002-2003 and 155 tonnes for the year 2003-2004, which represents specific sediment yields of approximately 0.3 t/km^2·y and 0.003 t/km^2·y, respectively (Table 3 (C3P2)). Bedload was transported during more time in 2002-2003 (e.g., 3% of time carried 95% of the load) than in 2003-2004 (1% of time carried 95% of the load) (Figure 9 (C3P2)). This fact is a reflection of the different hydrological behaviour between the two years (Figure 2 (C3P2)). Critical discharge (865 m^3/s, estimated by means of the Shields (1936) equation) was equalled or exceeded 7% of the time in 2002-2003 and only 1% of the time in 2003-2004.

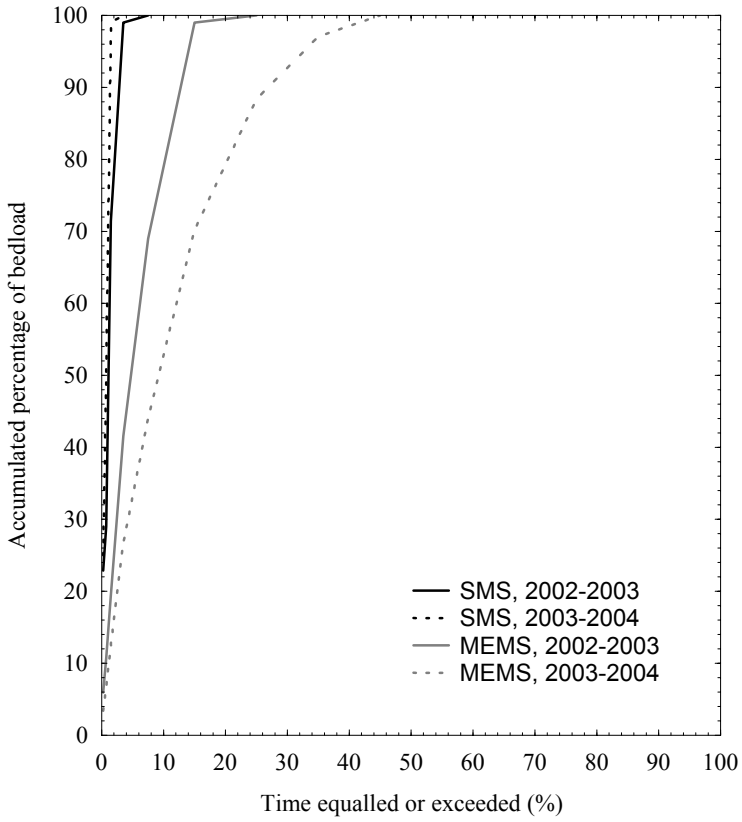

Figure 9 (C3P2). Frequency of bedload upstream and downstream from the dams during the hydrological years 2002-2003 and 2003-2004

6.5. Patterns of bedload transport and yield at MEMS

Bedload rates (i_b) of the Ebro River at the Móra d'Ebre Monitoring Section (MEMS) downstream from the dams showed a positive and statistically significant relation with discharge (Q) ($p<0.01$) for the two study years, 2002-2003 and 2003-2004 (Table 2 (C3P2), Figure 10a, b (C3P2)). As in the case of SMS, the degree of scatter is very high, indicating the importance of bedload variability and the possible operational effects (sampler uncertainty).

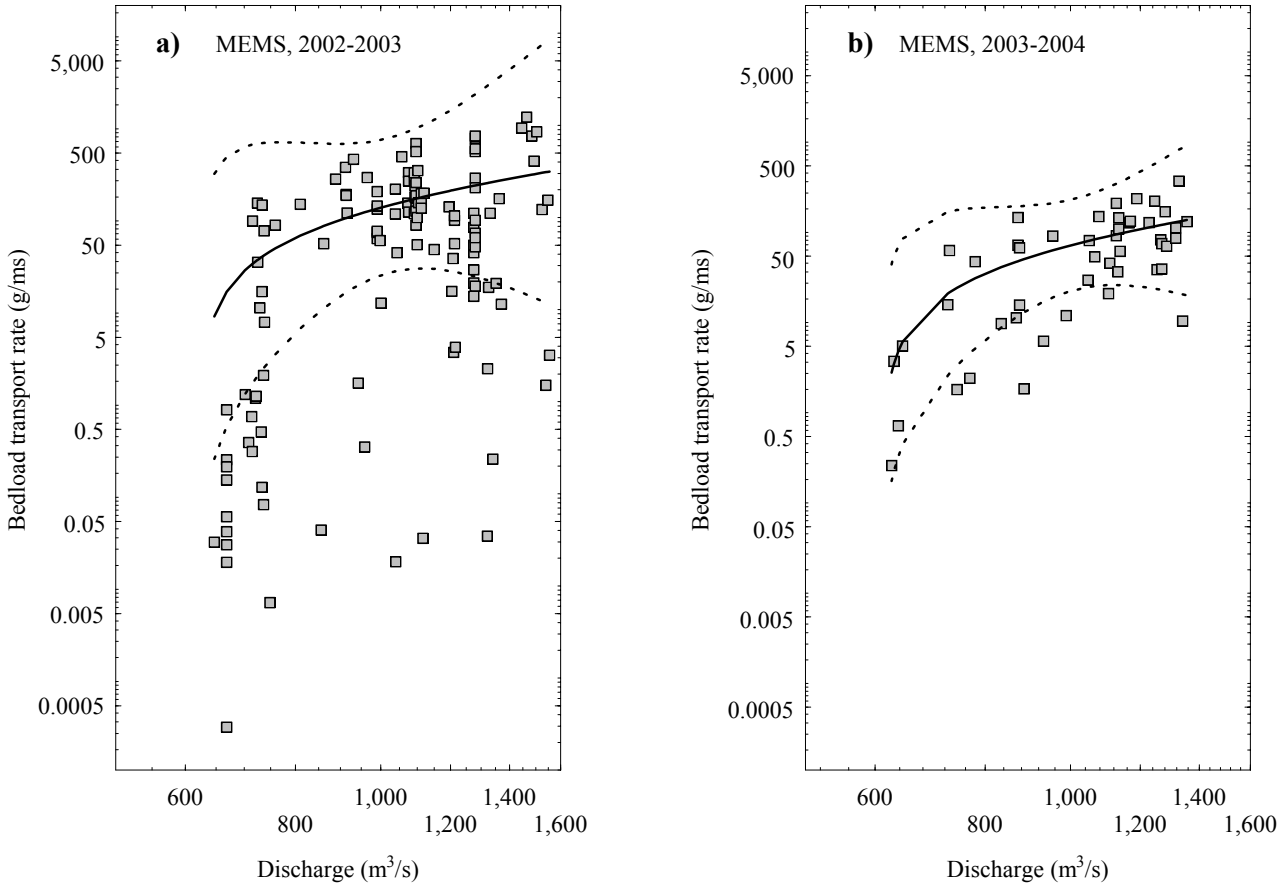

Figure 10 (C3P2). Bedload rating curves downstream from the dams at the Móra d'Ebre Monitoring Section for the hydrological years 2002-2003 and 2003-2004. Dashed lines represent the 0.95 confidence limits above and below the regression line (solid line) (see table 2 (C3P2) for equations)

Mean bedload rate (estimated as the mean of the measured rates) was 146 g/ms for a mean sampled discharge of 1,050 m^3/s in 2002-2003 and 68 g/ms for a mean sampled discharge of 1,020 m^3/s in 2003-2004. For comparison, Jones and Seitz (1980) reported for the Snake

River, Idaho, under discharges close to 1,000 m^3/s, bedload rates around 16 g/ms. For a given discharge, bedload rates were, on average, double during the first study year what they were during the second. Maximum rates were recorded during 2002-2003 (1,200 g/ms) under discharges close to 1,500 m^3/s. Maximum rates are an order of magnitude higher than those obtained at SMS under higher discharges (135 g/ms under 2,025 m^3/s). This fact clearly reflects the different bedload transport in both sections. The $D_{50\text{-bl}}$ in bedload samples collected during 2002-2003 varied from 1 mm to 72 mm. During 2003-2004 the bedload $D_{50\text{-bl}}$ varied from 4 mm to 44 mm. The upper limits (72 mm and 44 mm) correspond to the D_{75} and the D_{50} of the bed surface grain size distribution at MEMS, respectively. The lower limits (1 mm and 4 mm) are not present in the surface sediments, and represent D_5 and D_{22} of the subsurface grain size distribution. The range of variability in bedload $D_{50\text{-bl}}$ at MEMS is higher than at SMS and similar to the values reported by McLean *et al.* (1999) for the Fraser River in British Columbia, Canada. Mode of bedload D_{50} was 18 mm in 2002-2003 and 21 mm during 2003-2004, similar than to that at SMS. The $D_{max\text{-bl}}$ was 90 mm in bedload samples collected during 2002-2003 and 75 mm in samples collected during 2003-2004.

The mean annual bedload yield at the downstream section of MEMS was calculated at around $0.28 \cdot 10^6$ tonnes ($\pm$ $0.30 \cdot 10^6$ tonnes, reflecting the high variability, see 6.2) for the year 2002-2003 and $0.08 \cdot 10^6$ tonnes ($\pm$ $0.04 \cdot 10^6$ tonnes) for the year 2003-2004, which represents a specific sediment yield of approximately 3.4 $t/km^2 \cdot y$ and 0.9 $t/km^2 \cdot y$, respectively (Table 3 (C3P2)). The specific sediment yield is between 1 and 2 orders of magnitude higher than that obtained at SMS for 2002-2003 and 2003-2004, respectively. Bedload shows a different pattern between the two years (Figure 9 (C3P2)). Bedload was transported in much less time during 2002-2003 (e.g., 10% of time carried around 75% of the load) than during 2003-2004 (10% of time carried 50% of the load). Again, this fact is a reflection of the different hydrological behaviour between study years one and two (Figure 2 (C3P2)). In 2002-2003 the most important floods of the study period occurred, and they were responsible for most of the load (e.g., bedload yield during the February and March 2003 floods was around the 80% of the total load in 2002-2003). Bedload transport during 2003-2004 was more constant through time (e.g., during 45% of the time the flow had sufficient competence to transport coarse sediment) but bedload rates were lower than in the previous year.

Dams in the lower Ebro River trap 100% of coarse sediment moving from upstream, breaking the continuum of bedload material transfer. Under these conditions, the river bed of the lower Ebro should itself be the main source of coarse sediment. Possible sources from downstream tributaries are insignificant. The major tributary, the Siurana River, suffers from a large sediment deficit due to dams and instream gravel mining. These elements must be taken account in order to understand the incipient changes in river channel morphology (e.g., river bed degradation) observed in the Ebro River (e.g., Vericat and Batalla 2004)

7. Total load and sediment budget

7.1. Total load upstream from the dams

Total sediment load upstream from the dams (estimated as the sum of the measured suspended loads plus the bedload rates collected at the same time) was, on average, 894 kg/s for a mean sampled discharge of 1,350 m^3/s in 2002-2003, and 175 kg/s for a mean sampled discharge of 726 m^3/s in 2003-2004. The suspended load represents more than 99% of the total load. The maximum total load was recorded during the flood of February 2002-2003 at 3 t/s under a discharge close to 2,000 m^3/s. The minimum measured load was 0.4 kg/s.

The Ebro River at SMS transported a total of $2.31 \cdot 10^6$ tonnes of sediment in 2002-2003, 99% as suspended load (Table 3 (C3P2)). Almost all load was carried during the February and March floods (Vericat and Batalla 2005a). The suspended load during this year is higher than the annual maximum reported by Sanz *et al.* (1999), estimated from intermittent, non-frequent suspended sediment sampling upstream from Mequinenza Dam between 1975 and 1992. During our study period, only 1% of the total load was transported as bedload, indicating the low percentage of the coarse sediment transport within the annual sediment transport at this section. Total load was $0.97 \cdot 10^6$ t/y in 2003-2004. The proportion of suspended load was even higher (99.8%) during that year. Only 155 tonnes of coarse sediment were transported as bedload during the 1% of the time in

which the flow equalled or exceeded the critical discharge. During the two study years (2002-2004), the river at SMS transported a total of 3,285,000 tonnes into the Mequinenza reservoir, as we have indicated almost all in suspension (99.5%) (Table 3 (C3P2)).

7.2. Total load downstream from the dams

Total sediment load downstream from the dams (estimated as the mean of the measured suspended loads plus the bedload rates collected at the same time) was, on average, 34 kg/s (Q= 1,050 m^3/s) in 2002-2003 and 56 kg/s (Q= 1,020 m^3/s) in 2003-2004. Around 48% of the total load was carried in suspension and 52% as bedload in 2002-2003. The proportion of suspended load within the total load was considerably higher in 2003-2004 (79%), while bedload attained only 21%. The different hydrological behaviour between years (especially the magnitude of floods) is the main element that explains the different proportion between loads and years. Maximum load downstream from the dams was 210 kg/s, recorded during February 2002-2003 under a discharge around 1,500 m^3/s. This value is one order of magnitude lower than the maximum load measured at SMS upstream from the dams. The minimum measured load was 2.7 kg/s for a discharge close to 900 m^3/s, and it is six times higher than the minimum recorded upstream from the dams during the study period. The ration between maximum and minimum load is 7,500 at SMS and 80 at MEMS for a similar range of discharges. This fact (i.e., load variability) appears to be controlled by the sediment availability, much limited in the lower reach of the river, which prevents the flow carrying as much sediment as its capacity under unlimited supply.

The Ebro River at MEMS transported a total of $0.54 \cdot 10^6$ tonnes of sediment in 2002-2003 (Table 3 (C3P2)), around 85% of which was transported during the February and March major floods. The load in suspension represents only 11% of what was transported by the river at SMS, upstream from the dams. Considering that bank erosion downstream from the dams may supply fine material, trapping efficiency of the reservoirs easily could reach values around 95% during that year. A similar percentage of retention was estimated by Avendaño *et al.* (1997), based on reservoir sedimentation, Sanz *et al.* (1999), based on infrequent sampling, and Vericat and Batalla (2005a) following the method by Brune and data from two single floods.

At MEMS the river transported a total of $0.37 \cdot 10^6$ tonnes of sediment in 2003-2004, a value very close the total load in the previous year (Table 3 (C3P2)). However the proportion between suspended load (79%) and bedload (21%) is different. This fact has been previously explained as the consequence of the different hydrological behaviour between years (Figure 2 (C3P2)). Moreover, the 2002-2003 high floods changed the bed grain size distribution (i.e., percentage of material finer than 8 mm increased 10%, on average). Within this context, frequent discharges (1,000 m^3/s) were able to carry more sediment in suspension, explaining the different proportion between the two modes of transport. The annual suspended load in 2003-2004 is more than the value reported by Sanz *et al.* (1999) obtained immediately downstream from Flix Dam ($0.26 \cdot 10^6$ t/y). The difference between the values of Sanz *et al.* (1999) and values in this paper gives an indication of the potential amount of fine sediment that can be eroded from the river channel and transported by high mean discharges between the lowermost dam and the downstream monitoring site. Lateral erosion of the order of 0.5 m has been observed in some experimental sections upstream from MEMS (e.g. section Móra d'Ebre 1 and 2, Table 4 (C3P2)) during floods occurred between 2002 and 2004. The load in suspension represents 30% of what was transported by the river at SMS, upstream from the dams, illustrating again the high efficiency of reservoirs in trapping fine fractions. Similar retentions have been calculated in the Colorado River at Glen Canyon Dam, Arizona, where the supply of fine sediment was reduced between 81% and 85% for high flows (Topping *et al.* 2000).

Suspended transport downstream from the dams was very similar during the two study years. The difference concerns the proportion of suspended load and bedload within the total load, and this fact can be related to the different nature of the flow between the two years: a) the lesser competence of floods to carry coarse sediment during 2003-2004 explains the remarkable reduction of bedload during that year, and b) the higher occurrence of frequent discharges during 2003-2004 resulted in an increased sustained capacity of the river to transport suspended sediment during that year. A total of $0.91 \cdot 10^6$ tonnes of sediment were transported at MEMS during the period 2002-2004, 60% in suspension and 40% as bedload (Table 3 (C3P2)).

Table 4 (C3P2). Scour and fill in the riverbed and maximum particles mobilised in 7 experimental sections of the lower Ebro River for each hydrological year (2002-2004).

Measuring section	Distance from Flix Dam (km)	2002-2003 [1]		2003-2004 [5]	
		Net scour/fill (mm) [2]	D_{max} mobilised (mm) [3,4]	Net scour/fill (mm) [2]	D_{max} mobilised (mm) [3,4]
Presa Flix	0.850	-18	180	4	163
Meandre Flix	2.700	-175	70	-3	70
Flix	5.600	+523	71	26	35
Pas de l'Ase	18.300	-13	78	-9	116
Móra d'Ebre 1	25.200	-115	115	19	105
Móra d'Ebre 2	25.500	-22	70	-2	91
Móra d'Ebre 3 (MEMS)	27.000	-145	113	-41	150
Weighted mean		-4	97	0	104
Weighted mean without Flix section		-60		-3	

[1] Maximum discharge at MEMS during the hydrological year 2002-2003 was 2,498 m^3/s.
[2] Scour chains / - net scour, + net fill. Two scour chains were installed in each cross section from 2002. Measurement error is established as ± 20 mm.
[3] Painted pebbles. Lines of pebbles from 8 mm to 128 mm (size of b axis, half phi increments) were painted.
[4] Mean slope is 0.00085
[5] Maximum discharge at MEMS during the hydrological year 2003-2004 was 1,355 m^3/s.

7.3. Sediment budget of the lower Ebro River

The sediment budget of the lower Ebro River (Figure 11 (C3P2)) is characterized by two main factors: a) almost all the sediment load is trapped by dams and, b) below the dams the river transports around $0.45 \cdot 10^6$ tonnes of total load per year. The observed annual load is close to 3% of what was delivered at the beginning of the 20th century, according to the estimations of Bayerri (1934-1935) and Nelson (1990). At that time most sediment came presumably from the catchment (as suggested by concentrations up to 10 g/l), while now sediment is mainly entrained from the riverbed and the riverchannel. The annual load between the Flix Dam and MEMS is 3.8 times greater than the estimations by Guillén and Palanques (1992) from sediment transport measurements at the delta plain (120,000 t/y), therefore sedimentation may be occurring between MEMS and the delta plain (Figure 1 (C3P2)).

Bedload constitutes an important part (40%) of the total load downstream from the dams. Consequently, the river channel downstream from Flix Dam has to be the only source of

coarse sediment for the river (i.e., 356,000 tonnes during the study period 2002-2004). Assuming a regular supply of bedload over the 27-km study reach, an average channel width of 150 m, a submerged density of 1.65 t/m^3, and a porosity of riverbed deposits of 0.26 (data obtained experimentally in the field by the authors), mean incision after seven floods during the period 2002-2004 would have been around 65 mm. The greatest incision took place in 2002-2003 (53 mm), when the largest floods occurred (Figure 2 (C3P2)), and when bedload had the most important role in the total annual load (52%) (Table 3 (C3P2)). Most movable particles are in the range of 32 mm as indicated by lines of painted pebbles.

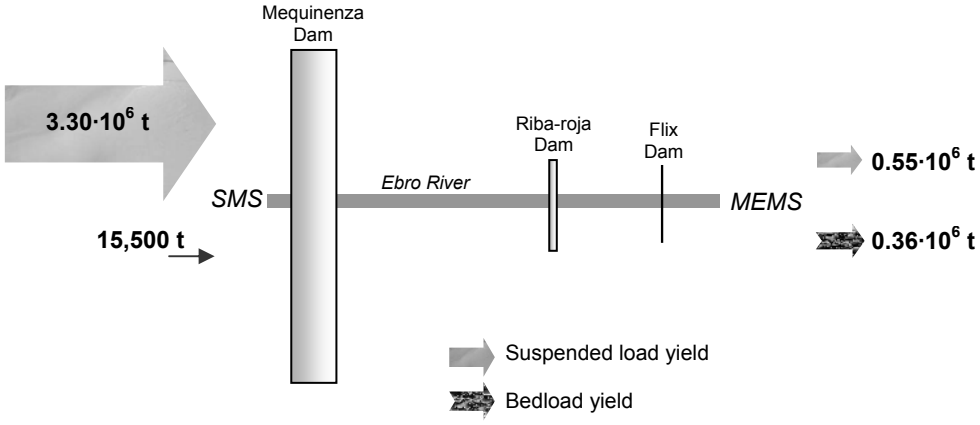

Figure 11 (C3P2). Sediment budget in the lower Ebro River for the period 2002-2004

According to scour chains at seven experimental sites located between the Flix Dam and MEMS (Vericat and Batalla 2005a), mean weighted erosion during 2002-2003 was 4 mm, with a measurement error of ± 20 mm (Table 4 (C3P2)). If we do not take into account the extreme value of 523 mm of net deposition in a single bar downstream from the Flix hydropower dam, mean erosion would be higher (60 mm) and much closer to the budget estimated after bedload measurements. The difference between the values of erosion estimated from bedload measurements and scour chains can also be attributed to the type and operation of the measuring techniques: a) bedload is measured in the active channel, while scour chains are located in bars that are not active the same amount of time in terms of bedload and, b) bedload at MEMS gives a temporal and spatial integration of bedload dynamics over a 27-km study reach, therefore assuming that all that is measured during one flood or one year is the product of upstream fluvial dynamics during that particular flood or year, in comparison with scour chains that inform on local dynamics in

representative bars (in the case of the lower Ebro almost all available bars have been monitored with chains). Scour chains are a technique that in a river as large as the Ebro will inform on erosion/deposition process over a long-term (i.e., decade), but the information should not solely be applied in short-term analysis. In this paper we report the data from scour chains to contextualize the order of magnitude of the riverbed incision extrapolated from the sediment budget, and to show that the tendency observed is consistent with the appearance that degradation is actually occurring. Net erosion/deposition was almost negligible during 2003-2004: 15 mm of mean erosion estimated from bedload measurements and 3 mm of erosion from scour chains, both values within the measurement error (Table 4 (C3P2)).

Maximum size of mobilised particles (Table 4 (C3P2)) gives an order of magnitude of riverbed mobilization. Maximum mobilised particles, determined by means of painted pebbles, ranged between sections from 70 mm to 180 mm during 2002-2003 and between 35 mm and 163 mm during 2003-2004. These values illustrate the competence of the river to remove almost all grain size classes in the riverbed, which are not replaced from upstream, therefore causing the long-term riverbed degradation that is occurring in the lower Ebro River.

8. Summary and final remarks

Sediment transport in a highly regulated large Mediterranean river (the lower Ebro) has been assessed from direct measurements during two average hydrological years (2002-2003 and 2004-2004). Special attention has been devoted to measuring sediment transport during floods upstream and downstream from Mequinenza and Riba-roja reservoirs. Main conclusions can be drawn as follows:

1. Mean annual total load upstream from the dams (SMS) is estimated at around $1.64 \cdot 10^6$ tonnes, of which 99.5% is transported in suspension. Mean annual total load downstream from the dams (MEMS) is estimated at around $0.45 \cdot 10^6$ tonnes, of which 60% was transported as suspended load and the remain 40% as bedload. This represents around 3% of what was transported at the beginning of the 20th century.

2. Specific sediment yield is three to four times higher at SMS than at MEMS. This fact is the consequence of the trapping of sediment by dams (around the 90% of suspended load and 100% of bedload), which otherwise would reach the lowermost reaches of the Ebro River and its delta plain.
3. Sediment load at SMS is mainly controlled by supply from the tributaries along the catchment, while at MEMS sediment is almost all entrained from the riverbed and eroded from banks, causing a mean riverbed incision of 30 mm per year. This value has been estimated from bedload measurements and the order of magnitude corroborated by means of scour chains and painted pebbles in the field. Suspended sediment is mainly supplied after bank collapses as erosion pins installed in the banks indicate at Móra d'Ebre 1 and 2 measuring sections.
4. At SMS the proportion of suspended load and bedload was very similar in both years. At MEMS the main difference pertains to the proportion of suspended load and bedload within the total load. This fact can be related to the different nature of the flow between the two years; the larger floods in 2002-2003 were able to carry larger amounts of bedload, while the higher occurrence of frequent discharges during 2003-2004 resulted in a higher capacity of the river to transport suspended sediment.

This study has pointed out the alteration of sediment transport and, subsequently, of the fluvial dynamics due to dam regulation in a large river system. What makes this case study of special interest is the combination of a relatively small reduction of sediment transporting flows (T*=0.97, Grant *et al*. 2003, i.e., the river keeps the competence and the capacity to entrain and carry sediment since the main dams were put into operation 40 years ago), and the almost complete disappearance of sediment supply. According to the initial hypothesis, the sediment supply downstream dams is remarkably lower than that observed upstream, a fact that is confirm by the low S* ratio of 0.27 (Grant *et al.* 2003). Under present conditions the riverbed and channel of the lower Ebro River will continue exporting sediment both during floods (>2,000 m^3/s, mostly bedload) and frequent high flows (1,000 m^3/s to 2,000 m^3/s) causing, eventually, continued degradation. Once the actual sediment deficit has been established, sediment transport information could be of use to design restoration programmes based on artificial sediment feeding and flow releases to ameliorate the sediment disequilibrium between the river and its delta and

coastline. Experimental flow releases (Figure 2 (C3P2)) have been already designed at the University of Lleida and carried out by Endesa, the Hydropower Company operating the dams in the lower Ebro (Palau *et al*. 2004). Sediment transport information obtained in the Ebro River could also be of use to inform restoration programmes in other large regulated fluvial systems, especially in the Mediterranean region.

Acknowledgements

This research was carried out within the framework of the research project REN2001-0840-C02-01/HID, which is funded by the Spanish Ministry of Science and Technology. The first author received a grant from the Spanish Ministry of Education. Hydrological data were supplied by the Ebro Water Authorities. The Móra d'Ebre Town Council provided logistic support during fieldwork. Albert Rovira at the University of Lleida assisted during fieldwork and labwork. Reviews by two anonymous referees greatly improved the manuscript.

References

Allayaud, W.K., 1985. Innovations in non-structural solutions to preventing coastal damage. In: *California's battered coast, Proceedings from a Conference on Coastal Erosion*, McGrath J. (ed.). California Coastal Commission: 260-280.

Avendaño, C., Cobo, R., Sanz, M.E., Gómez, J.L., 1997. Capacity situation in Spanish reservoirs. *I.C.O.L.D. Proceedings of the Nineteenth Congress on Large Dams* **74**(52): 849-862.

Avendaño, C., Sanz, M.E., Cobo, R., 2000. Embalses en el río Ebro: su influencia en la morfología del cauce y en los sólidos aportados al Delta. *Proceedings of the V Jornadas sobre encauzamientos fluviales*. Centro de Experimentación de Obras Públicas (CEDEX): Madrid; 1-12.

Batalla, R.J., Sala, M., Werritty, A., 1995. Sediment budget focused in solid material transport in a subhumid Mediterranean drainage-basin. *Zeitschrift Fur Geomorphologie* **39**(2): 249-264.

Batalla, R.J., 2003. Sediment deficit in rivers caused by dams and instream gravel mining. A review with examples from NE Spain. *Cuaternario y Geomorfología* **17**(3-4): 79-91.

Batalla, R.J., Kondolf, G.M., Gomez, C.M., 2004. Reservoir-induced hydrological changes in the Ebro River basin, NE Spain. *Journal of Hydrology* **290**: 117-136.

Bayerri, E., 1934-35. *Historia de Tortosa y su comarca*. Imprenta Moderna de Alguerri: Tortosa.

Brownlie W.R., Taylor, B.D., 1981. Sediment management for southern California mountains, coastal plains, and shoreline. Part C. Coastal sediment delivery in major rivers in southern California. Report 17-C, Environmental Quality Lab., California Institute of Technology: Pasadena.

Brune, G.M., 1953. The trap efficiency of reservoirs. *Transactions of the American Geophysical Union* **34:** 407-418.

Church, M., 1995. Geomorphic response to river flow regulation: case studies and time-scales. *Regulated Rivers: Research and Management* **11**(1): 3-22.

Csoma, J., 1973. Reliability of bed-load sampling. International Association for Hydraulic Research. *International Symposium on River Mechanics*, Bangkok, vol. B9: 97-107.

Day, J.W., Templet, P.H., 1989. Consequences of sea level rise: implications from the Mississippi delta. In *Expected effects of climate change on marine coastal ecosystems*, Benkema, J. *et al.* (eds.); 155-165.

Dietrich, W.E., 1982. Settling velocity of natural particles. *Water Resources Research* **18**(6): 1615-1626.

Emmett, W.W., 1980. *A Field Calibration Of The Sediment Trapping Characteristics Of The Helley-Smith Bedload Sampler*. US Geological Survey Professional Paper 1139.

Everts, C.H., 1985. Effects of small protective devices on beaches. In: *California's battered coast, Proceedings from a Conference on Coastal Erosion*, McGrath J. (ed.). California Coastal Commission; 127-138.

Fan, S., Springer, F.E., 1993. Major sedimentation issues at the Federal Energy Regulatory Commission. In: *Notes on sediment management in reservoirs,* Fan, S., Morris, G. (eds.). Water Resources Publications: Colorado, USA; 1-8.

Gibbs, C., Neill, C.R., 1972. *Laboratory testing of a VUV bed-load sampler*. Research Council of Alberta Open-File Report 1973-29.

Gomez, B., Naff, R.L., Hubbell, D.W., 1989. Temporal variations in bedload transport rates associated with the migration of bedforms. *Earth Surface Processes and Landforms* **14**: 135-156.

Grant, G.E., Schmidt, J.C., Lewis, S.L., 2003. A geological framework for interpreting downstream effects of dams on rivers. In *A peculiar river: geology, geomorphology, and hydrology of the Deschutes River, Oregon*, Grant, G.E., O'Connor, J.E. (eds.). Water Science and Application 7, AGU; 209-225.

Guillén, J., Palanques, A., 1992. Sediment dynamics and hydrodynamics in the lower course of a river highly regulated by dams: the Ebro River. *Sedimentology* **39**: 567-579.

Habersack, H.M., Laronne, J.B., 2001. Bed load texture in an alpine gravel bed river. *Water Resources Research* **37**(12): 3359-3370.

Habersack, H.M., Laronne, J.B., 2002. Evaluation and Improvement of bed load discharge formulas based on Helley-Smith sampling in an Alpine gravel bed river. *Journal of Hydraulic Engineering* **128**(5): 484-499.

Hamamori, A., 1962. A theoretical investigation on the fluctuations of bedload transport, *Rep. R4*, 14 p., Delft Hydraul. Lab., Delft, Netherlands.

Howard, A., Dolan, R., 1981. Geomorphology of the Colorado River in Grand Canyon. *Journal of Geology* **89**: 269-297.

Hubbell, D.W., 1987. Bed load sampling and analysis. In *Sediment transport in gravel-bed rivers*, Thorne C. R., Barthurst J.C., Hey R.D. (eds.). Chichester: John Wiley and Sons; 89-118.

Inbar, M., 1990. Effect of dams on montainous bedrock rivers. *Physical Geography* **11**(4): 305-319.

Inbar, M., 1992. Rates of fluvial erosion in basins with a Mediterranean type climate. *Catena* **19**: 393-409.

Inman D.L., 1976. *Man's impact on the California coastal zone*. Summary Report to California Department of Navigation and Ocean Development: Sacramento.

Jones, M.L., Seitz, M.R., 1980. *Sediment transport in the Snake and Clearwater Rivers in the vicinity of Lewiston, Idaho*. United States Geological Survey Open-File Report 80-690.

Kondolf, G.M., Matthews, W.V.G., 1993. *Management of coarse sediment in regulated rivers of California*. University of California Water Resources Center: Davis, California.

Kondolf, G.M., Wolman, M.G., 1993. The sizes of salmonid spawning gravels. *Water Resources Research* **29**: 2275-2285.

Kondolf, G.M., 1997. Hungry Water: Effects of Dams and Gravel Mining on River Channels. *Environmental Management* **21**(4): 533-551.

Leopold, L.P., Wolman, M.G., Miller, J.P., 1964. *Fluvial processes in geomorphology*. WH Freeman: San Francisco; 522pp.

Ligon, F., Dietrich, W.E., Trush, W.J., 1995. Downstream ecological effects of dams: a geomorphic perspective. *BioScience* **45**(3): 183-192.

Lvovich, M.I., Karasik, G.Y., Bratseva, N.L., Medvedeva, G.P., Maleshko, A.V., 1991. *Contemporary Intensity of the World Land Intracontinental Erosion*. USSR Academy of Sciencies, Moscow, Rusia.

McLean, D.G., Church, M., Tassone, B., 1999. Sediment transport along lower Fraser River 1. Measurements and hydraulic computations. *Water Resources Research* **35**(8): 2533-2548.

Meade, R.H., Parker, R.S., 1985. *Sediment in rivers of the United States*. U.S. Geological Survey Water-Supply Paper 2275.

Meyer-Peter, E., Favre, H., Einstein, H.A., 1934. Neuere versuchsresultate über den geschiebetrieb. *Schweiz Bauzeitung* **103**.

Milliman, J.D., Meade, R.H., 1983. World-wide delivery of river sediment to the oceans. *Journal of Geology* **91**: 1-21.

Nelson, C.H., 1990. Post Messinian deposition rates and estimated river loads in the Ebro sedimentary system. In *Marine Geology of the Ebro Continental Margin,* Nelson C.H., Maldonado A. (eds.). Marine Geology; **95**: 395-418.

Nordin, C.F., Richardson, E.V., 1971. Instrumentation and measuring techniques. In *River Mechanics*, Shen H. W. (ed.). Colorado State University, Fort Collins.

Novoa, M., 1984. Precipitaciones y avenidas extraordinarias en Catalunya. *Proceedings of the Jornadas de Trabajo sobre Inestabilidad de laderas en el Pirineo*: Barcelona; 1-15.

Palau, A., Batalla, R.J., Rosico, E., Meseguer, A., Vericat, D., 2004. Management of water level and design of flushing floods for environmental river maintenance downstream of the Riba-Roja Reservoir (Lower Ebro River, NE Spain). *Proceedings of the International Conference HYDRO 2004: A New Era for Hydropower*. Porto, Portugal, 18-21 October 2004.

Petts, G.E., 1984. *Impounded Rivers. Perspectives for Ecological Management*. Wiley, New York; 326 p.

Poff, N.L., Allan, J.D., Bain, M.B., Karr, J.R., Prestegaard, K.L., Richter, B.D., Sparks, R.E., Stromberg, J.C., 1997. The natural flow regime: a paradigm for river conservation and restoration. *Bioscience* **47**(11): 769-784.

Powell, D.M., Reid, I., Laronne, J.B., 2001. Evolution of bed load grain size distribution with increasing flow strength and the effect of flow duration on the caliber of bed load sediment yield in ephemeral gravel bed rivers. *Water Resources Research* **37**(5): 1463-1474.

Rinaldi, M., Simon, A., 1998. Bed-level adjustments in the Arno River, Central Italy. *Geomorphology* **22**: 57-71.

Sanz, M.E., Avendaño, C., Cobo, R., 1999. Influencia de los embalses en el transporte de sedimentos hasta el río Ebro (España). *Proceedings of the Congress on Hydrological and geochemical processes in large-scale river basins*. HIBAM: Shahin.

Shaw, E.M., 1983. *Hydrology in Practice*, Van Nostrand Reinhold: London; 539pp.

Shields, A., 1936. Anwendung der Ahnlichkeitsmechanik und der Turbulenzforschung auf die Geschiebebewegung. Mitt. Preussichen Versuchsanstalt für Wasserbau und Schiffbau, Berlin.

Shields, F.D., Simon, A., Steffen L.J., 2000. Reservoir effects on downstream river channel migration. *Enviromental Conservation* **27**(1): 54-66.

Topping, D.J., Rubin, D.M., Vierra, L.E., 2000. Colorado River sediment transport 1. Natural sediment supply limitation and the influence of Glen Canyon Dam. *Water Resources Research* **36**(2): 515-542.

United States Fish and Wildlife Service and Hooja Valley Tribe, 1999. *Trinity River Flow Evaluation, Final Report*. June 1999, 307 pp.

Vericat, D., Batalla, R.J., 2004. Efectos de las presas en la dinámica fluvial del curso bajo del río Ebro. *Cuaternario y Gemorfología* **18**(1-2): 37-50.

Vericat, D., Batalla, R.J., 2005a. Sediment transport in a highly regulated fluvial system during two consecutive floods (Lower Ebro River, NE Spain). *Earth Surface Processes and Landforms* (in press).

Vericat D., Batalla, R.J., 2005b. Bedload variability under low sediment transport conditions in the lower Ebro River (NE Spain). In *River/Catchment Dynamics: Natural Processes and Human Impacts*, Batalla, R.J. and Garcia, C. (eds.). IAHS Red Book (in press).

Walling D.A., Webb, B.W., 1983. Patterns of sediment yield. In: *Background to Paleohydrology,* K.J. Gregory (ed.). John Wiley and Sons: Chichester; 69-100.

Walling, D.E., 1984. Dissolved loads and their measurements. In *Erosion and sediment yield: Some methods of measurements and modeling*. Hadley R.F., Walling D.E (eds.). Geo Books: London; 111-177.

Walling D.A., Webb, B.W., 1996. Erosion and sediment yield: a global overview. *Proceedings of the IAHS Symposium on Erosion and sediment yield: Global and regional perspectives*. Exeter, IAHS Red Book 236; 3-19.

Ward, J.V., Stanford, J.A., 1979. *The Ecology of Regulated Streams*. Plenum Press, New York.

Ward, J.V., Stanford, J.A., 1995. Ecological connectivity in alluvial river ecosystems and its disruption by flow regulation. *Regulated Rivers: Research and Management* **11**: 105-119.

Wilcock, P.R., 1993. Critical shear stress on natural sediments. *Journal of Hydraulic Engineering* **119**: 491-505.

Wilcock, P.R., Kondolf, G.M., Matthews, W.V., Barta, A.F., 1996. Specification of sediment maintenance flows for a large gravel-bed river. *Water Resources Research* **32**: 2911-2921.

Williams, G.P., Wolman, M.G., 1984. *Downstream Effects of Dams on Alluvial Rivers*. US Geological Survey Professional Paper 128

CHAPTER 4
FLUVIAL ADJUSTMENTS

INDEX CHAPTER 4: FLUVIAL ADJUSTMENTS

Figure captions in the papers

Vericat, D., Batalla, R.J., Garcia, C. (2005): Grain-size distribution in a highly regulated large river: the Lower Ebro. 1. Temporal and spatial variation after large floods (to be submitted to an international journal)

Figure 1 (**C**hapter **4** **P**aper **1**). Location and main characteristics of the study reach in the lower Ebro Basin (NE Iberian Peninsula)

Figure 2 (C4P1). Mean daily discharges at the Móra d'Ebre bedload sampling section (Figure 1) during the hydrological year 2002-2003

Figure 3 (C4P1). (**a**) Surface and subsurface bed-material distributions of sections n.6 (highest armouring) and (**b**) n.3 (lowest armouring) observed in summer 2002 (Table 1 (C4P1))

Figure 4 (C4P1). Surface and subsurface grain-size distributions in the Móra d'Ebre monitoring reach in summer 2002 in relation to the envelope of bedload grain-size distributions estimated for each flood

Figure 5 (C4P1). Grain-size distribution of the four first bedload samples obtained during December 2002 in comparison with river-bed grain-size distributions. Sampling interval was 30 minutes and sampling time 3 minutes. Onset of bedload occurred 6 hours after entrainment threshold was reached. Bedload grain-size distribution was highly variable and showed an erratic behaviour in relation to bed-material fractions, even under almost constant discharge (in this case 1,500 m^3/s)

Figure 6 (C4P1). Mobility of river-bed sediment by fractions during winter 2002-03 floods in the lower Ebro River: (**a**) Proportion of bedload size *i* (P_i) in bed-material ($f_{i\text{-}bulk}$), (**b**) Proportion of bedload size *i* (P_i) in bed-material ($f_{i\text{-}bulk}$) during the rising and falling limbs of the December 2002 flood, and (**c**) Bedload transport per fraction *i* in (i_{bi} in g/ms) in relation to its frequency on river-bed sediments ($f_{i\text{-}bulk}$)

Figure 7 (C4P1). Downstream change of armouring (A_r) in the lower Ebro River in 2002 and 2003

Figure 8 (C4P1). Statistical relation between $D_{84\text{-}s}$ and degree of armouring in the lower Ebro River (2002 and 2003)

Figure 9 (C4P1). (**a**) Surface and subsurface bed-material distributions of sections n.1 (highest armouring) and (**b**) n.4 (lowest armouring) observed in summer 2003 (Table 1 (C4P1))

Vericat, D., Garcia, C., Batalla, R.J. (2005): Grain-size distribution in a highly regulated large river: the Lower Ebro. 2. River-bed armouring caused by small frequent floods (to be submitted to an international journal)

Figure 1 (**C**hapter **4** **P**aper **2**). Location of the Ebro River in the Iberian Peninsula and the study reach in the lower Ebro River

Figure 2 (C4P2). (**a**) Mean daily discharges and (**b**) flow frequency curve of the 2003-2004 hydrological year in the Móra d'Ebre sediment transport sampling section (Figure 1 (C4P2))

Figure 3 (C4P2). Surface and subsurface grain-size distributions of study reach in summer 2003 (data from Vericat *et al.*, this issue) in relation to the envelopes of bedload grain-size distributions estimated for each flood

Figure 4 (C4P2). Mobility of riverbed sediment by fractions during 2003-2004 floods in the lower Ebro River: (**a**) Proportion of bedload size *i* (P_i) in bed-material ($f_{i\text{-}bulk}$), and (**b**) Bedload transport per fraction *i* in (i_{bi} in g/ms) in relation to its frequency on river-bed sediments ($f_{i\text{-}bulk}$)

Figure 5 (C4P2). Surface and subsurface bed-material distributions of (**a**) section n.1 (highest armouring ratio) and (**b**) section n.4 (lowest armouring ratio) observed in summer 2004 (Table 1 (C4P2))

Figure 6 (C4P2). (**a**) Downstream change of armouring (A_r) in the lower Ebro River in 2004. Note the stabilization of A_r downstream the confluence with the Siurana River (see text for discussion). (**b**) Changes in proportion of surface sizes classes (f') after 2003-2004

Figure 7 (C4P2). Relation between total stream power (ω) and bedload transport rate for selected floods occurred during 2002-2004

Vericat, D., Batalla, R.J., Martínez, T.I. (2005): River-channel changes downstream large dams: the lower Ebro River. *Zeitschrift für Geomorphologie* (submitted)

Figure 1 (**C**hapter **4** **P**aper **3**). Location of the study reach in the lower Ebro River (NE Iberian Peninsula). For reference, we indicate the Flix Dam, built up in 1948 storing 11 hm^3 of water, and the associated hydroelectric power plant, holding a maximum generating discharge of 400 m^3/s

Figure 2 (C4P3). Disappearance of active areas due to vegetation encroachment and changes in bars configuration immediately downstream the Flix Dam between 1927 and 2002

Figure 3 (C4P3). Evolution of active areas (open bars) in the Flix Meander between 1927 and 2002

Figure 4 (C4P3). Vegetation encroachment in the lowermost reaches of the Flix Meander between 1927 and 2002

Figure 5 (C4P3). Progressive vegetation encroachment, occupation by agricultural fields and stabilization of channel banks in the Flix Meander between 1927 and 2002

Figure 6 (C4P3). Vegetation maps of the Flix Meander in 1927 and 2002

Figure 7 (C4P3). Riparian vegetation stabilising the channel edge in the Flix Meander, with *Tamaricetum canariensis* and *Rubio-Populetum albae* as the most common communities

Figure 8 (C4P3). Air photo and representative river cross section 1 km downstream from the Flix Dam. For reference, we indicate cross profiles of 2002, 2003 and 2004, water level at the peak discharge of the December 2002 flushing flow (Table 3 (C4P3)), and vegetation cover (symbols are not scaled)

Figure 9 (C4P3). Riverbed grain-size distribution 1 km downstream the Flix Dam

Table captions in the papers

Vericat, D., Batalla, R.J., Garcia, C. (2005): Grain-size distribution in a highly regulated large river: the Lower Ebro. 1. Temporal and spatial variation after large floods (to be submitted to an international journal)

Table 1 (C4P1). Bed-material characteristics, including armouring ratio in sampled sections of the lower Ebro River downstream from the Flix Dam in summer 2002 and summer 2003

Table 2 (C4P1). Flow and bedload main parameters measured at the Móra d'Ebre bedload sampling section during floods occurring in winter 2002-2003

Vericat, D., Garcia, C., Batalla, R.J. (2005): Grain-size distribution in a highly regulated large river: the Lower Ebro. 2. River-bed armouring caused by small frequent floods (to be submitted to an international journal)

Table 1 (C4P2). Bed-material characteristics, including armouring ratio, in the control sections of the lower Ebro River downstream from the Flix Dam (Figure 1 (C4P2)) in summer 2004

Vericat, D., Batalla, R.J., Martínez, T.I. (2005): River-channel changes downstream large dams: the lower Ebro River. *Zeitschrift für Geomorphologie* (submitted)

Table 1 (C4P3). Series of air photos used to characterise riverchannel changes and vegetation encroachment in the Flix Meander.

Table 2 (C4P3). Ground control points used to do geometric corrections of old series of air photos and to give them real coordinates.

Table 3 (C4P3). River hydraulics in a control section 1 km downstream the Flix Dam during the December 2002 experimental flood release (Figure 8).

1. INTRODUCTION

This chapter examines the fluvial adjustments of the Ebro River downstream from the Flix Dam. They are interpreted as the consequence of the drastic reduction of sediment supply and the frequent occurrence of competent flows. To illustrate this analysis we present three papers. Papers are presented maintaining their original format.

Small-scale adjustments are analysed from the grain-size distribution of river-bed sediments in two papers to be submitted to an international paper. In the papers we present the characteristics and the evolution of river-bed materials between Flix Dam and the monitoring section of Móra d'Ebre, a 27-km long river reach, during the study period 2002-2004. Changes in grain-sizes are related to flow competence during several flood events. The first paper reports on how high competent flows (2002-2003) were able to entrain most coarse surface material (armour layer), in turn increasing the availability of sediment to be transported (subsurface material). Incision of the riverbed was remarkable during those events. In contrast, second paper reports on how discharges were competent to move the surface material only partially during the year 2003-2004; the stream power was not high enough to move the coarser clasts. As a consequence, the surface river-bed material got progressively coarser and a re-armouring process occurred. In addition, both papers reports on spatial characteristics (i.e. downstream changes) of riverbed materials and on the particular evolution of grain-sizes in the control sections during the observed incision-armouring cycle.

Finally, large-scale adjustments have been analysed in a 5-km river reach below the Flix Dam. For this purpose we present the paper submitted to the journal *Zeitschrift für Geomophologie*. The evolution of the formerly active bars in the Flix Meander has been characterised by means of air photos analysis and fieldwork. Changes in river-channel form are related to the lack of sediment transport and the reduction of floods. Lost of sedimentary active areas, encroachment of vegetation and associated channel narrowing are seen as the main effects of the dams on river's morphology.

2. RIVER-BED MATERIAL

Vericat, D., Batalla, R.J., Garcia, C. (2005): Grain-size distribution in a highly regulated large river: the Lower Ebro. 1. Temporal and spatial variation after large floods (to be submitted to an international journal)

Grain-size distribution in a highly regulated large river: the Lower Ebro. 1. Temporal and spatial variation after large floods

Abstract

This paper reports variations of grain-size distribution and the armour layer at-a-section and downstream in relation to bedload after a series of floods in the strongly regulated lower Ebro River. Fieldwork was performed between summer 2002 and summer 2003, a wet hydrological year. River-bed grain-size distributions observed before floods indicated that surface material was coarser (mean $D_{50\text{-}s}$= 37 mm) and better sorted than subsurface sediments (mean $D_{50\text{-}ss}$= 16 mm). Mean armouring ratio was 2.3, although notable differences from section to section (1.0 to 4.4) were observed. The armour layer formed during the two previous years with relatively low flows. The December 2002 flood caused its initial breaking and the subsequent release of subsurface sediment that constituted the bulk of bedload during successive floods. Several hydraulic and geomorphological factors suggest the breaking of the armour, a) the extraordinary delay of bedload onset during first winter flood, b) the distinct mobility of the different bed-material fractions during successive floods, and c) the reduction of the armouring observed in summer 2003 in most of the investigated sections. The general net scour in the study reach points in the same direction. In addition, during the succession of floods, bedload grain-size distribution became progressively closer to subsurface grain-size distribution, a fact that indicates that the armour was removed. River-bed armouring in summer 2003 diminished to 2.0 and its reduction was more pronounced in sections with previously coarser surface sediments. Downstream sections were more prone to changes in armouring than those upstream (i.e., closer to dams), where river-bed structure and grain-size distribution proved to be more stable. Variation of river-bed and bedload grain-size distributions of the lower Ebro River has shown that a) armouring is an important active process in largely regulated fluvial systems, and that it is associated with disequilibrium between sediment transport (flow competence) and sediment supply, and b) armour stability is mainly controlled by flood magnitude.

Key words: dams, bedload transport, river-bed material, armouring

1. Introduction

Dams interrupt the continuity of sediment transfer and alter the downstream flow regime of rivers. On one hand, dams trap all coarse sediment (i.e., bedload) and important percentages of fine sediment (i.e., suspended load) that is being transported from upstream reaches (e.g., Meade and Parker, 1985; Topping *et al.,* 2000). On the other, dams tend to reduce flood frequency and magnitude (e.g., Kondolf and Matthews, 1993; Sear, 1995). These two main alterations cause several impacts in the downstream reaches, whose magnitude is directly related to dam size (i.e., impoundment ratio, Batalla *et al.,* 2004), fluvial regime, channel form and process, and the purpose and operation of the reservoir (Petts, 1984; Williams and Wolman, 1984; Friedman *et al.,* 1998; Brandt, 2000; Phillips, 2001 and 2003; Graf 2001).

Below dams floods may not be sufficiently competent to entrain and transport the incoming sediment from tributaries and the river-bed begins to aggrade (Howard and Dolan, 1981; Church, 1995; Topping *et al.,* 2000). In addition, deposition of fine material changes river-bed grain-size distribution and causes important ecological alterations, for instance on fish habitat (e.g., Suttle *et al.,* 2004). In contrast, when flows released from dams have greater transport capacity than the amount of sediment supplied and have sufficient competence to move most sediment fractions of the downstream river-bed, the main effect is channel degradation (Gomez, 1983; Kondolf, 1997; Surian and Rinaldi, 2003). For instance, Williams and Wolman (1984) reported channel incision of up to 6 meters downstream from the Davis Dam, in the Colorado River, Arizona. Finally, if mean bed shear stress is less than the critical stress needed to entrain the largest particles of the bed surface but sufficient to move the finer material, the surface becomes coarser and, consequently, an *armour layer* begins to develop (Parker and Klingeman, 1982; Parker and Sutherland, 1990; Gomez, 1994). In the Colorado River below the Glen Canyon Dam, Arizona, decreases in the supply of sediment have been interpreted as the main cause for the coarsening of the river-bed (Colby, 1964; Burkham, 1986; Topping *et al.,* 2000). In reaches where the sediment supply is weak, the degree of armouring relates directly to sediment availability and, as a consequence, determine the bedload transport rates. Thus, the degree of armouring of a river-bed influences bedload grain-size distribution and transport rates (i.e., reduction of sizes and amount of sediment transported, Parker and

Sutherland, 1990; Knighton, 1998) and, hence, alters the ecological functioning of the river (i.e., loss of spawning gravels, Kondolf and Wolman, 1993).

Different authors have attempted to identify the most relevant conditions for the development of an armoured surface, such as the sediment mixture that was originally exposed to the flow and the flow conditions (Gessler, 1965; Little and Mayer, 1976). In general, armouring has been explained as the consequence of: a) winnowing, both vertical and downstream (Gessler, 1971; Sutherland, 1987), b) equal mobility (Parker and Klingeman, 1982; Andrews and Parker 1987), and c) traction clogging (Moss, 1963; Dunkerley, 1990). In particular, the downstream winnowing hypothesis has been described as a short-term response to reduction of sediment supply (Andrews and Parker, 1987; Dietrich *et al.,* 1989), a phenomenon that is especially active below dams (e.g., Davies *et al.,* 1990). Armoured surfaces are coarser and better sorted than subsurface material and their stability is basically controlled by flow magnitude. They are stable in all flows of a lesser magnitude than the formative flow, and may only be disturbed by higher floods (Gomez, 1983). In some cases development of an armour layer can limit bed degradation below dams. For instance, river-bed degradation in the Nile River downstream from Aswan Dam, Egypt, ceased when 2 mm particles were concentrated into a 40 mm thick surface layer by about 1 meter of scour (Hammad, 1972). In the Hanjiang River below Danjiangkou Dam, China, the coarsening of river-bed material also increased the erosional resistence of the bed (Xu, 1996), a factor that enlarged bank erosion and widening channel (Xu, 1997). Within this context, two degrees of armouring can be differentiated: *stable* and *mobile armour*. Stable armour is formed when river-bed material is subjected to flows with insufficient magnitude to move the coarsest particles of the bed material combined with a clear limitation on the supply of sediment from upstream reaches (Sutherland, 1987; Gomez, 1995). The formation of a mobile armour is associated with small and persistent bedload transport. Grain-size distributions of bedload and subsurface are identical and as bedload transport decreases the bed surface progressively coarsens (Parker and Klingeman 1982, Andrews and Parker 1987). A limiting state of this development has been defined by the formation of a stable armour (Dietrich *et al.* 1989; Parker and Sutherland 1990, Lisle *et al.* 1993, Gomez 1995).

In this paper the term *armour layer* is applied to the semi-permanent bed surface that is developed in river-channels below dams as a consequence of hydrological and, especially, profound geomorphological alterations. The lower Ebro River downstream from the reservoir complex of Mequinenza-Riba-roja-Flix, the largest in the catchment and one of the largest in the Iberian Peninsula, has experienced important hydrological, morphological, and ecological alterations. Alterations include, a) reduction of flood magnitude (Batalla *et al.,* 2004), b) sediment deficit, bank erosion and river-bed degradation (Vericat and Batalla, 2004, 2005a) and, c) proliferation of aquatic vegetation (Palau *et al.,* 2004). Sediment supply below the lowermost dam is almost nonexistent because the main tributary, the Siurana River, is also largely regulated. Within this context, the channel and river-bed of the lower Ebro River provide a natural flume to assess adjustments of river morphology and sediment transport due to dams in large regulated fluvial systems. In particular, this paper reports on the variations of the river-bed grain-size distribution and the armour layer at-a-section and downstream, in relation to bedload, after a series of floods during a wet hydrological year. The authors are not aware of any previous attempt to systematically measure bed-material grain-size distributions below dams to compare them with bedload grain-size distribution as a way to understand the effects of reservoirs on the river-bed of large fluvial systems such as the lower Ebro River.

2. Study area

2.1. The Ebro basin

The Ebro River drains an area of 85,530 km^2 in the north-east part of the Iberian Peninsula (Figure 1 (C4P1)). Annual precipitation varies greatly across the area, with values above 2,000 mm in the Pyrenean Range and below 300 mm in the semiarid Ebro Depression. Mean annual water yield measured in Tortosa, the lowermost gauging station of the river, is 14,300 hm^3, which equals to a mean discharge around 450 m^3/s. Maximum discharge estimated in the Ebro River was around 12,000 m^3/s in Tortosa in 1907 (Novoa, 1984). A total of 187 reservoirs impound almost 60% of the catchment's annual runoff. Most dams, impounding 5,200 hm^3, were constructed between 1950 and 1975 (Batalla *et al.,* 2004). The maximum discharges recorded at Tortosa in the post-dams period has been 3,300 m^3/s

in 1982, much lower than that estimated for 1907. Mean annual sedimentation in reservoirs all over the basin is estimated at around 15 hm^3 (0.2% of total reservoir capacity in the catchment) (Sanz *et al.,* 1999; Batalla, 2003).

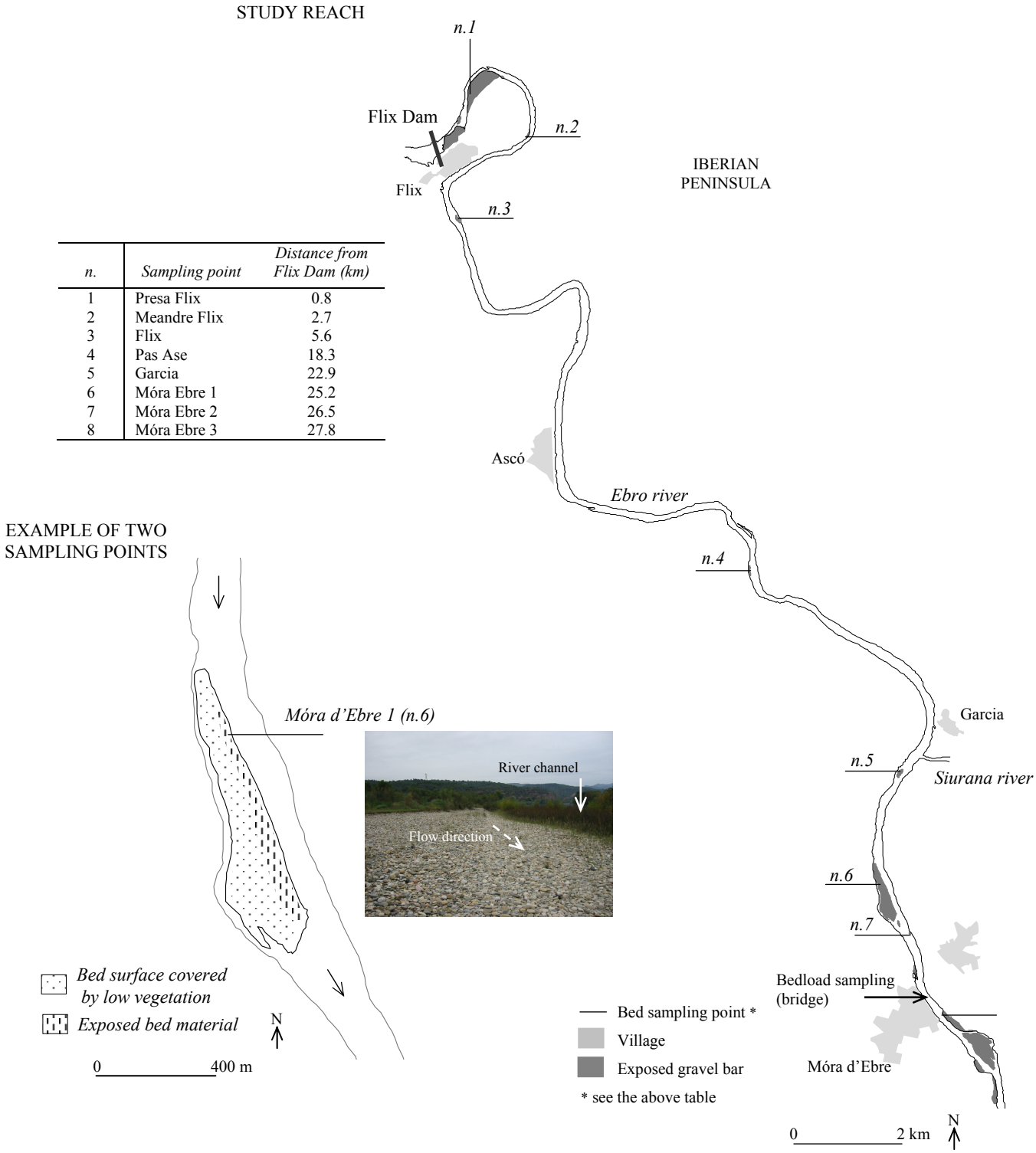

n.	*Sampling point*	*Distance from Flix Dam (km)*
1	Presa Flix	0.8
2	Meandre Flix	2.7
3	Flix	5.6
4	Pas Ase	18.3
5	Garcia	22.9
6	Móra Ebre 1	25.2
7	Móra Ebre 2	26.5
8	Móra Ebre 3	27.8

Figure 1 (C4P1). Location and main characteristics of the study reach in the lower Ebro Basin (NE Iberian Peninsula)

2.2. The lower Ebro River

We have selected as the study reach the lower Ebro River between the villages of Flix and Móra d'Ebre, a 27 km-long channel below the dams of Mequinenza (capacity of 1,534 hm^3, in operation since 1966), Riba-roja (207 hm^3, 1969) and Flix (11 hm^3, 1948), the lowermost impoundment constructions in the river mainstem (Figure 1 (C4P1)). Downstream from the Flix Dam the river flows as a single-thread meandering channel through the Ebro Depression. Further downstream the channel is constrained by bedrock outcrops when it crosses the Coastal Range at the Pas Ase section. The most important downstream tributary is the Siurana River, which debouches into the Ebro near the village of Garcia (Figure 1 (C4P1)). It is also heavily regulated and suffers from intensive gravel mining since the 1980s. In the lower Ebro, the magnitude of relatively frequent floods (Q_2-Q_{25}) has been reduced by 25% on average (Batalla *et al.*, 2004). Although the reduction is remarkable, the river still retains the capacity to transport sediment (Vericat and Batalla, 2004). Dams trap most fine sediment (90%) and all bedload that is being transported from upstream reaches (Vericat and Batalla, 2005b). Annual sediment contribution of the Ebro to its delta at the beginning of the 20th century was around $15 \cdot 10^6$ tons (e.g., Nelson, 1990), most of it transported in suspension. Vericat and Batalla (2005b) calculated from field measurements that the current mean annual sediment load of the river is $0.4 \cdot 10^6$ tonnes (half transported in suspension and half as bedload). Hence, a substantial change on sediment supply occurs in the lower Ebro River, a phenomenon that causes progressive changes in river-channel morphology and ecology (e.g., Sanz *et al.,* 1999; Vericat and Batalla, 2005b; Palau *et al.,* 2004). The reduction on sediment supply has been also identified as the main reason for the retreat of the Ebro Delta observed since the 1970s.

3. Methods

Members of the University of Lleida have undertaken since summer 2002, a sediment sampling programme in the lower Ebro River. Objectives are to estimate the sediment load upstream and downstream from the reservoir complex and to assess the main morphological effects that the expected change on sediment supply causes in the river-channel. The sampling program includes a) measurements of sediment transport, both in

suspension and bedload, at two upstream and downstream monitoring sections, especially during floods (Vericat and Batalla, 2005a) and b) survey of river morphology at selected representative cross sections and river reaches. Of particular interest for this paper is the study of river particle dynamics, including characterization of river-bed grain-size distribution and mobility.

3.1. River-bed sediment sampling

Bed-material samples were been obtained from almost all low-flow exposed bars located along the river reach between the Flix Dam and the Móra d'Ebre bedload station (Figure 1 (C4P1)). A total of 8 bars along the 27 km-long river reach were surveyed on sedimentologically equivalent positions (prevent e.g., bar fining). Bars are mainly central and have low vegetation cover (Figure 1 (C4P1)). Grain-size sampling was conducted in summer 2002 and summer 2003. In between, four floods occurred with peaks ranging from 1,500 m^3/s to 2,500 m^3/s ($Q_{2.5}$ and Q_8, respectively). The largest flood occurred in February 2003 (Figure 2 (C4P1)) and the last flood sampled before the sampling period occurred in March 2001, with a peak of almost 2,400 m^3/s (Q_7). Also in May 2003 occurred a flood (1,500 m^3/s, $Q_{2.5}$) that could not be sampled.

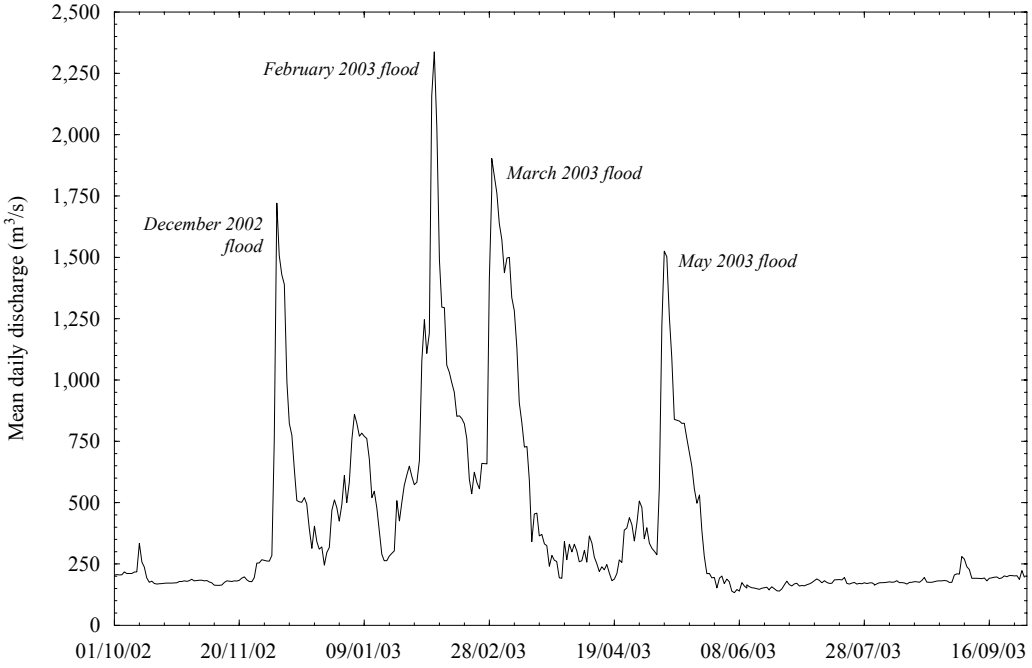

Figure 2 (C4P1). Mean daily discharges at the Móra d'Ebre bedload sampling section (Figure 1 (C4P1)) during the hydrological year 2002-2003

We sampled surface and subsurface material separately except in section n.2 located, 2.7 km below the Flix Dam (Figure 1 (C4P1)), where we took a total bulk sample because no difference was observed between surface and subsurface material.

The surface layer was characterised using the pebble count method (Wolman, 1954; Rice and Church, 1996). This technique allowed us to determine the sieve size range (b-axis) of a minimum of 100 particles by passing them through a template with square holes scaled at ½ phi (ϕ) intervals (e.g., Lisle and Madej, 1992). A total of 3,000 particles were measured in the 2002 and 2003 field campaigns. Simultaneously, the surface layer was also sampled using the area by weight technique (e.g., Lane and Carlson, 1953; Gomez, 1979). This method allows an accurate determination of the percentage of fine material (i.e., finer particles than 8 mm) that is considered to be underestimated by the pebble count method. Surface material was differentiated from the underlying sediment using spray paint (e.g., Lane and Carlson, 1953). Church *et al.* (1987) reported that spray paint does not exactly identify surface particles because paint might run down and infiltrate until the subsurface layer. In order to minimize this source of error, we used fast-dry paint that was sprayed from a sufficient distance to prevent the excess of paint percolating. The sampled area ranged from 1 m^2 to 3 m^2 and was calculated following Fripp and Diplas (1993) formula:

$$S = 400 \times (D_{max\text{-}s})^2$$

where, S is the area (m^2) of the river-bed surface that has to be painted and sampled, and $D_{max\text{-}s}$ is the b-axis (m) of the maximum exposed particle. A total of 21 m^2 (equivalent to 1,200 kg of material) were surveyed during the field campaigns of 2002 and 2003.

Subsurface material was sampled using the volumetric technique after removal of the surface layer. The largest particle in the subsurface layer ($D_{max\text{-}ss}$) did not exceed 1% of the sample weight (Church *et al.*, 1987). This technique was also used to characterise the river-bed grain-size distribution in section n.2. Almost 880 kg of material was sampled and sieved in the 2002 and 2003 field campaigns.

Both area by weight and volumetric samples were sieved at ½ ϕ intervals and weighed directly in the field. Samples containing wet material were taken to the laboratory and

dried prior to sieving and weighing. Area by weight samples were converted to volumetric values (equivalent to pebble count) (Kellerhals and Bray, 1971). A conversion factor of -0.5 was used in order not to generate equivalent particle size distributions whose median grain-size and standard deviation differed significantly from the extremes of the cumulative size-frequency curves (Gomez, 1983; Anastasi, 1984; Diplas and Sutherland, 1988; Diplas, 1989). If the percentage of fine particles (<8 mm) in the area by weight samples was higher than 5%, we generated combined surface grain-size distributions (Fripp and Diplas, 1993; Rice and Haschenburger, 2004). Consequently, particles finer than 8 mm were not so underrepresented as could have happened if only the pebble count distribution was used.

3.2. Bedload sampling

Bedload transport was sampled during floods at the Móra d'Ebre monitoring section (Vericat and Batalla, 2005a, 2005b), just few hundred meters upstream section n.8 (Figure 1 (C4P1)). Samples were taken by means of a 76-kg cable suspended Helley-Smith sampler with a 152-mm intake operated from a bridge by an automatic crane. Sampling time did not exceed 5 minutes, therefore preventing the sampler bag being filled to more than 50% of its capacity to ensure maximum sampling efficiency (Emmett, 1980; Habersack and Laronne, 2001). Sampling interval was thirty minutes and sample weight ranged from a few hundred grams to almost 13 kg. Samples were collected and brought to the laboratory, where they were dried, sieved, and weighted to obtain the corresponding grain-size distribution.

4. Results and remarks

4.1. River-bed grain-size distribution in summer 2002

4.1.1. Surface material

Median surface grain-size ($D_{50\text{-}s}$) for all sampled sections ranged from 9 mm to 71 mm (Table 1 (C4P1)). Mean $D_{50\text{-}s}$ was 37 mm with an error around the mean ($\varepsilon = \sigma/\sqrt{N}$, where

σ is the standard deviation and N the number of data) of ±8 mm. Maximum and minimum median size were observed in sections n.1 and n.4, respectively (Figure 1 (C4P1)). Surface material is coarser than the subsurface material in all sampling sections, except for section n.2, where no clear difference was observed. Section n.4 showed similar behaviour. Material finer than 8 mm was not prominent (i.e., <5%) in the river-bed, except for bar n.4 (Table 1 (C4P1)). Maximum surface material size ($D_{max\text{-}s}$) ranged from 195 mm to 45 mm, the mean being 137 mm ±19 mm (ε). Largest $D_{max\text{-}s}$ were measured in the uppermost and in the lowermost control bars (n.1 and n.8), where it attained 195 mm and 181 mm, respectively (Table 1 (C4P1)). Surface bed-material sorting ($\sigma_{F\&W}$), estimated from the Folk and Ward (1957) index, varied between 0.7 and 2.1, indicating moderately well sorted to very poorly sorted distributions, respectively (Table 1 (C4P1)). Mean sorting coefficient was 1.2 (i.e., poorly sorted). Sorting coefficient is higher than 2 in section n.4, the bar where surface material finer than 8 mm was significant (i.e., >5% of the area by weight sample). Poor sorting in section n.4 reflects the skewness towards fine material, and is associated with the bimodality (Wilcock, 1993) exhibited by the surface sediments at those locations (Table 1 (C4P1)). No statistically significant relation was found between surface median particle size and sorting, a fact that reflects the high variability of grain-size distributions along the study reach and the inability of $D_{50\text{-}s}$ to express sorting of grain-size distributions.

4.1.2. Subsurface material

Median subsurface grain-size ($D_{50\text{-}ss}$) varied from 8 mm to 25 mm. Mean $D_{50\text{-}ss}$ was 16 mm, with an error around the mean (ε) of ±2 mm, four times less than the error estimated for the surface material. This fact shows the smaller deviation of median subsurface material between bars in comparison to surface sediments. Maximum median size was sampled in section n.1 and minimum in section n.4, the same pattern observed for the surface material (Table 1 (C4P1)). Subsurface material showed poorer sorting than surface sediments, ranging from 2.8 to 0.9 (i.e., very poorly to moderate distributions, respectively). Mean subsurface sorting was 1.9 (Table 1 (C4P1)). Subsurface distributions are, in general, more skewed towards fine fractions than surface material. Values of bimodality higher than 2.3 were obtained for distributions with sorting coefficient higher than 2 (n.1, n.5 and n.6), all of them showing two well defined modes, one at coarse sand

and another at medium to coarse gravel. Better sorted distributions (n.3, n.4, n.7, and n.8) do not present bimodality (Table 1 (C4P1)). As in the surface material, no statistically significant relation was found between subsurface median particle size and sorting.

4.1.3. River-bed armouring

When gravel mixtures are subjected to competent discharges in the absence of sediment supply from upstream, the surface becomes progressively coarser than the subsurface. This hypothesis can be verified by estimating the bed armouring ratio (A_r), calculated as the ratio between median bed surface material ($D_{50\text{-}s}$) and median subsurface ($D_{50\text{-}ss}$) (e.g., Lisle and Madej, 1992). The armouring ratio approaches 1 in rivers with high sediment supply, whereas in a river in which transport capacity exceeds sediment supply, the ratio approaches 2 (e.g., Bunte and Abt, 2001).

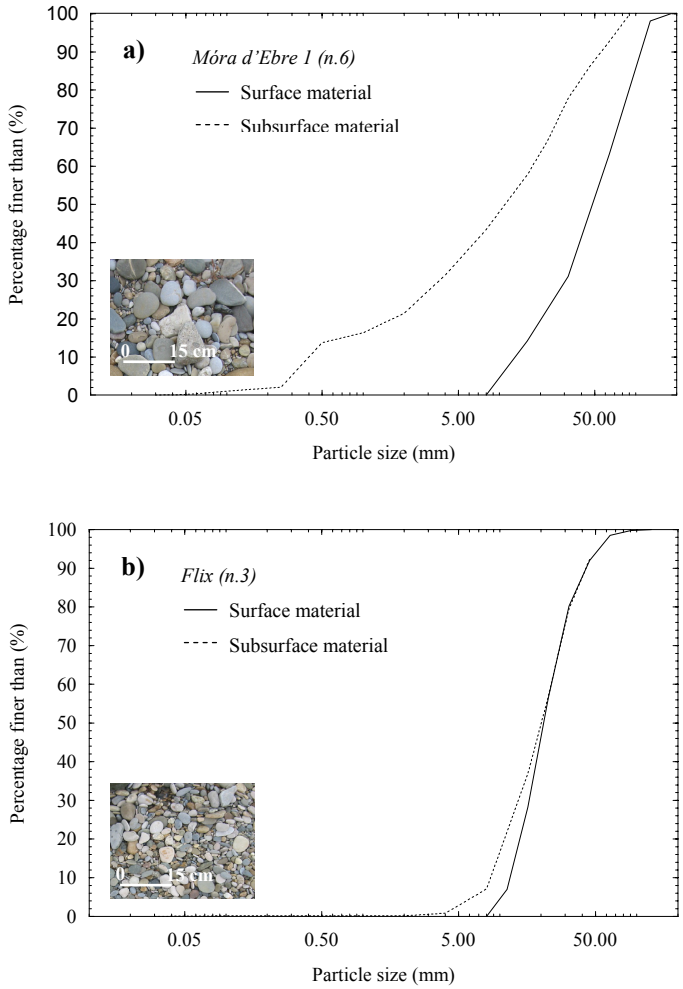

Figure 3 (C4P1). (**a**) Surface and subsurface bed-material distributions of sections n.6 (highest armouring) and (**b**) n.3 (lowest armouring) observed in summer 2002 (Table 1 (C4P1))

Table 1 (C4P1). Bed-material characteristics, including armouring ratio in sampled sections of the lower Ebro River downstream from

	2002									2003								
	Surface material					Subsurface material				Surface material					Subsurface material			
Sampling section[1]	$D_{50\text{-}s}$[3] (mm)	$D_{max\text{-}s}$[5] (mm)	$\sigma_{F\&W}$[6]	**B**[7]	**Fm**[8] (%)	$D_{50\text{-}ss}$[10] (mm)	$\sigma_{F\&W}$[6]	**B**[7]	A_r[11]	$D_{50\text{-}s}$[3] (mm)	$D_{max\text{-}s}$[5] (mm)	$\sigma_{F\&W}$[6]	**B**[7]	**Fm**[8] (%)	$D_{50\text{-}ss}$[10] (mm)	$\sigma_{F\&W}$[6]	**B**[7]	A_r[11]
Presa Flix (n.1)	70.5 [4]	195 [4]	0.7 [4]	- [4]	2	24.5	2.8	7.8	2.9 [4]	67.9 [4]	150 [4]	0.9 [4]	-	2	22.7	2.5	6.7	3.0 [4]
Meandre Flix (n.2)					-	12.9	1.3	-					-	-	12.5	2.2	3.6	
Flix (n.3)	20.9	150	0.7	-	<1	20.1	0.9	-	1.0	21.7	100	0.7	-	3	16.1	1.0	-	1.3
Pas Ase (n.4)	8.7	45	2.1	1.6	22 [9]	7.5	2.0	-	1.2	8.4	64	1.7	-	30 [9]	8.3	2.1	-	1.0
Garcia (n.5)	41.9	128	1.8	1.4	3	15.3	2.4	2.7	2.7	36.0	150	0.7	-	2	14.8	2.2	3.4	2.4
Móra d'Ebre 1 (n.6)	48.1	150	1.2	-	<5	11.0	2.6	2.3	4.4	35.1	123	2.8	-	9 [9]	14.5	2.5	6.2	2.4
Móra d'Ebre 2 (n.7)	19.7	111	0.7	-	3	14.2	1.0	-	1.4	34.9	155	1.7	-	9 [9]	16.3	2.5	4.4	2.1
Móra d'Ebre 3 (n.8)	49.6	181	1.0	1.2	<1	19.2	1.9	1.4	2.6	33.4	112	2.1	-	7 [9]	20.7	1.9	-	1.6
mean[2]	37	137	1.2			16	1.9		2.3	34	122	1.5			16	2.1		2.0
standard deviation	±22	±50	±0.6			±6	±0.7		±1.2	±18	±33	±0.8			±5	±0.5		±0.7

[1] Location of sections is presented in figure 1 (C4P1)
[2] Arithmetic mean
[3] Median surface material size (mm)
[4] Bed-material was sampled both surface and subsurface as a unique sample. Values are presented in the 'Subsurface' column according to the method used to sampling but have not included for the mean and standard deviation computations
[5] Maximum surface material size (mm)
[6] Folk and Ward's (1957) sorting index. For the subsurface material, sorting index in n.2 has not included for the computation
[7] Wilcock's (1993) bimodality index. B=1.7 corresponds to the bimodality threshold. Hyphen indicates than the distribution has only one mode
[8] Percentage of material finer than 8 mm in the surface distributions
[9] Bed surface grain-size distribution were done combining area by weight and pebble count samples
[10] Median subsurface material size (mm). Median size in n.2 has not been included in the computation
[11] Armouring ratio estimated as the ratio between median surface and subsurface material ($D_{50\text{-}s}/D_{50\text{-}ss}$) (e.g. $A_r > 2$ means that the river's transport capacity exceeds the sediment supply)

Mean armouring ratio for all sampled bars in the lower Ebro River is 2.3, with an estimated error around the mean (ε) of ±0.5 (Table 1 (C4P1)). Maximum armouring was obtained in section n.6 (A_r = 4.4, i.e., the median surface size is more than 4 times the median subsurface) (Figure 3a (C4P1)). In that bar, the percentage of surface fine material (<8 mm) is less than 5%, while 50% of the subsurface distribution is finer than 8 mm. No physical explanation has been found for the high degree of armouring observed in that section in 2002. Apart from section n.6, three other bars showed ratios higher than 2 (sections n.1, n.5, and n.8), an expression of both limitation of sediment supply from upstream reaches and occurrence of competent floods. Bar n.1 is located just a few hundred meters downstream from the Flix Dam and showed the coarsest bed-material, both surface and subsurface, in all the study reach. Bar n.5 is located some hundred meters downstream of the confluence of the Ebro and the Siurana rivers, a river that was an important source of sediment until the middle of the twentieth century, but suffers nowadays a severe sediment deficit due to upstream dams and instream gravel mining. The lowermost section in which armouring exceeded 2 was n.8, located a few meters below from the Móra d'Ebre bedload monitoring section (Figure 1 (C4P1)). We have no explanation for the armouring in that section in terms of sediment supply and influence of tributaries. Armouring ratio not exceeding 2 ranged from 1.0 to 1.5 (Table 1 (C4P1)). The lowest ratios were obtained at bars n.2, n.3 and n.4, between sections n.1 and n.5. There, the armouring ratio did not exceed 1.2 (Table 1 (C4P1), Figure 3b (C4P1)). Downstream reduction of armouring is thus remarkable and noticeable between sections n.1 and n.4. A similar tendency was reported in the lower Deschutes River below the Pelton-Round Butte dam complex, Oregon, where a clear but modest downstream decrease of armouring was assessed (Fassnacht *et al.*, 2003). The coarse surface layer observed in section n.1 was evidently not present anymore in the Meandre Flix section (n.2), where the median material is 5 times smaller, but it was also not observed in sections n.3 and n.4 (Table 1 (C4P1)).

4.2. The 2002-2003 winter floods

Four floods occurred below Flix Dam during winter 2002-2003 (Table 2 (C4P1) and Figure 2 (C4P1)). The first flood occurred in December 2002 and commenced as a flushing flow specifically designed to control the excess of aquatic vegetation in the river-channel

(Palau *et al.*, 2004). The experimental release was overcome after the peak by a four-day larger flood, which was the consequence of an upstream incoming natural flood. The floods of February, March and May 2003 were basically natural floods consequent on runoff contribution from tributaries in the catchment headwaters. Bedload was sampled at the Móra d'Ebre monitoring section (Figure 1 (C4P1)) during December, February, and March floods. A total of 134 samples (equivalent to 415 kg) were collected (Table 2 (C4P1)) (Vericat and Batalla, 2005a). Bedload during the May 2003 flood was not sampled.

Table 2 (C4P1). Flow and bedload main parameters measured at the Móra d'Ebre bedload sampling section during floods occurring in winter 2002-2003

Flood	Peak discharge (m^3/s)	Flood Duration (days)	Bedload Samples (number)	Mean[1] $D_{50\text{-}ib}$ (mm)	$D_{50\text{-}ib}$ standard deviation	Mean[1] $D_{max\text{-}ib}$ (mm)	$D_{max\text{-}ib}$ standard deviation	Mean[1] sorting[2]
December 2002	1,700	8	46	21	22	36	32	0.9
February 2003	2,500	20	59	19	10	53	15	1.0
March 2003	2,000	17	29	17	6	53	15	1.0
May 2003	1,500	11	-	-	-	-	-	-

[1] Arithmetic mean
[2] Folk and Ward's (1957) sorting index ($\sigma_{F\&W}$)

4.2.1. Bedload and bedload grain-size distribution

Flood occurred in December 2002 had a peak flow of 1,700 m^3/s, yielding an estimated peak bed shear stress of 47 N/m^2 (Figure 2 (C4P1)). Mean bedload transport rate (i_b) was 15 g/ms. Median size of bedload samples ($D_{50\text{-}ib}$) ranged from 3 mm to 105 mm. Mean $D_{50\text{-}ib}$ was 21 mm, with a standard deviation of ±22 mm and an estimated error around the mean (ε) of ±3 mm. Mean sorting ($\sigma_{F\&W}$) of the bedload grain-size distribution was 0.9 (i.e., moderately sorted), with a standard deviation (σ) of ±0.3. Maximum sampled particles ($D_{max\text{-}ib}$) ranged from 4 mm to 116 mm, with mean $D_{max\text{-}ib}$ of 36 mm, a standard deviation of ±31 mm, and an estimation error of ±4 mm (Table 2 (C4P1)).

Peak flow of the February 2003 flood was the maximum discharge attained during the 2002-2003 hydrological year (Figure 2 (C4P1)). It reached 2,500 m^3/s (i.e., 63 N/m^2). Mean bedload transport rate was 143 g/ms (Vericat and Batalla, 2005a). Median bedload size ($D_{50\text{-}ib}$) varied from 4 mm to 74 mm, with a mean diameter of 19 mm, a standard deviation of ±10 mm, and an error around the mean of ±1.4 mm. Mean $D_{50\text{-}ib}$ for all

samples was 19 mm, very similar to that obtained during the December 2002 flood; however the range of collected median sizes was smaller. As a consequence, standard deviation was also smaller. Mean sorting of bedload grain-size distributions was 1.0 (i.e., poorly to moderately sorted), with a standard deviation of ±0.2. Grain-size distributions are slightly less well sorted than those obtained during December 2002. Maximum collected particles ($D_{max\text{-}ib}$) ranged from 8 mm to 87 mm, with a mean of 53 mm. Mean $D_{max\text{-}ib}$ during the February 2003 flood was 17 mm coarser than that obtained during the December 2002 flood (Table 2 (C4P1)).

Maximum discharge during the March 2003 flood was 2,000 m^3/s (i.e., 52 N/m^2) (Figure 2 (C4P1)). Mean bedload transport rate was 350 g/ms (Vericat and Batalla, 2005a). The mean bedload rate, compared with that during the February 2003 flood (more hydraulically competent), indicates the higher sediment availability during the March 2003 flood. Median bedload grain-size ($D_{50\text{-}bl}$) ranged from 2 mm to 44 mm. Mean $D_{50\text{-}bl}$ was 17 mm, finer than that obtained during previous floods (Table 2 (C4P1)). Both standard deviation and estimation error of $D_{50\text{-}ib}$ were also smaller than that calculated for the samples of preceding floods. Mean sorting of bedload grain-size distribution was 1.0 with a standard deviation of ±0.2, both very similar values to that estimated for the February 2003 flood. Bedload $D_{max\text{-}ib}$ varied from 31 mm to 90 mm, with the mean at 53 mm (Table 2 (C4P1)).

4.2.2. Bedload and bed-material grain-size distributions

Figure 4 (C4P1) represents the relation between bed grain-size distribution obtained in summer 2002 and the envelopee of the bedload grain-size distributions for the different winter 2002-2003 floods. Bed grain-size distributions, both surface and subsurface, have been calculated from samples obtained at the eight sections (Figure 1 (C4P1)). Rennie *et al.* (2002) reported bedload velocities between 0.03 and 0.11 m/s under bedload rates up to 100 g/ms in the Fraser River, British Columbia. Median bedload grain-sizes and mean river-bed slope in their measurements were close to those reported in this paper for the lower Ebro River. On the assumption of continuous movement, the step distance for the bedload transport during the 2002-2003 floods in the Ebro can be probably related to one order of magnitude higher than the entire river reach below the Flix Dam (i.e., sediment obtained during bedload sampling in Móra d'Ebre was potentially travelling from section

n.1). Bed-material and bedload grain-size distributions were truncated at 1 mm in order to avoid particles that may be transported in suspension.

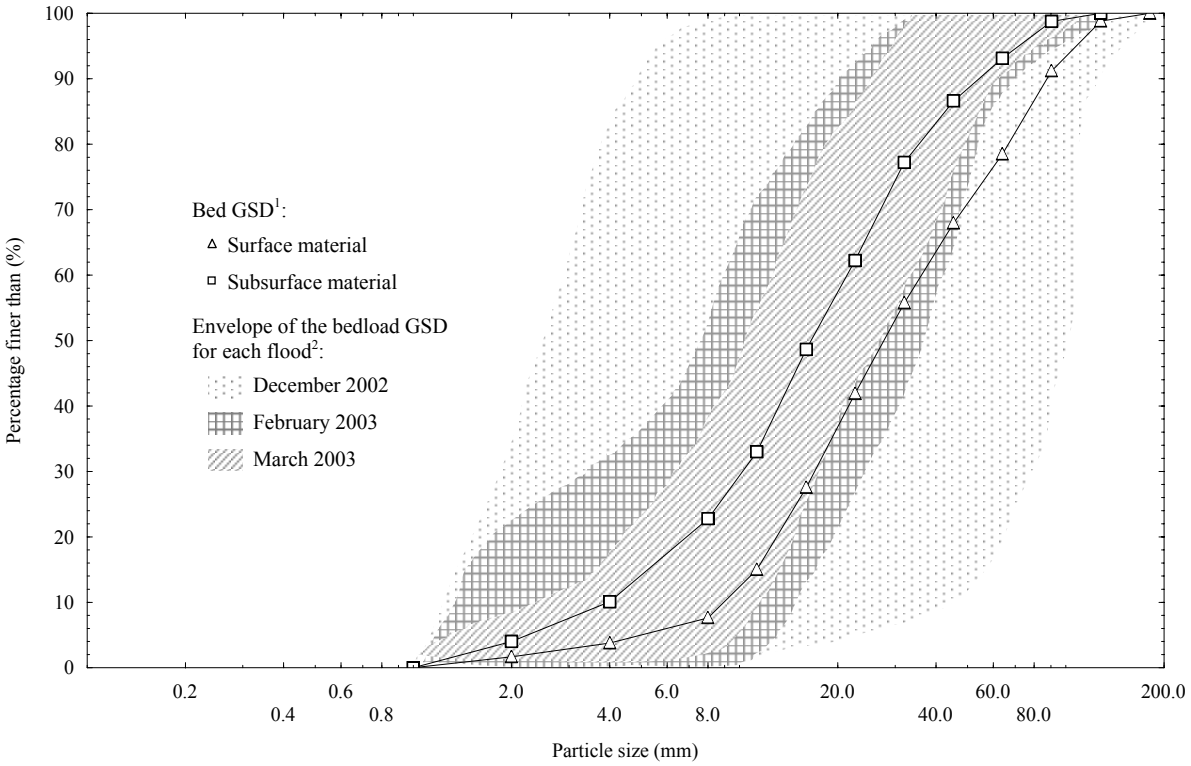

[1] Surface and subsurface bed grain-size distributions calculated as the unweighted sum of the distributions, both surface and subsurface, at the eight sampled sections in summer 2002. See the text for more details
[2] Range of bedload GSD for the samples collected on each flood

Figure 4 (C4P1). Surface and subsurface grain-size distributions in the Móra d'Ebre monitoring reach in summer 2002 in relation to the envelope of bedload grain-size distributions estimated for each flood

During the December 2002 flood mean bedload grain-size ($D_{50\text{-}ib}$=21 mm) was finer than the median size of the surface distribution ($D_{50\text{-}s}$=28 mm), and coarser than the median size of subsurface ($D_{50\text{-}ss}$=17 mm). The envelope of bedload sizes encompasses the river-bed grain-size distributions (surface and subsurface) within its limits. This fact indicates that most river-bed sediment fractions moved during the event. During the first flood the first finite bedload sample was collected under 1,525 m^3/s, while, according to Shields's (1936) equation, the critical discharge for the median surface material is 600 m^3/s (i.e., 25.4 N/m^2). That discharge was reached 6 hours before bed-material was set in motion, period in which no sediment (i.e., bedload) was collected. Delay of bedload was probably related to the strength of the armour (i.e., stable armour) after almost two years with no major

floods and also influenced by the unusual cover of the river-bed by macrophytes (Palau *et al.,* 2004). After the initial movement most of the river-bed surface fractions (coarser) began to move and, probably, subsurface fractions (finer) were mobilised. The combined flux of both types of materials can be pointed out as the main cause for the wide envelope of the bedload grain-size distributions. The high variability of the $D_{50\text{-ib}}$ between consecutive samples is also a consequence of the erratic behaviour of bedload and the combined role of surface and subsurface materials at the beginning of the flood (Figure 5 (C4P1)). The largest particles ($D_{max\text{-ib}}$) measured in the bedload samples also had a high variability as shown by the standard deviation (σ) of ±32 mm (Table 2 (C4P1)). Reduction of the $D_{50\text{-ib}}$ standard deviation in February 2003 (Table 2 (C4P1)) is the consequence of the reduction of the bedload grain-size envelope (Figure 4 (C4P1)). Mean $D_{50\text{-ib}}$ (19 mm) in February was very close to the median size of the subsurface distribution and 9 mm finer than the median size of the surface distribution. The envelope of the bedload grain-size distribution includes within its limits the subsurface grain-size distribution, but not the coarsest fractions of the surface, probably because of the change in the river-bed features after the December 2002 flood (Figure 4 (C4P1)).

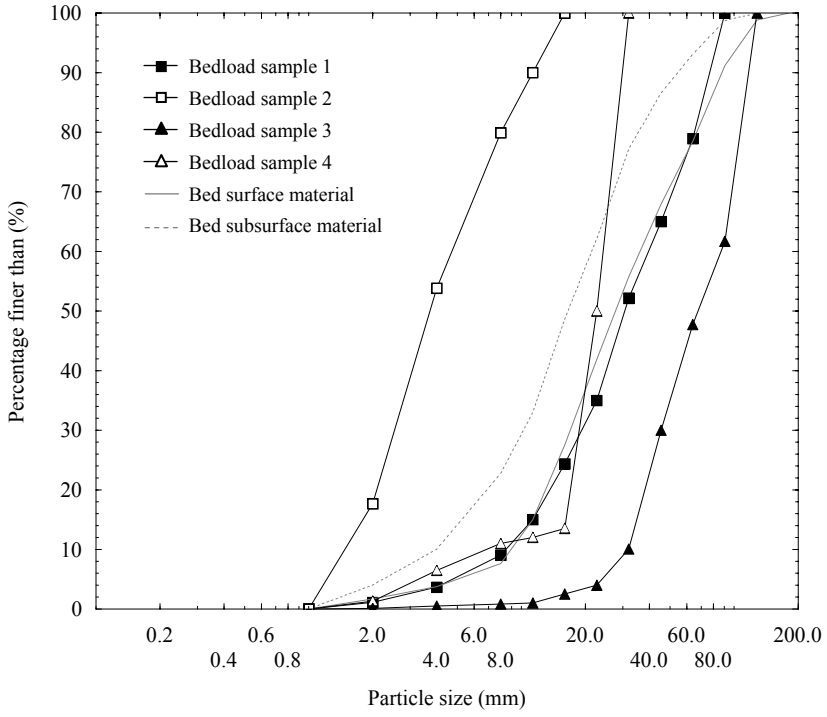

Figure 5 (C4P1). Grain-size distribution of the four first bedload samples obtained during December 2002 in comparison with river-bed grain-size distributions. Sampling interval was 30 minutes and sampling time 3 minutes. Onset of bedload occurred 6 hours after entrainment

threshold was reached. Bedload grain-size distribution was highly variable and showed an erratic behaviour in relation to bed-material fractions, even under almost constant discharge (in this case 1,500 m^3/s)

Following the tendency described for the February 2003 flood, the envelope of bedload grain-size distributions became narrower during the March 2003 flood and it was even closer to the bed subsurface distribution (Figure 4 (C4P1)). However, mean $D_{max\text{-}ib}$ and its standard deviation are equal than in the March 2003 flood. Mean $D_{50\text{-}ib}$ (17 mm) is practically the same as that of the subsurface distribution, and it is 12 mm finer than the median bed surface material (Figure 4 (C4P1), Table 2 (C4P1)). All sizes of the river-bed subsurface are contained within the envelope of the bedload grain-size distributions, while almost half of surface grain-sizes plots outside the envelope (Figure 4 (C4P1)). The close relation between subsurface and bedload grain-size distributions further strengthens the appearance of the dominance of subsurface material in the bedload transport during the March 2003 flood.

4.2.3. River-bed material mobility

Analysis of the mobility of various size classes provides relevant information on river-bed dynamics during 2002-2003 winter floods. For this purpose, the mean proportion of each grain-size in bedload samples (P_i) was scaled using the mean bulk sediment grain-size distribution ($f_{i\text{-}bulk}$) (Wilcock and Southard, 1988) taken as the reference material (Church and Hassan, 2002). Bedload samples were truncated at 1 mm in order to avoid particles that could be transported in suspension, and at 64 mm in order to prevent overrepresentation of large sizes, which might have been scooped, and therefore oversampled, by the Helley-Smith sampler during sampling operations.

Figure 6a (C4P1) suggests different behaviour between bed-material fractions and between floods. Very coarse sand appears to be under-transported in all floods (i.e., frequency of very coarse sand in bedload was lower than that in bed-material distribution, $P_i/f_{i\text{-}bulk}<1$). Similar results were reported by Church and Hassan (2002) in Harris Creek, British Columbia, a river with similar grain-size distribution than the lower Ebro. This phenomenon has been explained by the selective trapping of those sizes in the bed as the

flow strength increase (Laronne and Carson, 1976; Church and Hassan, 1992). Particles between 4 mm and 16 mm behave differently in the December 2002 flood in comparison to the February and March 2003 floods. On one hand, during December 2002 they were mostly under-represented in bedload, a fact that can be primarily related to the role of the armour in preventing those classes being set in motion, especially during the early phases of the flood (Figure 6b (C4P1)). On the other, during the February and, especially, March floods, fractions between 4 mm and 16 mm were over-represented in bedload, reflecting the increasing role of the subsurface sediments in the sediment transport. Figure 6c (C4P1) clearly exemplifies the greater availability ($i_{bi}/f_{i\text{-}bulk}$), hence presence in transport, of medium-size fractions (i.e., subsurface sediments) from flood to flood during winter 2003, after initial removal of the armour layer.

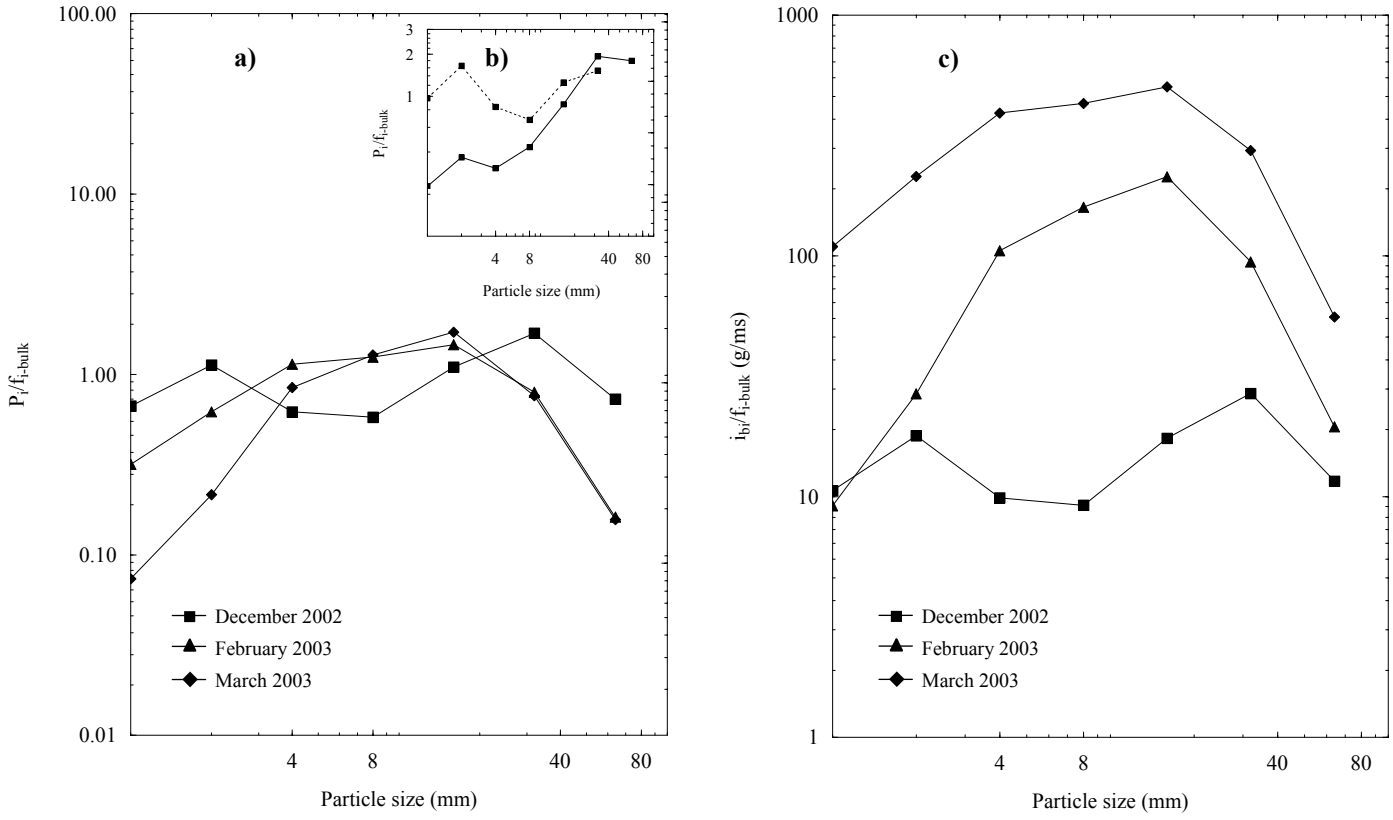

Figure 6 (C4P1). Mobility of river-bed sediment by fractions during winter 2002-03 floods in the lower Ebro River: (**a**) Proportion of bedload size *i* (P_i) in bed-material ($f_{i\text{-}bulk}$), (**b**) Proportion of bedload size *i* (P_i) in bed-material ($f_{i\text{-}bulk}$) during the rising and falling limbs of the December 2002 flood, and (**c**) Bedload transport per fraction *i* in (i_{bi} in g/ms) in relation to its frequency on river-bed sediments ($f_{i\text{-}bulk}$)

Finally, during the rising limb of the December 2002 coarser particles (32 mm and 64 mm size classes) were transported at higher frequency than their presence in the river-bed, illustrating the breaking of the bed during that flood phase (Figure 6b (C4P1)). Similarly, Gomez (1995) reported for the Snake River, Idaho (data from Jones and Seitz, 1980) that, before and during the disturbance of the armour layer, mobility was higher for particles close to the median size of the river-bed material (in the case of the Ebro River maximum mobility corresponds to 32 mm (i.e., fractions between 32 and 64 mm), the D_{55} of the surface material and the D_{65} of the bulk grain size distribution). Transport of different size-fractions was more even during the falling limb of the flood, the flood phase when, not surprisingly, particles of 64 mm were not in motion. This fact explains the mean flood ratio $P_i/f_{i\text{-}bulk}$ close to 1 (Figure 6a (C4P1)). During the February and March floods (Figure 6a (C4P1)) size-classes 32 mm and 64 mm experienced transport but were under-represented in bedload. This fact can be attributed to the major role of finer fractions in bedload. We do not think that under-representation indicates a hydraulic limitation, firstly because floods were competent to move them and secondly because the degree of armour decreased after the specified floods.

4.3. River-bed grain-size distribution in summer 2003

Bed-material dynamics during winter 2002-2003 floods were responsible for the new grain-size distribution of the lower Ebro river-bed obtained during the field campaign of summer 2003. Section n.2 showed again no difference between surface and subsurface layers and a volumetric sample was thus taken to analyse the sediment mixture. Except for section n.2, surface and subsurface material was sampled separately due to the presence of a coarse layer on the surface.

4.3.1. Surface material

Median size of surface material ($D_{50\text{-}s}$) ranged from 8 mm to 68 mm, almost the same limits obtained in 2002. Mean $D_{50\text{-}s}$ for the control sections was 34 mm, with an estimated error around the mean (ε) of $\pm$7 mm. Both values are similar to those obtained in 2002. Maximum and minimum $D_{50\text{-}s}$ were obtained in the Presa Flix (n.1) and in the Pas Ase (n.4) sections, as in 2002. One of the most remarkable features observed in summer 2003

was the notable increase of fine material (<8 mm) on the river-bed surface in comparison with summer 2002 (Table 1 (C4P1)). According to changes in the median grain-size of the surface material the study reach can be divided into two separate zones. The first comprises the river reach between sections n.1 and n.4 (both included), the first 17.5 km downstream the Flix Dam. There, $D_{50\text{-}s}$ did not significantly vary between 2002 and 2003. The second reach is located between sections n.5 and n.8 (both included), a 9.5 km-long river reach starting at the confluence with the Siurana River. Surface material became finer in sections n.5, n.6, and n.8 (sections showing highest degree of armouring in summer 2002). In contrast, median surface size at sections n.7 became coarser after winter 2002-2003 floods (Table 1 (C4P1)).

Mean $D_{max\text{-}s}$ in 2003 ranged from 155 mm to 64 mm, with a mean of 122 mm with an error around the mean of ±13 mm, that is, a reduction of 15 mm under the mean $D_{max\text{-}s}$ calculated in 2002 (Table 1 (C4P1)). Mean surface sorting ($\sigma_{F\&W}$) was 1.5 (i.e., poorly sorted), a value that reflects just a small reduction in comparison to 2002 (Table 1 (C4P1)). This fact could be related to the increase of fine material in the river-bed surface as a consequence of bedload dynamics during the winter 2002-2003 floods. The most important changes in occurred in bars n.5 and n.6 downstream from the confluence of the Siurana with the Ebro River (Table 1 (C4P1)). Sorting exceeded 2 in sections n.6 and n.8, where distributions were clearly skewed towards fine grain-sizes. No bimodality (B) was observed in those two sections (Table 1 (C4P1)). Median size of the composite distribution of section n.2 did not vary significantly (i.e., -0.4 mm) between 2002 and 2003. However, bed-material sorting increased to 2.2. In this case bimodality was estimated (B=3.6), with well defined modes, one fine mode at the coarse sand fraction and one coarse mode at medium coarse gravel (Table 1 (C4P1)).

4.3.2. Subsurface material

Median subsurface material size ($D_{50\text{-}ss}$) sampled in 2003 varied from 8 mm to 23 mm. Mean $D_{50\text{-}ss}$ was 16 mm, with an estimated error around the mean (ε) of ±2 mm. Overall, results show a small deviation of the median subsurface grain-size between sections. Maximum and minimum $D_{50\text{-}ss}$ were sampled in sections n.1 and n.4, respectively (Table 1 (C4P1)). A significant increase in the median size of the subsurface sediment occurred

after the winter floods in sections downstream from n.5. As was observed in summer 2002, subsurface material was poorly sorted compared to that on the surface. Sorting ($\sigma_{F\&W}$) ranged from 2.5 to 1.0 with the mean at 2.1 (Table 1 (C4P1)). Sorting changed very little in comparison with values calculated in 2002. The most important change occurred in section n.7 where the coefficient increased from 1 to 2.5. Bimodality of subsurface material (B>3.4) was observed in most of the grain-size distributions with sorting higher than 2, showing well defined modes at coarse sand and at medium to coarse gravel (Table 1 (C4P1)).

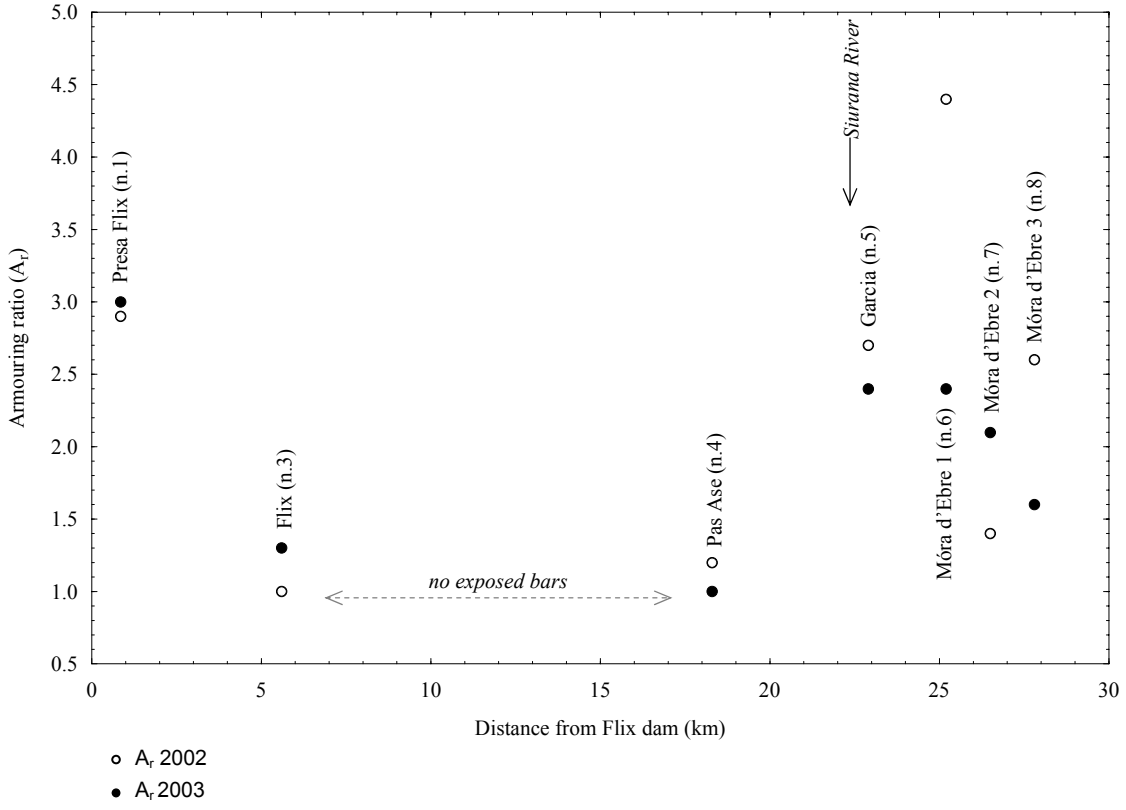

Figure 7 (C4P1). Downstream change of armouring (A_r) in the lower Ebro River in 2002 and 2003

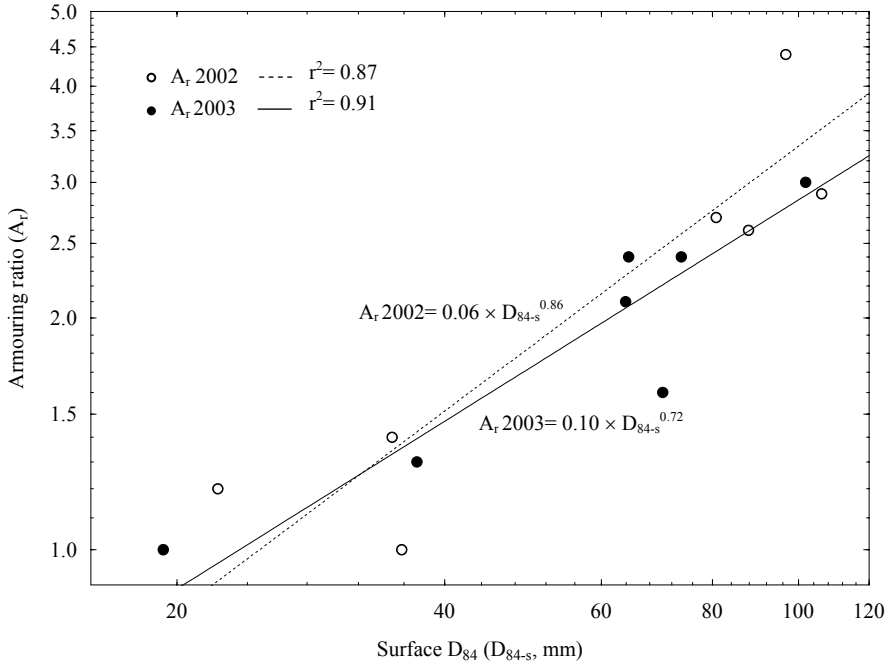

Figure 8 (C4P1). Statistical relation between $D_{84\text{-}s}$ and degree of armouring in the lower Ebro River (2002 and 2003)

4.3.3. Changes in river-bed armouring

As has been demonstrated, large particles were entrained from river-bed surface during December 2002 (Figure 4 (C4P1) and 6a (C4P1)) and, consequently, the armour layer was widely broken. As a consequence, the armouring ratio (A_r) experienced a remarkably general decrease in 2003 at part of the control sections (Table 1 (C4P1), Figure 7 (C4P1)). This fact can be related not only to the breaking but to the subsequent release of subsurface material, which was still evident on the river-bed surface in summer 2003, i.e., increase of surface fine material (<8 mm). A statistically significant relation was established between $D_{84\text{-}s}$ (i.e., percentile 84 of the surface distribution) and A_r ($p<0.01$) for both 2002 and 2003 years (Figure 8 (C4P1)), a fact that indicates the role of coarse fractions in the armour formation and stability. In 2002 the coarser the $D_{84\text{-}s}$ size the stronger the armouring, while in 2003 the coarser the grain-size distribution the more pronounced the reduction in armouring. The mean armouring ratio was 2.3 in 2002 and 2.0 in 2003, with an error around the mean (ε) of ± 0.3, 0.2 points inferior than the error estimated for 2002 (Table 1 (C4P1)). In particular, the most notable reduction was observed in section n.6 (from 4.4 to 2.4) (Figure 7 (C4P1)). Reduction was the consequence of both reduction of median

surface grain-size and increment of median subsurface grain-size (Table 1 (C4P1)). Maximum armouring (A_r=3.0) was estimated in section n.1 (Figure 9a (C4P1)), 0.8 km downstream the Flix Dam. There, the river-bed is quite stable and grain-size distributions do not greatly differ from year to year (Table 1 (C4P1)). Minimum armouring (A_r=1.0) was observed in section n.4 (Figure 9b (C4P1)). There, no change in river-bed grain-size distributions was observed in 2003 (Table 1 (C4P1)). As a consequence, breaking of the armour layer led to a) net scour (except for sections n.5 and n.7) mainly due to net export of subsurface material, and b) general reduction of the bars' mean elevation after the 2002-2003 winter floods, as reported by Vericat and Batalla (2005a, 2005b).

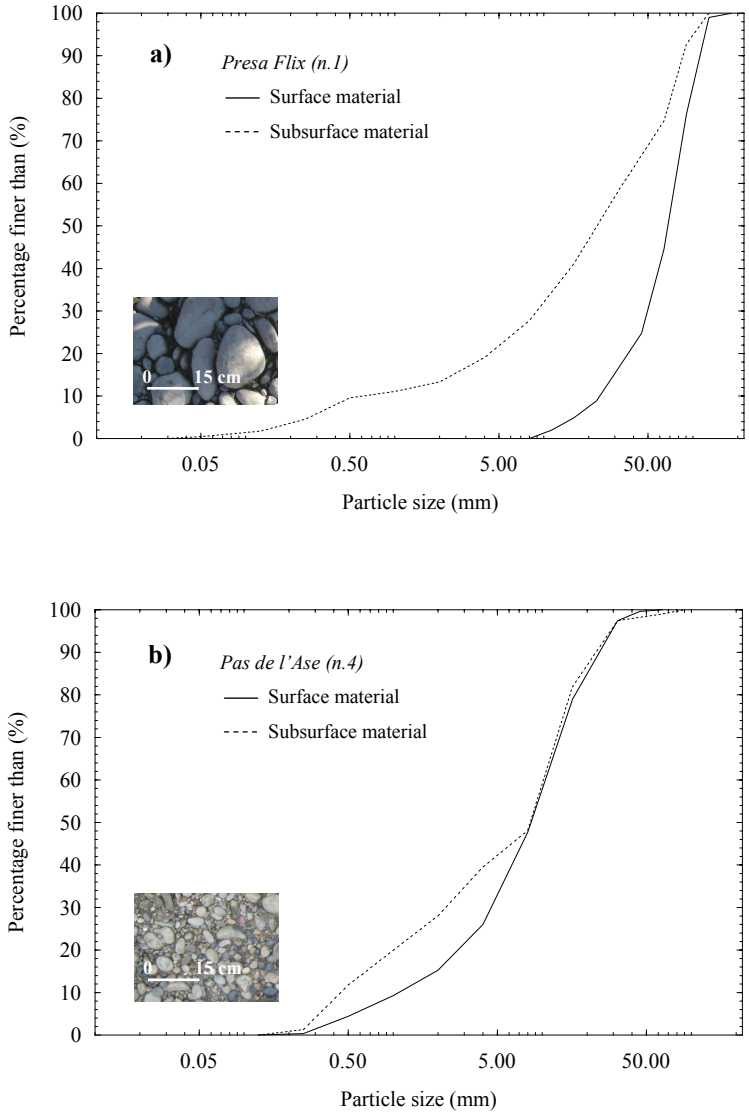

Figure 9 (C4P1). (**a**) Surface and subsurface bed-material distributions of sections n.1 (highest armouring) and (**b**) n.4 (lowest armouring) observed in summer 2003 (Table 1 (C4P1))

5. Summary and conclusions

River-bed grain-size distributions observed in summer 2002 in the lower Ebro River below the Flix Dam showed that surface material was clearly coarser and well sorted than material in the subsurface layer. Mean armouring ratio was 2.3, with notable differences from section to section (1.0 to 4.4). Fassnacht *et al.* (2003) reported a mean armouring of 4 in the lower Deschutes River, Oregon, below the Pelton-Round Butte dam complex, with values ranging from 1.3 to 11.9.

The magnitude of floods that occurred during winter 2002-2003 in the lower Ebro River allowed the breaking of the *stable armour layer* formed in some sections after two years of relatively low flows. A similar phenomenon was reported by Gomez (1983) for a small, non-regulated, gravel bed stream, the Sheepstor Beck, England. In the case of the Ebro River, there are several hydraulic and geomorphological factors that suggest the breaking of the armour, namely a) the extraordinary delay of bedload onset during the December 2002 flood, b) the distinct mobility of the different bed-material fractions during the first and successive floods, and c) the reduction of the armouring ratio observed in summer 2003 in most of the control sections. The low recovery of painted tracers after floods at the monitoring sections and the general net scour in the study reach (Vericat and Batalla, 2005b) point in the same direction. In addition, during the succession of floods bedload grain-size distribution got progressively closer to the subsurface grain-size distribution (Figure 4 (C4P1)), also a fact that indicates that the armour was removed (Gomez, 1995), increasing the role of subsurface material in bedload and increasing the availability of sediment overall in the study reach, thus increasing bedload transport rates from flood to flood. The main conclusions of the investigation are as follows:

1. A highly dynamic hydrological year, such as 2002-2003, was responsible for breaking the armour layer of the lower Ebro River, entraining and transporting most surface and subsurface sediment fractions, causing river-bed degradation (i.e., river-bed incision).
2. Subsurface material played an increasing role in bedload transport during the succession of floods, as a consequence of the progressive instability and break-up of the river-bed armour, increasing the availability of sediment and, consequently, the bedload rates.

3. Reduction in river-bed armouring was more pronounced in sections with coarser surface grain-size distribution. Downstream sections were more prone to changes in armouring than those upstream (i.e., closer to dams), where river-bed structure and grain-size distribution demonstrated greater stability.

Analysis of river-bed grain-size and bedload grain-size distributions in the lower Ebro River has shown that armouring is an important active process in largely regulated fluvial systems and that it is associated with disequilibrium between sediment transport (flow competence) and sediment supply. Stability of armouring is mainly controlled by flood magnitude. Continuous survey of grain-size distribution can be of great use to a) understand adjustments of river process, hence sediment transport, and forms, and b) to design and implement river restoration programmes (e.g., flushing flows) adequate for impounded fluvial environments.

Acknowledgments

This research was carried out within the framework of research project REN2001-0840-C02-01/HID, which is funded by the Spanish Ministry of Science and Technology. The first author received a grant from the Spanish Ministry of Education. Hydrological data was supplied by the Ebro Water Authorities. The Móra d'Ebre Town Council provided logistic support. Albert Rovira at the University of Lleida provided assistance during field and labwork. Michael Church at the University of British Columbia undertook a helpful review of the first version of the manuscript.

Notations

ϕ	Phi units (ϕ_i=-$\log_2$ D_i, where ϕ_i is the size in phi units of an unit of length D_i expressed in mm)
A_r	Armouring ratio (ratio between $D_{50\text{-}s}$ and $D_{50\text{-}ss}$, e.g., Lisle and Madej, 1992).
B	Bimodality index (Wilcock, 1993)
$D_{50\text{-}ib}$	Median bedload grain-size (mm)
$D_{50\text{-}s}$	Median surface grain-size (mm)
$D_{50\text{-}ss}$	Median subsurface grain-size (mm)
$D_{84\text{-}s}$	Percentile 84 of the surface grain-size distribution (mm)
$D_{max\text{-}ib}$	Maximum bedload grain-size (mm)
$D_{max\text{-}s}$	Maximum surface grain-size (mm)
$D_{max\text{-}ss}$	Maximum subsurface grain-size (mm)
$f_{i\text{-}bulk}$	Frequency of a given size *i* in bulk sediment deposits
i_b	Mean bedload transport rate (g/ms)
i_{bi}	Bedload transport rate by fraction *i* (g/ms)
$i_{bi}/f_{i\text{-}bulk}$	Bedload transport per fraction *i* (i_{bi} in g/ms) in relation to its frequency on river-bed sediments ($f_{i\text{-}bulk}$)
P_i	Frequency of a given transported size *i* in the bedload sample
$P_i/f_{i\text{-}bulk}$	Proportion of bedload size *i* in bed-material (bulk sediment)
Q_i	i-year flood calculated from the Tortosa gauging station flow series (Batalla *et al.*, 2004)
ε	Estimation error around the mean ($\varepsilon = \sigma/\sqrt{N}$, where σ is the standard deviation and N the number of data)
σ	Standard deviation
$\sigma_{F\&W}$	Sorting index (Folk and Ward, 1957)

References

Anastasi, G., 1984. Geschiebeanalysen im Felde unter Berücksichtigung von Grobkomponenten. [Field grain-size analyses with special attention to coarse material]. *Mitteilungen der Versuchsanstalt für Wasserbau, Hydrologie und Glaziologie der ETH Zürich*, Nr. **70**.

Andrews, E.D., Parker, G., 1987. Formation of a coarse surface layer as the response to gravel mobility. In *Sediment transport in gravel-bed rivers*, Thorne C. R., Barthurst J.C., Hey R.D. (eds.). Chichester: John Wiley and Sons; 269-300.

Batalla, R.J., 2003. Sediment deficit in rivers caused by dams and instream gravel mining. A review with examples from NE Spain. *Cuaternario y Geomorfología* **17**(3-4): 79-91.

Batalla, R.J., Kondolf, G.M., Gomez, C.M., 2004. Reservoir-induced hydrological changes in the Ebro River basin, NE Spain. *Journal of Hydrology* **290**: 117-136.

Brandt, S.A., 2000. Prediction of downstream geomorphological changes after dam construction: a stream power approach. *International Journal of Water Resources Development* **16**(3): 343-367.

Bunte, K., Abt, S.R., 2001. *Sampling surface and subsurface. Particle-size distributions in wadable gravel- and cobble-bed streams for analyses in sediment transport, hydraulics, and streambed monitoring*. U.S. Department of Agriculture, Forest Services, Rocky Mountain Research Station.

Burkham, D.E., 1986. Trends in selected hydraulic variables for the Colorado River at Lees Ferry and near Grand Canyon, Arizona -1922-1984. Report, 58 pp., Bur. of Recla., Glen Canyon Environ. Stud., Flagstaff, Arizona.

Church, M., 1995. Geomorphic response to river flow regulation: case studies and time-scales. *Regulated Rivers: Research and Management* **11**(1): 3-22.

Church, M., Hassan, M.A., 1992. Size and distance of travel of unconstrained clasts on a streambed. *Water Resources Research* **28**: 299-303.

Church, M., Hassan, M.A., 2002. Mobility of bed material in Harris Creek. *Water Resources Research* **38**(11).

Church, M., McLean, D.G., Wolcott, J.F., 1987. River bed gravels: sampling and analysis. In *Sediment transport in gravel-bed rivers*, Thorne C. R., Barthurst J.C., Hey R.D. (eds.). Chichester: John Wiley and Sons; 43-88.

Colby, B.R., 1964. Scour and fill in sand-bed streams. *U.S. Geol. Surv. Prof. Pap*., **462-D**, 32 pp.

Davies, D.A., Berrisford, M.S., Matthews, J.A., 1990. Boulder paved rivers: a case study of a fluvial periglacial landform. *Zeitschrift für Geomotphologie* **34**: 213-231.

Dietrich, W.E., Kirchner, J.W., Ikeda, H., Iseya, F., 1989. Sediment supply and the development of the coarse surface layer in gravel-bedded rivers. *Nature* **340**: 215-217.

Diplas, P., 1989. Areal sampling techniques. In *Sediment Transport Modeling*, Wang, S.S.Y. (ed.). New York: American Society of Civil Engineers; 380-385.

Diplas, P., Sutherland, A. J., 1988. Sampling techniques for gravel sized sediments. *Journal of Hydraulic Engineering* **114**(5): 484-501.

Dunkerley, D.L., 1990. The development of armour in the Tambo River, Victoria, Australia. Earth Surface Processes and Landforms **15**: 405-415.

Emmett, W.W., 1980. *A Field Calibration Of The Sediment Trapping Characteristics Of The Helley-Smith Bedload Sampler*. US Geological Survey Professional Paper 1139.

Fassnacht, H., McClure, E.M., Grant, G.E., Klingeman, P.C., 2003. Downstream effects of the Pelton-Round Butte hydroelectric project on bedload transport, channel morphology, and channel-bed texture, lower Deschutes River, Oregon. *Water science and Application* **7**: 175-207.

Folk, R.L., Ward, C., 1957. Brazos River bar: a study in the significance of grain size parameters. *Journal of Sedimentary Petrology* **27**(1): 3-26.

Friedman, J.M., Osterkamp, W.R, Scott, M.L., Auble, G.T., 1998. Downstream effects of dams on channel geometry and bottomland vegetation: Regional patterns in the Great Plains. *Wetlands* **18**: 619-633.

Fripp, J.B., Diplas, P., 1993. Surface sampling in gravel streams. *Journal of Hydraulic Engineering* **119** (4): 473-490.

Gessler, J., 1965. Der Geschiebetriebbeginn bei Mischungen untersucht an natuerlichen Abpflaesterungsercheinungen in Kanaelen. *Rep. 69*, Mitt. Der Vers. Für Wasswrbau und Erdbau, Zurich.

Gessler, J., 1971. Aggradation and degradation. In *River Mechanics*, Shen, H.W., (ed.). Fort Collins; Volume I.

Gomez, B., 1979. Bedload discharge in a small Devon stream. *Report of the Transactions of the Devonshire Association for the Advancement of Science* **111**: 31-48.

Gomez, B., 1983. Temporal variations in bedload transport rates: the effect of progressive bed armouring. Earth Surface Processes and Landforms **8**: 41-54.

Gomez, B., 1994. Effects of particle shape and mobility on stable armour development. Water Resources Research **30**(7): 2229-2239.

Gomez, B., 1995. Bedload transport and changing grain size distributions. In *Changing rivers channels*, Gurnell A., Petts, G. (eds.). Chichester: John Wiley and Sons; 177-199.

Graf, W.L., 2001. Damage control: restoring the physical integrity of America's rivers. *Annals of the Association of American Geographers* **91**: 1-27.

Habersack, H.M., Laronne, J.B., 2001. Bed load texture in an alpine gravel bed river. *Water Resources Research* **37**(12): 3359-3370.

Hammad, H.Y., 1972. River bed degradation. *Proceedings of the American Society of Civil Engineers, Journal of the Hydraulics Division* **98**: 591-607.

Howard, A., Dolan, R., 1981. Geomorphology of the Colorado River in Grand Canyon. *Journal of Geology* **89**: 269-297.

Jones, M.L., Seitz, M.R., 1980. Sediment transport in the Snake and Clearwater Rivers in the vicinity of Lewiston, Idaho. *United States Geological Survey Open-File Report* **80**-690.

Kellerhals, R., Bray, D. I., 1971. Sampling procedures for coarse fluvial sediments. *Journal of the Hydraulics Division, **ASCE**97*(HY8): 1165-1180.

Knighton, D., 1998. *Fluvial Forms and Processes: a New Perspective*. Arnold, London; 386 p.

Kondolf, G.M., 1997. Hungry Water: Effects of Dams and Gravel Mining on River Channels. *Environmental Management* **21**(4): 533-551.

Kondolf, G.M., Matthews, W.V.G., 1993. *Management of coarse sediment in regulated rivers of California*. University of California Water Resources Center: Davis, California.

Kondolf, G.M., Wolman, M.G., 1993. The sizes of salmonid spawning gravels. *Water Resources Research* **29**: 2275-2285.

Lane, E.W., Carlson, E.J., 1953. Some factors affecting the satbility of canals conbstructed in coarse granular materials. *Proceedings of the 5th Congress International Association for Hydraulic Research*, Delf, Netherlands.

Laronne, J.B., Carson, M.A., 1976, Interrelationships between bed morphology and bed-material transport for a small, gravel-bed channel. *Sedimentology* **23**: 67-85.

Lisle, T.E, Madej, M.A., 1992. Spatial variation in a channel with high sediment supply. In Dynamics of Gravel Bed Rivers, Billi, P., Hey, R.D., Thorne, C.R., Tacconi, P., (eds.), New York: John Willey; 277-291.

Lisle, T.E., Iseya, F., Ikeda, H., 1993. Response of channel width alternate bars to a decrease in supply of mixed bed load: a flume experiment. *Water Resources Research* **29**: 3623-3269.

Little, W.C., Mayer, P.G., 1976. Stability of channel beds by armouring. *Proceedings of the American Society of Civil Engineers, Journal of the Hydraulics Division*, **102**(Hy11): 1647-1661.

Meade, R.H., Parker, R.S., 1985. *Sediment in rivers of the United States*. U.S. Geological Survey Water-Supply Paper 2275.

Moss, A.J., 1963. The physical nature of the common sandy and pebbly deposits. Part II, *Am. J. Sci.*, **261**: 297-343.

Nelson, C.H., 1990. Post Messinian deposition rates and estimated river loads in the Ebro sedimentary system. In *Marine Geology of the Ebro Continental Margin,* Nelson C.H., Maldonado A. (eds.). Marine Geology; **95**: 395-418.

Novoa, M., 1984. Precipitaciones y avenidas extraordinarias en Catalunya. *Proceedings of the Jornadas de Trabajo sobre Inestabilidad de laderas en el Pirineo*: Barcelona; 1-15.

Palau, A., Batalla, R.J., Rosico, E., Meseguer, A., Vericat, D., 2004. Management of water level and design of flushing floods for environmental river maintenance downstream of the Riba-Roja Reservoir (Lower Ebro River, NE Spain). *Proceedings of the International Conference HYDRO 2004: A New Era for Hydropower*. Porto, Portugal, 18-21 October 2004.

Parker, G., Klingeman, P.C., 1982. On why gravel bed streams are paved. *Water Resources Research* **18**: 1409-1423.

Parker, G., Sutherland, A.J., 1990. Fluvial armour. *Journal of Hydraulic Research* **28**: 529-544.

Petts, G.E., 1984. *Impounded Rivers. Perspectives for Ecological Management*. Wiley, New York; 326 p.

Phillips, J.D., 2001. Sedimentation in bottomland hardwoods downstream of an east Texas dam. *Enviromental Geology* **40**: 860-868.

Phillips, J.D., 2003. Toledo Bend Reservoir and geomorphic response in the lower Sabine River. *River Research and Applications* **19**: 137-159.

Rennie, C. D., R. G. Millar, and M. A. Church., 2002. Measurement of bed load velocity using an acoustic Doppler current profiler. *Journal of Hydraulic Engineering-Asce* **128**:473-483.

Rice, S., Church, M., 1996. Sampling surficial fluvial gravels: the precision of size distribution percentile estimates. *Journal of Sedimentary Research* **66**(3): 654-665.

Rice, S.P., Haschenburger, J.K., 2004, A hybrid method for size characteritzation of coarse subsurface fluvial sediments. *Earth Surface Processes and Landforms* **29**: 373-389.

Richards, K.S., Clifford, N.J., 1991. Fluvial geomorphology - structured beds in gravelly rivers. *Progress in Physical Geography* **15**(4): 407-422.

Sanz, M.E., Avendaño, C., Cobo, R., 1999. Influencia de los embalses en el transporte de sedimentos hasta el río Ebro (España). *Proceedings of the Congress on Hydrological and geochemical processes in large-scale river basins*. HIBAM: Shahin, 1985

Sear, D.A., 1995. Morphological and sedimentological changes in a gravel-bed river following 12 years of flow regulation for hydropower. *Regulated Rivers: Research and Management* **10**: 247-264.

Shields, A., 1936. Anwendung der Aehnlichkeitsmechanik und der Turbulenzforschung auf die Geschiebebewegung. *Mitteilung der Preussischen Versuchsanstalt für Wasserbau und Schiffbau 26*, Berlin

Surian, N., Rinaldi, M., 2003. Morphological response to river engineering and management in alluvial channels in Italy. *Geomorphology* **50**: 307-326.

Sutherland, A.J., 1987. Static armour layer by selective erosion. In *Sediment transport in gravel-bed rivers*, Thorne C. R., Barthurst J.C., Hey R.D. (eds.). Chichester: John Wiley and Sons; 243-260.

Suttle, K.B., Power, M.E., Levine, J.M., McNeely, C., 2004. How fine sediment in riverbeds impairs growth and survival of juvenile salmonids. *Ecological applications* **14**(4): 969-974.

Topping, D.J., Rubin, D.M., Vierra, L.E., 2000. Colorado River sediment transport 1. Natural sediment supply limitation and the influence of Glen Canyon Dam. *Water Resources Research* **36**(2): 515-542.

Vericat, D., Batalla, R.J., 2004. Efectos de las presas en la dinámica fluvial del curso bajo del río Ebro. *Cuaternario y Gemorfología* **18**(1-2): 37-50.

Vericat, D., Batalla, R.J., 2005a. Sediment transport in a highly regulated fluvial system during two consecutive floods (Lower Ebro River, NE Spain). *Earth Surface Processes and Landforms* **30**.

Vericat, D., Batalla, R.J., 2005b. Sediment transport in the lower Ebro River (NE Iberian Peninsula). *Geomorphology* (submitted).

Wilcock, P.R., 1993. Critical shear stress on natural sediments. *Journal of Hydraulic Engineering* **119**: 491-505.

Wilcock, P.R., Southard, J.B., 1988. Experimental study of incipent motion in mixed size sediment, Water Resources Research **24**: 1137-1151.

Williams, G.P., Wolman, M.G., 1984. *Downstream Effects of Dams on Alluvial Rivers*. US Geological Survey Professional Paper 1986.

Wolman, M.G. 1954. A method of sampling coarse bed material. *American Geophysical Union Transactions*, **35**: 951-956.

Xu, J., 1996. Underlying gravel layers in a large sand bed river and their influence on downstream-dam channel adjustment. *Geomorphology* **17**:351-359.

Xu, J., 1997. Evolution of mid-channel bars in a braided river and complex response to reservoir construction: an example from the middle Hanjiang River, China. *Earth Surface Processes and Landforms* **22**: 953-965.

Vericat, D., Garcia, C., Batalla, R.J. (2005): Grain-size distribution in a highly regulated large river: the Lower Ebro. 2. River-bed armouring caused by small frequent floods (to be submitted to an international journal)

Grain-size distribution in a highly regulated large river: the Lower Ebro. 2. River-bed armouring caused by small frequent floods

Abstract

River-bed armouring during small frequent floods have been studied in the regulated lower Ebro River during 2003-2004. River-bed and bedload grain-size distributions have been compared to assess changes of river-bed surface material below the Flix Dam. River-bed grain-size distribution observed in summer 2004 showed that surface material was clearly coarser and better sorted than the material in the subsurface. Similar values were observed in summer 2002. Mean armouring ratio was 2.3, showing a clear stabilization at around 2.7 in section of the reach downstream from the confluence with the Siurana River. The low magnitude of flows during the winter 2003-2004 reinforced the formation of a new armour layer in most of the monitoring sections, a process probably initiated during small floods at the end of the winter 2002-2003. Consequently, river-bed armouring reduced the availability of sediment to be transported, leading to an average three-time decrease of the bedload transport rates hence minimising the river-bed incision. Grain-sizes between 8 and 32 mm were the most affected by the supply-limited conditions. The whole work reports on a complete two-year incision-armouring cycle in a large river under no-sediment supply conditions. Analysis of river-bed and bedload grain-size distributions has shown that armouring is an important process in regulated fluvial systems and that it is a fundamental fluvial process caused by the disequilibrium between sediment transport (flow competence) and sediment supply.

Key words: armouring, sediment availability, small floods, regulated river, Ebro River

1. Introduction

1.1. Sediment supply and riverbed armouring

Over long time scales the supply of sediment in natural alluvial channels can be considered in quasi-equilibrium with the transport capacity of the channel (Schumm, 1977; Kondolf, 1994; Topping *et al.*, 2000). River flow regulation modifies the pattern of sediment supply to downstream reaches and, consequently, alters the alluvial river regime (Petts, 1984). Petts (1980) defined three main factors in determining the response of the river channel downstream from dams: frequency of competent flows, sediment supply, and rate of channel colonization by riparian vegetation. The interaction between flow regulation and changes in sediment supply will characterize the alteration of the river channel, where rates of adjustment will vary over time (Sear, 1992; Brandt, 2000). For instance, below Danjiangkou Dam, in the Hanjiang River, China, two stages have been differentiated since the dam was closured (Xu, 1996). During the first seven years, the reservoir was operated for flood retention and small percentages of sediment were trapped into the reservoir. The river channel downstream suffered slow rates of degradation and river-bed material coarsened slowly. The operation mode of the reservoir changed after that period, water storage becoming the principal purpose, so that 95% of the sediment from upstream was intercepted. After three years, the rate of degradation downstream from the dam increased three times, and the river-bed material coarsened sharply (i.e., median material changed from 0.5 mm to 50 mm).

When competent floods occur frequently after dams are closed and downstream sediment supply relative to the flows' competence is low, river-bed degradation should take place downstream (Leopold *et al.*, 1964), its magnitude being governed by the interaction between the released flows and their capacity to transport downstream sediment (Gomez, 1983; Kondolf, 1997). River-bed coarsening has been reported as a process of channel degradation where mean flow competence is less than critical to transport the largest particles of the bed surface but sufficient to move finer material (Parker and Klingeman, 1982; Parker and Sutherland, 1990; Gomez, 1994). Consequently, the river-bed surface becomes coarser than the subsurface material and an armour layer develops. Therefore, the degree of armouring will be controlled by flow magnitude and river-bed material,

developing stable and mobile armoured river-beds. River-bed armouring reduces sediment availability and, consequently, determines bedload transport rate and bedload grain-size distribution. As armouring increases the transport capacity decreases, whereas the longer the period between bed-disrupting floods (i.e., floods competent to move coarser sizes), the larger the flood required disrupting the bed (Sear, 1992). Armouring also has been reported to have acute ecological impacts. For instance, Milhous (1982) showed that armouring of spawning riffles reduced fish stocks by 60% in the Sacramento River, California. As a general role, bed armouring appears in river reaches close to the dam and decreases downstream (e.g. Fassnacht *et al.*, 2003). The process migrates downstream as the supply of sediment is limited and the duration of competent although low magnitude discharges increases. The confluence of tributaries can interfere with the process (Williams and Wolman, 1984), and also with the river-bed forms sequence (e.g. riffle-pools, Sear, 1995).

1.2. The lower Ebro River. Antecedents on grain-size distribution

Bedload transport and riverbed material were sampled in 2002 and 2003 and subsequently analysed (Vericat *et al.*, this issue). In summary, high magnitude floods (Q_{10}) occurred during winter 2002-2003 were responsible for the changes in the grain-size distribution observed in the lower Ebro river (Figure 1 (C4P2)) in summer 2003. Floods attained 2600 m^3/s (shear stress of 63 N/m^2) and caused the breaking of the stable armour layer formed after two years of relatively low flows. That fact increased the availability of sediment and, consequently, the role of subsurface material in bedload transport during the succession of floods. Armouring ratio (i.e., $D_{50\text{-}s}/D_{50\text{-}ss}$) decreased from 2.3 to 2.0 along the study reach, on average.

In this paper we report on the changes of river-bed grain-size distribution towards armouring during a succession of low magnitude floods and frequent flows during the hydrological year 2003-2004.

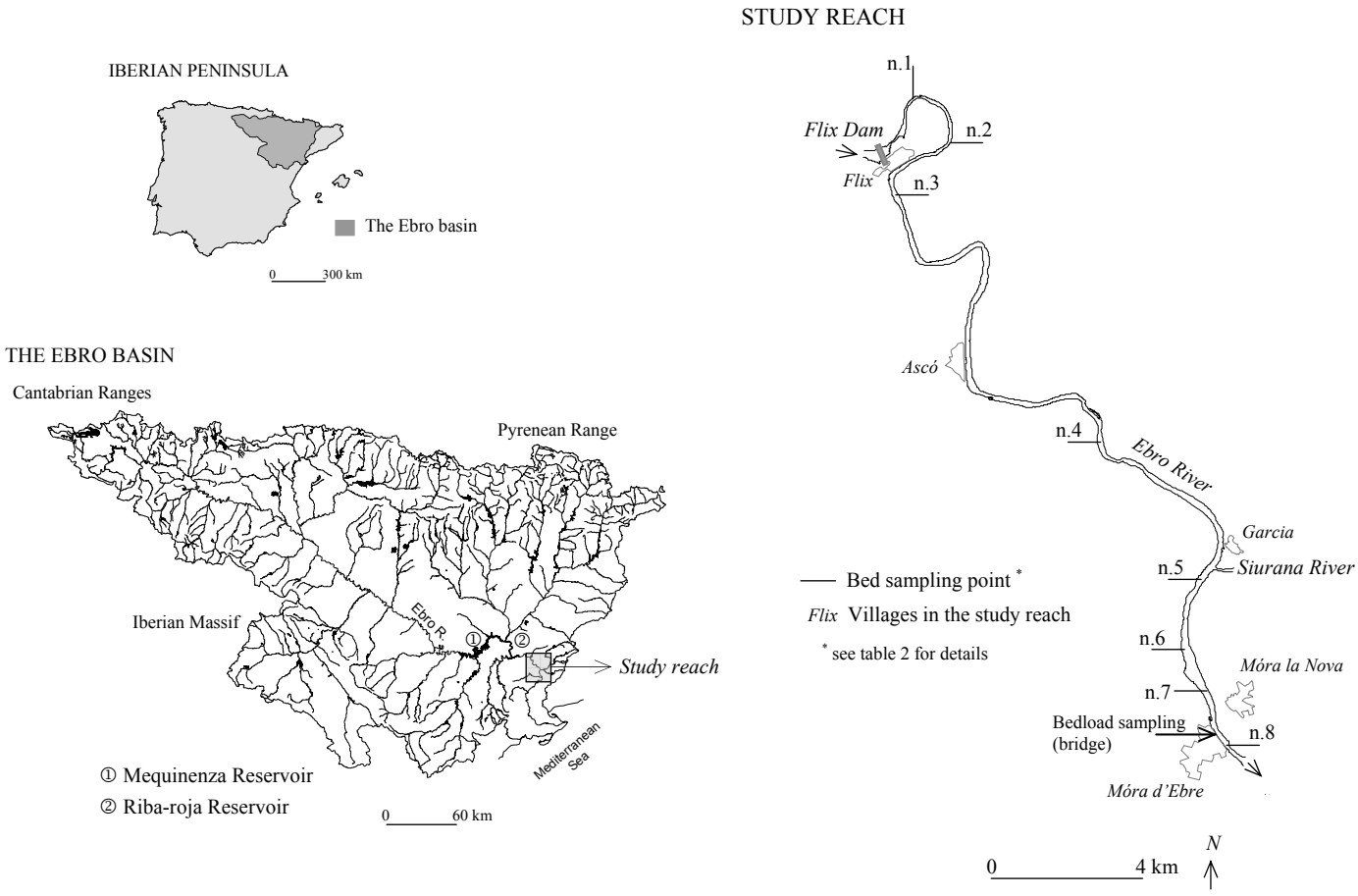

Figure 1 (C4P2). Location of the Ebro River in the Iberian Peninsula and the study reach in the lower Ebro River

2. Results

2.1. The 2003-2004 winter floods

Several floods occurred in the lower Ebro River during winter 2003-2004 (Figure 2a (C4P2)). In all cases the dams altered the hydrographs and, owing to dam operation policies, peak discharges systematically increased in comparison to the incoming flows. For instance, the flood of December 2003 had a maximum daily discharge of 600 m^3/s in the backwater of the Mequinenza Reservoir (Figure 1 (C4P2)), while downstream from the Flix Dam maximum mean daily flow reached 1,200 m^3/s. The first seasonal flood occurred in November 2003. It was a *flushing flow* specifically designed to control the excess of aquatic vegetation in the river channel, similar to the one carried out in December 2002

(Palau *et al.*, 2004),.Maximum instantaneous discharge occurred in the November 2003 flood was 1,355 m^3/s (Q_2) with an associated shear stress of 39 N/m^2. A discharge of 600 m^3/s (i.e., 25 N/m^2) is, according to Shields's (1936) equation, the critical flow for the entrainment of the median surface material. That discharge was equalled or exceeded 40% of the time during the year (Figure 2b (C4P2)), twice the time equalled or exceeded in 2002-2003.

2.1.1. Bedload and bedload grain-size distribution

A total of 51 bedload samples were obtained during the winter 2003-2004 floods. In particular, 36 samples were collected at the Móra d'Ebre bedload sampling section (Figure 1 (C4P2)) during the November 2003 flood (Figure 2a (C4P2)). Mean bedload transport rate (i_{b-m}) was 70 g/ms. Median grain-size in the bedload samples (D_{50-ib}) varied from 4 mm to 44 mm, similar to the range obtained during the March 2003 flood, whose maximum discharge was 700 m^3/s higher (Vericat *et al.*, this issue). Mean D_{50-ib} was 17 mm, with a standard deviation (σ) of ±7.0 mm and an estimated error around the mean ($\varepsilon = \sigma/\sqrt{N}$, where σ is the standard deviation and N the number of data) of ±1.2 mm. Mean sorting of bedload grain-size distribution ($\sigma_{F\&W}$), estimated from the Folk and Ward (1957) index, was 1.1 (i.e., poor sorted), with a standard deviation of ±0.1. Maximum size of collected particles (D_{max-ib}) ranged from 15 mm to 87 mm, with mean D_{max-ib} of 46 mm, a standard deviation of ±14.0 mm, and an estimated error of ±2.3 mm.

In addition, 15 bedload samples were collected during subsequent high flows after the November 2003 flood (Figure 2a (C4P2)). Discharges during sampling ranged from 725 m^3/s (i.e., 30 N/m^2) to 1,135 m^3/s (i.e., 37 N/m^2). Almost the whole range of winter flows was sampled. Mean bedload transport rate was 60 g/ms. Median bedload size (D_{50-ib}) varied from 12 mm to 30 mm, with a mean diameter of 19 mm, a standard deviation of ±4.5 mm, and an error around the mean of ±1.2 mm. Range of median sizes decreased in comparison to those observed during the November 2003 flood, showing a less range of sizes (i.e., more selected) and a coarser mean D_{50-ib}. Mean ($\sigma_{F\&W}$) was 1.0 (i.e., poorly to moderately sorted), with a standard deviation of ±0.2. Maximum collected particles (D_{max-ib}) ranged from 32 mm to 75 mm, with a mean of 48 mm.

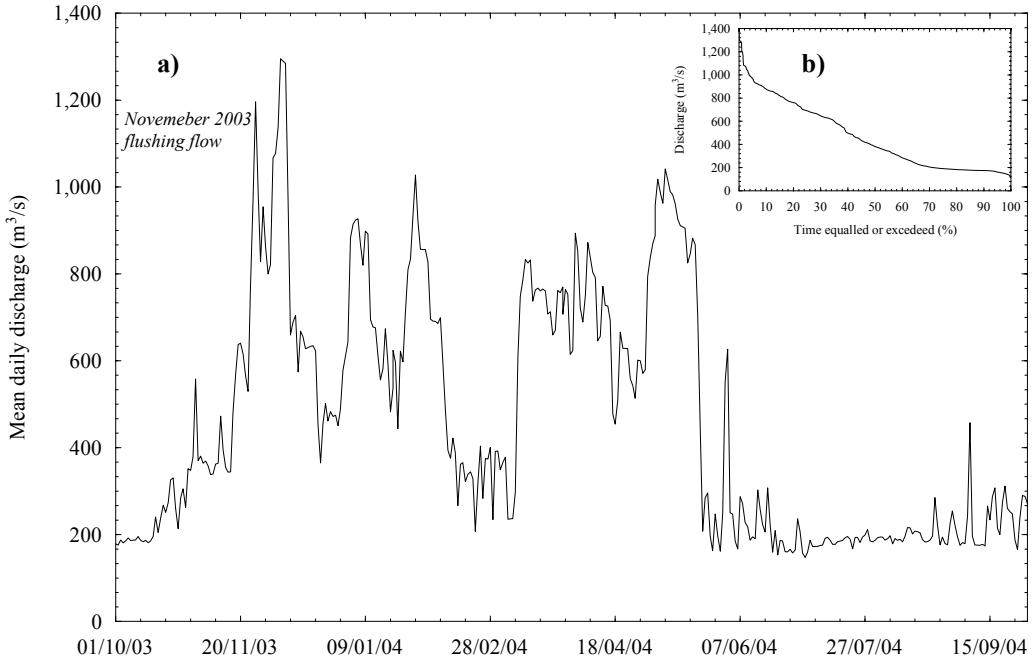

Figure 2 (C4P2). (**a**) Mean daily discharges and (**b**) flow frequency curve of the 2003-2004 hydrological year in the Móra d'Ebre sediment transport sampling section (Figure 1 (C4P2))

2.1.2. Bedload and bed-material grain-size distributions

The envelopes of the bedload grain-size distributions for the November 2003 flood and for the subsequent sampling period are compared with the river-bed grain-size distribution obtained in summer 2003 (Figure 3 (C4P2)). River-bed grain-size distributions both surface and subsurface, have been calculated as the unweighted sum of the samples (Vericat *et al.*, this issue) at the eight surveyed sections (Figure 1 (C4P2)). The step distance for the bedload transport is assumed to be the whole channel reach downstream from the Flix Dam (see for discussion Vericat *et al.*, this issue). Bed-material and bedload grain-size distributions were truncated at 1 mm in order to avoid particles that may be transported in suspension.

During the November 2003 flood mean bedload grain-size ($D_{50\text{-}ib}$=17 mm) was finer than the median size of the surface distribution ($D_{50\text{-}s}$=29 mm), and almost the same than the median size of the subsurface distribution observed in summer 2003. The envelope of bedload sizes encloses within its limits roughly 70% of the surface river-bed grain-size distribution and 90% of the subsurface distribution (Figure 3 (C4P2)). This fact suggests

that the transport of coarsest particles was hydraulic limited. This tendency increased during the high flows after the November 2003 floods, in which the mean bedload grain-size ($D_{50\text{-}ib}$=19 mm) was coarser. The $D_{50\text{-}ib}$ was finer than the median surface size and similar to the median subsurface material (Figure 3 (C4P2)). On one side, Only fine to medium gravels of the river-bed surface distribution and medium to coarse gravel of the subsurface material are contained between the limits of the envelope. Upper and lower limits of both river-bed surface and subsurface grain-size distributions plot outside the envelope, thus coarse sand to fine gravels and coarse gravels to cobbles were under-represented in the bedload and even not transported after November 2003. Transport of the coarsest sizes was hydraulically limited as it happened in the November 2003 flood. Finest fractions under-represented in bedload samples were, probably, supply limited, a phenomenon not observed during the November 2003 flood (Figure 3 (C4P2)). The higher selection of fractions transported during high flows after the November 2003 flood indicates that particles were more hydraulically and supplied limited, although the $D_{50\text{-}ib}$ remained coarser. This fact is corroborated by the decrease of the standard deviation of bedload grain-sizes after the November 2003 flood stated before

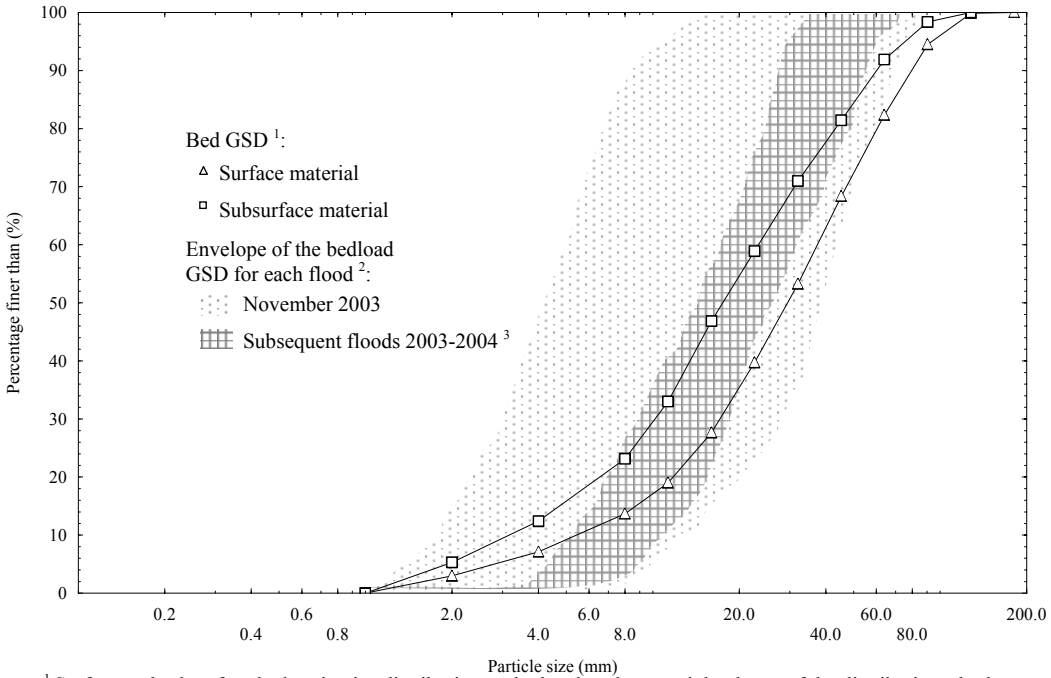

[1] Surface and subsurface bed grain-size distributions calculated as the unweighted sum of the distributions, both surface and subsurface, at the eight samples sections in summer 2003 (data from Vericat *et al.*, this issue)
[2] Range of bedload GSD for the samples collected on each flood
[3] Samples obtained during subsequent high flows after the November 2003 flood

Figure 3 (C4P2). Surface and subsurface grain-size distributions of study reach in summer 2003 (data from Vericat *et al.*, this issue) in relation to the envelopes of bedload grain-size distributions estimated for each flood

2.1.3. River-bed material mobility

The mean proportion of each grain-size in bedload samples (P_i) was scaled using the bulk sediment grain-size distribution ($f_{i\text{-}bulk}$) (Wilcock and Southard, 1988) taken as the references material (Church and Hassan, 2002) for all the sections in 2003. Bedload samples were truncated at 1 mm in order to avoid particles that could be transported in suspension. The largest particles collected were not larger than 64 mm hence no upper truncation was applied (Vericat *et al.*, this issue).

Figure 4a (C4P2) shows that sand fractions appear to be under-transported under all flows of the 2003-2004 hydrological year. After the November 2003 flood they have a smaller ratio $P_i/f_{i\text{-}bulk}$ probably because they were less available as a consequence of previous winnowing. During the 2002-2003 high flows sand had been less under-transported than during 2003-2004 and the ratio decreased as the flow strength increased (Vericat *et al.*, this issue).This phenomenon was not observed in 2003-2004. Proportion of fine gravels (2 mm) in bedload samples of 2003-2004 was lower than their frequency in river-bed material, and the difference increased after November 2003. Particles between 4 and 16 mm have relatively similar pattern of transport all along the period. Proportion ratios show that they were generally over-represented in bedload ($P_i/f_{i\text{-}bulk}>1$). Ratios varied randomly during the November 2003 flood and they were more constant during the subsequent period. For comparison, those sizes were under-transported during the December 2002, while during February and March 2003 floods they had ratios close to the unity (i.e., frequency of particles between 4 and 16 mm in bedload was practically the same than that in the bulk bed-material distribution) (Vericat *et al.*, this issue). Particles between 32 mm and 64 mm experienced transport but were under-represented in bedload, a fact suggesting that discharges during winter 2003-2004 were less competent than the precedent floods of February, March and May 2003 (Vericat *et al.*, this issue).

In general, the fractional scaled bedload transport ($i_{bi}/f_{i\text{-}bulk}$) during the November 2003 flood was higher than during the subsequent high flows, despite similar competence. Difference can be attributed to substantial reduction of the finest sizes (i.e., fine gravels to coarse sand) in transport (Figure 4b (C4P2)).

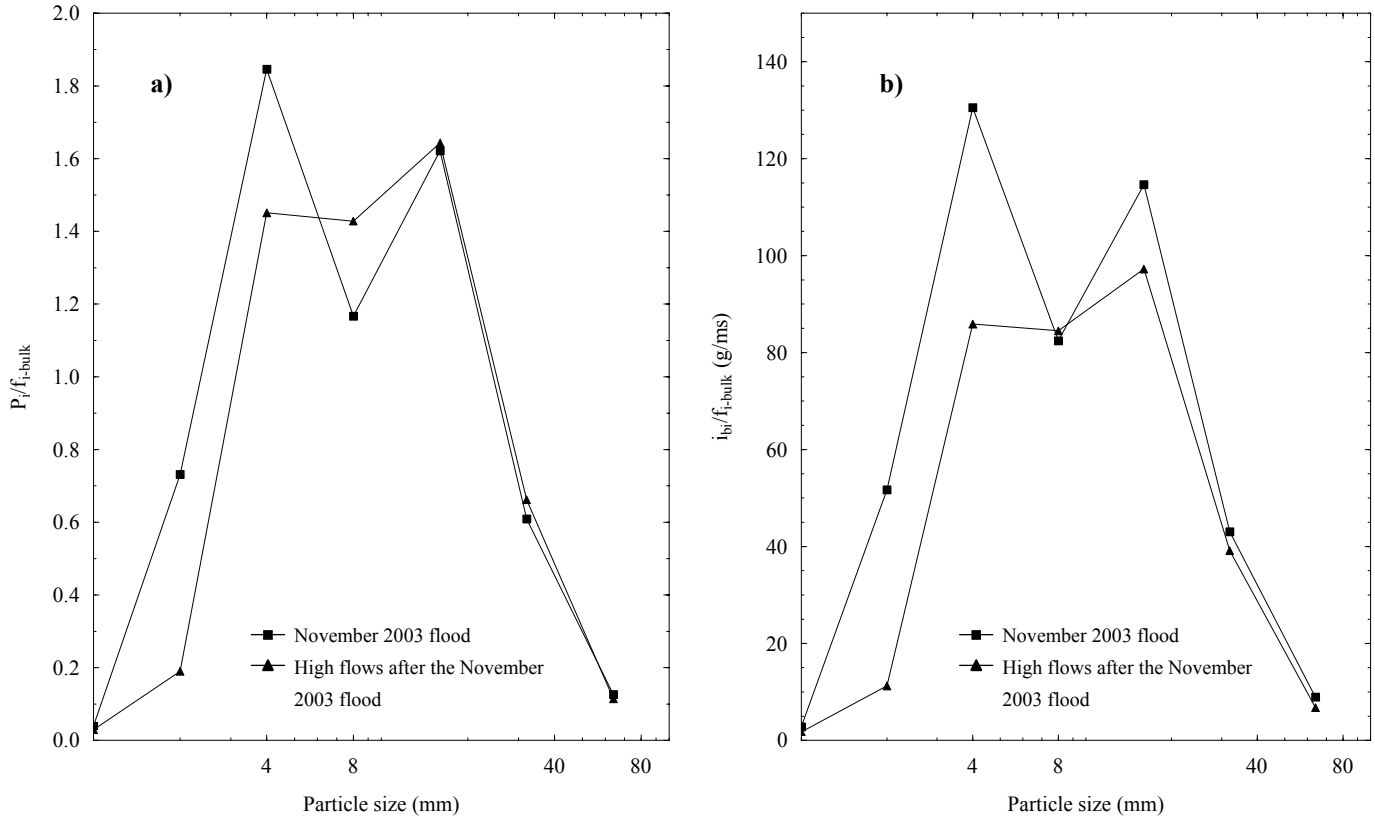

Figure 4 (C4P2). Mobility of riverbed sediment by fractions during 2003-2004 floods in the lower Ebro River: (**a**) Proportion of bedload size *i* (P_i) in bed-material ($f_{i\text{-}bulk}$), and (**b**) Bedload transport per fraction *i* in (i_{bi} in g/ms) in relation to its frequency on river-bed sediments ($f_{i\text{-}bulk}$)

Two grain-sizes had a minimum role in bedload transport during 2003-2004 (Figures 4a (C4P2) and 4b (C4P2)). On one side, particle sizes between coarse gravels and cobbles were hydraulically limited being entrained only sporadically as revealed by the range of maximum particles collected in bedload samples. On the other, hiding of small particles (<8 mm) beneath the coarse immobile layer explains their decreasing availability (Figure 4a (C4P2) and 4b (C4P2)). This process has been reported from flume experiments (e.g., Pender et. al., 2001). Limited entrainment of coarse sizes and hiding of small particles is clearly exemplified in figure 3 (C4P2) by the envelope of bedload grain-size distributions after the November 2003 flood. Particle-sizes between 4 and 16 mm had the largest role in the bedload transport during the 2003-2004 events (Figure 4b (C4P2)), a similar observation than that reported during the February and March 2003 floods (Vericat *et al.,* this issue), although less intense. The decline in bedload rates along 2003-2004 is probably related to the development of an armour layer during competent flows, which reduced

sediment availability and, consequently, lead to smaller bedload transport rates and limited mobility of grain-sizes.

2.2. River-bed grain size distribution in summer 2004

Surface and subsurface grain-size distributions were analysed separately in eight monitoring sections downstream from Flix Dam in summer 2004. The surveyed sections and the methodology used were the same than that reported by Vericat *et al.* (this issue). A total of 800 particles were measured and 8.5 m^2 (equivalent to 425 kg of material) were surveyed during the summer 2004 field campaign for the characterization of the surface material. A total of 510 kg of material were sampled and sieved to study the subsurface material grain-size distribution.

2.2.1. Surface material

Surface material was found to be coarser than the subsurface material in all sampling sections, except for section n.2 (Figure 1 (C4P2)), where no clear difference was observed hence a volumetric sample (i.e., composite by both surface and subsurface layers) was taken. Similar observation was reported in previous samplings (Vericat *et al.*, this issue). Presence of material finer than 8 mm in the riverbed surface decreased substantially in most bars in 2004, only section n.4 showing a proportion of fine material higher than 5%. Consequently, combined distributions (e.g., Fripp and Diplas, 1993) have been elaborated to determine surface grain-size distribution (Table 1 (C4P2)) (for details see Vericat *et al.*, this issue).

The estimated mean of the median surface material ($D_{50\text{-}s}$) was 43 mm, 9 mm coarser than in 2003, with an error around the mean (ε) of ±7.0 mm (Table 1 (C4P2)). Median size varied between 12 and 63 mm in the study reach, showing a coarsening trend in comparison with the median sizes observed in summer 2003. Only the sampling point n.1 showed a slight reduction of the median size, although it remains the coarsest section in the study reach. Minimum $D_{50\text{-}s}$ was again sampled in section n.4, although it was found to be 4 mm coarser than in 2003. Mean maximum surface material size ($D_{max\text{-}s}$) calculated for all the sections is almost the same than in 2003. Maximum $D_{max\text{-}s}$ was measured in section n.1,

while the minimum was observed in section n.4 as it was in 2003 (Table 1 (C4P2)). Surface bed-material sorting ($\sigma_{F\&W}$) varied between 0.5 and 1.5 (i.e., moderately well sorted to poorly sorted, respectively). Mean surface sorting for all sections was 1.0 (i.e., moderately-poorly sorted), substantially lower (i.e., better sorted) than in 2003. Maximum sorting was measured in section n.7, while the minimum was observed in section n.5, 23 km downstream from Flix Dam and few meters downstream from the confluence with the Siurana River. A general tendency to reduction in sorting was found in comparison with results of 2003. The maximum reduction occurred in section n.6, where the surface distribution changed from very poorly to moderately sorted (i.e., from 2.8 to 0.8). The generally better sorted surface distributions in 2004 reveal a smaller range of surface grain-sizes in the river-bed. This fact is probably a reflection of the bias in the balance between sediment supply and sediment transport in each section, altogether pointing towards a limitation of sediment supply so that some fractions were systematically transported without replacement.

Table 1 (C4P2). Bed-material characteristics, including armouring ratio, in the control sections of the lower Ebro River downstream from the Flix Dam (Figure 1 (C4P2)) in summer 2004

		Summer 2004								
		Surface material					**Subsurface material**			
Sampling section[1]	**ds** $_{\text{Flix Dam}}$[2] (km)	$D_{50\text{-}s}$[4] (mm)	$D_{max\text{-}s}$[6] (mm)	$\sigma_{F\&W}$[7]	**B**[8]	**Fm**[9] (%)	$D_{50\text{-}ss}$[11] (mm)	$\sigma_{F\&W}$[7]	**B**[8]	A_r[12]
Presa Flix (n.1)	0.8	63.1	154	1.2	1.7	1	29.1	2.0	2	2.2
Meandre Flix (n.2)	2.7	[5]	[5]	[5]	[5]	-	17.2	1.7	1.2	[5]
Flix (n.3)	5.6	24.5	90	0.8	-	4	12.4	1.7	-	2.0
Pas Ase (n.4)	18.3	12.5	75	1.4	-	13 [10]	10.7	1.5	-	1.2
Garcia (n.5)	22.9	42.6	138	0.5	-	4	15.6	2.2	1.7	2.7
Móra Ebre 1 (n.6)	25.2	47.2	113	0.8	-	3	17.4	2.5	1.0	2.7
Móra Ebre 2 (n.7)	26.5	54.2	135	1.5	-	4	20.4	1.6	1.4	2.7
Móra Ebre 3 (n.8)	27.8	57.6	148	0.8	-	4	21.4	2.2	-	2.7
mean[3]		43	122	1.0	-	-	18	1.9	-	2.3
standard deviation		±18	±30	±0.4	-	-	±6	±0.4	-	±0.6

[1] Location of sections is represented in figure 1 (C4P2)
[2] Localization of the sampling sections, distance from Flix Dam (km)
[3] Arithmetic mean
[4] Median surface material size (mm)
[5] Both surface and subsurface bed-material was sampled as a unique sample. Values are presented in subsurface field according the method used to sample but have not included in the mean and standard deviation computations.
[6] Maximum surface material size (mm)
[7] Folk and Ward's (1957) sorting index.
[8] Wilcock's (1993) bimodality index. B=1.7 corresponds to the bimodality threshold. Hyphen indicates that the distribution only has one mode
[9] Percentage of fine particles (<8 mm) in the surface distributions
[10] Bed surface grain-size distribution was formed by combining area by weight and pebble count samples
[11] Median subsurface material size (mm). Median size in n.2 was not included for the computation
[12] Armouring ratio estimated as the quotient between median surface and subsurface material ($D_{50\text{-}s}/D_{50\text{-}ss}$)

2.2.2. Subsurface material

Median subsurface material size ($D_{50\text{-}ss}$) sampled in summer 2004 (Table 1 (C4P2)) shows a weak coarsening trend compared with values obtained in 2003 (Vericat *et al.*, this issue). Mean $D_{50\text{-}ss}$ was 18 mm, ranging from 11 mm to 29 mm and with an estimated error around the mean (ε) of ±2.0 mm. Subsurface material was poorly sorted compared to that in the surface, similarly to the relation reported in 2002 and 2003. Sorting ($\sigma_{F\&W}$) ranged from 2.5 to 1.6 with the mean at 1.9 (Table 1 (C4P2)). Sorting changed very little in comparison with that of the surface grain-sizes and, overall, showed relatively better sorted distributions than in summer 2003. As in 2003, the greatest change occurred in section n.7 where the coefficient decreased from 2.5 to 1.6. Bimodality of subsurface material was observed in most grain-size distributions with sorting higher than 2 in 2003, and decreased with sorting in 2004 (Table 1 (C4P2)).

2.3. Changes in river-bed armouring

Armouring ratio ($A_r = D_{50\text{-}s}/D_{50\text{-}ss}$) experienced a generalised increase in 2004 in almost all sampling sections (Table 1 (C4P2)). On average, mean armouring ratio (A_r= 2.3, ε= ±0.2) increased 0.3 in relation to the ratio estimated in 2003 (A_r= 2.0, ε= ±0.3) (Vericat *et al.*, this issue). In contrast to the others, section n.1, located immediately below the Flix Dam (Figure 1 (C4P2)), presented a clear reduction in armouring owing to the decrease of the median surface material size and the increase of the subsurface median size (Table 1 (C4P2)). Scour chains and painted pebbles placed in that section did not show any significant behaviour that could explain the reduction of the armouring ratio. In any case, the degree of armouring shows that the river's transport capacity exceeded the sediment supply (A_r> 2, e.g., Bunte and Abt, 2001) during the 2003-2004 flood events.

Maximum armouring (A_r=2.7) was calculated between sections n.5 to n.8, both included (Table 1 (C4P2), Figure 1 (C4P2)). The increment of armouring compared to 2003 varied from 0.3 to 1.1. Maximum increase was observed in section n.8 (Figure 5a (C4P2)), few meters downstream from the sediment transport monitoring section (Figure 1 (C4P2)). Minimum armouring was estimated in section n.4 (Figure 5b (C4P2)), similarly to 2003 (Vericat *et al.*, this issue). Difference in changes of armouring reflects distinct sediment

supply in each monitoring section. Only in sections n.2 and n.4 (Figure 1 (C4P2)) the difference between surface and subsurface material was less than 2 (Table 1 (C4P2)). Those sections are located downstream armoured reaches and the tendency to coarsening is clear after 2004 too.

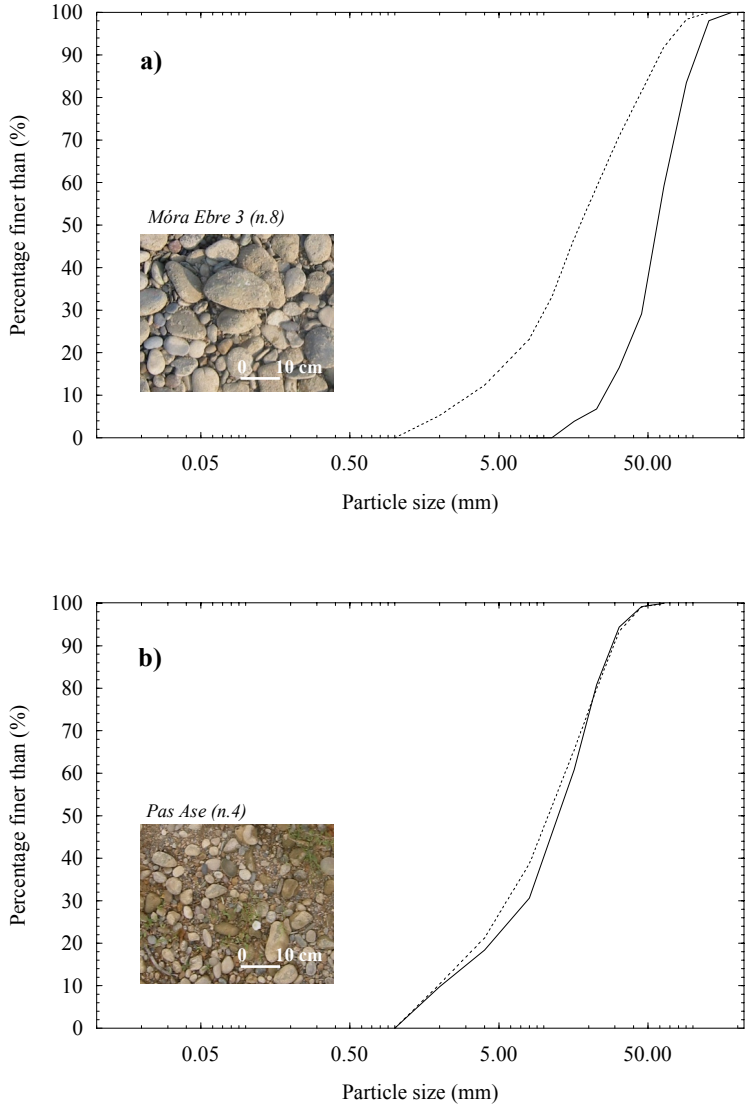

Figure 5 (C4P2). Surface and subsurface bed-material distributions of (**a**) section n.1 (highest armouring ratio) and (**b**) section n.4 (lowest armouring ratio) observed in summer 2004 (Table 1 (C4P2))

Two river reaches can be distinguished observing downstream changes in river-bed armouring (Figure 6a (C4P2)). First reach is limited by sections n.1 and n.4. It is an 18-km long section where armouring reduces downstream. As an example, distinction between surface and subsurface grain-size distributions disappears in section n.2 just 1.9 km

downstream from section strongly armoured section n.1. A similar relation was observed in field campaigns of 2002 and 2003 (Vericat *et al.*, this issue). Further downstream, in section n.4, river-bed surface and subsurface distributions are very similar again (Table 1 (C4P2)and Figure 6a (C4P2)). Second reach comprises sections n.5 to n.8 (Figure 1 (C4P2)). Downstream the confluence of the Ebro and the Siurana rivers (Figure 1 (C4P2)) armouring increases and remains rather constant (A_r= 2.7), with the highest values estimated in 2004 (Table 1 (C4P2) and Figure 6a (C4P2)).

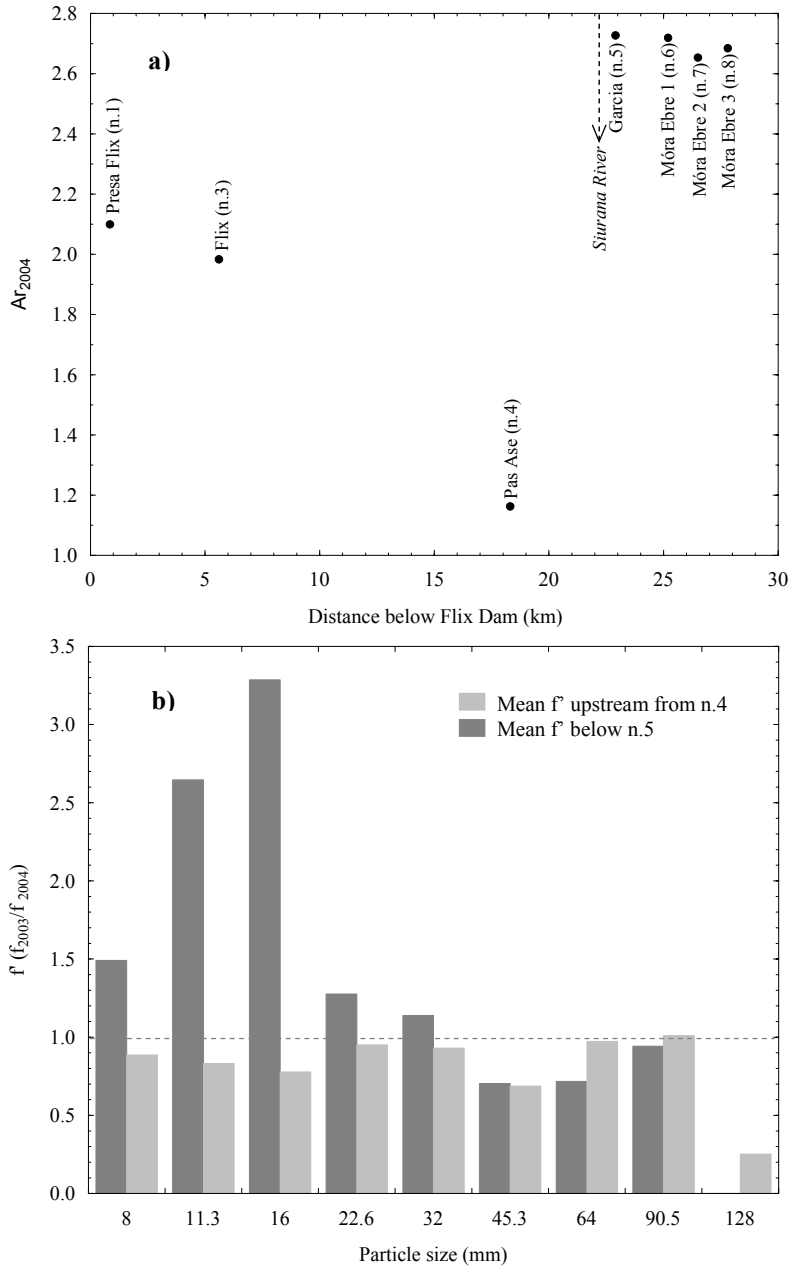

Figure 6 (C4P2). (**a**) Downstream change of armouring (A_r) in the lower Ebro River in 2004. Note the stabilization of A_r downstream the confluence with the Siurana River (see text for discussion). (**b**) Changes in proportion of surface sizes classes (f') after 2003-2004

Surface grain-size distributions of 2003 (Vericat *et al.*, this issue) and 2004 have been compared to assess changes on bed surface material after the 2003-2004 small floods. Distributions were truncated at 8 mm because finest fractions were not representative (i.e., <5%) in 2004. Frequency of each grain-size class in 2003 ($f_{i\text{-}s03}$) was divided the frequency in 2004 ($f_{i\text{-}s04}$). A quotient ($f'=f_{i\text{-}s03}/f_{i\text{-}s04}$) higher than 1 means that the proportion of a particle size *i* in the surface decreased in 2004, indicating that the fraction *i* became supply limited. In contrast, when f' is lower than 1 the proportion of a particle size *i* in the surface increased in 2004, owing to fractions whose transport was limited and, as a consequence of the winnowing of smaller particles, increased their frequency in the distribution. Figure 6b (C4P2) shows that the proportion of the different surface grain-sizes between sections n.1 and n.4 remains rather similar after floods occurred in winter 2003-2004. Only for the coarsest fraction *i*= 128 mm the ratio f' is clearly lower than 1, a fact controlled by the increase of large clasts in section n.1, the coarsest surface bar in the whole study reach. The supply and transport of sediment appear to be in balance in this reach. River-bed processes are different downstream section n.5 (second reach). Finer fractions (i.e., 8 to 32 mm) exhibit lower proportion in 2004 compared to 2003, indicating that those classes experienced supply-limited conditions. Scour chains and painted pebbles surveyed in summer 2004 strength this hypothesis. The transport of medium to coarse gravel occurred at a higher level than the supply from upstream reaches, a fact that is corroborated by the surface coarsening observed in the field (Table 1 (C4P2)). The Siurana River experiencing high flow regulation and gravel mining cannot mitigate the lack of sediment in the Ebro River.

2.4. Discussion

Under a general supply-limited scenario, the magnitude of floods that occurred in the lower Ebro River downstream from the Flix dam during the study period 2002-2004 controlled the degree of change of river-bed grain-size distribution. High magnitude events occurred in 2002-2003 caused the breaking of the stable armour layer present in several sections after two years of low flows, entraining and transporting most river-bed surface and subsurface size-classes, causing river-bed incision, and increasing the bedload transport during successive events (Vericat *et al.*, this issue). In contrast, low magnitude floods succeeded in 2003-2004 reformed and re-established the surface armour layer (Table 1

(C4P2)), increasing the stability of surface river-bed structure, and decreasing the supply of subsurface sediment during potentially competent high flows.

The comparison of the 2002 (Vericat *et al.*, this issue) and the 2004 surface grain-size distributions indicate that, overall, there is a sustained coarsening process in the study reach combined with a decrease of sediment sorting ($\sigma_{F\&W}$). In particular, downstream from section n.5 transport of particles between 8 and 32 mm was higher than their supply from upstream reaches, a phenomenon that progressively reduced the amount of sediment available for transportation during still competent flows in 2003-2004. The loss of gravels from the surface due to continuous winnowing poses ecological consequences such as fish habitat degradation.

Figure 7 (C4P2) shows the bedload transport rates during the 2002-2003 floods. Data reflects the erratic bedload pattern during the December 2002 flushing flow and the remarkable increase of bedload transport during February and March 2003 floods as a consequence of the breaking of the armour layer occurred in December 2002. The river experienced widespread incision (Vericat *et al.,* this issue). Bedload rates diminished during the November 2003 flood and the subsequent high flows. This fact would suggest the increasing role of the armour layer in controlling bedload transport. Armouring may have started during the small May 2003 flood but, unfortunately, bedload was not sampled (Vericat et al., this issue). However, selective transport occurred during the November 2003 flood reinforced the hypothesis of the on-going armouring of the river-bed (Figure 3 (C4P2)). No major incision was observed during 2003-2004 along the study reach.

Under natural conditions, competent floods entrain river-bed surface and subsurface sediments, maintaining river's ecological functioning and transferring sediment to the lowermost reaches. In contrast, under the absence of sediment supply from upstream, such floods cause incision. Further, sediment competence and transport decrease with flow magnitude, and under the same lack-of-sediment conditions, selective transport occurs and a tendency towards coarsening of the river-bed surface may be observed. This phenomenon affects the functioning of the river's ecosystem, increases the downstream sediment deficit but, in contrast, minimises incision. This work has described a complete two-year incision-armouring cycle in the lower Ebro River under no-sediment supply

conditions. Results are of fundamental use in the design and implementation of river restoration programmes seeking equilibrium between water, sediment and riverchannel processes in this as well as in other large regulated fluvial systems.

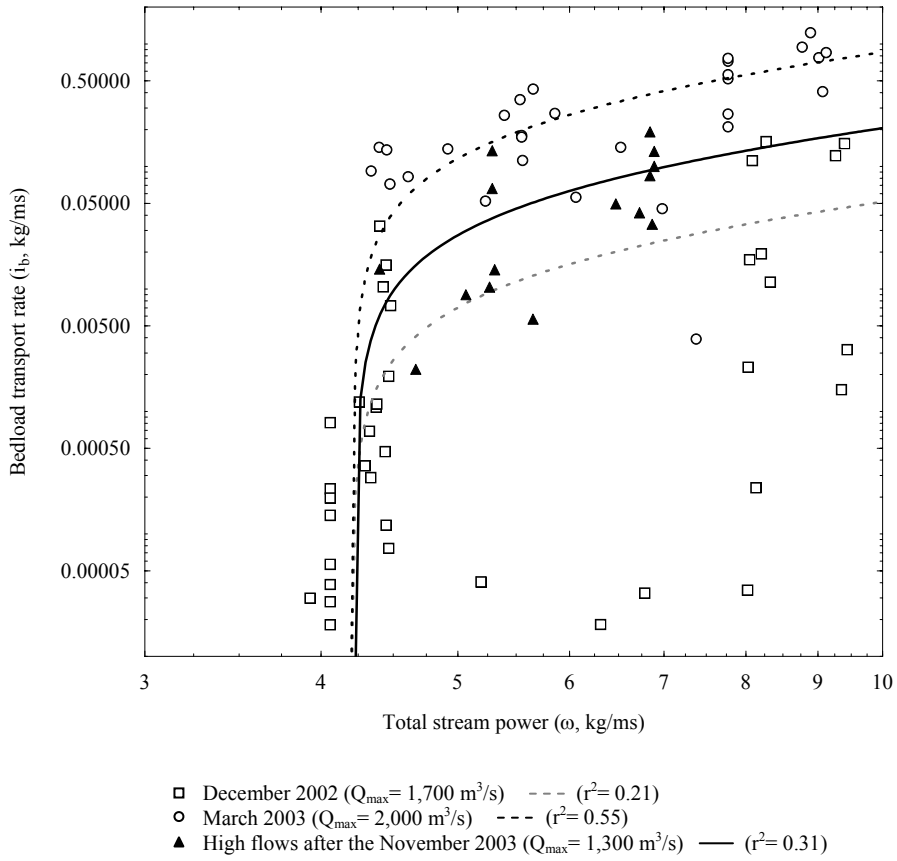

Figure 7 (C4P2). Relation between total stream power (ω) and bedload transport rate for selected floods occurred during 2002-2004

3. Conclusions

This paper reports on river-bed armouring observed after small frequent floods occurred in winter 2003-2004 in the lower Ebro River. Main conclusions can be drawn as follows:

- River-bed grain-size distribution observed in summer 2004 below the Flix Dam showed that surface material was clearly coarser and better sorted than the material in the subsurface, very similar to the results observed in summer 2002. Mean armouring ratio rose again to 2.3, showing a clear stabilization at around 2.7 in section of the reach downstream from the confluence with the Siurana River.

- The low magnitude of flows during the winter 2003-2004 reinforced the formation of a new armour layer in most of the monitoring sections, a process probably initiated during small floods at the end of the winter 2002-2003.
- River-bed armouring reduced the availability of sediment to be transported, leading to an average three-time decrease of the bedload transport rates hence minimising the river-bed incision. Grain-sizes between 8 and 32 mm were the most affected by the supply-limited conditions.

The papers have reported on a complete two-year incision-armouring cycle in a large river under no-sediment supply conditions. Analysis of river-bed and bedload grain-size distributions has shown that armouring is an important process in regulated fluvial systems and that it is the consequence of the disequilibrium between sediment transport (flow competence) and sediment supply.

Acknowledgements

This research was carried out within the framework of the research project REN2001-0840-C02-01/HID, which is funded by the Spanish Ministry of Science and Technology. The first author received a grant from the Spanish Ministry of Education. Hydrological data was supplied by the Ebro Water Authorities. The Móra d'Ebre Town Council provided logistic support. Albert Rovira at the University of Lleida provided assistance during fieldwork. Michael Church at the University of British Columbia undertook a helpful review of the first version of the manuscript.

Notations

A_r	Armouring ratio (quotient between $D_{50\text{-}s}$ and $D_{50\text{-}ss}$, e.g., Lisle and Madej, 1992).
B	Bimodality index (Wilcock, 1993)
$D_{50\text{-}ib}$	Median bedload grain-size (mm)
$D_{50\text{-}s}$	Median surface grain-size (mm)
$D_{50\text{-}ss}$	Median subsurface grain-size (mm)
d_i	Particle size *i* (mm)
$D_{max\text{-}ib}$	Maximum bedload grain-size (mm)
$D_{max\text{-}s}$	Maximum surface grain-size (mm)
$f_{i\text{-}bulk}$	Frequency of a given size *i* in bulk sediments
$f_{i\text{-}s03}$	Frequency of each surface grain-size class in 2003
$f_{i\text{-}s04}$	Frequency of each surface grain-size class in 2004
f'	Ratio between $f_{i\text{-}s03}$ and $f_{i\text{-}s04}$ reflecting changes of surface grain-size frequencies
i_b	Mean instantaneous bedload transport rate (g/ms)
i_{bi}	Bedload transport rate by fraction *i* (g/ms)
$i_{bi}/f_{i\text{-}bulk}$	Bedload transport of fraction *i* related to its frequency in river-bed sediments ($f_{i\text{-}bulk}$)
$i_{b\text{-}m}$	Mean bedload transport rate (g/ms)
P_i	Frequency of a given transported size *i* in a bedload sample
$P_i/f_{i\text{-}bulk}$	Proportion of bedload size *i* in bed-material (bulk sediment)
Q_i	i-year flood calculated from the Tortosa gauging station flow series (Batalla *et al.*, 2004)
Q_{max}	Maximum discharge (m^3/s)
ε	Estimation error around the mean ($\varepsilon = \sigma/\sqrt{N}$, where σ is the standard deviation and N the number of data)
σ	Standard deviation
$\sigma_{F\&W}$	Sorting index (Folk and Ward, 1957)
ω	Total stream power (kg/ms) (Bagnold, 1980)

References

Bagnold, R.A. 1980. An empirical correlation of bedload transport rates in flumes and natural rivers. *Proceedings of the Royal Society* **372A**: 453-473.

Batalla, R.J., Kondolf, G.M., Gomez, C.M., 2004. Reservoir-induced hydrological changes in the Ebro River basin, NE Spain. *Journal of Hydrology* **290**: 117-136.

Brandt, S.A., 2000. Prediction of downstream geomorphological changes after dam construction: a stream power approach. *International Journal of Water Resources Development* **16**(3): 343-367.

Bunte, K., Abt, S.R., 2001. *Sampling surface and subsurface. Particle-size distributions in wadable gravel- and cobble-bed streams for analyses in sediment transport, hydraulics, and streambed monitoring*. U.S. Department of Agriculture, Forest Services, Rocky Mountain Research Station.

Church, M., Hassan, M.A., 2002. Mobility of bed material in Harris Creek. *Water Resources Research* **38**(11).

Fassnacht, H., McClure, E.M., Grant, G.E., Klingeman, P.C., 2003. Downstream effects of the Pelton-Round Butte hydroelectric project on bedload transport, channel morphology, and channel-bed texture, lower Deschutes River, Oregon. *Water science and Application* **7**: 175-207.

Folk, R.L., Ward, C., 1957. Brazos River bar: a study in the significance of grain size parameters. *Journal of Sedimentary Petrology* **27**(1): 3-26.

Fripp, J.B., Diplas, P., 1993. Surface sampling in gravel streams. *Journal of Hydraulic Engineering* **119** (4): 473-490.

Gomez, B., 1983. Temporal variations in bedload transport rates: the effect of progressive bed armouring. Earth Surface Processes and Landforms **8**: 41-54.

Gomez, B., 1994. Effects of particle shape and mobility on stable armour development. Water Resources Research **30**(7): 2229-2239.

Kondolf, G.M., 1994. Geomorphic and environmental effects of instream gravel mining. *Landscape and Urban Planning* **28**: 225-243.

Kondolf, G.M., 1997. Hungry Water: Effects of Dams and Gravel Mining on River Channels. *Environmental Management* **21**(4): 533-551.

Leopold, L.B., Wolman, M.G., Miller, J.P., 1964. *Fluvial processes in Geomorphology*, San Francisco: W.H. Freeman; 522p.

Lisle, T.E, Madej, M.A., 1992. Spatial variation in a channel with high sediment supply. In *Dynamics of Gravel Bed Rivers*, Billi, P., Hey, R.D., Thorne, C.R., Tacconi, P., (eds.), New York: John Willey; 277-291.

Milhous, R.T., 1982. Effect of sediment transport and flow regulation on the ecology of gravel bed rivers. In *Gravel Bed Rivers*, Hey, R.D., Bathurst, J.C., Thorne, C.R., (eds.), Chichester: John Wiley and Sons; 819-842.

Palau, A., Batalla, R.J., Rosico, E., Meseguer, A., Vericat, D., 2004. Management of water level and design of flushing floods for environmental river maintenance downstream of the Riba-Roja Reservoir (Lower Ebro River, NE Spain). *Proceedings of the International Conference HYDRO 2004: A New Era for Hydropower*. Porto, Portugal, 18-21 October 2004.

Parker, G., Klingeman, P.C., 1982. On why gravel bed streams are paved. *Water Resources Research* **18**: 1409-1423.

Parker, G., Sutherland, A.J., 1990. Fluvial armour. *Journal of Hydraulic Research* **28**: 529-544.

Pender, G., Hoey, T.B., Fuller, C., McEwan, I.C., 2001. Selective bedload transport during the degradation of a well sorted graded sediment bed. *Journal of Hydraulic Research* **39**: 269-277.

Petts, G.E., 1980. Morphological changes of river channels consequent upon headwater impoundment. *J. Inst. Water Engrs Sci.* **34**(4): 374-382.

Petts, G.E., 1984. *Impounded Rivers. Perspectives for Ecological Management*. Wiley, New York; 326 p.

Schumm, S.A., 1977. *The fluvial system*. John Wiley and Sons, New York.

Sear, D.A., 1992. Impact of hydroelectric power releases on sediment transport processes in pool-riffle sequences. In *Dynamics of Gravel Bed Rivers*, Billi, P., Hey, R.D., Thorne, C.R., Tacconi, P., (eds.), New York: John Willey; 629-649.

Sear, D.A., 1995. Morphological and sedimentological changes in a gravel-bed river following 12 years of flow regulation for hydropower. *Regulated Rivers: Research and Management* **10**: 247-264.

Shields, A., 1936. Anwendung der Aehnlichkeitsmechanik und der Turbulenzforschung auf die Geschiebebewegung. *Mitteilung der Preussischen Versuchsanstalt für Wasserbau und Schiffbau 26*, Berlin

Topping, D.J., Rubin, D.M., Vierra, L.E., 2000. Colorado River sediment transport 1. Natural sediment supply limitation and the influence of Glen Canyon Dam. *Water Resources Research* **36**(2): 515-542.

Vericat, D., Batalla, R.J., 2005. Sediment transport in the lower Ebro River (NE Iberian Peninsula). *Geomorphology* (submitted).

Wilcock, P.R., 1993. Critical shear stress on natural sediments. *Journal of Hydraulic Engineering* **119**: 491-505.

Williams, G.P., Wolman, M.G., 1984. *Downstream Effects of Dams on Alluvial Rivers*. US Geological Survey Professional Paper 1986.

Xu Jiongxin, 1996. Underlying gravel layers in a large sand bed river and their influence on downstream-dam channel adjustment. *Geomorphology* **17**:351-359.

3. RIVER-CHANNEL MORPHOLOGY

Batalla, R.J., Vericat, D., Ida, T. (2005): River-channel changes downstream from dams in the lower Ebro River. *Zeitschrift für Geomophologie* (submitted)

River-channel changes downstream from dams in the lower Ebro River

Abstract

Changes in river morphology downstream from three large dams in the lower Ebro River (NE Iberian Peninsula) has been characterised by means of air photos analysis and fieldwork. The lack of sediment transport and the reduction of frequent floods below the lowermost dam of Flix are the main factors controlling riverchannel adjustments. Around 4 ha of sedimentary active areas were covered by vegetation between 1956 and 2002, thus decreasing sediment availability, and channel width has reduced around 20%, on average, thus reducing the active section of the channel. Overall 30% of the formerly open bars are nowadays occupied by mature riparian forest. *Tamaricetum canariensis* and *Rubio-Populetum albae* are the most common communities responsible of the shrub and tree-like revegetation of active areas. In addition, vegetation encroachment stabilises channel edges of the river and, consequently, alters flow hydraulics (e.g. roughness), hence riverbed processes (e.g. incision), particularly during flood events.

Keywords: flow regulation, sediment availability, river morphology, vegetation encroachment, Ebro River

1. Introduction

Dams disrupt the continuity of water and sediment transfer in river systems, which in turn affect river's morphology and ecology. A number of papers have discussed the effects of dams on river downstream flow regime (e.g. Williams & Wolman 1984, Richter et al. 1995). The effects of a given reservoir on flow regime will depend on its capacity in comparison with river runoff, its purpose (e.g. irrigation, hydroelectric generation, flood control), and its operating rules, precluding simple generalizations about the post-dam discharge distributions (Williams & Wolman 1984). Dams diminish the magnitude of floods, which transport the majority of sediment. In different rivers of the Sacramento-San Joaquin River system of California, the discharge with a 2-year recurrence interval (Q_2) was reduced below dams from 35% to 95% of pre-dam values, while the Q_{10} was reduced from 2% to 78%, depending on the reservoir size and operating rules (Kondolf & Mathews 1993). Similar trends have been reported for the whole Ebro basin (Batalla et al. 2004). In contrast, if floods are reduced and the flow released from dams cannot transport the sediment supplied by tributaries, sedimentation in the river channel may occur. For instance, in the Rio Grande, below Elephant Butte Dam, the material carried by tributaries caused important channel aggradation (Howard & Dolan 1981).

Dams alter the transference of sediment within the river system by trapping all bedload and an important part of the suspended load. As a consequence, dams release sediment-starved flows to downstream reaches, which may transport sand and gravel downstream without replacement from upstream, resulting in coarsening of the surface layer (armouring) (Williams & Wolman 1984), and may erode the bed, resulting in incision, and can undercut banks, thereby causing widening (Kondolf 1997). As an example, downstream from the Davis Dam, in the Colorado River, the channel has incised up to 6 metres (Williams & Wolman 1984). Channel changes caused by hungry water can cause notable alterations in river ecology and, at-a-long term, may damage foundations of bridges and other infrastructures.

Vegetation in and along channels downstream from the dams generally increases and, in some cases, encroachment of vegetation can be very extensive (Williams & Wolman 1984). The lack of floods prevent that seedlings of riparian plants be scoured to avoid

establishment of mature plants with roots resistant to scour (Kondolf & Wilcock 1996). With reduced flood flows, riparian vegetation can colonize the formerly active channel and induce deposition (within the vegetation) during subsequent high flows (Williams & Wolman 1984, Kondolf & Wilcock 1996), reducing the sediment availability from active channels. Vegetation encroachment and associated channel narrowing can reduce the hydraulic capacity of the channel and reduce the area of available aquatic habitat (Ligon et al. 1995).

Several works describing effects of altered flow regimes have addressed adjustments in channel form due to hydrologic change (e.g. Williams 1978). Within this context, this paper aims at characterising the changes in channel morphology of the Flix Meander in the lower Ebro River (NE Iberian Peninsula) downstream from dams. Changes occurred in the river channel during the 20^{th} century are described in relation to the reduction of floods and, especially, to the lack of sediment transport through the study reach. Encroachment of vegetation is taken as the main indicator to assess the river adjustments. The river does not receive any significant contribution of water and sediment along the study reach, so it can be considered a natural flume to analyse changes in fluvial dynamics due to dams during an almost eight-decade period.

2. Study area

The Flix Meander is located in the lower Ebro River, the second largest drainage basin in the Iberian Peninsula. It drains 85,530 km^2 along the southern-facing slopes of the Cantabrian Range and Pyrenees, and the northern-facing slopes of the Iberian Massif, and debouches into the Mediterranean downstream from Tortosa, 180 km south of Barcelona (Figure 1 (C4P3)). Mean annual precipitation varies from over 2000 mm in the Pyrenees to less than 400 mm in the arid interior. Mean annual runoff at Tortosa is 167 mm equivalent to a water yield of 14,300 hm^3 (e.g. 1 hm^3 = 1 x 10^6 m^3). Maximum peak flow was around 12,000 m^3/s in 1907 in Tortosa (NOVOA 1984).

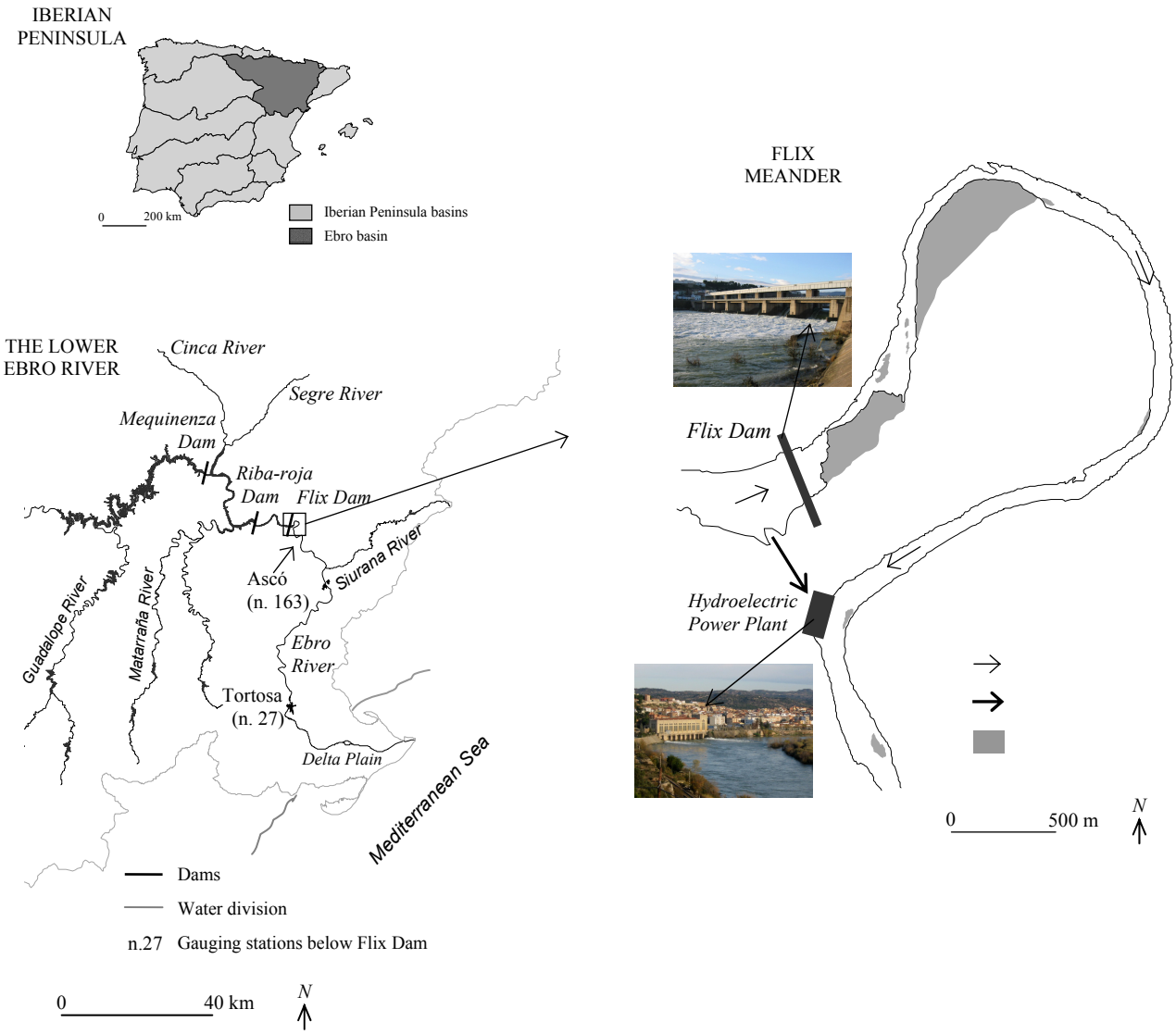

Figure 1 (C4P3). Location of the study reach in the lower Ebro River (NE Iberian Peninsula). For reference, we indicate the Flix Dam, built up in 1948 storing 11 hm^3 of water, and the associated hydroelectric power plant, holding a maximum generating discharge of 400 m^3/s

Almost one hundred ninety reservoirs regulate almost 60% of the Ebro River's total annual runoff. Virtually all dams were constructed during the 20th century, with 67% of reservoir capacity built in the 1950-1975 period. Mequinenza (1966) is the largest dam in the basin with a capacity of 1,534 hm^3 (11% of the river's annual runoff). The Ribarroja Dam (1969) has a capacity of 207 hm^3 and impounds the two largest tributaries of the Ebro (the Segre and the Cinca rivers). The lowermost impoundment is the Flix Dam (1948), with a capacity of 11 hm^3. The three of them complete a 120 km-long reservoir chain in the lower

Ebro (Figure 1 (C4P3)). The main purpose of the three dams is hydro-power generation. Of especial relevance for the objective of this paper is the location of the Flix Dam and the associated power plant. Water is diverted from the reservoir, hence upstream the meander, through a 12-m head tunnel at a maximum discharge of 400 m^3/s. After turbination water is released to the river at a section downstream the meander (Figure 1 (C4P3)). Most part of the year, water discharged from the dam to the meander is very low (few cubic meters per second) this fact inducing that, except during floods, water from the generation plant goes up the river and gently occupies the lowermost sections of the meander.

Dams have altered the downstream hydrology of the lower Ebro River. Downstream from the Mequinenza and Ribarroja dams, frequent floods responsible for most river's geomorphic work (e.g. Q_2 to Q_{25}) have been reduced by around 25%, on average (Batalla et al. 2004). Moreover, dams trap most of the sediment transported in the basin and in the river mainstem. Estimated total annual sedimentation in the basin's reservoirs is 15 hm^3 (Sanz et al. 1999, Batalla 2003). In particular, sediment trapping efficiency for suspended sediment in the Mequinenza and Ribarroja reservoirs has been estimated at around 90%, following the method of Brune (1953). According to data from Bayerri (1934-1935) and further estimates by Nelson (1990) the annual sediment contribution of the Ebro to its delta at the beginning of the 20^{th} century was around 15 x 10^6 tonnes, mostly in suspension. Recent estimates by Vericat & Batalla (2005b) annual sediment transport in suspension downstream dams is 0.25 x 10^6 tonnes. In addition, all bedload is trapped by reservoirs. The lower Ebro River does not receive coarse fractions from upstream dams, but it maintains a high level of bedload transport capacity since floods have not been dramatically reduced. Therefore, sediment is typically entrained from the riverbed and from lateral deposits, and deposited in the lowermost reaches of the river (Vericat & Batalla 2004). The lack of sediment and the reduction of floods have caused changes in river channel morphology, mainly revegetation of formerly active areas, riverbed coarsening, and erosion of channel banks (e.g. Sanz et al. 1999, Vericat & Batalla 2004).

The Flix Meander is located below the Flix Dam (Figure 1 (C4P3)). It is a single-thread channel reach of 5.5 km with a sinuosity index (Leopold et al. 1964) of 3.5. Mean channel width is 78 m and mean slope is 8.5 x 10^{-4}. Mean particle size ranges from 17 to 60 mm in

the surface and at around 12 mm in the subsurface. Analysis of riverbed materials shows armouring (Vericat & Batalla 2005b) as the common grain-size pattern in several reaches of the river. Riverine vegetation is dominated by associations such as *Tamaricetum canariensis*, *Rubio-Populetum albae*, and *Hedero-Ulmetum minoris*.

3. Methods

3.1. Image processing

The long-term evolution of the Flix meander has been analysed by means of a series of air photos and orthophotos taken before (1927 and 1956) and after (1995, 1999 and 2002) the construction of the large Mequinenza and Ribarroja dams (Table 1 (C4P3)). Images were processed by means of a series of specialised software, such as ArcView GIS 3.2.®, ENVI 3.4.®, ERDAS 8.6.® and IDRISI 32®. In order to study the riverchannel changes consecutives images of the same river reach have to be superimposed, hence all images of the 1927, 1956 and 1995 series were geometrically corrected to give them the real coordinates. The air-photo series of 1999 was taken as reference. A simple linear regression model was used to transform original coordinates to reference coordinates (Chuvieco 1995). Table 2 (C4P3) presents the control points and the Root Mean Square Error (RMSE) for each air-photo series. Acceptable errors were established at 2 pixels for the 1927 series and 1.5 pixels for the 1956 and 1995 series. Digital Levels -DL were transferred to the corrected positions were done by means of bilinear interpolation resulting from the averaged mean DL of the four closest pixels (Chuvieco 1995).

Table 1 (C4P3). Series of air photos used to characterise riverchannel changes and vegetation encroachment in the Flix Meander

Air-photo series	Date	Scale	Spatial resolution	Image Type
1927	-[1]	1:10,000	1 m	Orthophoto
1956	06/09/1956	1:34,000	3 m	Air photo
1995	15/04/1995	1:32,000	3 m	Panchromatic photo
1999	-[1]	1:10,000	1 m	Panchromatic photo
2000	June 2002	1:5,000	0.5 m	3-band photo (A,V, R)

[1] unknown

Table 2 (C4P3). Ground control points used to do geometric corrections of old series of air photos and to give them real coordinates

Air-photo series	GCP[1]	RMSE (X)[2]	RMSE (Y)[3]	Total RMSE[4]	Total RMSE (m)[5]
1927	11	1.50	0.47	1.75	1.75
1956	8	0.81	0.95	1.38	4.14
1995	8	1.31	0.49	1.40	4.20

[1] Ground Control points
[2] Root Mean Square Error for the X coordinates (in pixel)
[3] Root Mean Square Error for the Y coordinates (in pixel)
[4] Total Root Mean Square Error (in pixel)
[5] Total Root Mean Square Error (in meters)

The series of air-photos have been analysed in order to determine changes in riverchannel morphology and vegetation. Special attention has been paid to the differentiation of active and vegetated areas along the meander during the 20th century (Figure 2 (C4P3)). Several degrees of vegetation cover and structure have been established and used to determine progressive vegetation encroachment in formerly active areas. Changes in channel width along the study period have also been documented. Daily discharge registered at the downstream gauging station of Ascó (n. 163) (Figure 1 (C4P3)) at the day the air photos were taken varied from 98 m^3/s in the 1956 series to 225 m^3/s in the 1999 series, resulting in a difference of few centimetres in water depth and few decimetres in channel width in the study reach. Therefore no major interpretation error related to the discharge is expected. Remarkably, since 1948 most river flow, especially below 400 m^3/s, does not circulate through the meander but it is diverted from the reservoir through the hydroelectric power plant (Figure 1 (C4P3)). In terms of flow duration, 400 m^3/s is a discharge equalled or exceeded 25% of the time.

3.2. Fieldwork

Fieldwork was done in the Flix meander in June 2004 to verify features observed in recent air-photos related to: a) riverchannel morphology, b) vegetation species and communities, and c) land uses in the vicinity of the river. Two cross sections were surveyed by means of an ecosound Lowrance LCX-15 (decimetric resolution) and a total station (Vericat & Batalla 2005b). Riverbed material was sampled in 2002, 2003 and 2004 in order to characterise its grain size distribution and evolution (Vericat & Batalla 2005b). We sampled surface and subsurface material separately. The surface layer was characterised

using the pebble count method measuring the b axis of 400 particles (Wolman 1954, Rice & Church 1996). The subsurface material was sampled using the volumetric technique, in which the D_{max} did not exceed 1% of sample weight (Church et al. 1987).

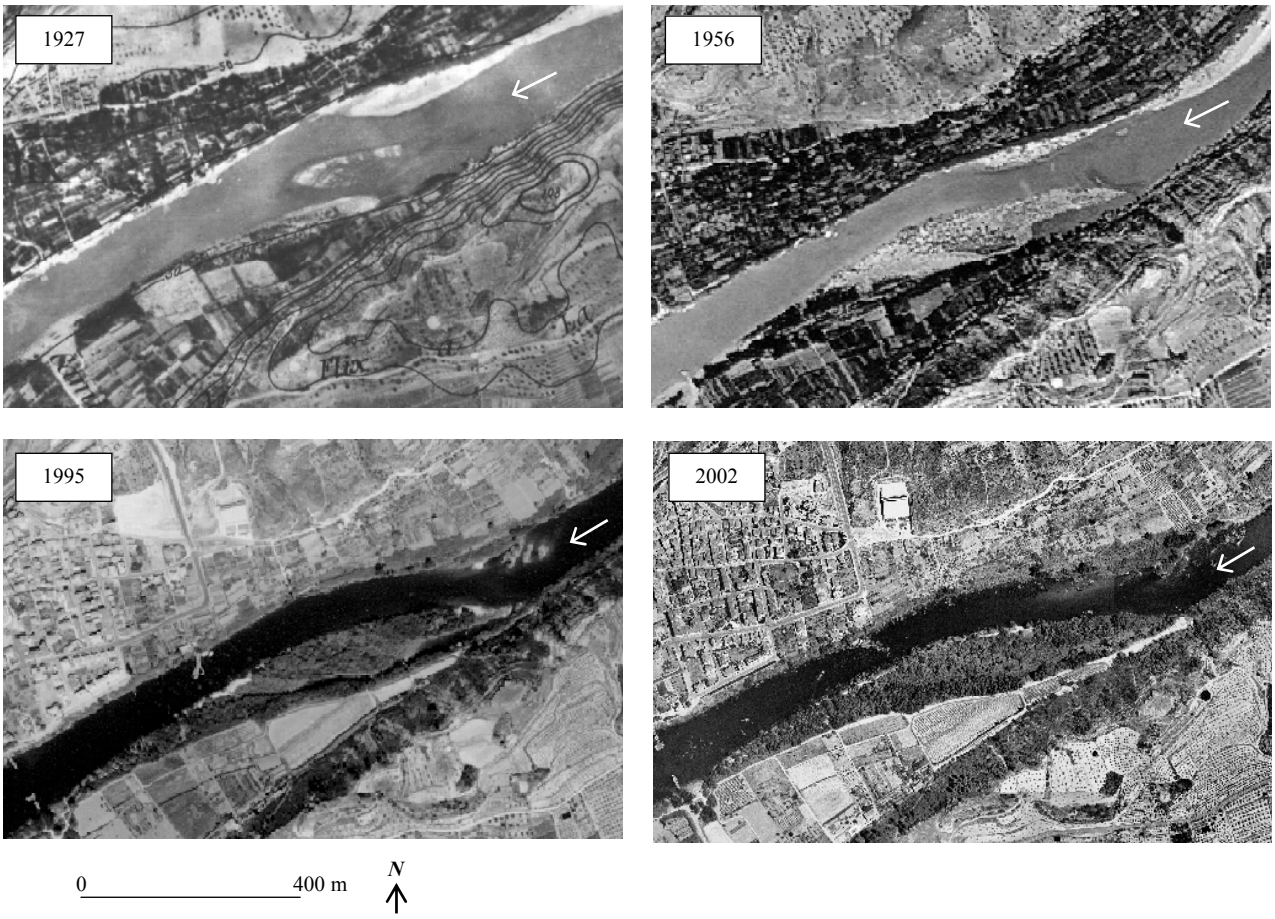

Figure 2 (C4P3). Disappearance of active areas due to vegetation encroachment and changes in bars configuration immediately downstream the Flix Dam between 1927 and 2002

Once the fieldwork campaign was finished, information was used to determine the changes-by-area of river morphology (e.g. active areas, channel width) and the evolution of vegetation encroachment within each study period (1927-1956, 1956-1995, and 1995-2000). Cross sections and grain-size were used to determine the hydraulic characteristics (e.g. stream power) of selected floods in the study reach. Data from field observations and image interpretation were put together in a GIS database as bases for future studies in the Ebro River.

4. Results

4.1. Riverchannel changes

Changes related to river morphology and sedimentary characteristics observed in the Flix meander between 1927 and 2002 are twofold: a) aggradation (i.e. creation of new active sedimentary areas) until 1956, and degradation (i.e. loss of active areas) from 1956 until 2002 (Figures 2 (C4P3) and 3 (C4P3)), and b) strong reduction of channel width between 1927 and 1956 and stabilization after that.

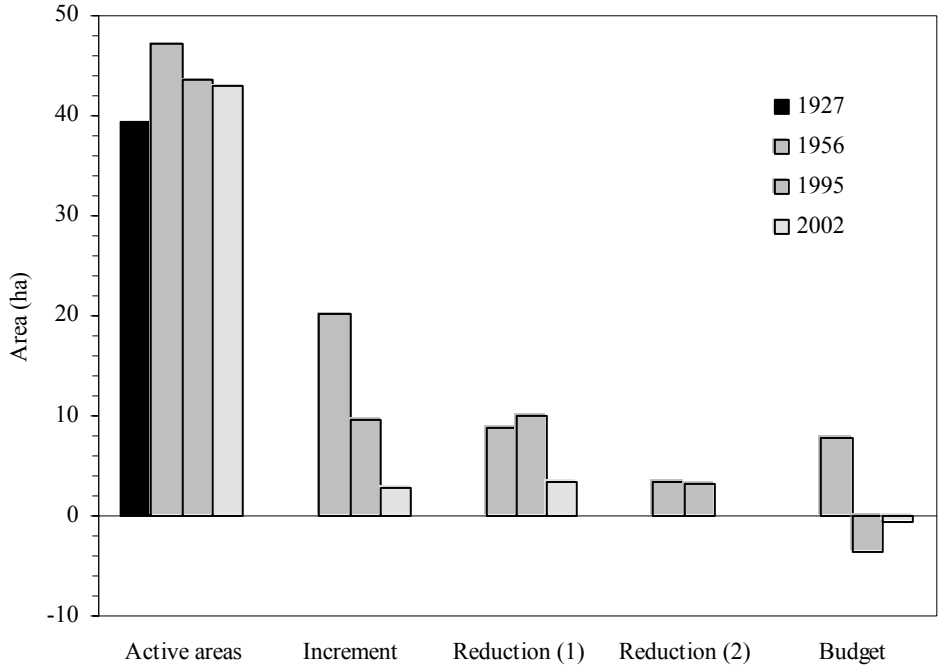

Figure 3 (C4P3). Evolution of active areas (open bars) in the Flix Meander between 1927 and 2002

Aggradation in the riverchannel is evident before 1956, especially in the reach immediately below the dam, a fact that could hypothetically be the consequence of two successive events: the extraordinary flood of 1937 and the immediate construction of the Flix Dam from 1940 and its closure in 1948. Large bars such as those observed below the dam in the air photo of 1956 are reported to built up during high energetic floods (e.g. Smith 1974), as the one occurred in the Ebro in 1937 (the second largest during the 20th century with an estimated discharge of the order of 10,000 m^3/s in Tortosa). After 1948 bars got progressively stabilized due to the drastic reduction of river competent discharges that flow through the meander since the closure of the dam. As described, the intake

located upstream the dam diverts water through a tunnel to the hydroelectric plant at a capacity of 400 m^3/s, a value equivalent to the river mean discharge. Only when the discharge excesses that value the flow is released to the meander. As a direct effect, the meander receives a minimum discharge of few cubic meters per second most part of the year. This fact, in turn, leaved areas (bars), which were habitually submerged prior the construction of the dam, opened. Changes in bars configuration can also be observed (Figure 2 (C4P3)). Between 1956 and 1995 there was a general reduction of sediment active areas in direct relation to the progressive encroachment of vegetation, especially on marginal bars (Figure 2 (C4P3)). Sanz et al. (1999) reported similar observations downstream from the Flix meander. Lateral bar migration has also been observed.

Degradation of the riverchannel can be assessed analysing the evolution of bars. The river had 15 open (marginal) bars in 1956 and 7 of the same characteristics in 2002. In addition, agricultural fields occupied formerly active areas taking advantage of the evident reduction of high flows in the meander from the 1950s. Some erosion is observed immediately below the dam and in few points along the meander, a typical phenomenon in rivers downstream dams, as reported elsewhere (e.g. Williams & Wolman 1984, Chien 1985).

Channel width (w) at low flows had clearly diminished all over the meander by 1956 as a consequence of both, the reduction of discharges downstream from the dam and the progressive revegetation of active areas. Since then, width has become rather stable, except for few places where episodic retreats are observed due to local erosion. Reduction in width was relatively more pronounced in the river reach immediately below the dam (23% from w=97m in 1927 and w=69m in 2002) than further downstream (19% from w=102m in 1927 and w=82m in 2002). The smaller width reduction observed in the lowermost reaches of the meander could be related to the backwater discharges coming from the outlet of the hydroelectric power plant, which normally inundate the area (Figure 1 (C4P3)).

4.2. Vegetation encroachment

Riparian vegetation has particular biological and functional characteristics that allow a quick adaptation to changes in riverchannel physical conditions. Species are of rapid

growth, show high regeneration capacity, and are able to form mature communities in a relatively short period of time. As stated, vegetation in and along channels downstream from the dams generally increase and, in some cases, encroachment of vegetation can be very extensive (Williams & Wolman 1984).

Vegetation in the Flix meander experienced a broad expansion on formerly active areas, especially after 1948 (Figure 4 (C4P3)). First evidences of this phenomenon can be already seen on the air photo series of 1956 (Figure 5 (C4P3)). In 1927, around 57% of the bars had less than 10% of vegetation -*class 1*. In 1956 the proportion of class 1 had reduced to 52%, and in 2002 the proportion was 3%. In contrast, *class 6* (>60% of tree-like vegetation cover) constituted 5% of the total vegetation cover in 1927 and 1956, and rose up to more than 30% in 2002. Nowadays most bars of bars are occupied by vegetation in 30% or more of their surface (14 ha that are equivalent to the 72% of the emerged area). Intermediate classes show similar trends, altogether indicating a clear tendency towards the encroachment of vegetation along the study reach (Figures 4 (C4P3) and 6 (C4P3)). In addition, approximately 3.5 ha of formerly active sediment surfaces have become agricultural fields during the study period, mostly in areas far from the active channel. The lack of periodical high flows is seen as the main reason for that.

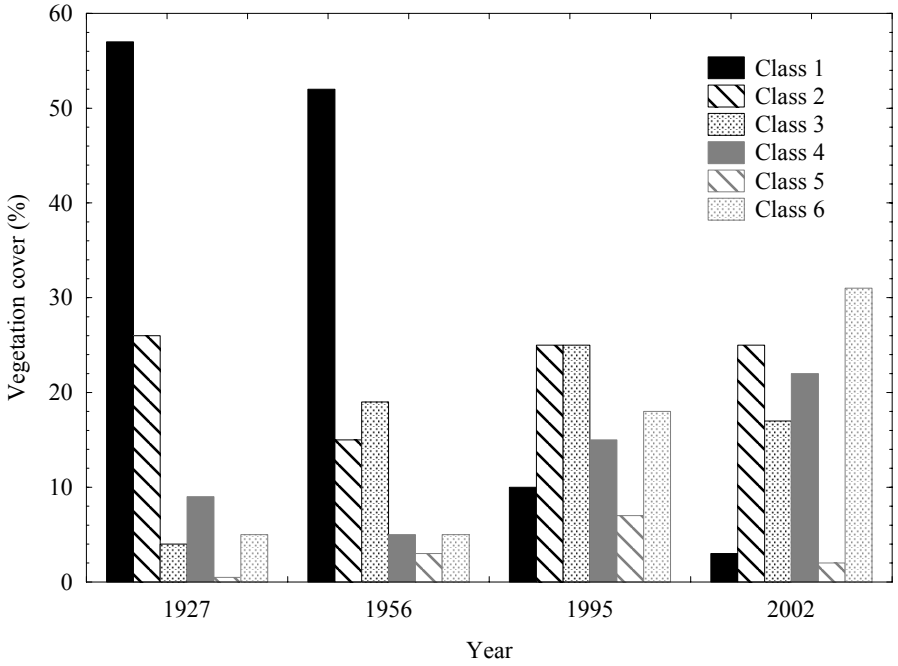

Figure 4 (C4P3). Vegetation encroachment in the lowermost reaches of the Flix Meander between 1927 and 2002

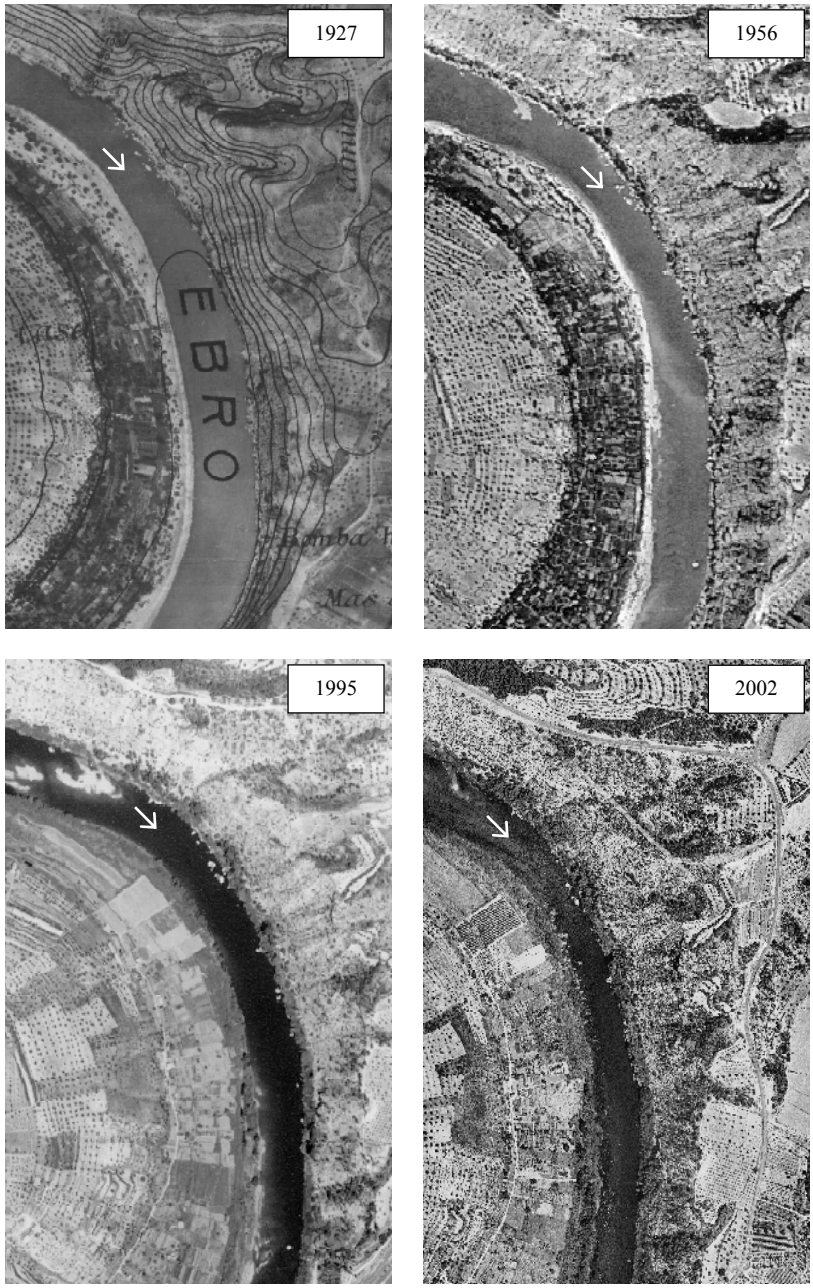

Figure 5 (C4P3). Progressive vegetation encroachment, occupation by agricultural fields and stabilization of channel banks in the Flix Meander between 1927 and 2002

The period 1927-1956 was very active in terms of sediment transport and bar formation. Numerous bars become emerged after the closure of the Flix Dam in 1948. During the second period 1956-1995 vegetation encroachment progresses everywhere in the meander, stabilising most of the formerly active areas. During the third period 1995-2002, tree-like

cover became common in the meander. Therefore, in half century vast open areas become covered by mature riparian forest. The reduction of floods prevents seeds being periodically scoured thus favouring the quick installation of individuals that generate complex communities in few years/decades. In addition, most secondary channels got collapsed by sediments and subsequently revegetated. Only the central-right part of the large island below the dam remains open with small vegetation cover (Figure 6 (C4P3)). Few areas experience erosion and subsequent disappearing of vegetation. In contrast, channel edges are completely vegetated, thus stable, preventing most of them from erosion during high flows and concentrating water energy in just the active watercourse. A representative example is given in figure 7 (C4P3).

Tamaricetum canariensis and *Rubio-Populetum albae* are the most common communities responsible of the shrub and tree-like revegetation of active areas in the Flix Meander. Figure 8 (C4P3) shows the vegetation cover in the largest bar below the dam including a representative cross-section surveyed during the period 2002-2004. Vegetation appears distributed in parallel bands perpendicular to the watercourse, being the nearest the more resistant to floods and periodical inundation. The higher centre of large bars appears to resist opened, a fact that can be related to the difficulty of most species in accessing to groundwater. In former secondary channels, nowadays completely full of sediments, is were vegetation reaches the highest degree of development, showing a well-developed riparian forest in which species such as *Populus alba* and *Populus nigra* are predominant, together with species of *Rubus* sp., and *Crataegus* sp. (Figures 7 (C4P3) and 8 (C4P3)).

4.3. Flow hydraulics

Revegetation of formerly active bars may cause channel narrowing and, as a consequence of that, channel may suffer incision (Williams & Wolman 1984, Kondolf & Wilcock 1996). Unfortunately, we do not have historical data to describe the evolution of the riverbed of the Flix meander since 1948, although signs of incision have been widely documented during 2002-2004 in the whole channel reach of the Ebro River from Flix to Mora d'Ebre, 27 km downstream (Vericat & Batalla 2005a). River-bed armouring, a common phenomenon in reaches downstream dams (e.g. Williams & Wolman 1984), slow downs and, at a long-term, stops incision.

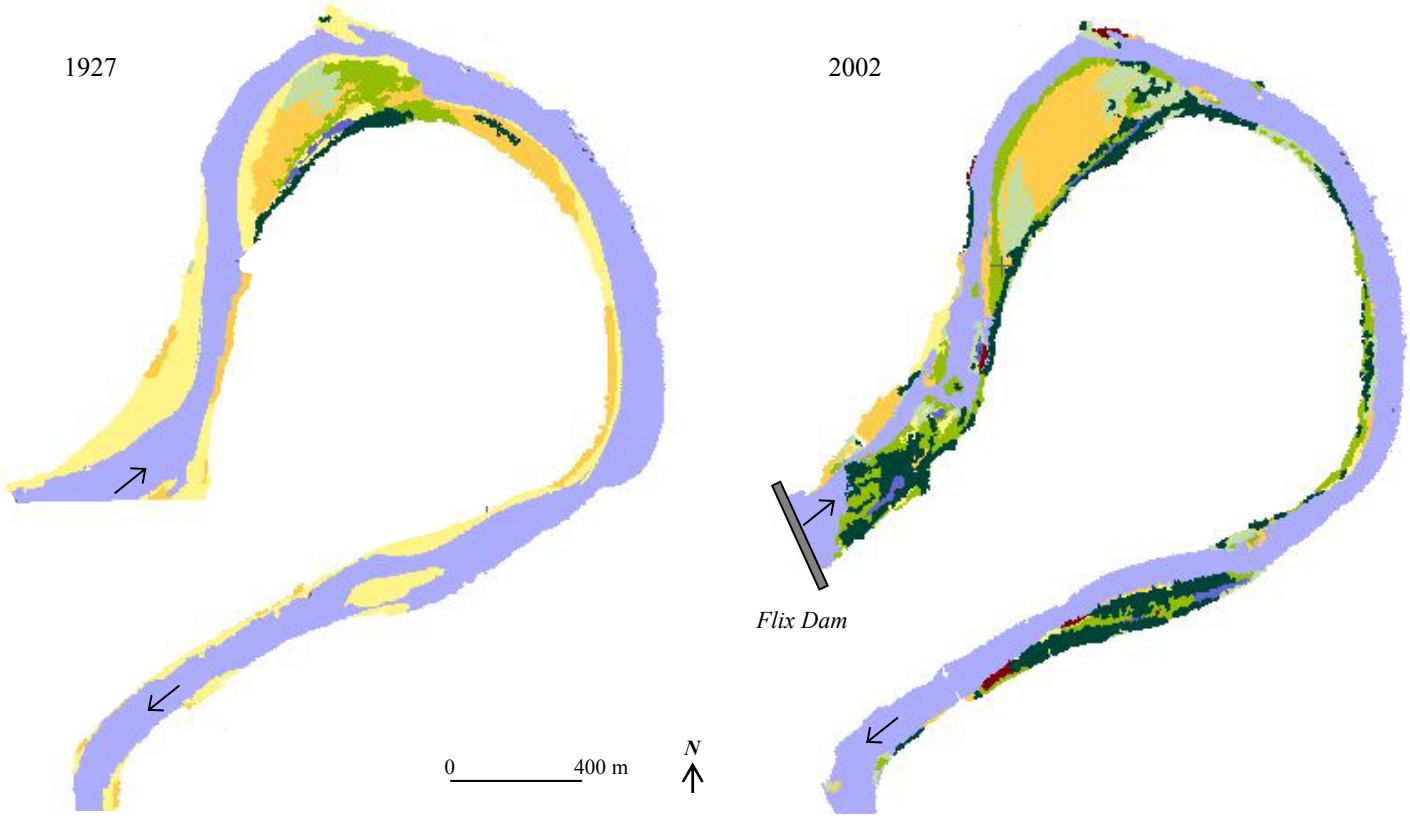

Vegetation class	Cover (%)	Stratum
Class 1[1]	0-10	Undifferentiated
Class 2[2]	10-30	Undifferentiated
Class 3[3]	30-60	Shrubby (<30% of the total)
Class 4[4]	>60	Shrubby (<30% of the total)
Class 5[5]	30-60	Tree-like (>30% of the total)
Class 6[6]	>60	Tree-like (>30% of the total)

[1] Active areas under continuous change or recently formed
[2] Active areas recently occupied by pioneer communities
[3, 4, 5] Intermediate evolution states
[6] Mature riparian forest with high diversity of species and cover

Figure 6 (C4P3). Vegetation maps of the Flix Meander in 1927 and 2002

Figure 7 (C4P3). Riparian vegetation stabilising the channel edge in the Flix Meander, with *Tamaricetum canariensis* and *Rubio-Populetum albae* as the most common communities

Vegetation encroachment results in changes in flow hydraulics. Roughness increases in vegetated areas (e.g. Yang 1996) thus reducing flow velocity onto them and redistributing flood discharge thus flow energy in the cross section. Table 3 (C4P3) shows river hydraulics during a flushing experimental flow released from the Flix Dam in December 2002 (Palau et al. 2004), with a peak discharge of 1,450 m^3/s (1.5 to 2 years of recurrence period under regulated flow conditions, Batalla et al. 2004). Based on field data (discharge, slope, riverchannel width, mean and maximum depth at flood peak) (Figure 8 (C4P3)), we estimated the river-bed total roughness at n=0.042, roughness due to grain-size at n=0.030 (in the centre of the channel), and composite roughness due to grain-size and vegetation at n=0.049 (in the channel edges and banks, and in the vegetated bar), using Manning and Strickler equations (Table 3 (C4P3)). Total discharge resulting from the sum of the discharges of the three subsections is 1,530 m^3/s (4% higher than the actual peak flow discharged from the dam). Mean stream power at the monitored section (Figure 8 (C4P3)) was estimated at 77 W/m^2 during the peak flow (Table 3 (C4P3)), estimated from the stream power formula per unit of width that is per unit of bed area (Leopold et al. 1964):

$$\omega = g\ Q\ \rho'\ s/w$$

where g is the acceleration due to gravity (9.8m/s^2), Q is the discharge (m^3/s), ρ' is the fluid density (kg/m^3), s is the slope and w is the channel width (m). Most of the flow (80%) during the peak of discharge circulated through the channel centre subsection (nr. 2, representing 39% of the total channel width), with an associated stream power of 160 W/m^2. In contrast, only 20% of the peak discharge flowed through lateral subsections (nr.1 and nr.3), with a mean stream power of 23 W/m^2. This fact indicates different flow competence thus scour capacity in different zones of the cross section, favouring incision in non-vegetated areas (channel centre). Therefore, incision could have been a common phenomenon in several reaches of the Flix Meander until river-bed become progressively armoured (Figure 9 (C4P3)). Armouring ratio, defined as the ratio between median surface and subsurface material, is 3.0 in this reach (Vericat & Batalla 2005b). Moreover, we have not observed river-bed degradation or aggradation, or remarkable changes in grain-size distribution, in this particular section of the river after seven floods during the monitoring period 2002-2004 (Figure 8 (C4P3)).

This information has been the bases to support the hydraulic design of flushing flows prescribed to enhance ecological functioning of the river in particularly altered reaches, such as the Flix Meander in the lower Ebro River (Palau et al., 2004).

Table 3 (C4P3). River hydraulics in a control section 1 km downstream the Flix Dam during the December 2002 experimental flood release (Figure 8 (C4P3))

	Q (m^3/s)	**w (m)**	**d (m)**	**v (m/s)**	**n**
Total section	1,470	165	4.75	1.88	0.042[1]
Subsection 1 (Left Bank)	35	13	2.89	0.93	0.049[2]
Subsection 2 (Channel Centre)	1,245	65	6.50	2.95	0.030[3]
Subsection 3 (Right Bank)	250	87	2.65	1.09	0.049[2]

[1] Estimated using Manning's equation $n = 1/v\ R^{2/3}\ s^{1/2}$, where *n* is the total roughness, *v* is the velocity, R is the hydraulic radius, and s is the slope ($8.5 \cdot 10^{-4}$).
[2] Weighted roughness estimated from total roughness and roughness of subsection 2.
[3] Roughness estimated from Strickler equation $n = (D_{50}^{1/6})/21.1$, where D_{50} is the median surface grain-size of the river-bed from VERICAT & BATALLA (2005a).

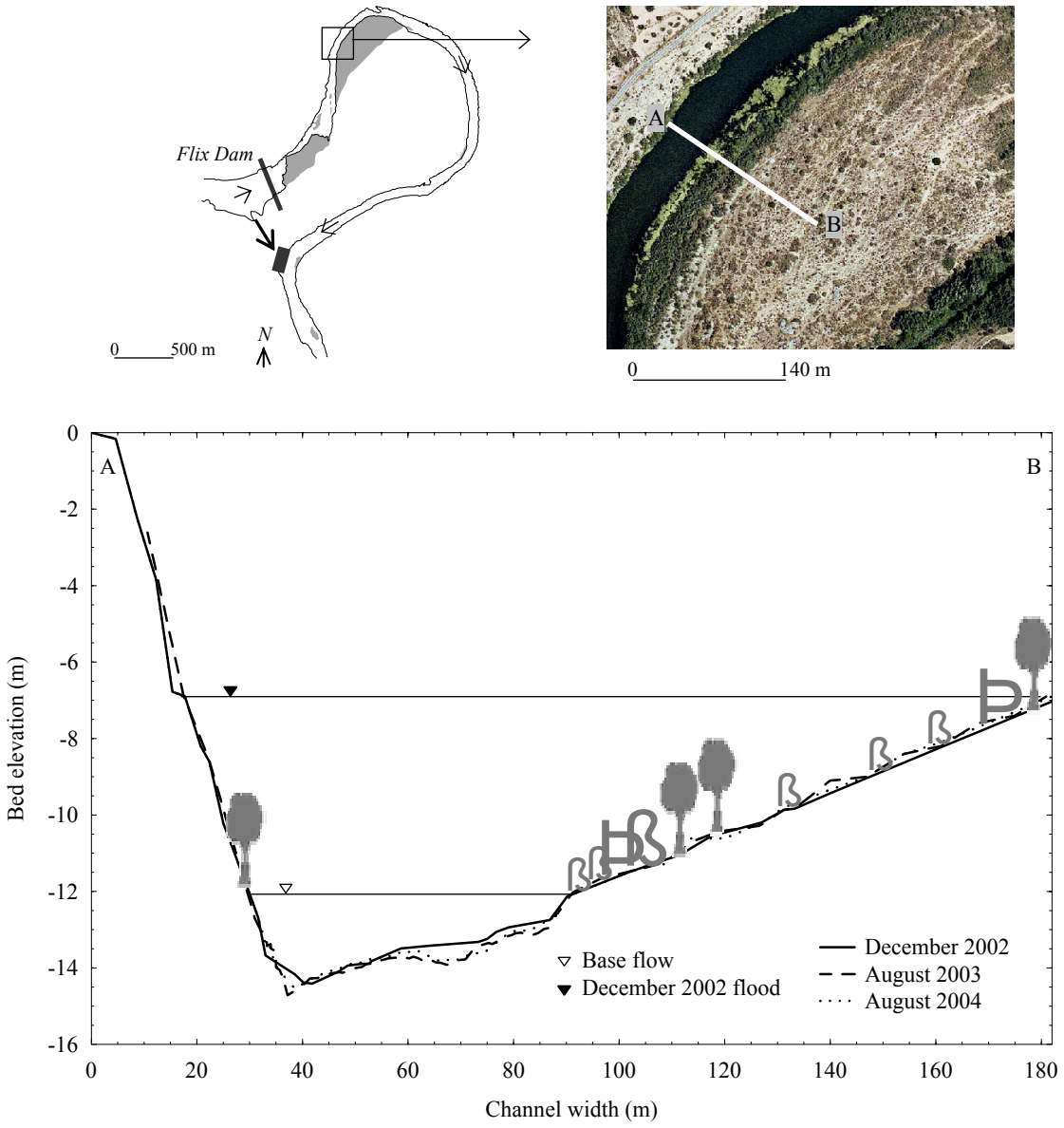

Figure 8 (C4P3). Air photo and representative river cross section 1 km downstream from the Flix Dam. For reference, we indicate cross profiles of 2002, 2003 and 2004, water level at the peak discharge of the December 2002 flushing flow (Table 3 (C4P3)), and vegetation cover (symbols are not scaled)

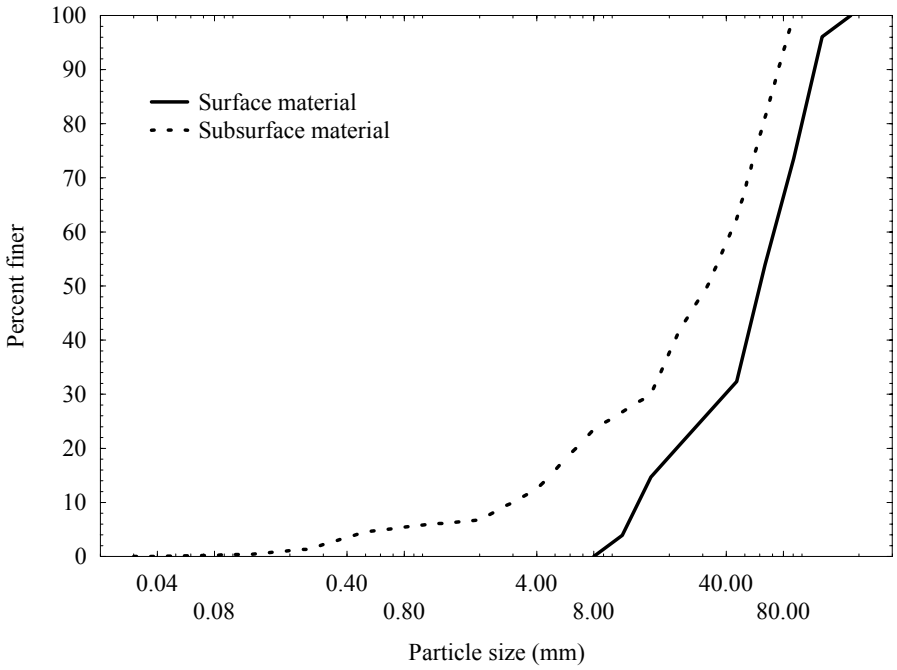

Figure 9 (C4P3). Riverbed grain-size distribution 1 km downstream the Flix Dam

5. Conclusions

Changes in river morphology of the Flix Meander since upstream dams closured in 1948, 1966 and 1969 has been characterised by means of air photos analysis and fieldwork. Changes in riverchannel form are related to the lack of sediment transport and the drastic reduction of floods. Lost of sedimentary active areas, encroachment of vegetation and associated channel narrowing are seen as the main effects of the dams. Around 4 ha of active sediment were lost from 1956 to 2002, 30% of formerly open bars are nowadays occupied by mature riparian forest (i.e. *Rubio-Populetum albae*), and channel width has reduced around 20%, on average. Vegetation of formerly active bars stabilises channel edges of the river and thus alters flow hydraulics, especially during flood events. Approximately 80% of the discharge, hence flow competence, is concentrated in the centre 40% of the river cross section. Stream power is eight times higher in the channel centre than in the lateral vegetated subsections. This fact may have caused incision along the meander in years after dams' closure, but lately ceased due to riverbed armouring. No

evidences of degradation have been seen in this particular year after seven floods monitored between 2002 and 2004.

Acknowledgements

This research was carried out within the framework of the research project REN2001-0840-C02-01/HID, which is funded by the Spanish Ministry of Science and Technology. The first author received a grant from the Spanish Ministry of Education. Hydrological data were supplied by the Ebro Water Authorities and ENDESA. Albert Rovira assisted during fieldwork.

References

Batalla, R.J. (2003): Sediment deficit in rivers caused by dams and instream gravel mining. A review with examples from NE Spain. *Cuaternario y Geomorfología* **17**(3-4): 79-91.

Batalla, R.J., G.M. Kondolf, C.M. Gomez (2004): Reservoir-induced hydrological changes in the Ebro River basin, NE Spain. *Journal of Hydrology* **290**: 117-136.

Bayerri, E. (1934-35): Historia de Tortosa y su comarca. Tortosa, Imprenta Moderna de Alguerri.

Brune, G.M. (1953): The trap efficiency of reservoirs. -Transactions of the American Geophysical Union 34: 407-418.

Chien, N. (1985): Changes in the river regime after the construction of upstream reservoirs. *Earth Surface Processes and Landforms* **10**: 143-159.

Church, M., D.G. Mclean, J.F. Wolcott (1987): River bed gravels: sampling and analysis. In: THORNE C. R., J.C. BARTHURST & R.D. HEY (eds.): Sediment transport in gravel-bed rivers. Chichester, John Wiley and Sons; 43-88.

Chuvieco, E. (1995): Fundamentos de teledetección especial. Madrid, Rialp, 453 p.

Howard, A., R. Dolan (1981): Geomorphology of the Colorado River in Grand Canyon. *Journal of Geology* **89**: 269-297.

Kondolf, G.M., P.R. Wilcock (1996): The flushing flow problem: Defining and evaluating objectives. *Water Resources Research* **32**(8): 2589-2599.

Kondolf, G.M., W.V.G. Matthews (1993): Management of coarse sediment in regulated rivers of California. University of California Water Resources Center, Riverside, Report No.80.

Kondolf, G.M. (1997): Hungry water: effects of dams and gravel mining on river channels. *Environmental Management* **21**(4): 533-551.

Leopold, L.B., M.G. Wolman, J.P. Miller (1964): Fluvial Processes in Geomorphology. New York, Dover Publ.

Ligon, F.K., W.E. Dietrich, W.J. Trush (1995): Downstream ecological effects of dams, a geomorphic perspective. *Bioscience* **45**(3): 183-192.

Nelson, C.H. (1990): Post Messinian deposition rates and estimated river loads in the Ebro sedimentary system. In NELSON C.H., & A., MALDONADO (eds.): Marine Geology of the Ebro Continental Margin. Marine Geology 95: 395-418.

Novoa, M. (1984): Precipitaciones y avenidas extraordinarias en Catalunya. -In: Ponencias y comunicaciones de las Jornadas de Trabajo sobre Inestabilidad de laderas en el Pirineo, 1, 1-15, Barcelona.

Palau, A., R.J. Batalla, E. Rosico, A. Meseguer, D. Vericat (2004): Management of water level and design of flushing floods for environmental river maintenance downstream of the Riba-roja reservoir (lower Ebro River, NE Spain). In: HYDRO 2004– A new era for Hydropower. Porto, Portugal, 18-20 Octubre 2004.

Rice, S., M. Church (1996): Sampling surficial fluvial gravels: the precision of size distribution percentile estimates. *Journal of Sedimentary Research* **66**(3): 654-665.

Richter, B.D., J.V. Baugartuer, J. Powell, D.P. Braun (1995): A method for assessing hydrologic alteration within ecosystems. *Conservation Biology* **10**(4): 1163-1174.

Sanz, M.E., C. Avendaño, R. Cobo (1999): Influencia de los embalses en el transporte de sedimentos hasta el río Ebro (España). In: Proceedings of the Congress on Hydrological and geochemical processes in large-scale river basins. HIBAM: Shahin, 1985

Vericat, D., R.J. Batalla (2004): Efectos de las presas en la dinámica fluvial del curso bajo del río Ebro. *Cuaternario y Gemorfología* **18**(1-2): 37-50.

Vericat, D., R.J. Batalla (2005a): Sediment transport in a highly regulated fluvial system during two consecutive floods (Lower Ebro River, NE Spain). *Earth Surface Processes and Landforms* **30**.

Vericat, D., R.J. Batalla (2005b): Sediment transport in the lower Ebro River (NE Spain). *Geomorphology* (accepted, in press).

Williams, G.P., M.G. Wolman (1984): Downstream Effects of Dams on Alluvial Rivers. US Geological Survey Professional Paper 1986, 83 p.

Williams, G.P. (1978): The case of the shrinking channels. The North Platte and the Platte Rivers in Nebraska. US Geological Survey Circular 781, 48 p.

Wolman, M.G. (1954): A method of sampling coarse bed material. American Geophysical Union Transactions 35: 951-956.

Yang, C.T. (1996): Sediment Transport: Theory and Practice, New York, McGraw Hill Co.; 396 p.

CHAPTER 5
DISCUSSION AND CONCLUSIONS

INDEX CHAPTER 5: DISCUSSION AND CONCLUSIONS

1. DISCUSSION

Human activities alter the sediment load of rivers. Deforestation and land cultivation are known to increase up to 3.5 times the suspended sediment load of large rivers (Dedkov and Mozzherin, 1996). In contrast, dams trap an important part of the sediment load that is transported from upstream, reducing the transfer to downstream reaches. This phenomenon has been studied in the Ebro River on the bases of systematic and comprehensive direct measurements of total load (in suspension and, especially, as bedload) upstream and downstream from a complex of large reservoirs. Retention of sediment in the Mequinenza and Riba-roja reservoirs was first assessed by Varela *et al.* (1986) at 85% (1974-1979). Palanques (1987) reported a 72% of retention for the period 1983-1986. Lately, Avendaño *et al.* (1997) gave an estimation from bathymetrical surveys at around 75% of retention of the river's sediment load. Sanz *et al.* (1999) reported similar values from sparse suspended sediment data obtained under low range of discharges. Recently, Roura (2004) estimated the retention in the Mequinenza Reservoir at 95% from daily suspended sediment data. Using a different approach, Brune's curve yields mean sediment retention of 90%. Our results point out to the same order of magnitude - 85% of the total annual sediment load is retained within the reservoir chain. However, it is worth to notice that our estimations of sediment deficit do not take into account the sediment input to the Riba-roja reservoir from the Segre and Cinca rivers, the largest tributaries in the catchment. If that was case, the sediment deficit would have plotted even higher. For comparison, around 98% of the suspended load is retained by the Aswan Dam in the Nil River, Egypt (Shalash, 1982).

Upstream the Mequinenza Dam the river transported an annual average load of $1.64 \cdot 10^6$ tonnes of sediment during 2002-2004, 99% of which in suspension. Annual load was higher than the calculated by Palanques (1987, $0.35 \cdot 10^6$ t/y), and by Roura (2004, $0.5 \cdot 10^6$ t/y). It was even higher than the annual maximum load reported by Sanz *et al.* (1999, $1.44 \cdot 10^6$ t/y). Differences can be basically attributed to the distinct hydrological patterns (i.e., annual runoff and frequency and magnitude of floods) during the several sampling periods. For instance, mean annual runoff during the sampling period in 1998-2000 (Roura, 2004) was 5,771 hm^3/y with a maximum sampled discharge of 850 m^3/s, while in our case the mean annual runoff was 7,588 hm^3/y and the maximum discharge attained

2,600 m^3/s. Varela *et al.* (1986) reported a mean annual suspended load of $1.76 \cdot 10^6$ tonnes, an estimation obtained under similar hydrological conditions than the present study.

Below the Flix Dam the river mean annual load was $0.45 \cdot 10^6$ tonnes. The observed annual load represents 1.5% of what was transported by the Ebro at the end of the 19th century (Gorría, 1877) and 3% of what was delivered at the beginning of the 20th century (Bayerri, 1934-1935; Nelson, 1990), when practically no dams were present in the catchment. Those values are in the range of the annual sediment loads estimated in basins with similar drainage area but with 3 times more annual runoff, for instance the Rhone River (France) and the Po River (Italy) (Jansen *et al.*, 1979). The annual load calculated in this study confirms the drastic reduction of the sediment load occurred in the Ebro along the 20th century. Values reported here are 4 times higher than that estimated by Guillén and Palanques (1992) from sediment transport measurements in the delta plain (120,000 t/y) and similar to that obtained by Sanz *et al*. (1999) for suspended sediment. These facts suggest that a) the river reach downstream the monitoring section acts as a sink of sediment (e.g., coarse fractions) not reaching the delta, and b) there exist a stable pattern of the transport of fine sediment below the Flix Dam, that is quite independent of the flow regime and is mostly controlled by phenomenon such as local bank erosion.

In addition to the sediment retention, dams modify the pattern of sediment transport. Bedload constitute around 10% of the total load in alluvial systems under natural conditions (Dedkov and Mozzherin, 1996). However, the proportion may shift in regulated rivers due to both the reduction of the suspended load and the increase of bedload, in case that competent flows are frequently released from dams. In the case of the Ebro River, 60% of the solid load is transported in suspension and 40% as bedload. This result is seen as one major contributions of this work. Furthermore, bedload transport and flood magnitude below the Flix Dam control the dynamics of river-bed material. The floods occurred during the winter 2002-2003 caused the breakup of the armour layer formed in several sections of the study reach after two years of relatively low flows. Gomez (1983) reported a similar phenomenon for a small, non-regulated, gravel bed stream, the Sheepstor Beck, England. Incision of the river-bed of the Ebro was remarkable during that year. In contrast, the smaller floods occurred during 2003-2004 reestablished the surface armoured layer, increasing the stability of bed-material and decreasing the supply of subsurface

sediment, hence minimising the river-bed incision. This observation constitutes another major finding of this thesis. Mean armouring ratio in 2004 was 2.3, although differences were observed from section to section. Fassnacht *et al.* (2003) reported a mean armouring of 4 in the lower Deschutes River, Oregon, below the Pelton-Round Butte dam complex.

At the long-term and at a larger scale, changes in the river-channel morphology below Flix Dam has been related to the lack of sediment supply and the reduction of floods (Batalla *et al.*, 2004). Lost of sedimentary active areas, encroachment of vegetation and associated channel narrowing are found to be the main effects of the dams. Similar results have been reported elsewhere (e.g., Williams and Wolman, 1984; Grant *et al.*, 2003).

Experimental data on bedload and bed-material dynamics in the Ebro River support the design and implementation of restoration measurements, such as the flushing flows (e.g. Kondolf and Wilcock, 1996). Two experimental flushing flows were designed and performed in the lower Ebro River during the course of the Thesis. Hydraulic design of floods was based on bed-material and bedload process directly measured in the river, thus providing a sound bases for this type of river restoration actions taken downstream from the dams. Floods have became a key hydrological disturbance, for instance, for the control of the populations of aquatic plants and exotic species, both fish and, in particular, the two bivalves that have been introduced (zebra mussel and Asian clam). They may also contribute to reducing the deficit of fine sediment at the delta mouth, and contribute to the fertilisation of the estuarine area of the river and therefore to fish yields in this area and off the adjacent coastline (Palau *et al.*, 2004). The experience achieved in the Ebro can be used to implement river restoration programmes in other large regulated gravel-bed rivers.

2. CONCLUSIONS

This work has presented the sediment transport and the associated fluvial processes in the large impounded Ebro River during two average, thus representative, hydrological years (2002-2004). Main conclusions can be drawn as follows:

1. Sediment transport in the lower Ebro is highly affected by the reservoirs, since they reduce the downstream transfer of sediment and change the pattern of transport. The mean annual total load upstream from the dams is estimated at $1.64 \cdot 10^6$ tonnes (99% in suspension). In contrast, the mean annual total load below the dams is estimated at $0.45 \cdot 10^6$ tonnes, of which 60% is transported in suspension and 40% as bedload. Almost all the sediment is entrained from the river-bed and the riverchannel, causing a mean incision of 30 mm per year.

2. Instantaneous sediment load is remarkably different upstream and downstream from the dams during floods of similar magnitude. Suspended sediment transport is particularly high at the upstream monitoring section, with a mean concentration of 0.5 g/l; mean bedload rates are lower than 100 g/ms. In contrast, suspended sediment transport is an order of magnitude lower in the downstream river reach, with a mean concentration of 0.05 g/l; mean bedload rates are higher than 150 g/ms.

3. Bedload transport is highly variable, even under steady flow conditions: i) the bedload transport rate at individual sampling verticals varied up to 3.7 times the mean rate computed for the same vertical, and ii) the highest bed load transport rates and highest variance around the sampling mean were observed in the channel centre and both the transport rate and variance diminished toward the channel margins.

4. Changes in river-bed grain-size distributions along the control 27-km channel reach downstream the Flix Dam are related to flow competence and sediment availability during flood events: i) high competent discharges are able to entrain most coarse surface material (i.e., armour layer), increasing the availability of sediment to be transported (subsurface material), hence causing incision of the river-bed and ii) small floods are not competent enough to move coarse clasts and, as a consequence, the river-bed material got progressively coarser and the armour layer re-established. The observations constitute the first description of a complete incision-armouring cycle in the lower Ebro River.

5. The lack of sediment transport and the reduction of frequent floods below the lowermost dam of Flix are seen as the main factors controlling river-channel adjustments during the second half of the 20^{th} century: i) lost of sedimentary active areas that were covered by

vegetation, thus decreasing sediment availability and modifying rivers' hydraulics, and ii) reduction of channel width thus reducing the active section of the channel.

6. For the methodological perspective, the Ebro River data on bedload confirms that the blockage and the hanging of bedload samplers are important sources of bias on bedload measurements and computations. The sampler's nozzle size needs to be adapted to the expected size of the largest material likely to move in the streambed in order to reduce this source of interference.

3. LIMITATIONS OF THE THESIS AND FUTURE WORK

Measurement of bedload transport can be seen as one of the main limitations of the type of experimental work carried out in this thesis and, at the same time, it can be taken as one of the bases to propose future work related to sediment transport in large gravel-bed rivers such as the Ebro.

Chapter 2 reports on some of the main sources of bias on bedload transport measurement and computations. Differences of instantaneous bedload rates using two scaled Helley-Smith samplers at the Móra d'Ebre Monitoring Section (MEMS) have been reported in the first paper of the chapter 2. According to the results, the use of the largest sampler (152-mm intake) seems to be more appropriate compared with the performance of the smaller sampler (76-mm intake). However, samples could also be bias using this largest sample and it would be thus important to analyse that source of error. For this, estimates of the *real* bedload transport would be necessary, despite difficulties in employing other field techniques (e.g. traps, acoustic devices) to measure bedload in such large rivers. Furthermore, characteristics of the river-bed material at the Sástago Monitoring Section (SMS) recommended the use of the 76-mm intake Helley-Smith sampler. However, we did not analyse the bias of this sampler there in comparison with the largest one. Therefore, a bedload sampling programme may be developed for the study of the bias to support the use of a specific sampler in that section.

Spatial and temporal bedload variability is specifically examined in the second paper presented in chapter 2. There we have reported on the bedload variability both spatial and temporal at MEMS. The results show how important is to take in account bedload variability on sediment transport programmes in the lower Ebro River and similar large gravel-bed rivers. The sampling at a single vertical allows assessing accurately the temporal variability. Spatial variability was also important although has not been taken into account in the computation of sediment load. Therefore, the sediment sampling programme could be redefined to include multiple vertical sampling. In addition, bedload variability should also be analysed at SMS.

Other important source of errors associated with experimental work can be summarized as follows:

1. Errors associated to discharge computation using flow routing method. The Muskingum method tended to systematically overestimate discharges at the monitoring sections, especially for low flows. Mean overestimation is about 10% at SMS and 3% at MEMS.

2. Errors associated to data collection and hydraulic inferences than can be made from them. They are a) the small number of control sections that are limited by the number of open bars with low vegetation cover exposed during low flows, and b) the sampling location in control sections, since bed-material dynamics can be somewhat different in the active channel than in the bars. Unfortunately, monitoring techniques such scour chains and painted pebbles could not be used in the watercourse.

At the light of these various limitations that have arisen during the course of the experimental work, several aspects need to be considered before defining future work on sediment transport, especially on bedload, in the lower Ebro River:

1. To improve the monitoring of sediment transport:
   - Increasing sampled verticals at both monitoring sections according to the observed spatial bedload transport variability.
   - Obtaining continuous suspended sediment measurements in order to integrate short-term variability in the load computation.

2. To improve the analysis of sediment transport and budget:
   - Carrying simultaneous measurements of sediment transport during floods in the main tributaries of the lower Ebro River such as the Segre, the Cinca, the Matarranya and the Guadalope rivers, as they were the main sources of sediment before dams set in operation.
   - Monitoring suspended sediment transport just below the Flix Dam in order to quantify how much suspended sediment passes the reservoirs in comparison with the amount that is entrained from the river-channel below the dam.
   - Monitoring sediment transport in the main tributary downstream the Flix Dam, the Siurana River. Nowadays, dams and gravel mining profoundly alter this river. However, in spite of the drastic reduction of the sediment supply, the Siurana River could still transfer sediment to the lower Ebro River during high flows, acting a potential source of sediment below the dams.

3. To improve the survey of river-bed processes:
   - Sampling or recording grain-size of river-bed materials in different river morphologies such as riffles and pools, in order to define the extension and strength of armouring in the river.
   - Tracing particle entrainment using radio-transmitters. Painted magnetic pebbles placed at the monitored sections below the Flix Dam have shown a low degree of recover. This is an important source of information to design hydraulically efficient flows to restore geomorphological functioning of the river.

4. REFERENCES

Avendaño, C., Cobo, R., Sanz, M.E., Gómez, J.L. (1997): Capacity situation in Spanish reservoirs. *I.C.O.L.D. Proceedings of the Nineteenth Congress on Large Dams* **74**(52): 849-862.

Batalla, R.J., Kondolf, G.M., Gomez, C.M. (2004): Reservoir-induced hydrological changes in the Ebro River basin, NE Spain. *Journal of Hydrology* **290**: 117-136.

Bayerri, E. (1934-35): *Historia de Tortosa y su comarca*. Imprenta Moderna de Alguerri: Tortosa.

Dedkov, A.P., Mozzherin, V.I. (1996): Erosion and sediment yield on the Earth. In *Erosion and Sediment Yield: Global and Regional Perspectives*. IAHS Publ. 236: 29-33.

Fassnacht, H., McClure, E.M., Grant, G.E., Klingeman, P.C. (2003): Downstream effects of the Pelton-Round Butte hydroelectric project on bedload transport, channel morphology, and channel-bed texture, lower Deschutes River, Oregon. *Water Science and Application* **7**: 175-207.

Gomez, B. (1983): Temporal variations in bedload transport rates: the effect of progressive bed armouring. *Earth Surface Processes and Landforms* **8**: 41-54.

Gorría, H. (1877): *Desecación de las marismas y terrenos pantanosos denominados de Los Alfaques*. Imprenta la Giralda, Madrid.

Grant, G.E., Schmidt, J.C., Lewis, S.L. (2003): A geological framework for interpreting downstream effects of dams on rivers. In *A peculiar river: geology, geomorphology, and hydrology of the Deschutes River, Oregon*, Grant, G.E., O'Connor, J.E. (eds.). Water Science and Application 7, AGU; 209-225.

Guillén, J., Palanques, A. (1992): Sediment dynamics and hydrodynamics in the lower course of a river highly regulated by dams: the Ebro River. *Sedimentology* **39**: 567-579.

Jansen, P. Ph., Van Bendegom, L., Van den Berg, J., De Vries, M., Zanen, A. (1979): *Principles of River Engineering*. Pitman, London, 509 pp.

Kondolf, G.M., Wilcock, P.R. (1996): The flushing flow problem: Defining and evaluating objectives. *Water Resources Research* **32**(8): 2589-2599.

Nelson, C.H. (1990): Post Messinian deposition rates and estimated river loads in the Ebro sedimentary system. In *Marine Geology of the Ebro Continental Margin,* Nelson C.H., Maldonado A. (eds.). Marine Geology; **95**: 395-418.

Palanques, A. (1987): *Dinámica Sedimentaria, Minerología y Microcontaminantes Inorgánicos de las Suspensiones de los Sedimentos Superficiales en el Margen Continental del Ebro.* Instituto de Ciencias del Mar (CSIC), Barcelona, 438 pp.

Palau, A., Batalla, R.J., Rosico, E., Meseguer, A., Vericat, D. (2004): Management of water level and design of flushing floods for environmental river maintenance downstream of the Riba-Roja Reservoir (Lower Ebro River, NE Spain). *Proceedings of the International Conference HYDRO 2004: A New Era for Hydropower*. Porto, Portugal, 18-21 October 2004.

Roura, M. (2004): *Incidència de l'embassament de Mequinensa en el transport de sòlids en suspensió i la qualitat de l'aigua del riu Ebre*. PhD Thesis, Facultat de Biologia, Universitat de Barcelona, Barcelona, 145 pp.

Sanz, M.E., Avendaño, C., Cobo, R. (1999): Influencia de los embalses en el transporte de sedimentos hasta el río Ebro (España). *Proceedings of the Congress on Hydrological and geochemical processes in large-scale river basins*. HIBAM: Shahin.

Shalash, S. (1982): Effects of sedimentation on the storage capacity of the High Aswan Dam Reservoir. *Hydrobiology* **92**: 623-639.

Varela, J., Gallardo, A., López de Velasco, A. (1986): Retención de sólidos por los embalses de Mequinenza y Ribarroja. Efectos sobre los aportes al Delta del Ebro. In *El sistema integrado del Ebro*, M. Mariño (ed.). Gráficas Hermes, Madrid, 200-219.

Williams, G.P., Wolman, M.G. (1984): *Downstream Effects of Dams on Alluvial Rivers*. US Geological Survey Professional Paper 1286.

ANNEXES

1. RAINFALL AND RUNOFF DATA

Table 1. Annual rainfall in the Ebro Basin: (source: SAIH, Ebro Water Authorities)

Number	Code	Name	Annual precipitation (mm) 2002-2003	2003-2004	Observations
1	A017	Cinca en Fraga	552.8	495.4	
2	A089	Gallego en Zaragoza	435.3	257.4	
3	A260	Arba en Tauste	352.0	401.5	
4	C028	Cola Pardinas, Bardenas	161.6	560.9	lost of data 2002-2003
5	E002	Embalse de Flix	324	345.1	
6	E003	Embalse de Mequinenza	216.4	300.4	
7	E004	Embalse de Ribarroja	200.7	241.9	
8	E046	Embalse de Mediano	733.9	637.4	
9	E047	Embalse de Grado	650.6	416.8	
10	E282	Toma de Canal de Lodosa			no data available
11	M001	Estación Meteorológica de Egea	185.7	243	lost of data 2003-2004
12	P001	Soto	917.6	1056.6	
13	P002	Pto. del Escu	699.4	817.6	
14	P003	Basconcillos del Tozo	841.8	732.4	
15	P004	Tobes y Rahedo	563.00	559.40	
16	P005	Berberana	780.2	657.3	
17	P006	Vallarta de Bureba	514.5	520.8	
18	P007	Ajamil	332.2	700.2	
19	P008	Lagran	463.8	797	
20	P009	San Vicente de	832.00	846.20	
21	P010	Sierra Urbasa	1489.2	1334.2	lost of data 2003-2004
22	P011	Valloria	653.4	761.8	
23	P012	Beruete	1807	1806.4	
24	P014	Fuentes de Agr	646.8	530.6	
25	P015	Hecho	1144	1060.4	
26	P016	Ansó	1107	1083.8	
27	P017	Lobera de Onsella	594.8	745.3	
28	P018	Beratón	483.6	271.8	
29	P019	Judes	491.6	513.6	
30	P020	Almazul	415.8	448.2	
31	P021	Cubillejo del Sitio	446.8	514.2	
32	P022	Collado de Brinzol	589.4	474.8	
33	P023	Ojos Negros	426	485	
34	P024	Sta. Eulalia	340	307.6	
35	P025	Cucalón	585	428.2	
36	P026	El Cebollar	941.6	780.2	lost of data 2003-2004
37	P027	Vivel del Río Martín	242.6	574.2	
38	P028	El Coscollar	742.7	701.6	lost of data 2002-2003
39	P029	Samper	816	1014.2	lost of data 2002-2003
40	P030	Las Paules	1016	899.2	
41	P031	Casallera	583.2	702.5	lost of data 2002
42	P032	Castilgaleu	455.7	532.8	lost of data 2002
43	P034	Castelnou	621.6	754.2	lost of data 2002
44	P035	La Guardia	638.8	641.8	lost of data 2002
45	P036	Boixols	675.4	733.4	
46	P037	Benavent	916	918.4	
47	P038	Os de Balaguer	732.8	916.4	
48	P039	Arcalis	1002	810.2	
49	P040	Bordas de Seturia	967	849.4	
50	P041	Grau Roig	546	700.6	

51	P043	Estana	500.2	820.4	
52	P044	Viliella	611	586.6	
53	P045	Fornolls	502.4	608.4	
54	P046	Pinell	475.6	592	
55	P047	Cervera	379.8	281.8	
56	P048	Vilosell	458	650.5	
57	P049	La Iglesuela del Cid	545.4	504	
58	P050	Morella	760.8	633.8	
59	P051	Michavilla	627.2	602.4	
60	P052	Arnés	516.8	743.2	
61	P053	Bot	469.2	555.8	
62	P054	Brazuelo	477.4	608	
63	P055	Savalla	403.2	511.4	
64	P056	Arnedillo	640.9	461.8	
65	P062	Trasobares	614.8	547.8	

Table 2. Annual discharge and runoff in the Ebro basin (source: SAIH, Ebro Water Authorities)

Code	Station Name	River	Hydrological year 2002-2003			Hydrological year 2003-2004		
			Maximum discharge[1]	Mean discharge[1]	Annual runoff [2]	Maximum discharge[1]	Mean discharge[1]	Annual runoff [2]
A002	Castejón	Ebro	3,320.0	258.6	8,155.9	1,431.6	222.2	7,008.3
A004	Funes	Arga	932.8	41.5	1,307.5	418.2	44.5	1,403.1
A005	Caparroso	Aragón	1,218.5	40.0	1,260.5	542.5	38.1	1,200.0
A011	Zaragoza	Ebro	2,988.0	277.4	8,747.1	1,217.7	240.5	7,584.6
A014	Híjar	Martín	7.7	0.5	16.8	45.0	1.1	33.7
A017	Fraga	Cinca	536.7	40.9	1,290.5	469.8	55.1	1,738.8
A025	Serós	Segre	309.2	100.9	3,181.2	356.0	104.1	3,283.3
A026	Arroyo	Ebro	46.3	8.5	269.7	108.8	8.7	273.2
A027	Tortosa	Ebro	2,475.2	389.7	12,290.0	1,206.9	441.9	13,935.0
A089	Zaragoza	Gállego	582.7	26.2	826.7	706.2	23.7	747.5
A120	Mendavia	Ebro	2,159.6	133.8	4,218.6	188.5	17.7	559.2
A216	Zaragoza	Huerva	75.8	4.7	147.9	80.7	3.1	96.5
A278	Chodes	Jalón	59.4	3.2	102.0	59.2	12.6	398.6

[1] Discharge in m^3/s
[2] Runoff in hm^3

2. PHOTOGRAPHS

Figure 1. Portable cranes used for sediment transport sampling

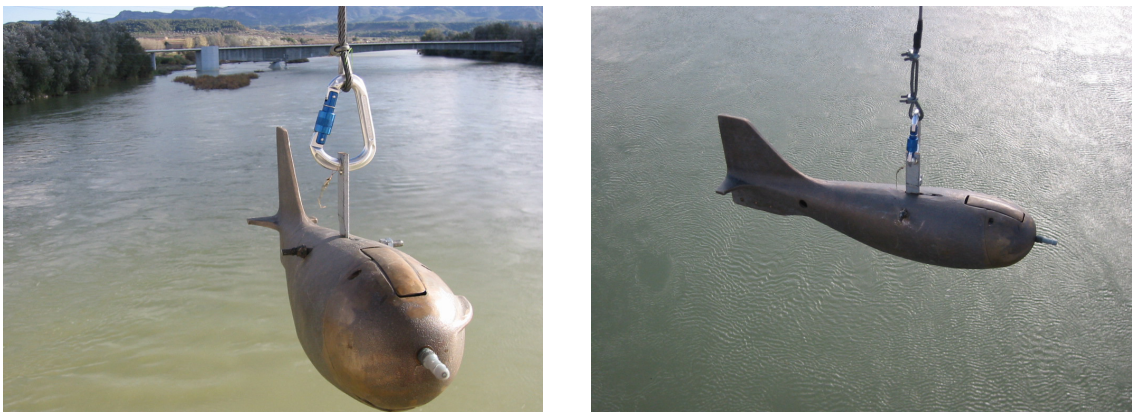

Figure 2. Depth-Integrating suspended sediment sampler USGS DH-74

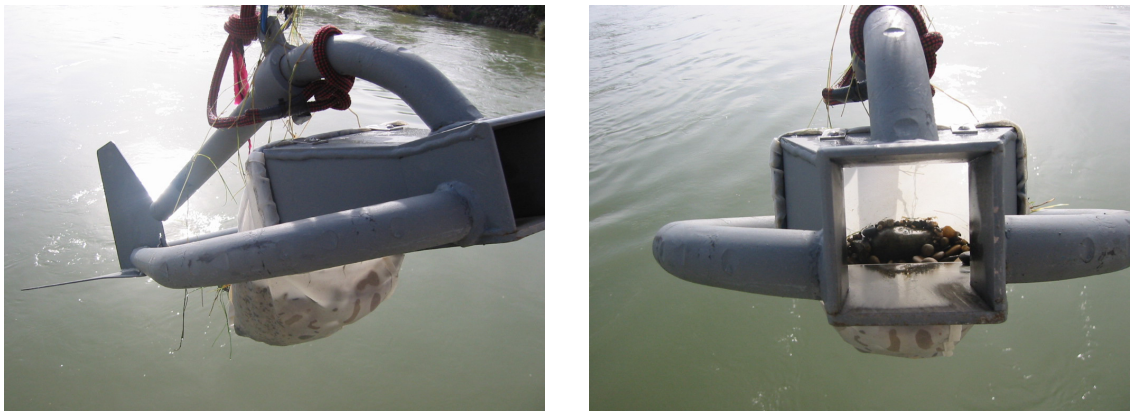

Figure 3. Helley-Smith bedload sampler 76-mm intake

Figure 4. Helley-Smith bedload sampler 152-mm intake

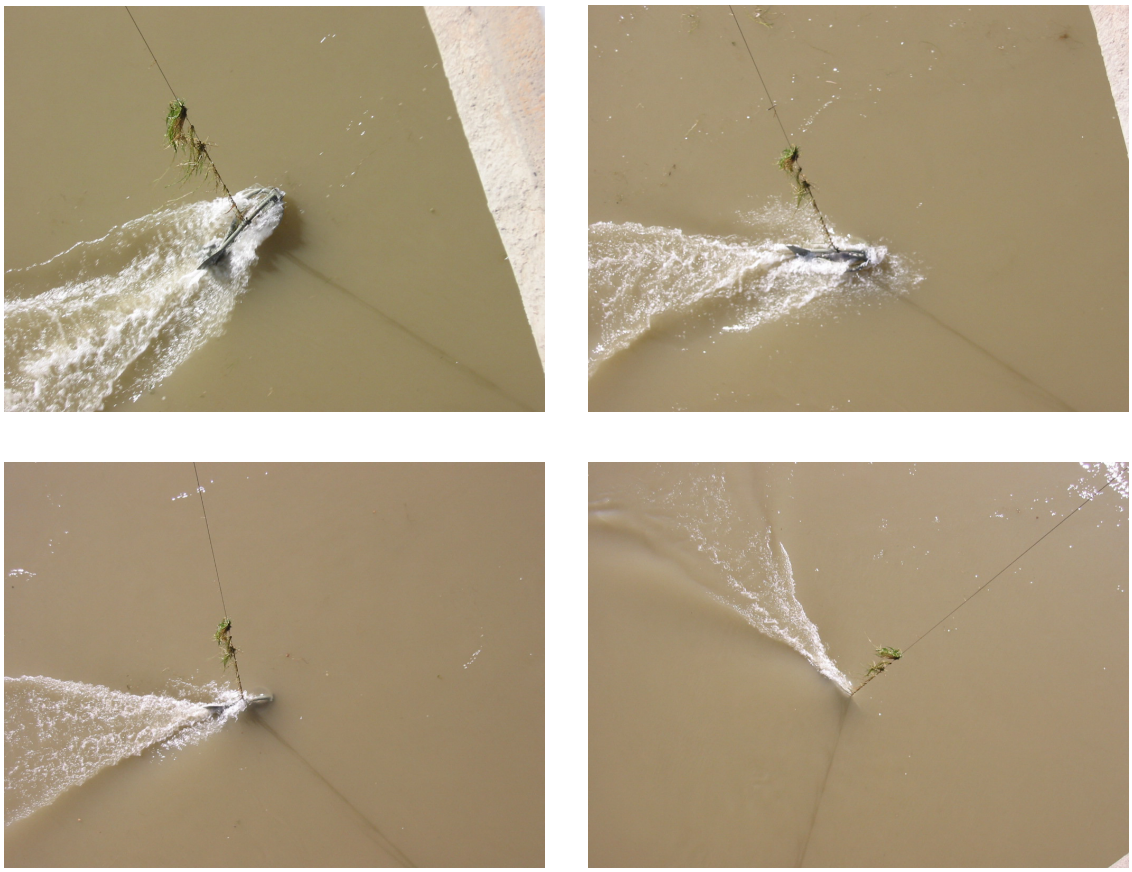

Figure 5. Deployment of a 76-mm intake Helley-Smith 76-mm sampler during February 5th 2003 at the Móra d'Ebre Bridge Monitoring Section

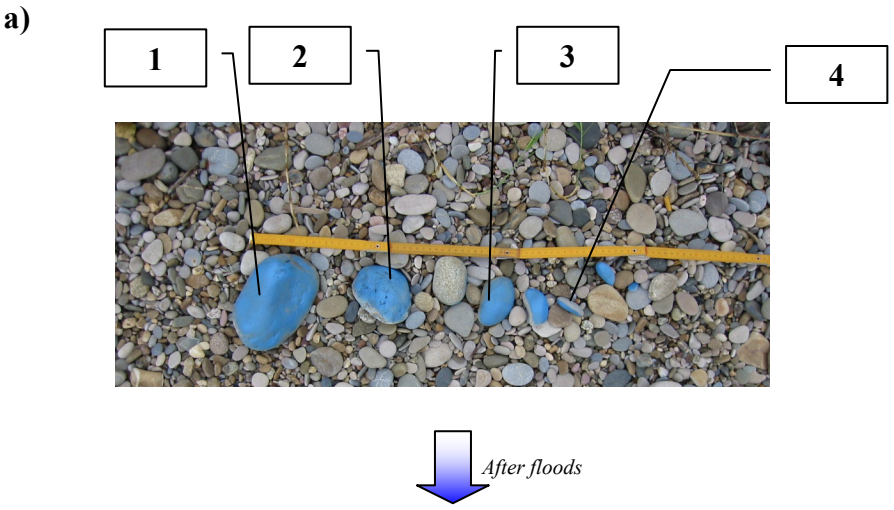

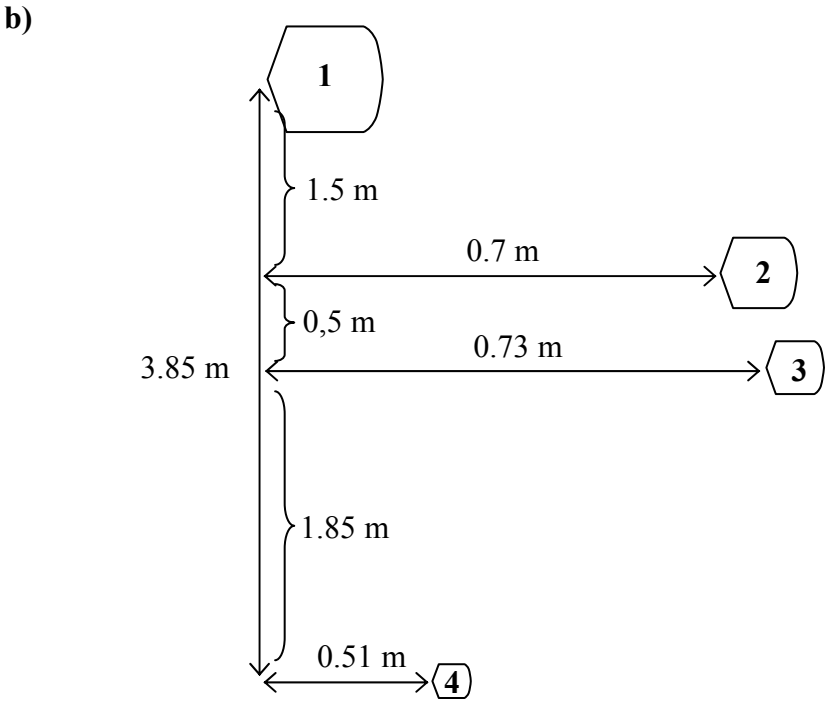

Figure 6. (a) Painted pebbles at the Flix control section placed the 29th of November 2002. (b) Diagram showing movement of the pebbles after a peak flow of 1,600 m^3/s. Survey done during the field campaign of December 24th 2002

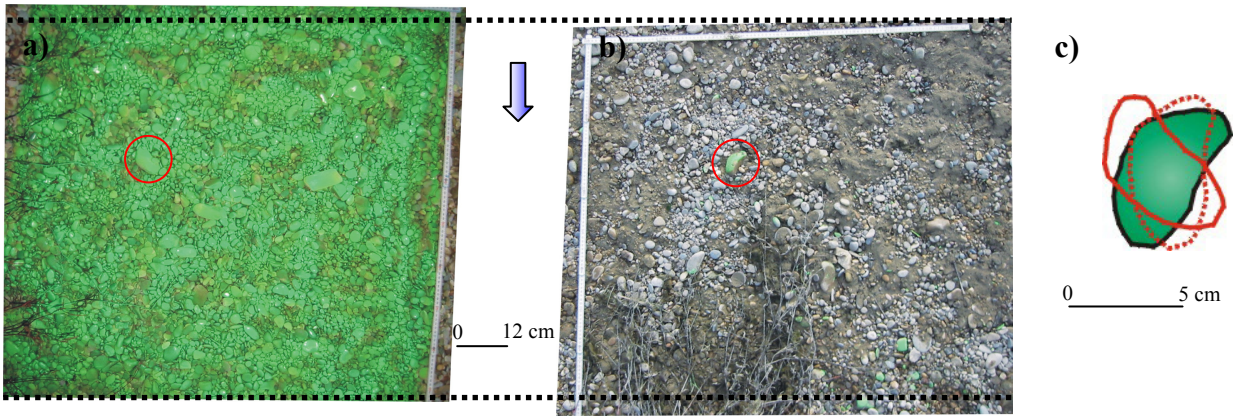

Figure 7. (a) Painted pebbles at the Meandre Flix control section placed the 29th of November 29th, (b) Winnowing of finest particles after a peak flow of 1,600 m^3/s can be observed, and (c) Largest particle were not set in motion but experienced some movement. Survey done during the field campaign of December 24th 2002

Figure 8. Painted pebbles at the Pas de l'Ase control section placed the 25th of February 2005

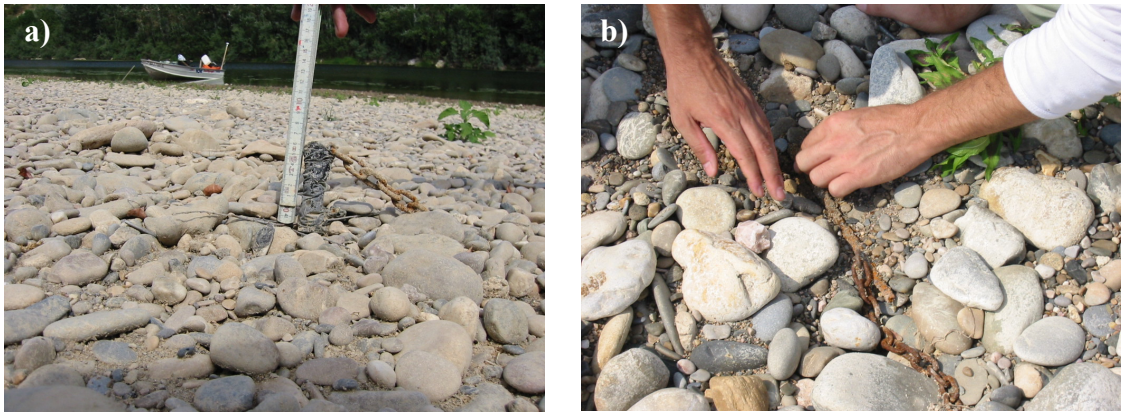

Figure 9. Scour chain at the Meandre Flix (a) and the Móra d'Ebre 3 (b) control sections surveyed on July 14th 2003 after the winter floods 2002-2003

Figure 10. General view of the Presa Flix control section after a peak flow of 1,600 m^3/s. Photograph taken during the field survey of December 24th 2002

Figure 11. General view of the Pas de l'Ase control section after a peak flow of 1,500 m^3/s. Photograph taken during the field survey of February 25th 2004

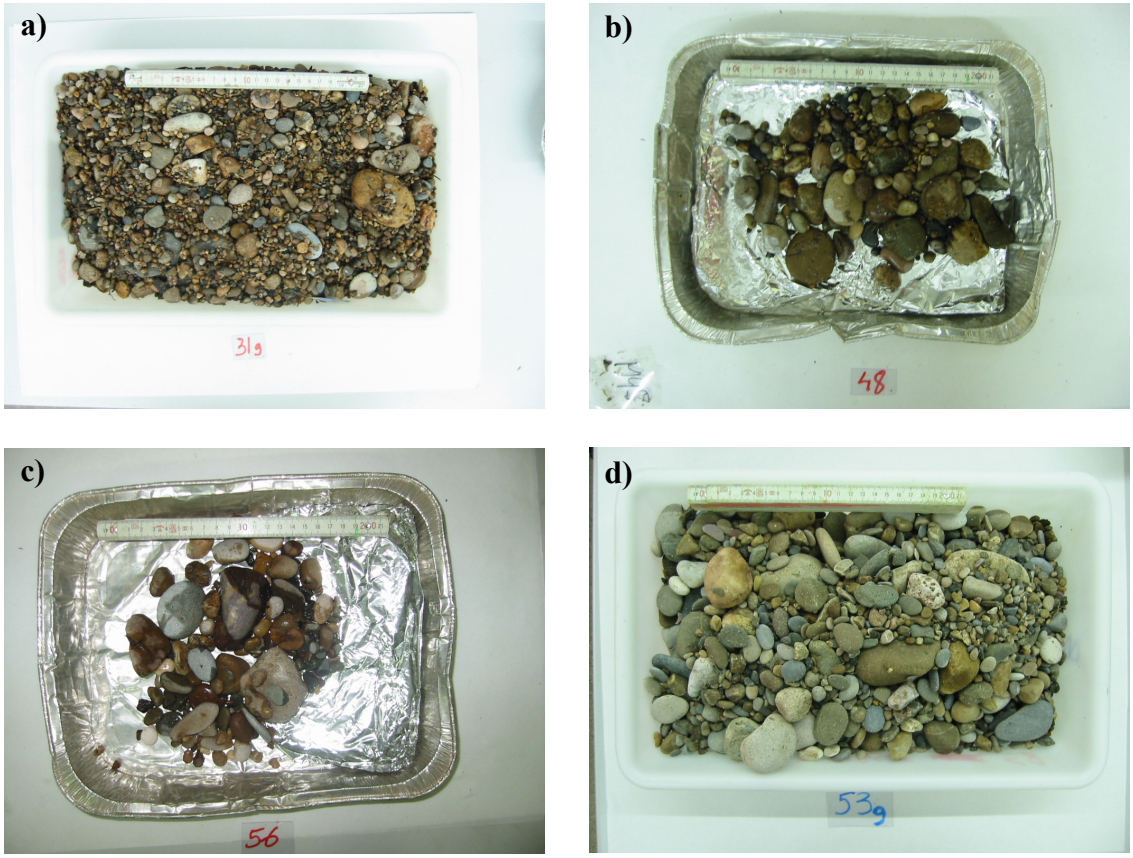

Figure 12. Bedload samples obtained at the Móra d'Ebre Bridge Monitoring Section during the winter 2003-2004 floods: (a) D_{50}= 12 mm, i_b= 353 g/ms, Q= 1,328 m^3/s; (b) D_{50}= 20 mm, i_b= 50 g/ms, Q= 1,284 m^3/s; (c) D_{50}= 27 mm, i_b= 38 g/ms, Q= 1,130 m^3/s; and (d) D_{50}= 22 mm, i_b= 210 g/ms, Q= 1,127 m^3/s (i_b is the instantaneous bedload rate and Q is the associated discharge)

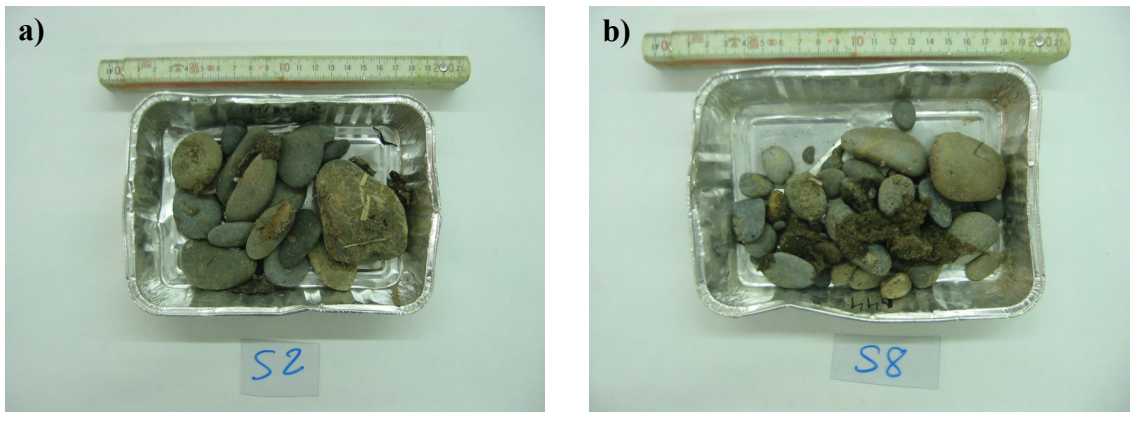

Figure 13. Bedload samples at the Sástago Bridge Monitoring Section during the winter 2003-2004 floods: (a) D_{50}= 14 mm, i_b= 5 g/ms, Q= 830 m^3/s; and (b) D_{50}= 19 mm, i_b= 3.5 g/ms, Q= 875 m^3/s (i_b is the instantaneous bedload rate and Q is the associated discharge)

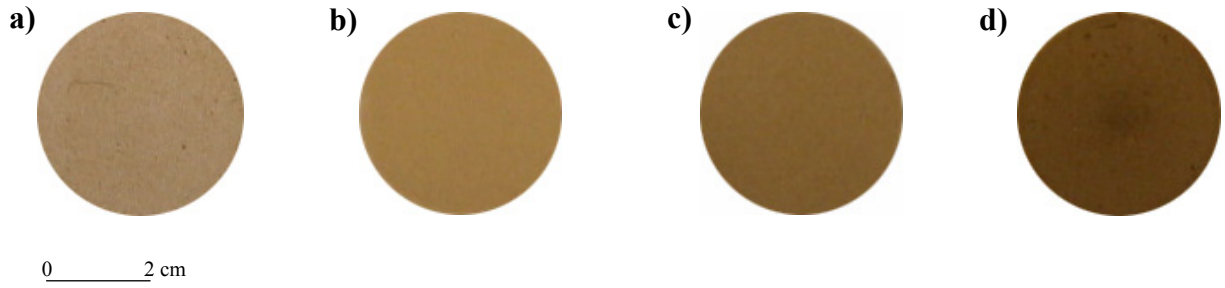

Figure 14. Suspended sediment deposited in filters corresponding to samples obtained in the lower Ebro River during winter 2003-2004 floods: (a) Móra d'Ebre Bridge Monitoring Section, C_i= 8.3 mg/l, Q= 720 m^3/s; (b) Móra d'Ebre Monitoring Section, C_i= 14 mg/l, Q= 930 m^3/s; (c) Sástago Monitoring Section, C_i= 130 mg/l, Q= 1,160 m^3/s; and (d) Sástago Bridge Monitoring Section, C_i= 1,500 mg/l, Q= 1,965 m^3/s (C_i is the instantaneous suspended sediment concentration (mg/l), and Q is the associated discharge (m^3/s)

3. PUBLICATION STATUS OF THE PAPERS

Table 3. Publication status of the papers presented in this thesis (May 14th, 2005)

Chapter	Papers [1]	Journal [2]	State
1. Introduction	- C1P1	- CyG	- published
2. Methods	- C2P1	- WRR	- accepted
	- C2P2	- IAHS	- in press
3. Sediment transport	- C3P1	- ESPL	- published
	- C3P2	- GEO	- accepted
4. Fluvial adjustments	- C4P1	- WRR[3]	- to be submitted
	- C4P2	- WRR[3]	- to be submitted
	- C4P3	- ZfG	- submitted

[1] Where C1P1indicates the position of the paper in the Thesis, in this case **C**hapter **1** **P**aper **1**
[2] CyG: *Cuaternario y Geomorfología*; WRR: *Water Resources Research*; IAHS: *IAHS Publication (Red Book)*; ESPL: *Earth Surface Processes and Landforms*; GEO: *Geomorphology*, and ZfG: *Zeitschrift für Geomorphologie*
[3] Papers are being reviewed by an external referee before submission to Water Resources Research